

https://dspace.org/

Biocatalytic asymmetric synthesis of beta-amino acids for peptidomimetics

Phathutshedzo, Masithi

2019
https://hdl.handle.net/10539/28835

Downloaded from a DSpace repository. https://dspace.org/

Biocatalytic asymmetric synthesis of *beta*-amino acids for peptidomimetics

By

Masithi Phathutshedzo

Supervisor: Prof. Dean Brady

Co-Supervisors: Prof. Moira Bode

Dr. Maya Makatini

Declaration

I declare that this thesis is my own and was supervised by Prof Dean Brady, Prof Moira Bode and Dr Maya Makatini. It is being submitted for the degree of Master of Science in the University of the Witwatersrand, Johannesburg, and has not been submitted before for any degree or examination in any other university.



……

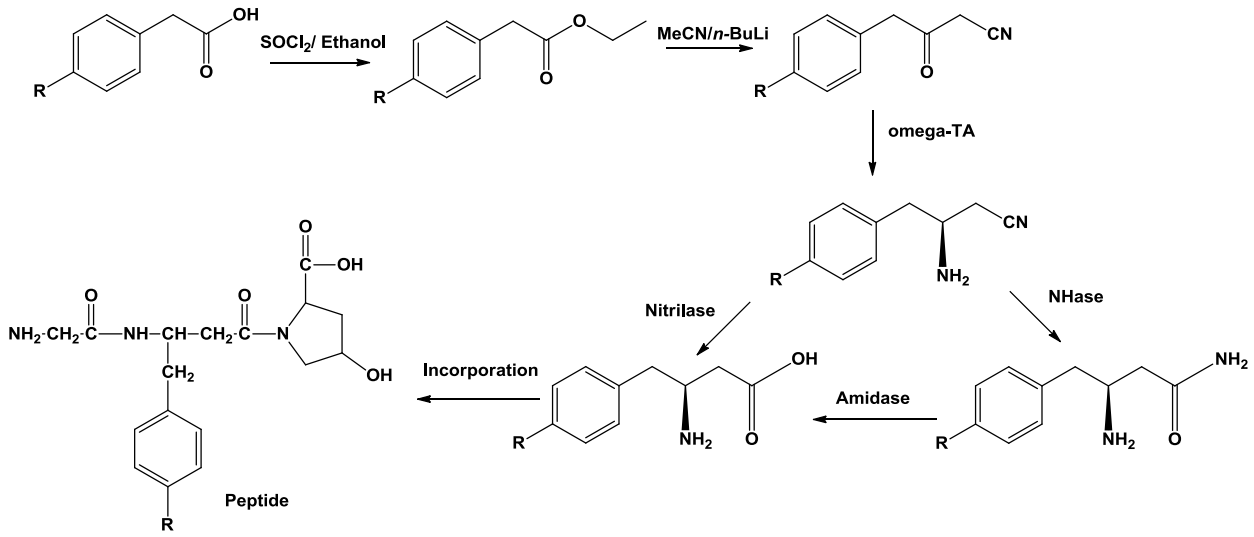
20/06/2019

Masithi Phathutshedzo

ABSTRACT

There is an increasing demand for enzymes that can transform synthetic compounds with high regio-, chemo-, and enantioselectivity. Single enantiomer compounds are in high demand from the agrochemical and pharmaceutical industries for the improvement of the compound's efficacy and reduction in side-effects. Synthesis of optically pure aromatic β-amino acids has recently attracted attention for their application in many pharmacologically active compounds. However, to date there are still no efficient synthetic methods for their preparation. Omega-transaminases (ω-TAs) are stereospecific enzymes that can either be applied for the asymmetric synthesis of β-amino acids from their corresponding ketones or kinetic resolution of racemic β-amino acids. The asymmetric synthesis is more advantageous because it leads to 100% of β-amino acid product, and is therefore a major focus of this dissertation.

In previous studies, ω-transaminases could not be applied efficiently on asymmetric synthesis of enantiopure aromatic β-amino acids due to the decarboxylation of β-keto acids. In this study, we report an asymmetric synthesis strategy to circumvent the decarboxylation problem via reductive amination hydrolysis (RAH) of stable aromatic β-ketonitrile substrates.



R: (a) H, (b) F, (c) Me, (d) OMe

In this work, aromatic carboxylic acids were initially converted to carboxylic esters using thionyl chloride, and then subsequent nucleophilic substitution by lithiated acetonitrile resulted into aromatic β-ketonitriles. The thermodynamically stable aromatic β-ketonitriles were converted to aromatic β-aminonitriles using ω-TA in using the LDH pyruvate removal mixture as well as in the presence of the diamine donor *o*-xylylenediamine dihydrochloride. However low yields were obtained due to side-

reactions and low enzyme activity, and therefore the subsequent steps in the project were demonstrated using commercial material.

Hydrolysis of racemic aromatic β-aminonitriles into β-aminoamides as a first step towards conversion to carboxylic acids, was achieved using isolated nitrile hydratase from *Rhodococcus rhodochrous* ATCC BAA-870 (NHase). For determination of substrate specificity, NHase was also tested on β-ketonitrile substrates.

Enantiopure aromatic β-amino acids were incorporated into wound healing peptides. The synthesis of these peptides was performed using solid phase peptide synthesis (SPPS). Successful synthesis of the wound healing peptides has been achieved, as well as their modification by attaching palmitic acid and adamantane for improving their membrane permeability. The biological activity of these peptides will be evaluated in future work.

Acknowledgements

We would like to thank the University of the Witwatersrand for the resources needed to complete this work. Financial support from the Department of Science and Technology Biocatalysis Initiative (Grant 0175/2013) and the NRF Bursary Scheme was greatly appreciated.

I would like to thank my supervisor **Prof Dean Brady** for the great support and the best opportunity to pursue this degree under his supervision.

Prof Moira Bode, my co-supervisor, I am so grateful for your support and for improving my scientific thinking and reasoning capacity. The suggestions you gave me throughout my research years are really appreciated. I am very grateful for the assistance with NMR data analysis.

Dr Maya Makatini, my co-supervisor, I was really a one lucky student to have you throughout my master's research years. The enormous support and guidance you gave me is really appreciated.

Wits organic group (Peter, Robyn, Eric, Thapelo, Refilwe, Dennis, Tebogo, Gciniwe, Ntombi, Kate, Kennedy, Dubekile, Akhona, Jean, Mudzuli, Pious, Thabo, Xolani, Songz, William, Memory, Charles, Donald and Khanani)

Mashimbye Khuthadzo Lucia, you are the best person I ever had in my life, thanks for the support you gave me, without you I don't think I would've made it.

I would like to thank my family and friends for their unconditional support and love they gave me all these years.

I would also like to thank **God**, his love is unconditional and without him I would not have made it through, in him I will always believe.

List of abbreviations

CSIR	Council of Scientific and Industrial Research
DCM	Dichloromethane
DMSO	Dimethyl Sulfoxide
DMF	*N,N*-dimethylformamide
EtOAc	Ethyl acetate
IR	Infrared
LDH	Lactate Dehydrogenase
NADPH	Nicotinamide adenine phosphate
MS	Mass Spectroscopy
CMPs	Collagen mimetic peptides
NMR	Nuclear Magnetic Resonance
TLC	Thin Layer Chromatography
PTSA	*p*-Toluenesulfonic acid
TFA	Trifluoroacetic acid
TIS	Triisopropylsilane
$SOCl_2$	Thionyl chloride
HRMS	High resolution mass spectroscopy
PLP	Pyridoxal phosphate
NaOH	Sodium hydroxide
n-BuLi	*n*-Butyllithium
KO^tBu	Potassium *tert*-butoxide
$NaBH_3CN$	Sodium cyanoborohydride
HCl	Hydrochloric acid
MBA	Methylbenzylamine
ω-TA	Omega-transaminase
HEPES	4-(2-Hydroxyethyl)piperazine-1-ethanesulfonic acid
GDH	Glucose dehydrogenase

SPPS	Solid-phase peptide synthesis
DIPEA	*N,N*-Diisopropylethylamine
HBTU	(2-(1H-benzotriazol-1-yl)-1,1,3,3-tetramethyluronium hexafluorophosphate
HOBt	Hydroxybenzotriazole
Fmoc	Fluorenylmethyloxycarbonyl
Boc-phenylalanine	*N*-(*tert*-Butoxycarbonyl)-L-phenylalanine
Gly	Glycine
Phe	Phenylalanine
Hyp	Hydroxyproline
Arg	Arginine
Asp	Aspartic acid
Pal	Palmitic acid
Ada	Adamantane
m/z	Mass to charge ratio

Table of contents

Abstract i

Acknowledgement ii

List of abbreviations iv

CHAPTER 1: **INTRODUCTION** 1

1.1. Collagen mimetic peptides for wound healing 1

1.1.1. Chronic wounds challenges 2

1.1.2. Wound healing phases 2

1.1.3. Importance of peptides as components of wound dressings 3

1.1.4. Importance of Integrins and collagen sequences 6

1.1.5. Sequence of interest 7

1.2. Beta-amino acids 7

1.2.1. The importance of beta-amino acids in pharmaceuticals 9

1.2.2. Methods for the production of beta-amino acids 10

1.3. Transaminases 13

1.3.1. Reaction mechanism for omega-transaminases 14

1.3.2. Biotransformation methods 15

1.3.3. Equilibrium problem for omega-transaminases 17

1.3.4. Overcoming thermodynamic equilibrium difficulties 18

1.3.5. Conversion of various substrates using omega-TA 19

1.4. Nitrile hydrolyzing enzymes 20

1.4.1 Nitrilases 20

1.4.2 Nitrile hydratases 21

1.4.3 Amidases 22

1.5 Proposed reaction sequence ……..23

1.6. Overall project aim …… 24

1.6.1 Aims and objectives ……24

1.6.2 Hypothesis and questions ……25

2. Experimental procedure ……26

2.1 Chemicals and reagents ……26

2.2 Instrumentation ……26

2.3 Initial test for biocatalysis using transaminases ……..27

2.3.1 Analytical scale deamination of amine substrates using pyruvate amine acceptor ……27

2.3.2 Analytical scale reductive amination of ketone substrates using diamine donor ……28

2.3.3 Analytical scale reductive amination of ketone substrates using LDH/GDH pyruvate removal system ……...28

2.4 Initial test for the hydrolysis of beta-ketonitriles into beta-ketoamides ……28

2.5 General synthetic procedures ……28

2.5.1 Attempted preparation of β-ketonitriles 49 exemplified by compound 49a (Method 1) ……28

2.5.2 Procedure for the synthesis of esters (48a-d) from carboxylic acids (46a-d) (Method 2) ……29

2.5.2.1 Synthesis of ethyl 2-phenylacetate **48a** ……30

2.5.2.2 Synthesis of ethyl 2-(*p*-fluorophenyl)acetate **48b** ……30

2.5.2.3 Synthesis of ethyl 2-(*p*-tolyl)acetate **48c** ……31

2.5.2.4 Synthesis of ethyl 2-(*p*-methoxyphenyl)acetate **48d** ……31

2.5.3 Procedure for the synthesis of β-ketonitriles (**49a-d**) from esters (**48a-d**) ...32

2.5.3.1 Synthesis of 3-oxo-4-phenylbutanenitrile **49a** ……...32

2.5.3.2 Synthesis of 4-(4-fluorophenyl)-3-oxobutanenitrile **49b** ……....32

2.5.3.3 Synthesis of 3-oxo-4-(*p*-tolyl)butanenitrile **49c** ……33

2.5.3.4 Synthesis of 4-(*p*-methoxyphenyl)-3-oxobutanenitrile **49d** ……33

2.6 Conventional synthesis of β-aminonitrile standard product ……..34

2.6.1 Synthesis of *tert*-butyl (1-hydroxy-3-phenylpropan-2-yl)carbamate **52i** ..…34

2.6.2 Attempted approach towards synthesis of 3-amino-3-(*p*-tolyl)acrylonitrile **55** ……...36

2.6.3 Synthesis of 3-amino-3-(*p*-tolyl)acrylonitrile **55** ……36

2.7 General Synthetic procedure using transaminases ……37

2.7.1 Preparative scale biotransformation of methylbenzylamine using pyruvate amine acceptor ……37

2.7.2 Reductive amination of ketone substrates using LDH/GDH pyruvate removal system ……..37

2.7.2.1 Asymmetric synthesis of methylbenzylamine **57** using LDH/GDH mixture ..……...37

2.7.3 Preparative scale reductive amination of ketone substrates using diamine donor or amine donor ……38

2.7.3.1 Asymmetric synthesis of methylbenzylamine **58** using L-alanine as amine donor ……38

2.7.3.2 Asymmetric synthesis of methylbenzylamine 58 using Isopropylamine as amine donor ……39

2.7.3.3 Asymmetric synthesis of methylbenzylamine 57 using diamine donor ……39

2.7.3.4 Asymmetric synthesis of 3-amino-3-(p-tolyl)propanenitrile 56c using diamine donor ……..39

2.8 Procedure for hydrolysis of nitrile substrates using nitrile hydratase ……...40

2.8.1 Synthesis of 3-amino-3-(*p*-tolyl)propanamide **65** ……40

2.8.2 Synthesis of 3-oxo-3-(*p*-tolyl)propanamide **66c** ……...40

2.8.3 Synthesis of 3-(*p*-methoxyphenyl)-3-oxopropanamide **66d** ……...41

2.9 Synthetic procedure for wound healing peptides ……41

2.9.1 α-peptides **60…**……42

2.9.2 *β*-peptides **61……..**……43

2.10 Synthesis of 2-((((9H-fluoren-9-yl)methoxy)carbonyl)(methyl)amino)-3-phenylpropanoic acid (Fmoc-N-α-MePhe-OH) **62** ……45

3. Results and discussion ……..47

3.1 Approach towards synthesis of β-aminonitriles ……...47

3.1.1 Attempted synthesis of β-ketonitriles via acyl chloride (Method 1) ...48

3.1.2 Synthesis of β-ketonitriles via esters (Method 2) ……50

3.1.2.1 Synthesis of esters from carboxylic acids ……..50

3.1.2.2 Synthesis of *beta*-ketonitriles from esters ……..54

3.2 Synthesis of racemic *beta*-aminonitrile standards ……..58

3.2.1 First attempted approach towards *beta*-aminonitrile standards **50a** ……...58

3.2.1.1 Synthesis of *tert*-butyl (1-hydroxy-3-phenylpropan-2-yl)carbamate **52i** ……59

3.2.2 Second approach towards beta-aminonitrile standards **56c** ……..61

3.2.2.1 Attempted synthesis of 3-amino-3-(*p*-tolyl)acrylonitrile **55** ..62

3.2.2.2 Synthesis of 3-amino-3-(*p*-tolyl)acrylonitrile **55** ……64

3.2.3 Synthesis of 3-amino-3-(p-tolyl)propanenitrile **56c** ……..65

3.3 Transaminase activities ……...66

3.3.1 LC-MS analysis of the standards **57** and **58** ……68

3.3.1.1 Screening of the transaminase using **57** ..……68

3.3.1.2 Screening of the transaminase using **58** ……70

3.3.2 Substrate and product inhibition ……73

3.3.2.1 Determining product inhibition by amine product **57** ……73

3.3.2.2 Investigating substrate inhibition by **58** ……74

3.3.3 Displacing the unfavourable equilibrium ……..75

3.3.3.1 Employing LDH pyruvate removal system ……75

3.3.3.2 Employing isopropyl as amine donor ……76

3.3.3.2 Employing xylylenediamine dihydrochloride diamine donor ……78

3.4 Asymmetric synthesis of *beta*-aminonitriles ……81

3.5 Reaction controls using **54c** and **56c** ……85

3.6 Hydrolysis of nitrile substrates using nitrile hydratase ……87

3.6.1. Hydrolysis of β-aminonitrile ……87

3.6.2 Hydrolysis of β-ketonitriles ……..88

3.7 Approach towards synthesis of wound healing peptides ……..90

3.7.1 Synthesis of *alpha*-peptides ……90

3.7.2 Synthesis of *beta*-peptides ……..97

3.7.3 N-methylation of α-phenylalanine ……100

4. Conclusion and future work ……103

4.1 Conclusion ……..103

4.2 Future work ……104

References ……..106

Appendix ……..114

1. INTRODUCTION

The human body relies on the biological functions of proteins such as structural proteins, hormones, enzymes, receptors, and antibodies.[1] Proteins are a chain of peptides formed by a linkage of amino acids through the peptide bond.[1] Peptides play an important role as cytokines, growth factors, enzyme inhibitors, hormones, neurotransmitters, neuromodulators, and in various other biological functions such as wound healing.[2] However, when an individual suffers from diseases such as diabetes these natural peptides may take a longer time to regenerate to aid wound healing. Therefore there is a need for supporting synthetic peptides that would mimic natural wound healing peptides. Hence it is crucial for us to be able to synthesise peptides that mimic the functions or structural properties of the peptides or proteins.[1] These are considered as peptidomimetics or protein mimics.[1]

Amino acids are important components of peptidomimetics. The peptide linkages in synthetic and natural biopolymers adopt ordered conformations which are crucial to their functions in biological systems.[3] Therefore, there is an increasing interest in researching synthetic peptides which mimic the functions of the backbones of these natural biopolymers.[3b] The peptidomimetics can also be synthesised in the laboratory with various modifications to avoid hydrolysis by proteases, thereby extending their active duration. The β-amino acids **1** (**Figure 1**) when linked together form stable β-peptides. These β-peptides have received a great deal of attention due to the additional carbon atom at position 3 in the β-amino acids (**Figure 1**), which renders β-amino acids more flexible[3a] than the corresponding α-amino acids **2** (**Figure 1**).[4,5] The aim of this study is to design and synthesise novel wound healing peptides and the β-amino acid components of these peptides.

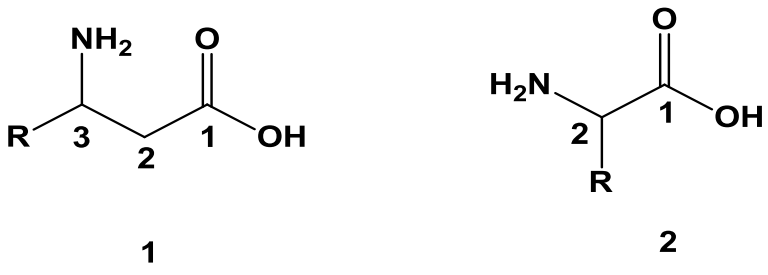


Figure 1. Illustration of β-amino acid (**1**) and α-amino acid (**2**)

1.1. Collagen mimetic peptides for wound healing

1.1.1. Chronic wounds challenges

The skin has the essential role of protecting our bodies from different infections.[4,6] Damage to the skin's integrity leads to infections.[6] Chronic wounds mainly affect the adult population who suffer from diabetes and obesity[6,7] and are an emerging therapeutic and economic issues in health care.[8,9] Chronic wounds are described as the wounds that take an inappropriate length of time to heal and as a result of damage to the skin's integrity are often associated with systemic diseases.[8,9] The management of chronic wounds is very challenging and difficult, which poses an economic and health burden, which results in emotional stress as most of the people can't access medical care due to the very high cost of hospitalization.[8,10]

1.1.2. Wound healing phases

Following harm to the skin's integrity, the tissue recovery for fixing the injury begins.[11] Wound mending includes a progression of steps in particular; hemostasis, inflammation, cellular migration and proliferation, wound contraction and remodeling as show in **Figure 2**.[9]

This process is defined as three major phases: Inflammation, Proliferation and Remodeling.[6,11] The process of wound healing is very complex as it includes dissolvable mediators, *extracellular matrix* (ECM) development, and cell migration.[6] The *Inflammation* stage is the underlying advance following the damage and it is intervened by physiological factors, such as cytokines, chemokines and fibronectin.[9,11] The proinflammatory cells are required for eliminating microorganisms and expulsion of debris in the wound, and are also in charge of the penetration of neutrophils and macrophages.[9,11] Macrophages animate the angiogenesis, fibroplasia and the creation of ECM, thereby initiate proliferation phase.[8] The *Proliferation* stage includes angiogenesis, fibroplasia, and re-epithelialization, where angiogenesis and fibroplasia happens in the meantime to generate ECM and granulation tissue.[9,11] The *Remodeling* stage, is the last stage where the ECM redesigns the collagens into collagenous structure, fibroblast into myofibroblast and wound contraction, which is the place the injury development happens with arrangement of scar tissue because of the decline in cellularity.[12]

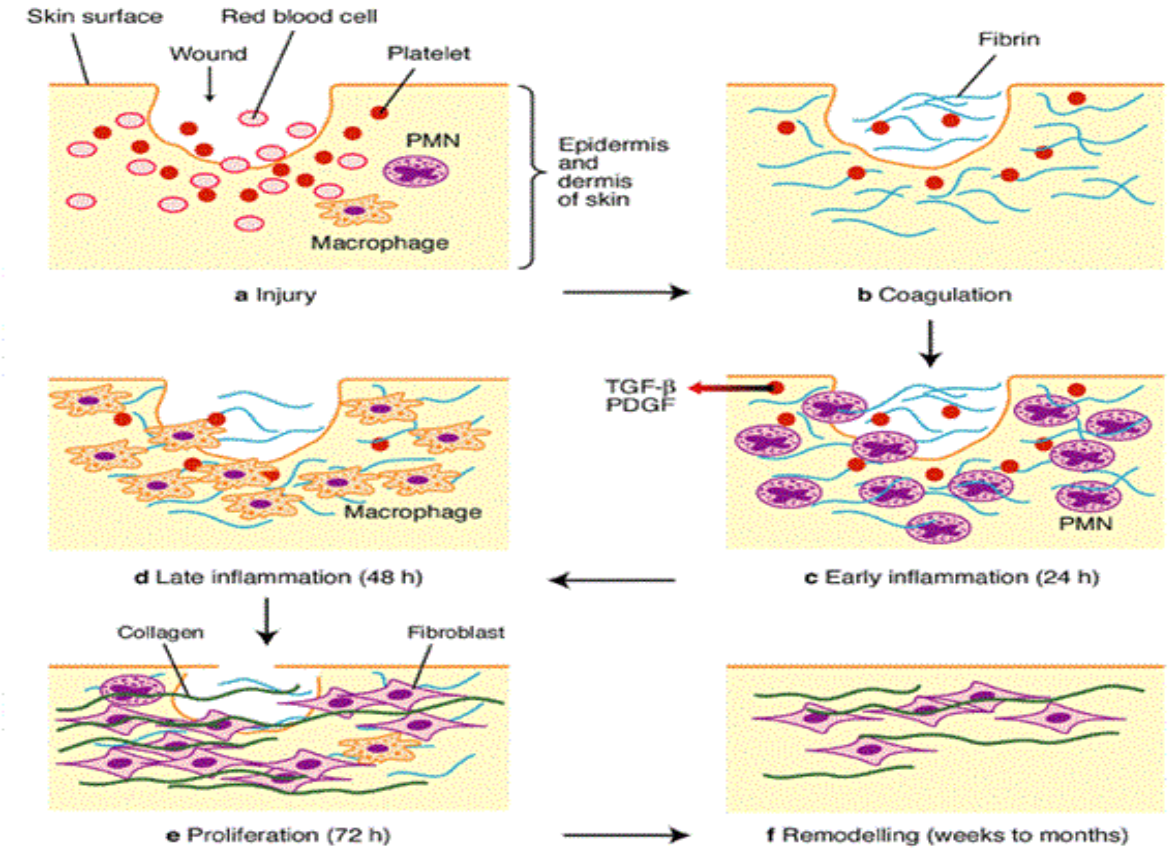


Figure 2. Wound healing phases (https://www.pilonidal.org/surgery-aftercare/wound-healing-in-depth/).

1.1.3. Importance of peptides as components of wound dressings

Currently, there is ongoing research into the properties of biological agents that mimic the structural properties and functions of the ECM that can be incorporated into physical (dressings) or chemicals pharmaceuticals for wound care treatments.[13] In spite of the fact that there are some unmistakable advantages seen in clinical examinations, there is a need for further research in this area. The most common type of wound mending support is wound dressings which are made utilizing polymers, for example, chitosan, hyaluronic acid,[14] polyurethane,[15] silk fibroin, hydrocolloids, silicon and collagen.[6,16,17] However, this work will concentrate on the examination of the collagen mimetic peptides (CMP's). Collagens are the most abundant proteins in the ECM and are characterised by a triple helical structure (**Figure 3**).[18,19]

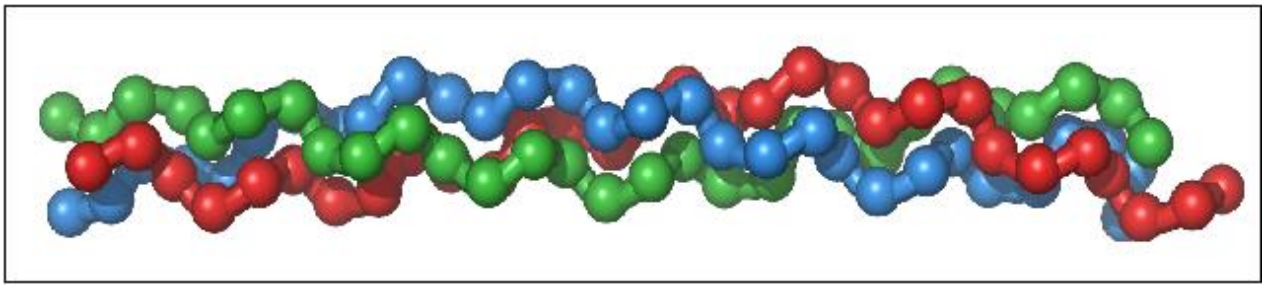


Figure 3. A diagram of collagen peptides triple helix in complex (http://www.ebi.ac.uk/interpro/potm/2009_1/Protein_focus_2009_01-Collagen.html).

They have fundamental functions in the human body including tissue framework, cell grip, cancer, cell relocation, angiogenesis, tissue morphogenesis and tissue repair.[20] The triple helix comprises of three individual polypeptide chains (green, red and blue in **Figure 3**) with repeating glycine-X–Y units, where X and Y are occupied by proline (P) and hydroxyproline (O).[14,16] The cross-linking between these three alpha chains is facilitated by hydrogen bonding, shown as dotted lines (**Figure 4**).[19,20]

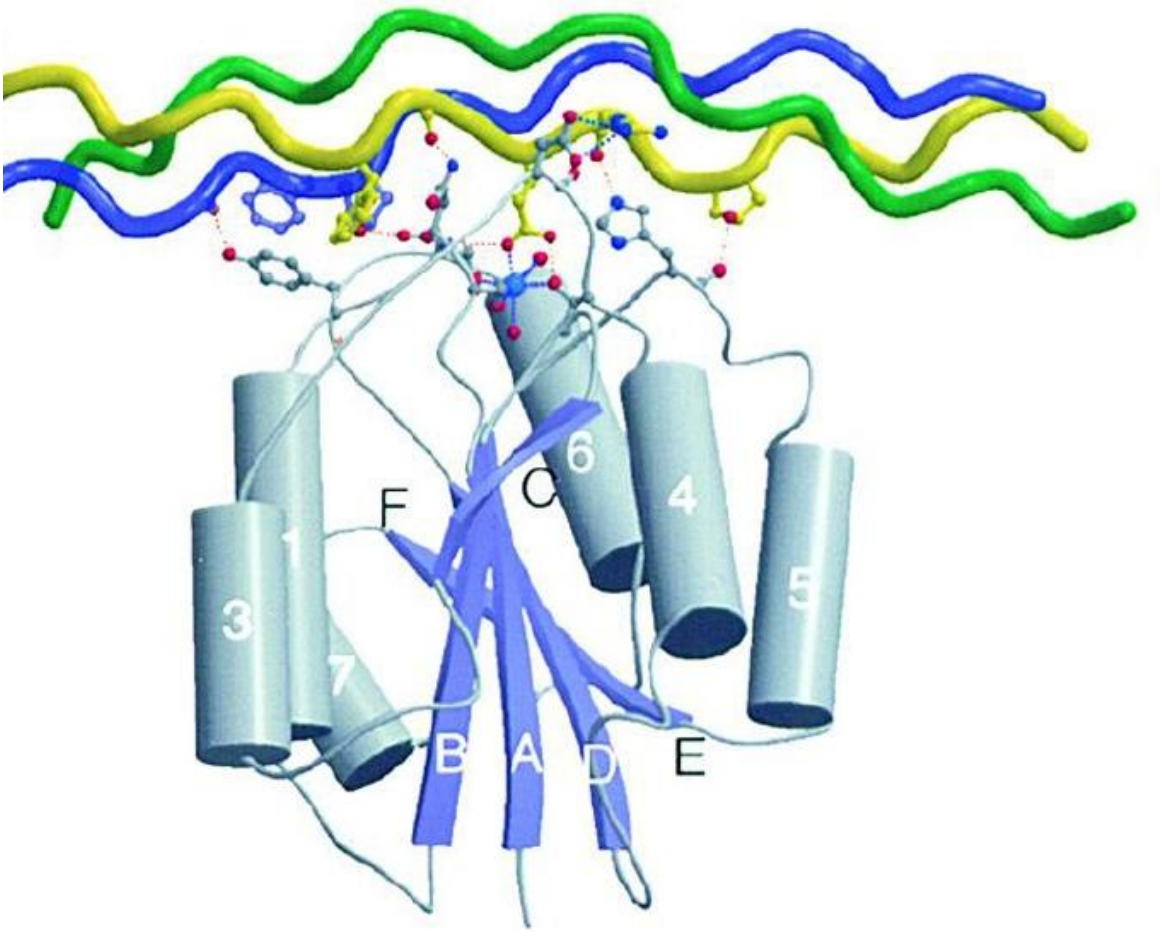


Figure 4. A schematic of the detailed collagen-integrin interface, reproduced from Ref 19.[19]

Collagen turnover is a basic process for ECM *remodeling*, which requires the matrix-metalloproteinases (MMP's). The MMPs make the collagens accessible for the cell receptors (integrins).[21] Integrins are transmembrane receptors intervening the migration, attachment to the ECM,[20] and differentiation during the healing process.

Integrins are made out of heterodimeric *alpha* and *beta* subunits.[22,23] These subunits comprise of an extensive extracellular space (N-terminus), a short cytoplasmic area (C-terminus) and a transmembrane space, and furthermore contains the metal binding site that is depicted as the *metal ion-dependent adhesion site* (MIDAS); represented as a blue sphere in **Figure 5**.[23,24]

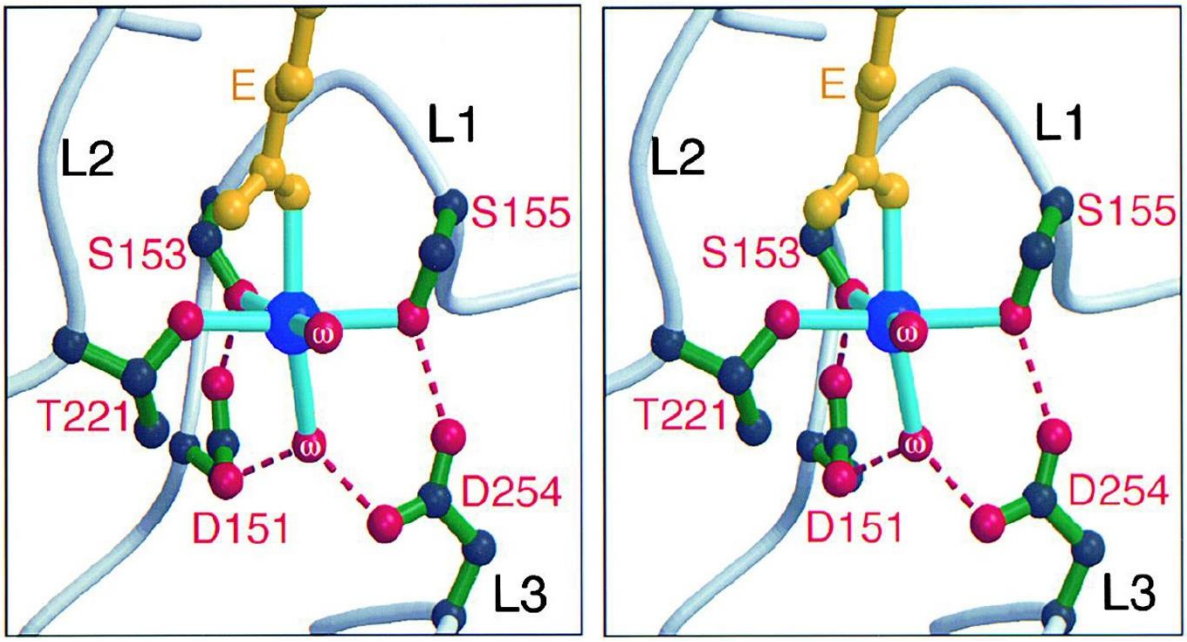


Figure 5. A stereo molecular diagram representing MIDAS. Reproduced from Ref 19.[19]

The MIDAS is vital for the communication between the collagens and integrins in the ECM interceded by the I-domains, which are in charge of the ligand recognition. The binding of I-domains to the collagens relies on a divalent cation magnesium (Mg^{2+}) which is coordinated an octahedral geometry that includes the glutamate side chain (E – in yellow) in the center strand of the triple helical peptide.[21,25,26]

1.1.4. Importance of Integrins and collagen sequences

The αI domain is part of the I-domain and it is the central collagen binding site in the integrins.[22] The main integrin receptors for collagens are the $\alpha_1\beta_1$ and $\alpha_2\beta_1$ integrins, both of which recognise collagen type I containing the peptide sequence Gly-Phe-Hyp-Gly-Glu-Arg (**G-F-O-G-E-R**) which is a high affinity binding site (**Figure 6**).[19,26]The collagen-binding to the integrins includes coordination of a collagen carboxyl group (glutamate, **E**) with the divalent cation at the highest point of the I-domain.[23] The glycine(**G**) is imperative for the collapsing of the triple helix and does not interface with the I-domain.[19,20] Hydroxyproline (**O**) is in charge of hydrogen bonding to N154 and the stereoelectronic impact when binding with the integrin. The hydrophobic interface is made by phenylalanine (**F**) interacting with N154.[19,20] The existence of a hydrophobic effect impacts the development of fibres and aggregation platelets.[20] The arginine (**R**) makes a salt bridge with the negatively charged part of the integrin.[20]

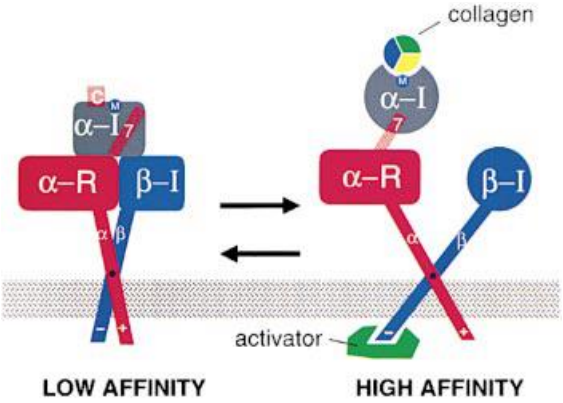


Figure 6. Diagram depicting the integrin binding site.[19]

1.1.5. Sequence of interest

The arginine-glycine-aspartic acid (RGD) has been reported as the principal sequence with strong affinity for the integrin in the ECM.[27] Thus designing peptides with this sequence will improve cell adhesion of the peptidomimetic. The sequence GFO is responsible for the hydrophobic interaction of the peptide when binding to the integrin[27], therefore the conjugation of this sequence with the RGD sequence will result in a peptidomimetic of the sequence GFOGRGD. The Phenylalanine (F) will be replaced by the enantiopure *beta*-amino acids to enhance the selectivity of the β-peptides. The incorporation of these *beta*-amino acids will improve the peptides' resistance to peptidases, physicochemical properties and conformational secondary structures due to the extra methylene carbon as compared to *alpha*-amino acids.[28,29] The different substituents on the aromatic ring of the β-amino acid will also improves the binding of these peptides to the integrins. These peptides will be further modified by the attachment of methyl, palmitic acid or adamantane at the *N*-terminal. These modifications will enhance the peptide's affinity for the membrane, which subsequently improves the permeability of the CPM's amid the application on the injury dressing,[30] and are less easily degraded than typical peptides since they improve the conformational rigidity nature of the peptide.[31] Such modifications will potentially provide an improved wound healing peptide.

1.2. *Beta*-amino acids

In the 1960's, β-amino acids were discovered in nature in the form of poly-β-aspartic acid, poly-β-alanine and the β-lactam rings of penicillin.[32] These poly-β-amino acids show ordered secondary conformational structures such as helices,[33,34,35] turns[36,37] and β-sheets[33c,38,39] as observed in the natural peptides (poly-αββ-amino acids) and proteins.[3a,5] The secondary structures are due to the intramolecular forces (hydrogen bonding) between the amide proton (NH) and the carbonyl oxygen of the *C*-terminus as well as the torsion angles (**Figure 7**).[36,40]

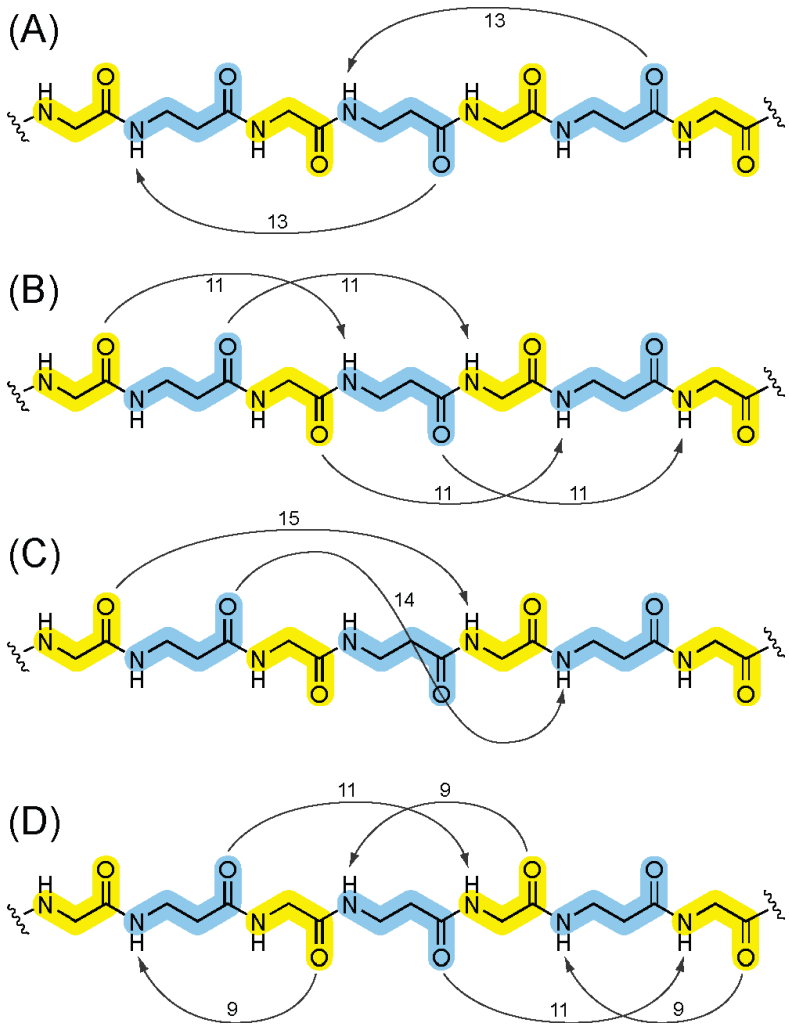


Figure 7. Intramolecular hydrogen bonding possibilities in helices of *alpha* and *beta*-amino acid containing peptides. The alpha amino acid residues are highlighted yellow while the *beta*-amino acid residues are highlighted blue. The hydrogen bonding is indicated by the arrows in different helices from A to D.[36] Reproduced from reference 36.[36]

The α-amino acids have been utilised for the synthesis of chiral biologically active compounds and are the building blocks of natural peptides, enzymes and proteins.[41,42] However, short-chain α-peptides containing α-amino acids do not fold into secondary conformations because their backbone have three torsion angles compared to the β-peptides which have more torsion variables (**Figure 8**).[3a]

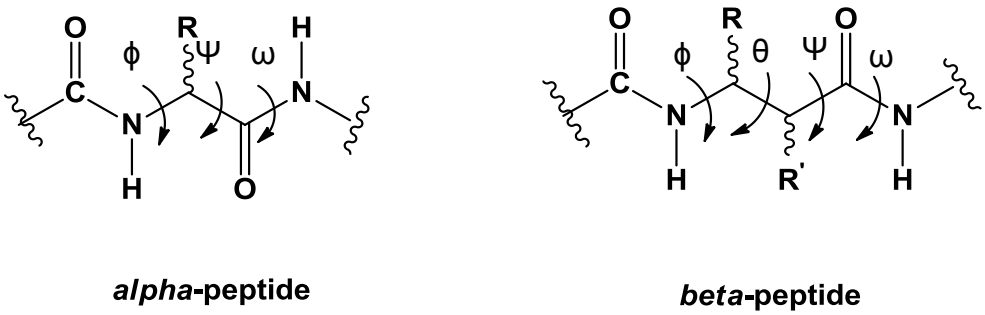


Figure 8. A diagram depicting torsion angles for *alpha* and *beta*-peptide.[3a]

In the case of β-peptides, short-chains of β-amino acids fold into secondary conformations resulting in resistance to cleavage by peptidases. The susceotibility of α-peptides to enzyme degradation led to the investigation of homologues of α-amino acids, such as β-amino acids.[43] Hence the asymmetric synthesis of β-amino acids and their incorporation into peptides.[41]

In contrast with the poly-α-peptides, poly-β-peptides have demonstrated stable conformations in aqueous media and fold into the required secondary structures that display resistance to degradation by proteases.[44,45] The additional carbon atom in the β-amino acids builds the open door for R,R'-substitutions by various functional groups and expands the amide linkage space which improves solubility, brings down the melting point and increases stability to heat when compared to α-amino acids (**Figure 8**).[3a,4]

1.2.1. The importance of *beta*-amino acids in pharmaceuticals

β-Amino acids are important for the biological activity of the drugs such as the antitumour drug Taxol,[46,47] the antidiabetic drug Sitagliptin (**Figure 9**, with the β-moiety circled by a dotted line),[47,48] the antifungal antibiotic Cispentacin[49] and protease inhibitors against HIV.[50]

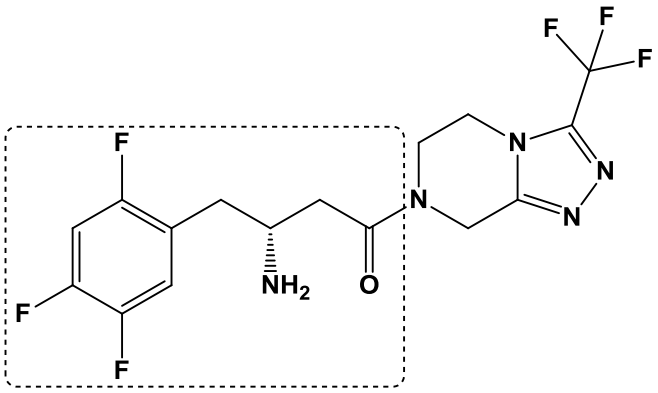


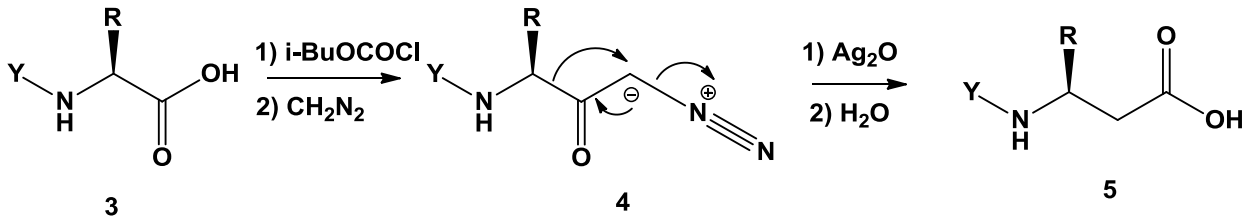
Figure 9. Structural representation of Sitagliptin.

This makes them good building blocks[51] for the synthesis of various pharmaceutical[52,53,54] and agrochemical ingredients.[55,56] The pharmaceutical industry has an expanding interest in the asymmetric synthesis of β-amino acids as they have novel pharmacological properties and β-peptides show selectivity for bacterial cells with low hemolytic activity for mammalian red blood cells.[40,41,43]

About 80% of pharmaceutical items are optically active.[57] Enantiomerically pure chiral β-amino acids,[58] alcohols and amines are utilised progressively for the improvement of the physiological impacts of pharmaceutical and agrochemical compounds.[59,60] Enantiopurity of β-amino acids is required to decrease the dose of the medication and for the improvement of the drug's efficacy.[57,60]

1.2.2. Methods for the production of *beta*-amino acids

So far we have discussed the importance of β-amino acids in pharmaceuticals, but how are they made? The methods for readily and efficiently producing enantiopure β-amino acids are still under investigation.[48] There are two general synthetic methods available for the production of optically active β-amino acids: *chemical and biocatalytic* methods. There are several chemical methods available, including, for example, Wolff rearrangement (**Scheme 1**)[61], addition of enantiopure amines to Michael adduct (**Scheme 2**)[41] and the Curtius rearrangement (**Scheme 3**).[62]



Scheme 1. Synthesis of β-amino acids from α-amino acids via Wolff rearrangement.[61]

The most import step in the reaction scheme above is the Wolff rearrangement of compound **4** in the presence of silver oxide.[61] The elimination of N_2 generates the intermediate ketene (**Figure 10**) which, on addition of water, is converted into the corresponding β-amino acid **5** (**Scheme 1**).[61]

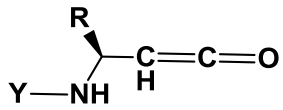
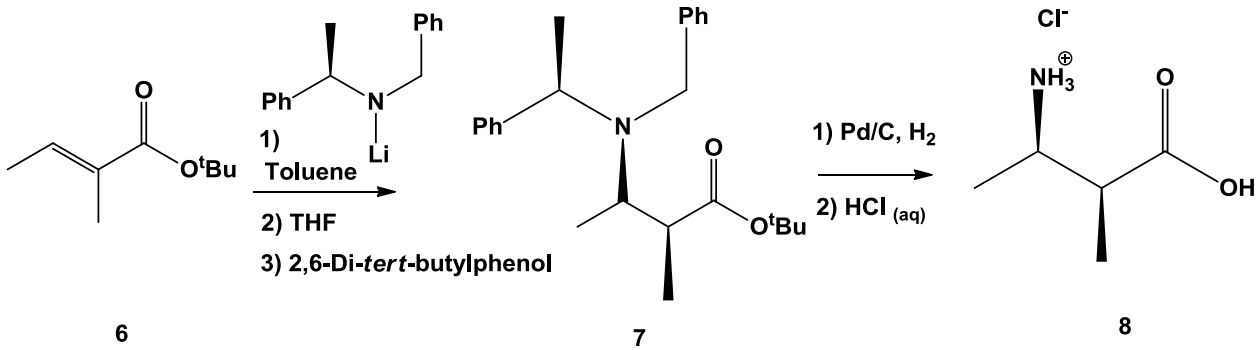


Figure 10. Ketene intermediate resultant from Wolff rearrangement

However this method gives moderate yields, uses poisonous and expensive reagents, and reaction conditions are explosive.[63]

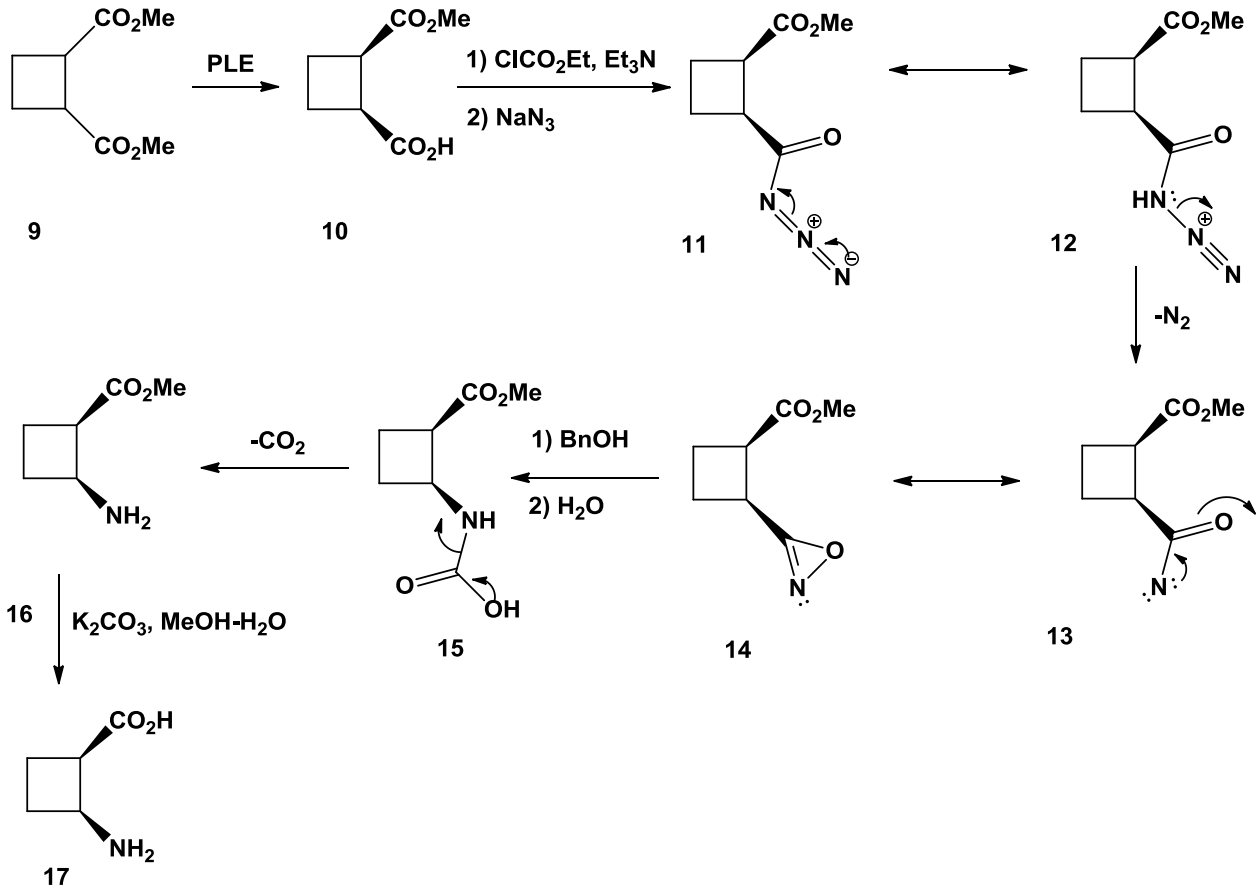
The second method which involves the Michael adduct is shown in **Scheme 2**.



Scheme 2. Michael addition of the enantiopure amine.[41]

The enantiopure amine added in step one acts as a nucleophile when reacting with the *tert*-butyl acrylate **6** in toluene followed by the addition of THF to dilute the reaction mixture. Upon completion, 2,6 di-*tert*-butylphenol, a hindered acid is added to quench the reaction.[41] Upon reduction of the amine with carbon supported palladium and ester hydrolysis with aqueous hydrochloric acid, β-amino acid **8** is obtained. The drawback of this method is that the yields are very low.

The pig liver esterase (PLE) was used to first catalyse the desymmetrisation of **9** to **10** (**Scheme 3**).[62]



Scheme 3. A stepwise Curtius rearrangement of di-esters **9**.[64,65,66]

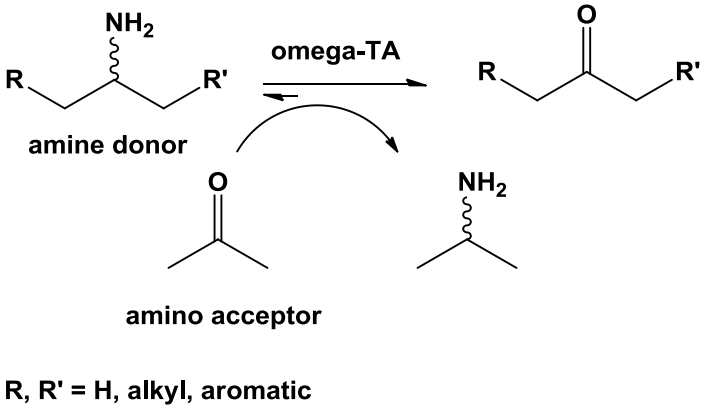
The acyl azide **11** was prepared by treating **10** with ethyl chloroformate/ triethylamine followed by sodium azide.[64] The Curtius rearrangement of acyl azide **11** generates the acyl nitrene **13**, followed by the formation of aziridene **14**.[65] The ring opening of aziridene **14** was performed under heat in the presence of benzyl alcohol, followed by hydrolysis resulting into carbamic acid **15**.[64,66] The decarboxylation of carbamic acid generates amino ester **16**.[66] The resulting amino ester **16** was hydrolysed by potassium carbonate

in the presence of methanol/water to generate the β-amino acid **17**.[62,64] However there is still no efficient chemical method for the production of optically pure amino acids due to the use of expensive metal catalysts, additional purification steps and generation of by-products which reduces the percentage yield.[57,59b]

Increasing understanding of biological systems that use chirally selective catalytic enzymes for many biological reactions has led to the increase in research focusing on biocatalysis to synthesise bioactive compounds in the pharmaceutical industries.[60] The use of biocatalytic methods is advantageous due to their regioselectivity,[67] chemoselectivity[68,69] and stereoselectivity[70,71] properties in the biotransformation of substrates into optically active products.[68,72] This strategy has several advantages over chemical synthetic routes because reactions are carried out under ambient conditions, consequently preventing the use of harsh conditions which cause problems with isomerization and racemization.[69] Immobilization of the enzyme can be done for reuse, thus reducing the creation of waste and cost.[68,69] Most of the reactions are carried out in aqueous medium which diminishes the utilization of organic solvent, hence promoting environmental friendliness and safety.[68,73] These properties make biocatalysis one of the greener synthetic routes for enantiopure bioactive intermediates.[70]

1.3. Transaminases

Transaminases[74,75] catalyze the reversible deamination[76] of the amino group from the donor to the amino acceptor using a cofactor pyridoxal 5'-phosphate (PLP) as an electron shuttle (**Scheme 4**).[77,78]



Scheme 4. Deamination of amino group involving transaminases.[78]

Transaminases can be classified as *alpha*-transaminase (α-TA) or *omega*-transaminase (ω-TA) based on the position of the amino group to be deaminated relative to the carboxyl group in the starting material.[78] The α-TA accepts only α-keto acids and α-

amino acids as the substrates.[78,79] In contrast to α-TAs, ω-TAs exhibit enantioselectivity for a wide range of substrates that have more than one methyl group between the carboxyl group and the substituents including aryl-substituents.[80,81]

There are two types of ω-TA's: *R*-selective ω-Transaminases (*R*-ω-TA) [82] and *S*-selective Transaminases (*S*-ω-TA). The *R*-ω-TA's belong to fold class type IV whereas the *S* -ω-TA's belong to fold class type I.[82] A larger number of *S*-ω-TA's are found in many different micro-organisms: *Alcaligenes denitrificans Y2k-2, Arthrobacter citreus, Bacillus megaterium SC6394, Bacillus thuringiensis JS64, Chromobacterium violaceum, Klebsiella pneumoniae JS2F, Mesorhizobium and Vibrio fluvialis JS17.*[83] Only a few R-ω-TA's have been discovered: in *Aspergillus fumigatus,*[82] *Nectria,*[84] *Arthobacter sp. KNK168*[83] *and ATA117.*[83]

These two types of ω-TA's both consist of two binding active site pockets between the homodimers: large and small pockets as illustrated in **Figure 11**.[82,85,86]

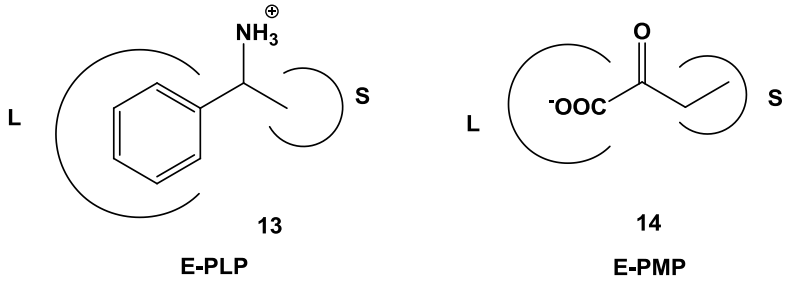


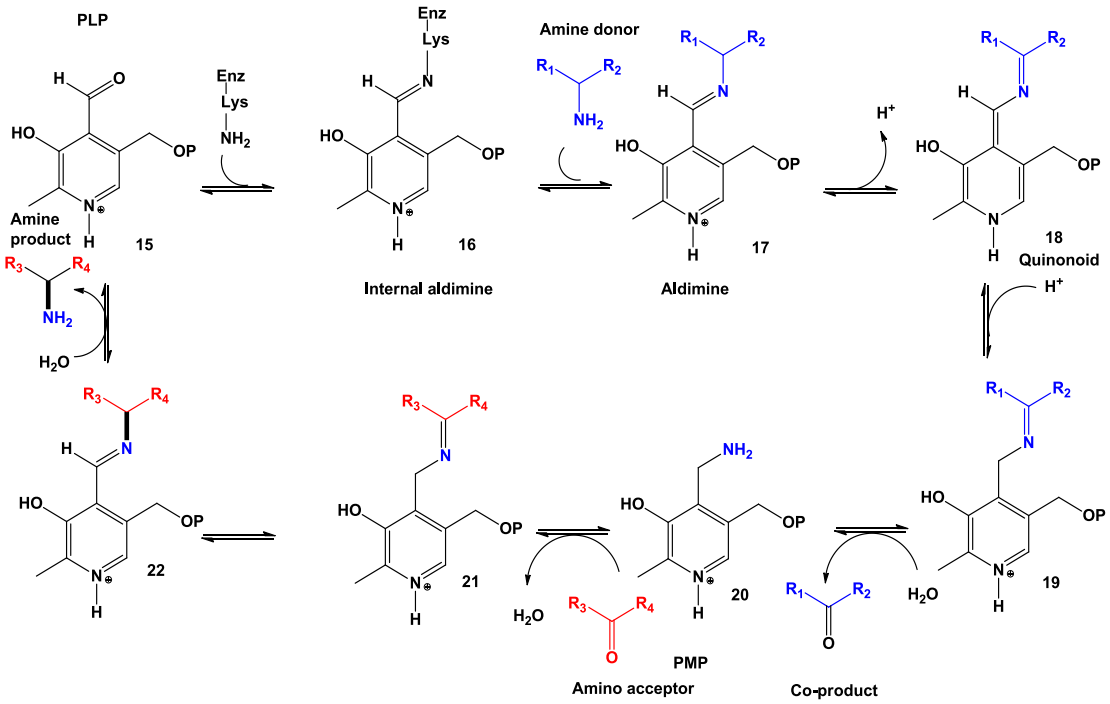
Figure 11. ω-Transaminase substrate binding depicting the large (L) and small (S) pockets of the PLP form of the enzyme occupied by methylbenzylamine (**13**) and 2-oxobutyrate (**14**).[87]

The large pocket shows acceptance of both hydrophobic and carboxylate groups, while the small pocket shows recognition for groups not larger than ethyl and resistance to carboxylate groups due to strong repulsion.[88] The newly discovered ω-TA's that overcome the above problem are found in *Paracoccus denitrificans* (PDTA) and *Arthrobacter sp*, which are a *S*-ω-TA and a *R*-ω-TA respectively.[88]

1.3.1. Reaction mechanism for omega-transaminases

The cofactor PLP **15** is covalently bound to the lysine in the active site of the enzyme through a Schiff base to form an internal aldimine **16** and lies at the bottom of the active site between the small and large pockets (**Scheme 5**).[74,84,89] There are two half-reactions in the proposed mechanism of TA's .[84] In the first half-reaction the cofactor forms the Schiff base with the amino donor to produce the aldimine **17** and after proton abstraction it forms the quinonoid intermediate **18**.[74,84] The rearrangement of the proton and hydrolysis reaction leads to the formation of PMP **20**.[74,84] In the second half-reaction the

2-oxobutyrate on the pyridoxamine 5'-phosphate active site (PMP) transfers the amino group to the amino acceptor (ketone) yielding PLP **15** and the amine product as a single enantiomer (**Scheme 5**).[84]



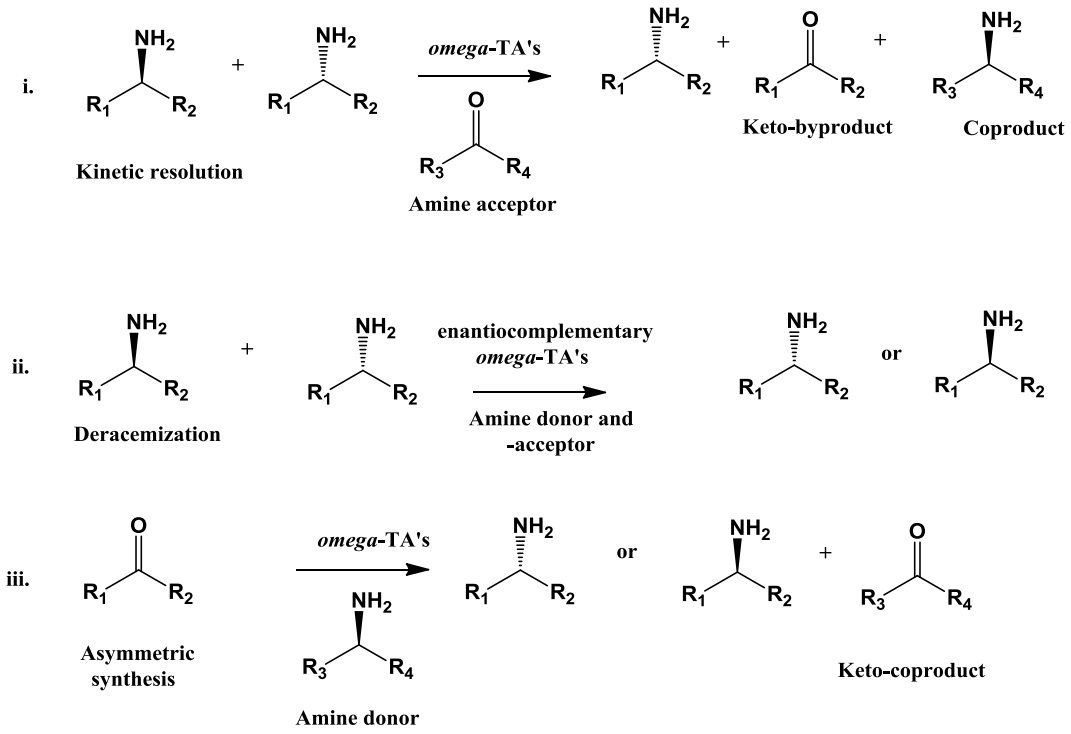
Scheme 5. The schematic representation of transaminases mechanism involving the PLP cofactor.[84]

The quinonoid **18** plays an important role in determining the stereoselectivity of the enzyme where-in if the *Si*-side of the quinonoid intermediate is exposed to solvent, it is an *R*-selective-TA and if the *Re*-side is exposed to the solvent, it is an *S*-selective-TA.[82,83,84]

1.3.2. Biotransformation methods

The biotransformation of relevant substrates into chiral amines and amino acids has been carried out using lipases, hydantoinases and acylases.[52] These are the hydrolytic enzymes used originally, however there are now more recently discovered enzymes for the production of chiral amines and amino acids including omega-transaminases[52,47,77], nitrile hydratase,[90,91] amidases[90,91] and nitrilases.[91] Omega-transaminases (ω-TA) have received increasing interest as biocatalysts for the reductive amination of prochiral ketones or aldehydes and oxidative deamination of primary amines.[83,76] Transaminases are a new class of biocatalyst that are not well established as compared to other enzymes e.g. lipases.[68] Therefore, screening studies need to be conducted to explore transaminase enzymes as they have attracted great attention for the production of β-

amino acids. Naturally occurring ω-TAs are used in the three different biotransformation methods described in **Scheme 6**.[92,88]



Scheme 6. Different methods for the biotransformation of substrates into pure enantiomers.[74]

There are two major methodologies for chiral biotransformation: asymmetric[93] synthesis (iii) and kinetic resolution of enantiomers (i).[94] The kinetic resolution relies on the stereoselective *transformation* of the one enantiomer using a chiral enzyme catalyst, while asymmetric synthesis is based on the stereogenic *formation* of one enantiomer from given substrates and theoretically gives a 100% yield.[94] The main disadvantage of kinetic resolution is that it only converts one enantiomer to the desired chiral product, thus has a maximum yield of 50%. This disadvantage led to the development of *deracemization*, a new method which improves the theoretical yield to 100% (**Scheme 6, ii**).[95,96,90]

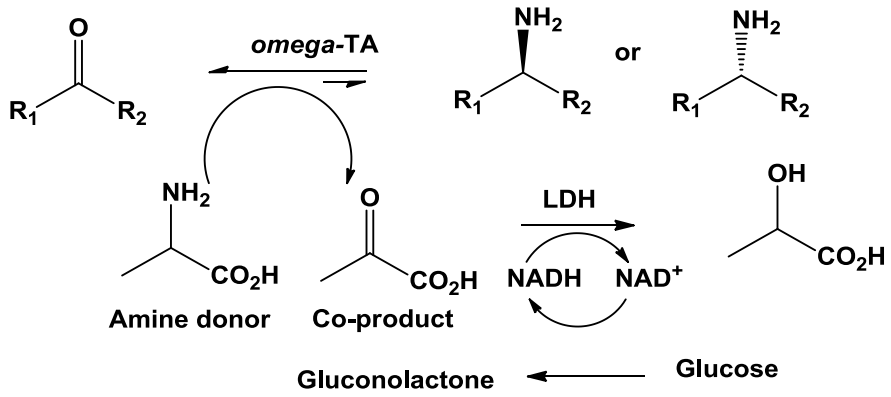
The deracemization reaction is carried out by using *two* enantiocomplementary omega-transaminases, a complex method that requires two steps in a one-pot process redox reaction (**Scheme 6**).[74] In the first step, the omega-transaminases displaying stereopreference and an amine acceptor (ketone) are used to kinetically resolve the racemic mixtures into chiral amine and intermediate ketone; in the second step, an omega-transaminase displaying opposite stereopreference to the first omega-

transaminase is used to convert the intermediate ketone into chiral amine in the presence of an amine donor.[74]

Therefore, asymmetric synthesis would be the preferred method to carry out this research as theoretically it has 100% yield, one step reaction process and fewer limitations as compared to other methods.

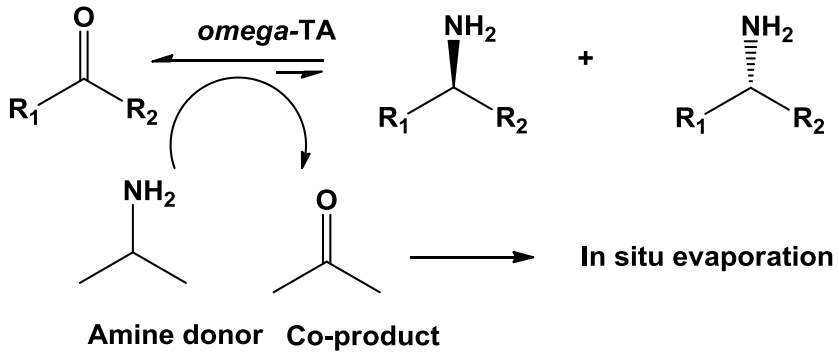
1.3.3. Equilibrium problem for omega-transaminases

The stereochemistry of the amine product can either be *R* or *S* depending on the type of ω-TA used for biotransformation. However, good conversion of the prochiral-ketone to the chiral amine product depends highly on the removal of the co-product which is formed during the deamination of the amine donor to shift the equilibrium to the chiral amine product.[83,86,97] The unfavourable equilibrium reaction for chiral product in the asymmetric synthesis is due to the fact that the transaminases favour the formation of ketone starting material.[98,99] This major problem can be overcome by removing the co-product using lactate dehydrogenase (LDH), nicotinamide adenine dinucleotide (NAD^+) and glucose dehydrogenase (GDH) coupled with the ω-TA. The co-product is converted to a lactone (**Scheme 7**) and undergoes decarboxylation to yield acetaldehyde and carbon dioxide.[77,88,99]



Scheme 7. Example of the removal of coproduct using LDH coupled with omega-transaminase.[77]

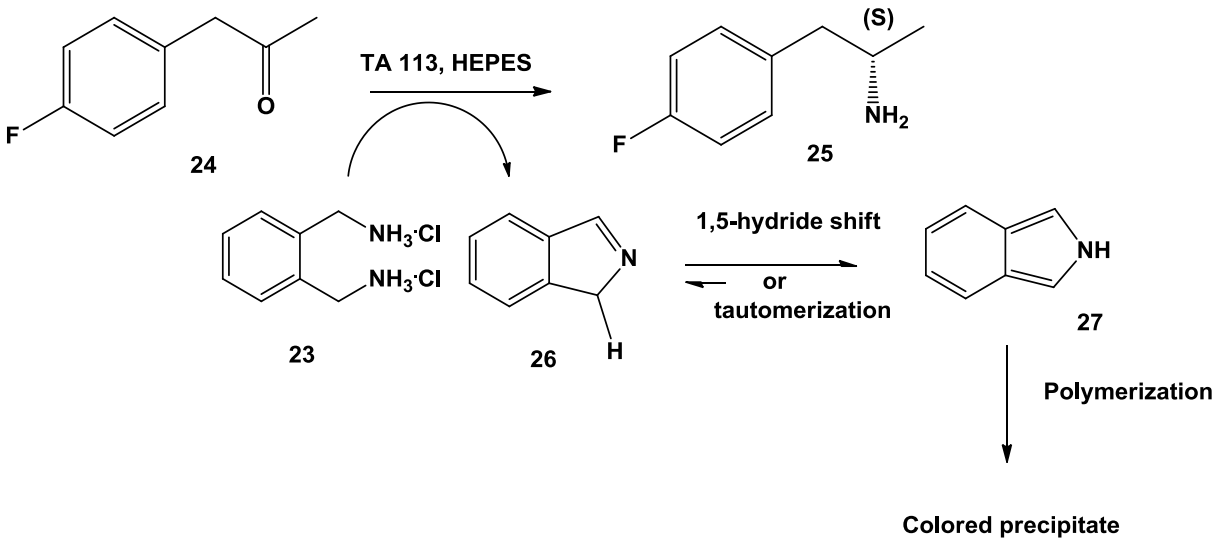
The coupling of LDH, NAD^+ and GDH with ω-TA also requires a large excess of the amino donor and this method is favoured for small to medium reaction scales.[99] The types of amino donor also influence the thermodynamic equilibrium of the biotransformation. Isopropylamine has been used as an amino donor in larger scale reaction processes, however it is used in large excess and the removal of the acetone coproduct is needed to drive the reaction to completion (**Scheme 8**).[76,99]



Scheme 8. Selected example for larger scale reaction using isopropylamine.[99]

1.3.4. Overcoming thermodynamic equilibrium difficulties

An alternative method was recently discovered in which the ketone co-product is spontaneously converted into a phenol tautomer which is more stable, however their high cost poses difficulties for the use of this approach.[99] This problem led to the new alternative approach whereby the low cost and achiral diamine donor was used to drive the unfavourable thermodynamic equilibrium towards the product.[99] The diamine donor xylylenediamine dihydrochloride (**23**) is commercially available at low cost and was used for the conversion of the 4-fluorophenyl acetone (**24**) (>99%,>99% *ee*) at one equivalent of amine donor (**Scheme 9**).[99]



Scheme 9. Conversion of **24** into (*S*)-**25** using diamine donor (**23**) at 1.1 equivalent. HEPES = 4-(2-hydroxyethyl)-piperazine-1-ethanesulfonic acid.[99]

The reaction equilibrium towards the product was favoured by the spontaneous tautomerization or 1,5-hydride shift of coproduct **26** into the more stable compound **27** (isoindole) which is the more effective method for the removal of this by-product from the system.[99] The spontaneous polymerization of by-product **27** gives coloured moieties.[99] This diamine donor can also be used in a large scale-reaction process.[99] The temperature, solvent, pH of the buffer, types of buffer and substrate concentration also affect the stability and activity of the enzyme, hence optimum conditions and a suitable solvent along with the minimal required substrate concentration must be used.[89,98]

1.3.5. Conversion of various substrates using omega-TA

ω-TA's have previously been used for the conversion of the aromatic β-keto acids using methylbenzylamine (MBA) as amino donor. However the major drawback of this reaction is the spontaneous decarboxylation of the β-keto acid starting material (**Figure 12**).[53] Hence ω-TA's have been demonstrated in very few studies for the synthesis of β-amino acids with the *beta*-keto acids used as the substrates.[53] Starting with the more stable *beta*-keto ester which was then hydrolysed by a lipase enzyme was found useful for the synthesis of *beta*-keto acids in a one pot biocatalytic cascade reaction with the combination of ω-TA's in the asymmetric synthesis of enantiopure β-amino acids (**Scheme 10**).[53]

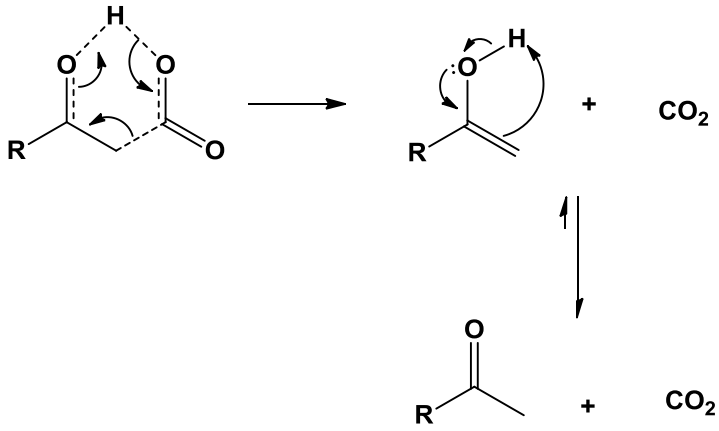
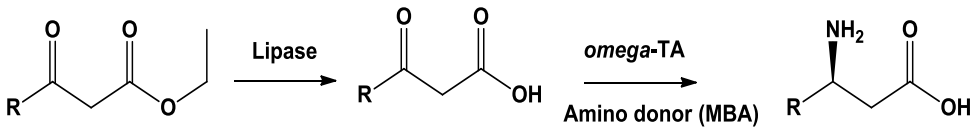


Figure 12. Decarboxylation mechanism through a cyclic transition state mechanism.[53]



Scheme 10. Combination of lipase and transaminases for asymmetric synthesis of *beta*-amino acids using hydrolysis-reductive amination (HRA).[53]

Mathew *et* al[53] prevented the decarboxylation of β-keto acids by the optimization of the lipase concentration during the conversion of β-keto esters to β-keto acids and then subsequent reductive amination using transaminases.[53] However, this approach requires a great amount of lipase enzyme to efficiently hydrolyse esters. Therefore, we decided our approach would adopt the use of nitrile containing substrates instead of esters and nitrile hydrolyzing enzymes instead of lipases to investigate the broad activity of ω-TA with the diamine donor and other amine donors in which the biotransformation would be carried out under reductive amination-hydrolysis (RAH) with β-ketonitriles preventing the decarboxylation problem. This change in reaction order from HRA to RAH would prevent the decarboxylation transition state as the β-ketonitriles are more stable and do not have the acid moiety which is involved in the hydrogen bonding during the decarboxylation process. These β-ketonitriles would be aminated by ω-TA in the presence of the amino donor followed by nitrile hydrolysis using nitrile hydrolysis enzymes into β-amino acids.

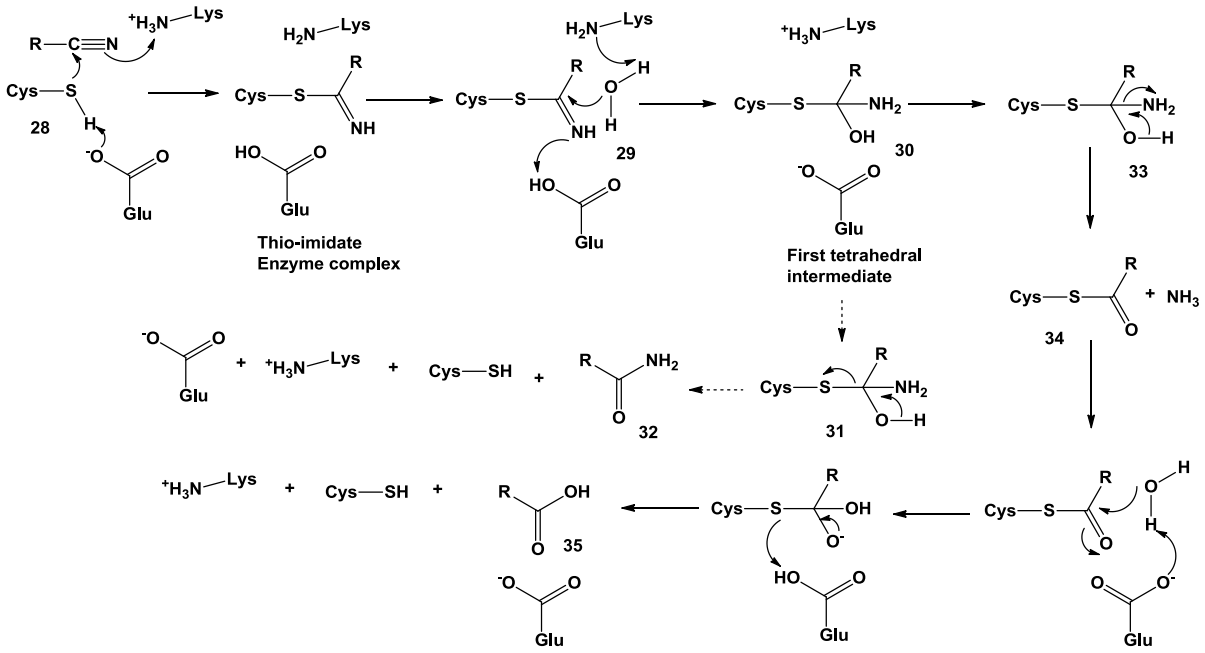
1.4. Nitrile hydrolyzing enzymes

Nitrilases,[100,101] nitrile hydratases[102,103] and amidases[104] are able to hydrolyse nitrile substrates into amides and amino acids.[105] These enzymes display regioselectivity and enantioselectivity, therefore these enzymes have received a great deal of attention in the biotransformation of nitriles.[44,100,101] These naturally occurring enzymes are used as bioremediation enzymes in the environment, examples of which include toxic effluents, cyanide remediation and herbicide degradation.[101] Nitrile hydrolyzing enzymes are derived from several microbes and plants which convert arylacetonitrile, aromatic and aliphatic nitriles into the corresponding amides and acids.[101,103]

1.4.1 Nitrilases

Nitrilases require two molecules of water to catalyze the biotransformation of nitriles into acids and ammonia in a two-step mechanism.[101,103] They belong to the nitrilase enzyme superfamily and they do not have a metal ion in the active site.[100,101] Nitrilase active sites contain three different amino acids: cysteine, glutamate and lysine in a catalytic triad.[101,105] Glutamate serves as a general base at the active site and lysine stabilizes the tetrahedral intermediate through a hydrogen bond with the nitrile nitrogen.[101] The role of

cysteine at the active site is to act as a nucleophile as it attacks the cyano group through its thiol group (**Scheme 11**).[101,103,105]



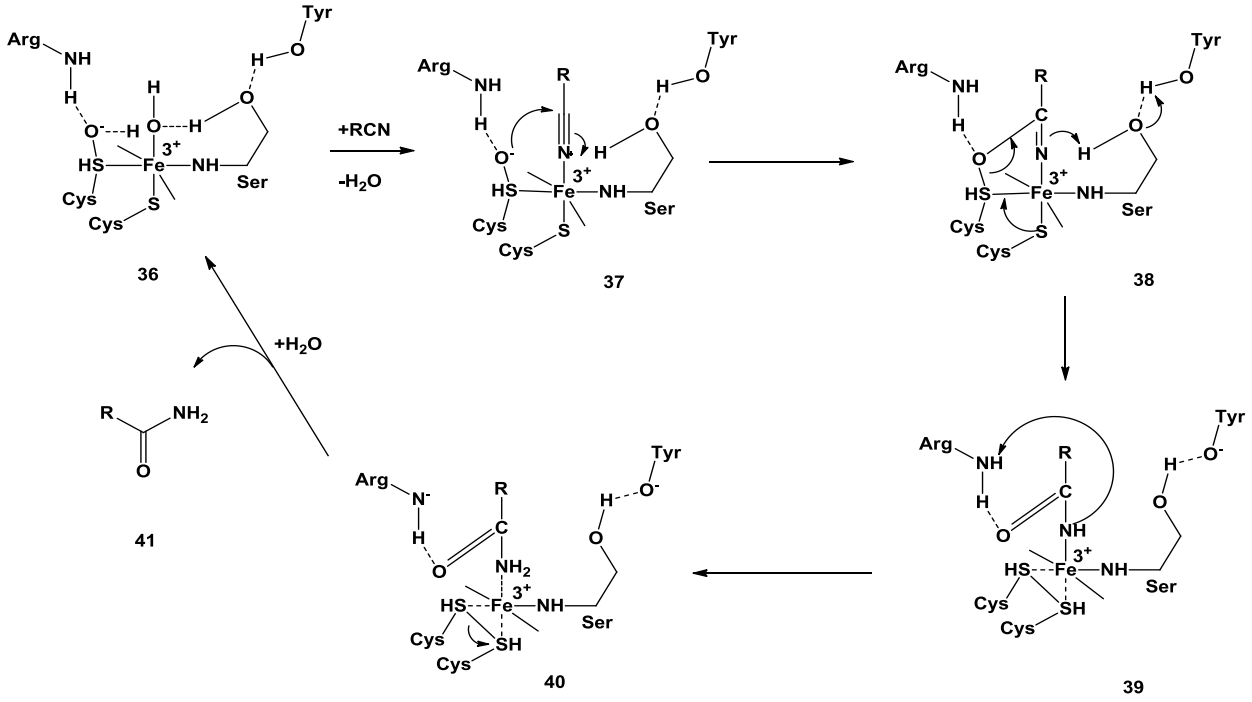
Scheme 11. Nitrilase hydrolysis mechanism for nitrile substrates.[101]

The complete mechanism (**Scheme 11**) of nitrilases involves the nucleophilic attack by the cysteine's SH-group **28** on the substrates nitrile carbon atom producing compound **29**. The addition of the first water molecule hydrolyzes the covalent thioimidate **29** into tetrahedral intermediate **30**.[100] It has been reported that the scissile bond in **30** is not well defined and with the delay in addition of the second water molecule can lead to the cleavage of the sulfur-carbon bond as illustrated in **31** to produce amides **32**.[101] In contrast, when the amine is the leaving group after the protonation of nitrogen in **33** this leads to the release of thioester **34** and ammonia.[101,105] The cleavage of the carbon-nitrogen bond in **33** and addition of the second water molecule are key to formation of the carboxylic acid moiety **35** (**Scheme 11**).[101]

1.4.2 Nitrile hydratases

Nitrile hydratases (NHase) are enzymes discovered from bacteria, plants and fungi,[105] and have been used for the biotransformation of aromatic and aliphatic nitriles into the corresponding amides.[101,103] They have a conserved low-spin metal ion cofactor at the active site namely Fe(III) or Co(III).[105,106] The two cysteines at the active site exist as the cysteine sulfenic and cysteine sulfinic acid.[105,106] The other residues present at the active site include tyrosine, serine and arginine (**Scheme 12**).[106] The mechanism of NHase is

proposed to be similar regardless of which metal ion cofactor is contained at the active site.[105] The first step of the mechanism involves the attack of a metal bound hydroxyl group on the nitrile substrate (**Scheme 12**).[105,106]

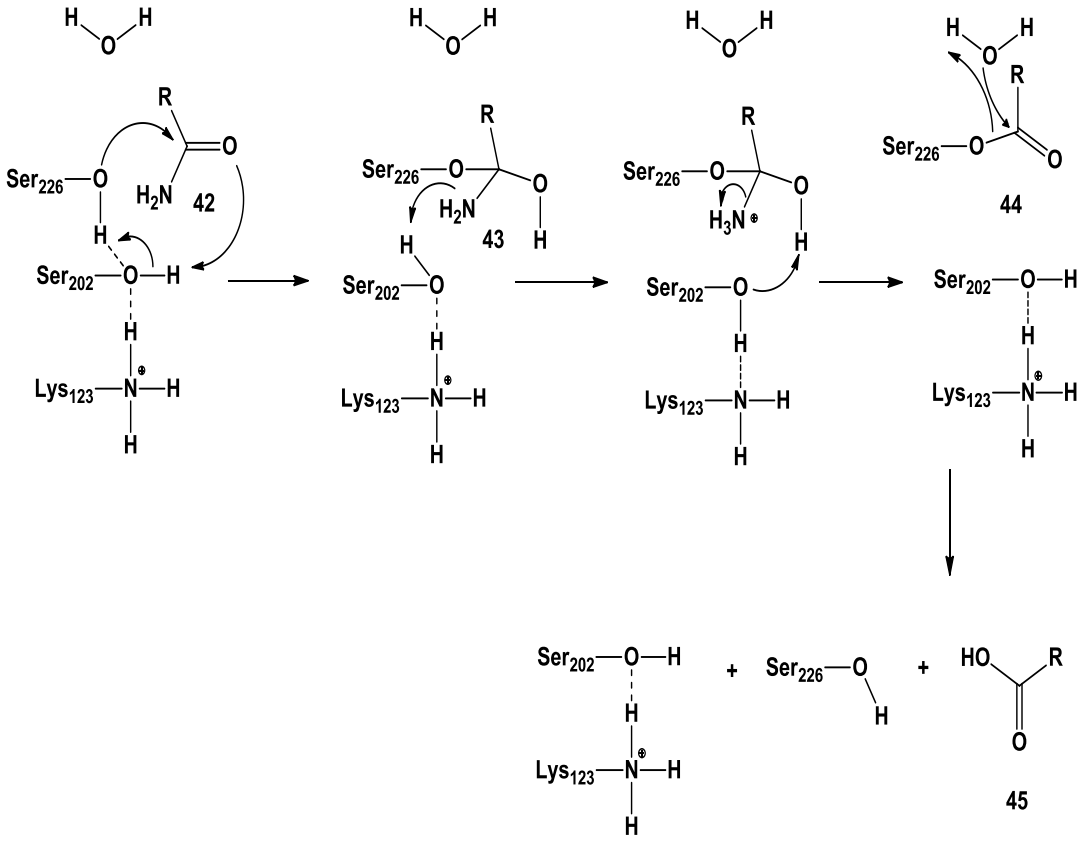


Scheme 12. The NHase mechanism for conversion of nitrile to amide.[106]

The nucleophilic attack by Cys-SO$^-$ **37** on the nitrile substrate facilitates the formation of the cyclic intermediate **38**.[106] The oxygen from the cysteine is transferred to the nitrile as seen at **39** and is then incorporated in the amide product.[106] The abstraction of a proton from arginine produces **40** and subsequent addition of water leads to the release of amide product **41** and the formation of a metal-hydroxyl complex **36**.[105,106]

1.4.3 Amidases

The amidases further hydrolyze the amide product into the corresponding acid and ammonia.[107] Amidases are regioselective and have broad substrate specificity.[107] These enzymes have conserved serine and lysine residues at the active site where the serine residue plays a very important role initiating nucleophilic attack on the amide carbonyl carbon atom (**Scheme 13**).[107]

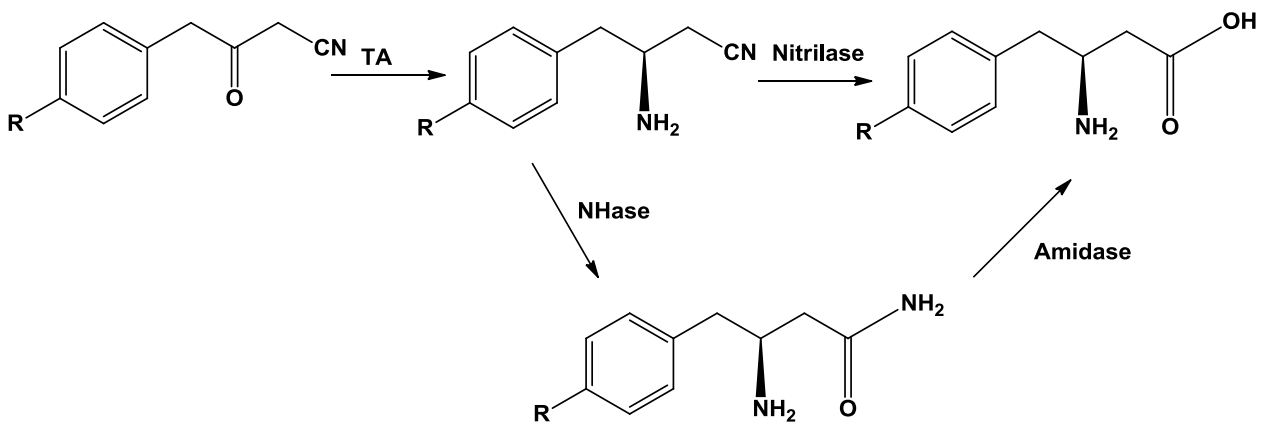


Scheme 13. Amidase mechanism for the biotransformation of amide into acid.[107]

The nucleophilic attack by the Ser226 oxygen is key to formation of tetrahedral intermediate **43**.[107] The deprotonation of Ser226 by Ser202 increases the nucleophilicity of the oxygen.[107] The protonation of the amino group by Ser202 increases the electrophilic properties of the substrate carbon atom in the intermediate **43**. Deprotonation of the hydroxyl group by Ser202 leads to the dissociation of ammonia and formation of a carbonyl group in **44** (**Scheme 13**).[107] The addition of water leads to the hydrolysis from Ser226 and protonation, leading to formation of the acid product **45**.[107]

1.5 Proposed reaction sequence

The RAH sequence would involve the reductive amination of β-ketonitriles into β-aminonitriles using omega-transaminase followed by nitrile hydrolysis using either nitrilase or nitrile hydratase\amidase to produce β-amino acids (**Scheme 14**).



Scheme 14. RAH reaction cascade

1.6. Overall project aim

The overall aim is to produce a wound healing peptide that is not rapidly degraded by cellular proteases. To achieve this we intend to incorporate enantiopure *beta*-amino acids into the peptide chain. These *beta*-amino acids can be generated using omega-transaminases, but as *beta*-keto carboxylic acids spontaneously decarboxylate, we are going to use *beta*-keto-nitriles as the substrates and use a sequential biocatalysis reaction (*ω*-TA – NHase/amidases) to achieve this.

1.6.1 Aims and objectives

- The aim is to synthesise enantiopure *beta*-amino acids using transaminases and nitrile hydratases/amidases for incorporation into wound healing peptides
- Synthesise the *beta*-aminonitrile standards from *beta*-ketonitriles
- Synthesise the β-ketonitrile substrates from aromatic carboxylic acids
- Evaluate the β-ketonitriles as starting materials using omega-transaminases
- Identify the optimal reaction conditions for maximising the transaminases activity
- Identify one or more good amine donors that significantly drive reaction equilibrium towards the product
- Screen different transaminases for conversion of ketone substrates
- Use nitrile hydrolyzing enzymes for hydrolysis of the resultant *beta*-aminonitriles
- Synthesise peptidomimetics by incorporating the *beta*-amino acids into wound healing peptide sequences
- Analyse the components using HPLC-MS

1.6.2 Hypothesis and questions

1.6.2.1 Hypothesis

- The nitrile hydrolyzing enzymes will convert the optically pure β-aminonitriles into the corresponding β-amino acids

1.6.2.2 Research questions

- It is possible to synthesise β-amino acids from nitrile substrates using omega-transaminases?
- Can a multi-enzymes one pot reaction process drive the unfavourable equilibrium towards the product?

2. EXPERIMENTAL PROCEDURE

2.1 Chemicals and reagents

Hexane, ethyl acetate, methanol and acetone were purchased from Sigma Aldrich. Acetone was used to clean apparatus. Acetonitrile and tetrahydrofuran (THF) were purchased from Mallinckrodt. Sodium was purchased from Sigma Aldrich and used for preparation of dry THF under nitrogen gas. Distillations were done under nitrogen gas (purchased from TriGas) using calcium hydride for drying dichloromethane (DCM). *Beta*-amino acids were purchased from Bepharm. 2-Chlorotrityl resins were purchased from Sigma Aldrich.

Triisopropylsilane (TIS), hexafluorophosphate azabenzotriazole tetramethyl uronium (HATU), hydroxybenzotriazole (HOBt) and Fmoc protected L-amino acids were purchased at DLD Scientific. Bromoacetic acid, 2-chlorotrityl chloride resin, diethyl ether, trifluoroacetic acid (TFA), N,N'-diisopropylcarbodiimide (DIC), thionyl chloride ($SOCl_2$), piperidine, chloroform ($CHCl_3$), 1,2-Ethanedithiol (EDT), dimethyl sulfoxide (DMSO), acetic acid (AcOH), aluminium trichloride ($AlCl_3$), sodium hydrogen carbonate ($NaHCO_3$), magnesium sulphate ($MgSO_4$), diisopropylethylamine (DIPEA), triethylsilane, formic acid, hexane, ethyl acetate, paraformaldehyde, p-toluenesulfonic acid, toluene, iodine, *n*-butyllithium (*n*-BuLi), acetone, methanol (MeOH), sodium hydroxide (NaOH) and ascorbic acid were purchased at Sigma Aldrich. N,N'−dimethylformamide (DMF) and acetonitrile (ACN) were purchased from DLD Scientific.

Enzymes: transaminases (Enzymicals TA001-TA008) from Enzymicals AG (Germany) (ECS), omega-Transaminase *Aspergillus fumigatus* purchased from Sigma Aldrich, transaminases (Prozomix-TA001-TA050) purchased from Prozomix Limited in Northumberland, lactate dehydrogenases (LDH) and glucose dehydrogenase (GDH) both purchased from Sigma Aldrich, were used without further purification. Nitrile hydratase *Rhodococcus rhodochrous* ATCC BAA-870 was supplied by ZABiotech and CSIR Biosciences (South Africa). Nicotinamide adenine dinucleotide (NAD^+) and pyridoxal 5'-phosphate (PLP) were purchased from Sigma Aldrich. The diamine donor o-xylylenediamine dihydrochloride and 4-(2-Hydroxyethyl)piperazine-1-ethanesulfonic acid (HEPES) were purchased from Sigma Aldrich.

2.2 Instrumentation

Thin layer chromatographic (TLC) analysis was done on Merck Aluminium foil backed plates coated with silica gel 60, F_{254} and a UV lamp (245 nm) was used to monitor the reaction progress. Macherey-Nagel silica gel 60 (particle size 0.063 nm to 0.200 nm) was used as the solid phase column packaging.

The ^{1}H and ^{13}C Nuclear Magnetic Resonance spectra were acquired on a Bruker 500 or 300 MHz spectrometer at room temperature. The deuterated solvent was used as specified for each compound. The internal standard tetramethylsilane (TMS, 0.05% v/v) was contained in deuterated chloroform ($CDCl_3$). MestreNova Software under license from Mestrelab Research, CA, USA was used for data processing.

The abbreviations for multiplicities were labelled as follows: singlet = s, doublet = d, triplet = t, doublet of doublet = dd, quartet = q, multiplet = m.

Mass spectra were recorded on a Thermo Scientific Dionex Ultimate 3000 Ultra-High Performance Liquid Chromatography (UHPLC) instrument coupled to a Bruker Compact Q-TOF high mass spectrometer. An electrospray ionisation source (ESI) in the positive ion mode was used for the analysis. A Phenomenex C18 column (5 µm, 100 Å, 250 mm × 21.2 mm) was utilized for HPLC separation.

The purity of compounds was determined using an Agilent 1260 Infinity semi-preparative HPLC system equipped with a Phenomenex C18 column (5 µm, 100 Å, 250 mm × 21.2 mm) coupled to a UV-Vis detector (operating at 215 nm and 254 nm) and an automated fraction collector. Acetonitrile-water (both containing 0.1 % formic acid) was used as the mobile phase (Gradient: 5 – 95 % acetonitrile in 25 minutes + 5 minutes at 95%, flow 15.0 mL/min).

Infra-red (IR) spectra were recorded on a Bruker Tensor-27 Fourier Transform infrared spectrometer.

Chiral analysis were performed on a Dionex Ultimate 3000 chiral HPLC instrument furnished with a photodiode array detector. The mobile phase utilized on Lux 3 µm cellulose-2 (250 × 4.6 mm) comprised of hexane and isopropyl alcohol (IPA) (90:10); flow rate = 1 mL/min).

2.3 Initial test for biocatalysis using transaminases

2.3.1 Analytical scale deamination of amine substrates using pyruvate amine acceptor

All biocatalysis reactions were performed at 30°C for 12 h in HEPES buffer (100 mM, 850 µL, pH 7.5) containing PLP (2 mM) in a 2 mL-Eppendorf tube. The corresponding amine substrate (5 mM) was dissolved in 15% v/v DMSO and added to the buffer solution (850 µL) containing transaminase (2 mg) with the amine acceptor pyruvate (0.5 equiv). The reaction mixture was agitated at 30°C. TLC and HRMS were used to monitor the generation of the ketone product. The reaction was quenched by the addition of sodium hydroxide (150 µL, 5 N) followed by extraction using ethyl acetate (3 × 500 µL).

The organic layers were combined and dried over $MgSO_4$. The reactions were analysed by HRMS.

2.3.2 Analytical scale reductive amination of ketone substrates using diamine donor

All biocatalysis reactions were performed at 30°C for 12 h in HEPES buffer (100 mM, 850 µL, pH 7.5) containing PLP (2 mM) in a 2 mL-Eppendorf tube. The corresponding ketone substrate (5 mM) was dissolved in 15% v/v DMSO and added to the buffer solution (850 µL) containing transaminase (2 mg) with diamine donor (1.1 equiv). The reaction mixture was agitated at 30°C. TLC was used to monitor the generation of the amine product. The reaction was quenched by the addition of sodium hydroxide (150 µL, 5 N) followed by extraction using ethyl acetate (3 × 500 µL). The organic layers were combined and dried over $MgSO_4$. The reactions were analysed by HRMS.

2.3.3 Analytical scale reductive amination of ketone substrates using LDH/GDH pyruvate removal system

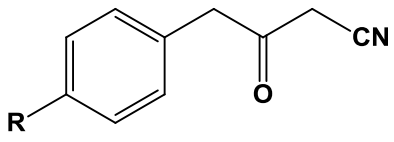
The biotransformation reactions were performed at 30°C in a 2 mL Eppendorf tube. Transaminase (2 mg) and PLP (2 mM) were rehydrated in HEPES buffer (100 mM, 850 µL, pH 7.5). The amine donor L-alanine (75 mM) was added to the solution and allowed to equilibrate for 2h. Corresponding ketone substrate (15 mM) was dissolved in DMSO (150 µL), pyruvate reductase mix (=LDH/GDH mix) (40 mg, mixture of lactate dehydrogenase, glucose dehydrogenase, glucose, NAD^+), were added to the solution and the reaction mixture was allowed to stir at 30°C for 24 h. The progress of the reaction was monitored by TLC. The reaction was quenched by the addition of aqueous NaOH (200 µL, 5 N) solution, followed by extraction with ethyl acetate (3 × 500 µL). The combined organic layers were dried over $MgSO_4$ and concentrated under reduced pressure. The reactions were monitored by HRMS.

2.4 Initial test for the hydrolysis of *beta*-ketonitriles into *beta*-ketoamides

The hydrolysis test was conducted at 30°C for 8 h in Tris-buffer (100 mM, pH 9) in a 2 mL-Eppendorf tube. The substrate 3-oxo-3-(*p*-tolyl)propanenitrile (20 mM) was dissolved in methanol 10% v/v and added to the buffer (850 µL) containing nitrile hydratase enzyme (5 mg). After 8 h the reaction was quenched by the addition of HCl (200 µL, 2 N) followed by the extraction with ethyl acetate (3 × 500 µL). The organic layers were combined and dried over $MgSO_4$. The reactions were monitored by TLC and HRMS.

2.5 General synthetic procedures

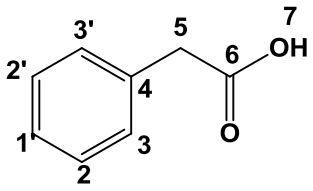
2.5.1 Attempted preparation of β-ketonitriles 49 exemplified by compound 49a (*Method 1*)



49

R: a.H, b.F, c.CH_3, d.OMe

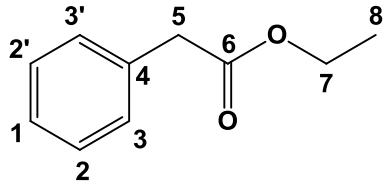
2-Phenylacetic acid **46a** (1.01 g, 7.351 mmol) was dissolved in dry DCM (1.1 mL) and thionyl chloride (7.0 mL) was added. The reaction was stirred at room temperature for 2 h. The excess $SOCl_2$, and the by-products HCl and SO_2 were removed under reduced pressure to give 2-phenylacetyl chloride **47a** (100% yield). Acetonitrile (1.2 mL, 22.970 mmol) was added drop-wise to the solution containing *n*-BuLi (4.0 mL, 42.462 mmol) in dry THF (8 mL) stirring at -78°C for 1 h. The crude product 2-phenylacetyl chloride **47a** was dissolved in dry THF (3 mL) and added to the reaction mixture. The reaction was stirred at -78°C for 4 h and then quenched by the addition of HCl (5 mL, 2 M). Water (5 mL) was added followed by the extraction using ethyl acetate (5 × 5 mL). The organic layers were combined, dried over $MgSO_4$ and instead of the anticipated product, the original starting material 2-phenylacetic acid **46a**[108] (0.87 g, 87%) was recovered as an oil product. R_f (30% EtOAc/Hexane) 0.60. *M.p*. 74-76°C (lit. *m.p*. 76-78°C).[108] **^{1}H NMR (300 MHz, $CDCl_3$):** δ 7.36 – 7.21 (5H, m, H1, H2, H2', H3 and H3'), 3.64 (2H, s, H5). **^{13}C NMR (75 MHz, $CDCl_3$):** δ 177.8 (C-6), 133.3 (C-4), 129.4 (C-3 and C-3'), 128.6 (C-2 and C-2'), 127.3 (C-1), 41.1 (C-5) (lit. Sigma Aldrich).[108]



46a

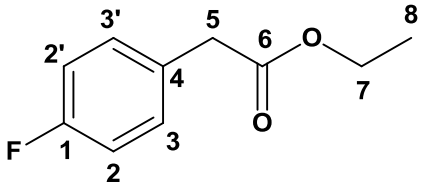
2.5.2 Procedure for the synthesis of esters (48a-d) from carboxylic acids (46a-d) (*Method 2*)

2.5.2.1 Synthesis of ethyl 2-phenylacetate 48a[109]



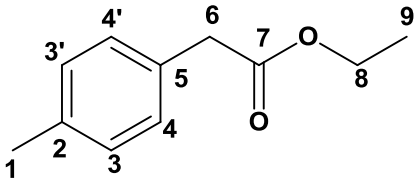
2-Phenylacetic acid (1.00 g, 7.351 mmol) was dissolved in ethanol (6 mL). Thionyl chloride (0.026 mL) was added to the clear solution. TLC was used to monitor the consumption of the starting material. The reaction was concentrated under reduced pressure. Water (8 mL) was added followed by extraction with ethyl acetate (3 × 5 mL). The organic layers were combined, washed with brine solution and dried over $MgSO_4$. The crude product was purified by silica gel column chromatography yielding ethyl 2-phenylacetate **48a** (1.03 g, 85%) and was isolated as a clear oil. R_f (30% EtOAc/hexane) 0.85. **^{1}H NMR (300 MHz, $CDCl_3$):** δ 7.37 – 7.19 (5H, m, H1, H2, H2', H3 and H3'), 4.13 (2H, q, *J* = 7.1 Hz, H8), 3.59 (2H, s, H5), 1.23 (3H, t, *J* = 7.1 Hz, H8). **^{13}C NMR (75 MHz, $CDCl_3$):** δ 171.5 (C-6), 134.2 (C-4), 129.2 (C-3 and C-3'), 128.5 (C-2 and C-2'), 127.0 (C-1), 60.8 (C-7), 41.4 (C-5), 14.2 (C-8) (lit. Liu *et al*[109]).

2.5.2.2 Synthesis of ethyl 2-(*p*-fluorophenyl)acetate 48b[110]



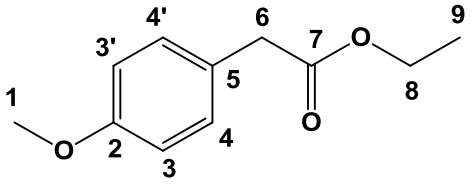
2-(*p*-Fluorophenyl)acetic acid (1.00 g, 6.490 mmol) was dissolved in ethanol (6 mL). Thionyl chloride (0.026 mL) was added to a clear solution. TLC was used to monitor the consumption of the starting material. The reaction was concentrated under reduced pressure. Water (8 mL) was added followed by extraction with ethyl acetate (3 × 5 mL). The organic layers were combined, washed with brine solution and dried over $MgSO_4$. The crude product was purified by a silica gel column chromatography yielding ethyl 2-(p-fluorophenyl)acetate **48b** (1.09 g, 89%) and was isolated as a clear oil. R_f (30% EtOAc/hexane) 0.82. **^{1}H NMR (300 MHz, $CDCl_3$):** δ 7.25 (2H, dd, *J* = 8.7, 5.4 Hz H3 and H3'), 7.01 (2H, t, *J* = 8.7 Hz H2 and H2'), 4.16 (2H, q, *J* = 7.1 Hz, H7), 3.58 (2H, s, H5), 1.25 (3H, t, *J* = 7.1 Hz, H8). **^{13}C NMR (75 MHz, $CDCl_3$):** δ 171.8 (C-6), 162.4 (C-1, d, $^1J_{C-F}$ = 245.1 Hz), 131.2 (C-3 and C-3', d, $^3J_{C-F}$ = 8.0 Hz), 130.3 (C-4, d, $^4J_{C-F}$ = 3.3 Hz), 115.7 (C-2 and C-2', d, $^2J_{C-F}$ = 21.4 Hz), 61.3 (C-7), 40.8 (C-5), 14.5 (C-8) (lit. Busto *et al*[110]).

2.5.2.3 Synthesis of ethyl 2-(*p*-tolyl)acetate 48c[111]



2-(*p*-Tolyl)acetic acid (1.02 g, 6.671 mmol) was dissolved in ethanol (6 mL). Thionyl chloride (0.026 mL) was added to a clear solution. TLC was used to monitor the consumption of the starting material. The reaction was concentrated under reduced pressure. Water (8 mL) was added followed by extraction with ethyl acetate (3 × 5 mL). The organic layers were combined, washed with brine solution and dried over $MgSO_4$. The crude product was purified by a silica gel column chromatography yielding ethyl 2-(*p*-tolyl)acetate **48c** (1.00 g, 85%) and was isolated as a clear oil. R_f (30% EtOAc/hexane) 084. **^{1}H NMR (300 MHz, $CDCl_3$):** δ 7.13 (2H, d, *J* = 6.6 Hz, H4 and H4'), 7.06 (2H, d, *J* = 7.1 Hz, H3 and H3'), 4.08 (2H, q, *J* = 7.1 Hz, H8), 3.51 (2H, s, H6), 2.27 (3H, s, H1), 1.18 (3H, t, *J* = 7.2 Hz, H9). **^{13}C NMR (75 MHz, $CDCl_3$):** δ 171.8 (C-7), 136.7 (C-2), 131.4 (C-5), 129.4 (C-3 and C-3'), 129.3 (C-4 and C-4'), 60.8 (C-8), 41.1 (C-6), 21.2 (C-1), 14.3 (C-9) (lit. Song *et al*).[111]

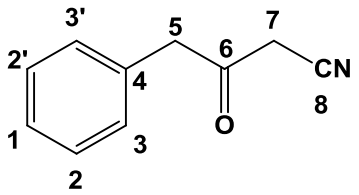
2.5.2.4 Synthesis of ethyl 2-(*p*-methoxyphenyl)acetate 48d[110]



2-(*p*-Methoxyphenyl)acetic acid (1.00 g, 6.021 mmol) was dissolved in ethanol (6 mL). Thionyl chloride (0.026 mL) was added to a clear solution. TLC was used to monitor the consumption of the starting material. The reaction was concentrated under reduced pressure. Water (8 mL) was added followed by extraction with ethyl acetate (3 × 5 mL). The organic layers were combined, washed with brine solution and dried over $MgSO_4$. The crude product was purified by a silica gel column chromatography yielding ethyl 2-(*p*-methoxyphenyl)acetate **48d** (0.93 g, 80%) and was isolated as clear oil. R_f (30% EtOAc/hexane) 0.84. **^{1}H NMR (300 MHz, $CDCl_3$):** δ 7.18 (2H, d, *J* = 8.7 Hz, H4 and H4'), 6.84 (2H, d, *J* = 8.7 Hz, H3 and H3'), 4.12 (2H, q, *J* = 7.1 Hz, H8), 3.75 (3H, s, H1), 3.53 (2H, s, H6), 1.23 (3H, t, *J* = 7.1 Hz, H9). **^{13}C NMR (75 MHz, $CDCl_3$):** δ 171.1 (C-7), 158.0 (C-2), 129.5 (C-5), 125.6 (C-4 and C-4'), 113.2 (C-3 and C-3'), 59.9 (C-8), 54.3 (C-1), 39.7 (C-6), 13.4 (C-9) (lit. Busto *et al*).[110]

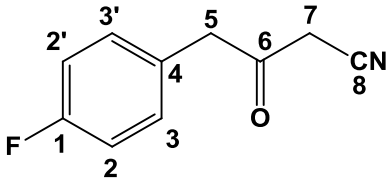
2.5.3 Procedure for the synthesis of β-ketonitriles (49a-d) from esters (48a-d)

2.5.3.1 Synthesis of 3-oxo-4-phenylbutanenitrile 49a[112]



To a solution containing *n*-BuLi/hexane (11.220 mmol, 2.3 equiv) in dry THF was added dry acetonitrile (9.760 mmol, 2.0 equiv) drop wise. After stirring the reaction at -78°C for 1 h, ethyl 2-phenylacetate (0.80 g, 4.881 mmol) dissolved in dry THF was added to a reaction mixture. The reaction was stirred at -78°C for 4 h and then quenched by the addition of HCl (5 mL). Water (5 mL) was added followed by the extraction using ethyl acetate (5 × 8 mL). The organic layers were combined and dried over $MgSO_4$. The crude product was purified by a silica gel column chromatography yieldings 3-oxo-4-phenylbutanenitrile **49a** (0.61 g, 78%) and was isolated as red-brown crystalline solid. R_f (30% EtOAc/hexane) 0.60. M.*p*. 90-95°C. **^{1}H NMR (300 MHz, $CDCl_3$):** δ 7.35 – 7.25 (3H, m, H1, H2 and H2'), 7.15 (2H, d, *J* = 6.3 Hz, H3 and H3'), 3.77 (2H, s, H7), 3.46 (2H, s, H5). **^{13}C NMR (75 MHz, $CDCl_3$):** δ 196.2 (C-6), 132.6 (C-4), 129.9 (C-3 and C-3'), 129.4 (C-2 and C-2'), 128.1 (C-1), 114.4 (C-8), 49.3 (C-5), 31.7 (C-7) (lit. Foehlisch *et al*).[112] **IR (ν_{max} /cm^{-1}):** 2225 (C≡N), 1590 (C=C).

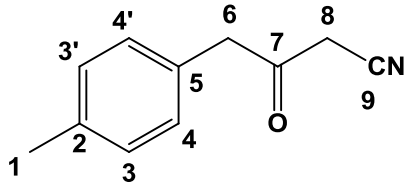
2.5.3.2 Synthesis of 4-(*p*-fluorophenyl)-3-oxobutanenitrile 49b



To a solution containing *n*-BuLi/hexane (10.223 mmol, 2.3 equiv) in dry THF was added dry acetonitrile (8.801 mmol, 2.0 equiv) drop wisely. After stirring the reaction at -78°C for 1 h, ethyl 2-(*p*-fluorophenyl)acetate (0.80 g, 4.401 mmol) dissolved in dry THF was added to a reaction mixture. The reaction was stirred at -78°C for 4 h and then quenched by the addition of HCl (5 mL). Water (5 mL) was added followed by the extraction using ethyl acetate (5 × 8 mL). The organic layers were combined and dried over $MgSO_4$. The crude product was purified by a silica gel column chromatography yielding 4-(*p*-

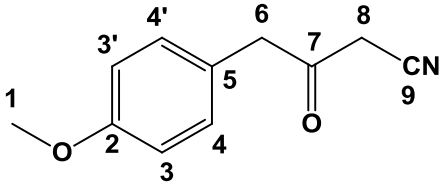
fluorophenyl)-3-oxobutanenitrile **49b** (0.64 g, 82%) and was isolated as red-brown crystalline solid. R_f (30% EtOAc/hexane) 0.52. *M.p*. 101-104°C. **^{1}H NMR (300 MHz, $CDCl_3$):** δ 7.21 – 7.13 (2H, m, H3 and H3'), 7.03 (2H, t, *J* = 8.7 Hz, H1 and H1'), 3.82 (2H, s, H7), 3.53 (2H, s, H5). **^{13}C NMR (75 MHz, $CDCl_3$):** δ 195.1 (C-6), 161.9 (C-1), d, $^1J_{C\text{-}F}$ = 246.6 Hz), 130.8 (C-3 and C-3', d, $^3J_{C\text{-}F}$ = 8.2 Hz), 127.4 (C-4, d, $^4J_{C\text{-}F}$ = 3.3 Hz), 115.6 (C-2 and C-2', d, $^2J_{C\text{-}F}$ = 21.6 Hz), 113.4 (C-8), 47.6 (C-5), 31.0 (C-7). **IR (ν_{max} /cm^{-1}):** 2220 (C≡N), 1610 (C=C), 1355 (C-F).

2.5.3.3 Synthesis of 3-oxo-4-(*p*-tolyl)butanenitrile 49c



To a solution containing *n*-BuLi/hexane (10.223 mmol, 2.3 equiv) in dry THF was added dry acetonitrile (8.901 mmol, 2 equiv) drop wisely. After stirring the reaction at -78°C for 1 h, ethyl 2-(*p*-tolyl)acetate (0.80 g, 4.491 mmol) dissolved in dry THF was added to a reaction mixture. The reaction was stirred at -78°C for 4 h and then quenched by the addition of HCl (5 mL). Water (5 mL) was added followed by the extraction using ethyl acetate (5 × 8 mL). The organic layers were combined and dried over $MgSO_4$. The crude product was purified by a silica gel column chromatography yieldings 3-oxo-4-(*p*-tolyl)butanenitrile **49c** (0.57 g, 73%) and was isolated as red-brown crystalline solid. R_f (30% EtOAc/hexane) 0.55. *M.p*. 100-103°C. **^{1}H NMR (300 MHz, $CDCl_3$):** δ 7.13 (2H, d, *J* = 8.0 Hz, H4 and H4'), 7.05 (2H, d, *J* = 8.1 Hz, H3 and H3'), 3.73 (2H, s, H8), 3.47 (2H, s, H6), 2.31 (3H, s, H1). **^{13}C NMR (75 MHz, $CDCl_3$):** δ 196.5 (C-7), 137.7 (C-2), 130.0 (C-5), 129.7 (C-4 and C-4'), 129.5 (C-3 and C-3'), 114.5 (C-9), 48.9 (C-6), 31.5 (C-8), 21.3 (C-1). **IR (ν_{max} /cm^{-1}):** 2210 (C≡N), 1593 (C=C).

2.5.3.4 Synthesis of 4-(*p*-methoxyphenyl)-3-oxobutanenitrile 49d[113]



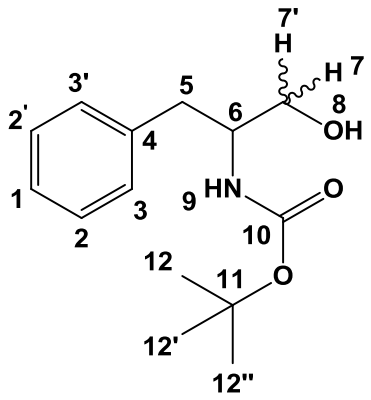
To a solution containing *n*-BuLi/hexane (10.211 mmol, 2.3 equiv) in dry THF was added dry acetonitrile (8.880 mmol, 2 equiv) drop wisely. After stirring the reaction at -78°C for

1 h, ethyl 2-(*p*-methoxyphenyl)acetate (0.80 g, 4.441 mmol) dissolved in dry THF was added to a reaction mixture. The reaction was stirred at -78°C for 4 h and then quenched by the addition of HCl (5 mL). Water (5 mL) was added followed by the extraction using ethyl acetate (5 × 8 mL). The organic layers were combined and dried over $MgSO_4$. The crude product was purified by a silica gel column chromatography yieldings 4-(*p*-methoxyphenyl)-3-oxobutanenitrile **49d** solid (0.66 g, 79%) and was isolated as brown crystalline. R_f (30% EtOAc/hexane) 0.51. *M.p*. 103-108°C. **^{1}H NMR (300 MHz, $CDCl_3$):** δ 7.10 (2H, d, *J* = 8.6 Hz, H4 and H4'), 6.87 (2H, d, *J* = 8.7 Hz, H3 and H3'), 3.77 (3H, s, H1), 3.74 (2H, s, H8), 3.49 (2H, s, H6). **^{13}C NMR (75 MHz, $CDCl_3$):** δ 195.7 (C-7), 158.8 (C-2), 130.1 (C-4 and C-4'), 123.6 (C-5), 114.1 (C-9), 113.6 (C-3 and C-3'), 54.8 (C-1), 47.8 (C-6), 30.7 (C-8) (lit. Katritzky *et al*).[113] **IR (v_{max}/cm^{-1}):** 2222 (C≡N), 1595 (C=C).

2.6 Conventional synthesis of β-aminonitrile standard product

The synthesis of the standard β-aminonitriles were attempted using the following methods:

2.6.1 Synthesis of *tert*-butyl (1-hydroxy-3-phenylpropan-2-yl)carbamate 52i[114]

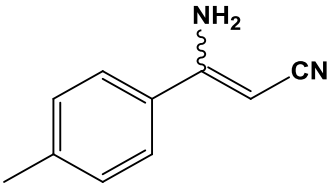


52i

2-((tert-Butoxycarbonyl)amino)-3-phenylpropanoic acid **51** (2.02 g, 7.551 mmol) was dissolved in THF (10 mL) at 0°C and iodine (2.03 g, 8.501 mmol) was added to the solution. $NaBH_4$ (0.31 g, 8.502 mmol) was added to the green solution and the reaction was allowed to stir at 0°C for 2 h, then refluxed for another 2 h. $NaHCO_3$ (15 mL) was added to the reaction mixture, and the solution was extracted with ethyl acetate (3 × 10 mL). The organic layers were combined, dried over $MgSO_4$ and concentrated under reduced pressure. The crude product was purified by silica gel column chromatography yielding tert-butyl (1-hydroxy-3-phenylpropan-2-yl)carbamate **52i** (0.15 g, 8%) as a colourless oil. R_f (50% EtOAc/hexane) 0.54. **^{1}H NMR (300 MHz, $CDCl_3$):** δ 7.47 – 7.05

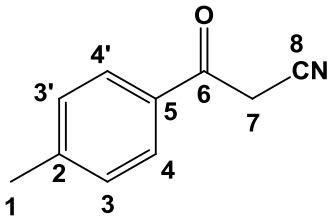
(5H, m, H1, H-2, H-2', H3 and H3'), 5.58 (1H, s, H8), 5.54 – 5.34 (1H, m, H6), 4.50 – 4.25 (1H, m, H7), 3.94 – 3.70 (1H, m, H7'), 3.27 – 2.56 (2H, m, H5), 1.31 (9H, s, H12). **^{13}C NMR (75 MHz, $CDCl_3$):** δ 156.1 (C-11), 136.9 (C-4), 130.1 (C-2 and C-2'), 129.0 (C-3 and C-3'), 127.4 (C-1), 80.7 (C-11), 63.1 (C-7), 57.0 (C-6), 38.5 (C-5), 28.5 (C-12, C-12' and C-12'') (lit. Nagendra *et al*).[114]

2.6.2 Attempted approach towards synthesis of 3-amino-3-(*p*-tolyl)acrylonitrile 55[44]



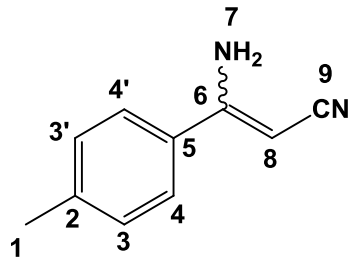
55

4-Methylbenzonitrile **53** (4.50 g, 8.551 mmol) was dissolved in THF (15 mL), and added to a solution of acetonitrile (2.1 mL, 38.290 mmol) with *n*-BuLi/Hexane (1 M, 45 ml, 477.682 mmol). The reaction mixture was allowed to stir at -78°C for 8 h. HCl (20 mL, 2 M) was added to the reaction mixture to quench the excess base and the resulting mixture was extracted with ethyl acetate (3 × 10 mL). The organic layers were combined, dried over $MgSO_4$ and concentrated under reduced pressure. The crude product was purified by silica gel column chromatography yielding the unexpected β-ketonitrile 3-oxo-3-(*p*-tolyl)propanenitrile **54** (1.03 g, 76%) as a white crystalline solid. R_f (30% EtOAc/hexane) 0.78. **^{1}H NMR (300 MHz, $CDCl_3$):** δ 7.82 (2H, d, *J* = 8.3 Hz, H3 and H3'), 7.32 (2H, d, *J* = 8.0 Hz, H4 and H4'), 4.05 (2H, s, H7), 2.44 (3H, s, H1). **^{13}C NMR (75 MHz, $CDCl_3$):** δ 186.3 (C-6), 145.7 (C-2), 131.6 (C-5), 129.5 (C-3 and C-3'), 128.3 (C-4 and C-4'), 113.6 (C-8), 28.9 (C-7), 21.5 (C-1) (Katritzky *et al*).[115]



54

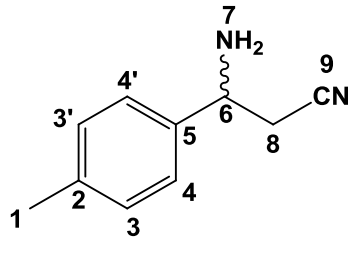
2.6.3 Synthesis of 3-amino-3-(*p*-tolyl)acrylonitrile 55[44]



55

4-Methylbenzonitrile **53** (2.03 g, 17.10 mmol) was dissolved in dry toluene (15 mL), and added to a solution of acetonitrile (1.3 mL, 24.89 mmol) with potassium *tert*-butoxide (3.80 g, 34.20 mmol). The reaction mixture was allowed to stir at room temperature for 8 h. HCl (20 mL, 2 M) was added to the reaction mixture to quench the excess base and the resulting mixture was extracted with ethyl acetate (3 × 10 mL). The organic layers were combined, dried over $MgSO_4$ and concentrated under reduced pressure. The crude product was purified by silica gel column chromatography yielding 3-amino-3-(*p*-tolyl)acrylonitrile **55** (1.83 g, 68%) as white crystalline solid. R_f (50% EtOAc/hexane) 0.48. **^{1}H NMR (300 MHz, $CDCl_3$):** δ 7.38 (2H, d, *J*=6.3 Hz, H3 and H3'), 7.20 (2H, d, *J*=7.8 Hz, H4 and H4'), 5.07 (2H, s, H7), 4.16 (1H, s, H8), 2.35 (3H, s, H1). **^{13}C NMR (75 MHz, $CDCl_3$):** δ 161.8 (C-6), 141.3 (C-2), 132.4 (C-5), 129.6 (C-3 and C-3'), 125.9 (C-4 and C-4'), 119.9 (C-9), 62.4 (C-8), 21.3 (C-1) (lit. Chhiba *et al*).[44] **IR (v_{max} /cm^{-1}):** 2230 (C≡N), 1670 (C=C), 3350 (N-H), 1100 (C-N).

2.6.4 Synthesis of 3-amino-3-(*p*-tolyl)propanenitrile 56c[44]



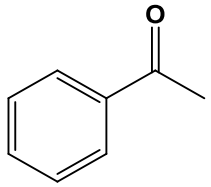
56c

3-Amino-3-(*p*-tolyl)acrylonitrile **55** (0.20 g, 1.27 mmol) was dissolved in ethanol (5 ml). Sodium cyanoborohydride (86.18 mg, 1.39 mmol) was added, followed by bromocresol green (1 drop of 0.5% solution in ethanol). Concentrated HCl (32%) was added dropwise until the solution gave a permanent yellow colour. The reaction was allowed to stir at

room temperature for 3 h. Water (3 mL) was added, followed by concentrated aqueous ammonia (25%) to pH 11. The aqueous solution was extracted with diethyl ether (3 × 5 mL). The combined organic layers were dried over $MgSO_4$ and concentrated under reduced pressure. The crude product was purified by silica gel column chromatography yielding 3-amino-3-(*p*-tolyl)propanenitrile **56c** (0.10 g, 50%) as a yellow oil. R_f (60% EtOAc/hexane) 0.43. **^{1}H NMR (300 MHz, $CDCl_3$):** δ 7.25 (2H, d, *J* = 8.1 Hz, H3 and H3'), 7.16 (2H, d, *J* = 8.0 Hz, H4 and H4'), 4.30 – 4.22 (1H, m, H6), 2.62 (2H, dd, *J* = 6.4, 4.1 Hz, H8), 2.33 (3H, s, H1), 1.71 (2H, s, H7). **^{13}C NMR (75 MHz, $CDCl_3$):** δ 139.1 (C-5), 137.4 (C-2), 129.1 (C-3 and C-3'), 125.4 (C-4 and C-4'), 117.6 (C-7), 51.9 (C-5), 28.0 (C-6), 20.6 (C-9) (lit. Chhiba *et al*[44]). **IR (v_{max} /cm^{-1}):** 3400 (N-H), 2220 (C≡N), 1594 (C=C), 1250 (C-N). **HRMS *m/z***: calculated for $C_8H_{13}N$: 161.1035 *m/z*, observed: $[M+H]^+$ 161.1067 *m/z*.

2.7 General Synthetic procedure using transaminases

2.7.1 Preparative scale biotransformation of methylbenzylamine using pyruvate amine acceptor



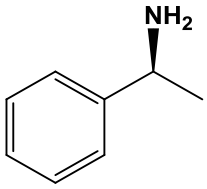
58

All biocatalysis reactions were performed at 30°C for 12 h in HEPES buffer (100 mM, pH 7.5) containing PLP (2 mM) in a round bottom flask (50 mL). Methylbenzylamine **57** substrate at various concentrations (10 mM, 20 mM, 50 mM, 100 mM and 250 mM) was dissolved in 15% v/v DMSO and added to the buffer solution (8.50 mL) containing transaminase (5 mg) with amine acceptor pyruvate (10 mM). The reaction mixture was agitated at 30°C with the use of TLC and HRMS to monitor the generation of the ketone product. The reaction was quenched by the addition of sodium hydroxide (15 mL, 5 M) followed by the extraction using ethyl acetate (3 × 15 mL). The organic layers were combined, dried over $MgSO_4$ and concentrated under reduced pressure yielding a trace amount of the product **58**. **HRMS *m/z***: calculated for C_8H_9O: 121.0609, observed: $[M+H]^+$ 121.0656.

2.7.2 Reductive amination of ketone substrates using LDH/GDH pyruvate removal system

The biotransformation reactions were performed at 30°C in a 2 mL Eppendorf tube. Transaminase (2 mg) and PLP (2 mM) were rehydrated in HEPES buffer (850 µL) pH 7.5. The amine donor L-alanine (250 mM) was added to the enzyme solution and allowed to equilibrate for 2 h. Corresponding ketone substrate (50 mM) was dissolved in 15% v/v DMSO (150 µL), pyruvate reductase mix (=LDH/GDH mix) (40 mg, mixture of lactate dehydrogenase, glucose dehydrogenase, glucose, NAD^+), were added to the solution and the reaction mixture was allowed to stir at 30°C for 24 h. The progress of the reaction was monitored by TLC. The reaction was quenched by the addition of aqueous NaOH solution (200 µL, 5 M), followed by extraction with ethyl acetate (3 × 500 µL). The combined organic layers were dried over $MgSO_4$ and concentrated under reduced pressure. The reactions were monitored by HRMS.

2.7.2.1 Asymmetric synthesis of methylbenzylamine 57 using LDH/GDH mixture



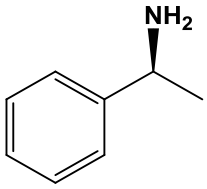
57

To a buffer solution containing PLP (2 mM), LDH/GDH mix, L-alanine (250 mM) and transaminase (2 mg) was added acetophenone (50 mM) **58** dissolved in DMSO. The reactions yielded trace amounts of products **57**. **HRMS *m/z***: calculated for $C_8H_{12}N$: 122.0925 *m/z*, observed: $[M+H]^+$ 122.0964 *m/z*.

2.7.3 Preparative scale reductive amination of ketone substrates using diamine donor or amine donor

All biocatalysis reactions were performed at 30°C for 24 h in HEPES buffer (100 mM, pH 7.5) containing PLP (2 mM) in a round bottom flask (50 mL). The corresponding ketone substrate at various concentrations (10 mM, 20 mM, 50 mM, 100 mM) was dissolved in 15% v/v DMSO and added to the buffer solution (8.50 mL) containing omega-transaminase (5 mg) with diamine donor **7** (1.1 equiv). For comparison, L-alanine (50 mM, 10 equiv, 100 mM, 20 equiv or 250 mM, 45 equiv) and isopropylamine (100 mM, 20 equiv or 250 mM, 45 equiv) were also tested as amine donor under the same reaction conditions. The reaction mixture was agitated at 30°C for 24 h and with the use of TLC to monitor the generation of the amine product. The reaction was quenched by the addition of sodium hydroxide (15 mL, 5 M) followed by the extraction using ethyl acetate (3 × 15 mL). The organic layers were combined, dried over $MgSO_4$ and concentrated under reduced pressure.

2.7.3.1 Asymmetric synthesis of methylbenzylamine 57 using L-alanine as amine donor



57

To a buffer solution containing PLP (2 mM), various concentrations of L-alanine (50 mM, 10 equiv, 100 mM, 20 equiv or 250 mM, 45 equiv) and transaminase (5 mg) was added various concentrations of acetophenone **58** dissolved in DMSO. The reactions were monitored by HRMS and no product was detected.

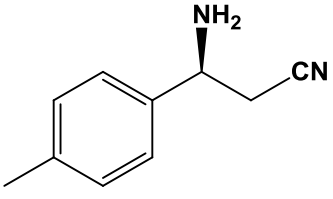
2.7.3.2 Asymmetric synthesis of methylbenzylamine 57 using Isopropylamine as amine donor

To a buffer solution containing PLP (2 mM), various concentrations of Isopropylamine (100 mM, 250 mM) and transaminase (5 mg) was added various concentrations of acetophenone **58** dissolved in DMSO. The reactions were monitored by HRMS and no product was detected.

2.7.3.3 Asymmetric synthesis of methylbenzylamine 57 using diamine donor

To a buffer solution containing PLP (2 mM), various concentrations of diamine donor (1.1 equiv) and transaminase (5 mg) was added various concentrations of acetophenone **57** dissolved in DMSO. The reactions yielded trace amounts of products **58**. **HRMS *m/z***: calculated for $C_8H_{12}N$: 122.0925 *m/z*, observed: $[M+H]^+$ 122.0966 *m/z*.

2.7.3.4 Asymmetric synthesis of 3-amino-3-(*p*-tolyl)propanenitrile 56c using diamine donor



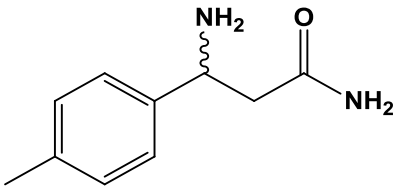
56c

To a buffer solution containing PLP (2 mM), various concentrations of diamine donor and enzyme (5 mg) was added to various concentrations of 3-oxo-3-(*p*-tolyl)propanenitrile **54c** in DMSO. The reactions yielded trace amounts of products. **HRMS *m/z***: calculated for $C_{10}H_{13}N_2$: 161.1035 *m/z*, observed: $[M+H]^+$ 161.1075 *m/z*.

2.8 Procedure for hydrolysis of nitrile substrates using nitrile hydratase

The hydrolysis test was conducted at 30°C for 24 h in Tris-buffer (100 mM, pH 9) in a 2 mL-Eppendorf tubes. The corresponding nitrile substrate (20 mM) was dissolved in methanol 10% v/v and added to the buffer (850 µL) containing nitrile hydratase *Rhodococcus rhodochrous* ATCC BAA-870 (5 mg). After 24 h the reaction was stopped by centrifugation at 10 000 rpm × 15 min followed by extraction of the supernatant with ethyl acetate (3 × 500 µL). The organic layers were brine washed before combined and dried over $MgSO_4$. The product was not isolated.

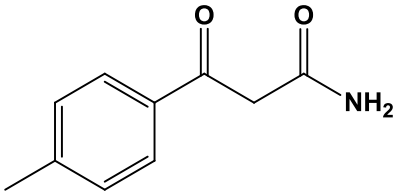
2.8.1 Synthesis of 3-amino-3-(*p*-tolyl)propanamide 65[44]



65

To a buffer solution containing nitrile hydratase (2 mg) was added 3-amino-3-(*p*-tolyl)propanenitrile (20 mM) dissolved in methanol. The reaction mixture was incubated at 30°C. The reaction mixture was monitored by TLC and HRMS yielding trace amounts of the product as detected by HRMS. **HRMS *m/z***: Calculated for $C_{10}H_{14}N_2O$: 179.1140 *m/z*, observed: $[M+H]^+$ 179.1181 *m/z*.

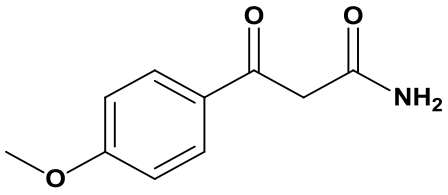
2.8.2 Synthesis of 3-oxo-3-(*p*-tolyl)propanamide 66c



66c

To a buffer solution containing nitrilehydratase (2 mg) was added 3-oxo-3-(*p*-tolyl)propanenitrile (20 mM) dissolved in methanol. The reaction mixture was incubated at 30°C. The reaction mixture was monitored by TLC and HRMS. The reaction mixture was not isolated. **HRMS *m/z***: Calculated for $C_{10}H_{12}NO_2$: 178.0823 *m/z*, observed: $[M+H]^+$ 178.0861 *m/z*.

2.8.3 Synthesis of 3-(*p*-methoxyphenyl)-3-oxopropanamide 66d



66d

To a buffer solution containing nitrilehydratase (2 mg) was added 3-(*p*-methoxyphenyl)-3-oxopropanenitrile (20 mM) dissolved in methanol. The reaction mixture was incubated at 30°C. The reaction mixture was monitored by TLC and HRMS. **HRMS *m/z***: Calculated for $C_{10}H_{12}NO_3$: 194.0772 *m/z*, observed: $[M+H]^+$ 194.0809 *m/z*.

2.9 Synthetic procedure for wound healing peptides

Manual solid phase peptide synthesis (SPPS) was carried out in a reaction vessel under inert nitrogen gas atmosphere. 2-Chlorotrityl resin (500 mg) was weighed into two different tubes. The resins were first activated by reacting them with thionyl chloride (1 mL) and dry DCM (10 mL). After filtering and washing the resins with dry DCM, the first amino acid Fmoc-Gly (0.70 g, 4 equiv) was attached to the resin through the carboxylic-terminal. The amino acid was first dissolved in dry DCM (10 mL). This solution (5 mL) was added to the resin (500 mg) with DIPEA (1.74 mL) and the reaction was gently mixed by bubbling nitrogen for 45 min. The reaction was filtered and the resin was washed with DMF (3 × 5 mL) followed by DCM (3 × 5 mL) and DMF (3 × 5 mL) to remove excess reagents and byproducts.

The Fmoc group is removed by the piperidine and that is how the loading capacity is measured. The loading capacity of the resin-Gly was determined by weighing duplicate samples of 10 mg loaded resin into Eppendorf tubes, 20 % piperidine/DMF (1 mL) was added and shaken for 20 min, then centrifuged for 5 min. The supernatant solution (100 µL) was added to a vial containing DMF (10 mL). Pure DMF (2 mL) was pipetted into each of two cells (reference and sample cell) and the spectrophotometer was set to zero. The sample cell was emptied and the solution containing the sample (2 mL) was

transferred to the sample cell, and the absorbance observed three times at 301 mm. These absorbance were used to calculate the theoretical yields.

The stock solution of 1M DIPEA in DMF was prepared. HBTU (7.58 g, 0.2 M) was added into 100 mL of DMF to prepare the stock solution. The other stock solution prepared was 20% piperidine in DMF.

The resin-Gly was filtered and washed with DMF (3 × 5 mL). The 20% piperidine solution (10 mL) was added to the resin to remove the Fmoc protecting group for 15 minutes and after which the resin was washed with DMF (3 × 5 mL) followed by DCM (3 × 5 mL) and DMF (3 × 5 mL) to remove excess reagents.

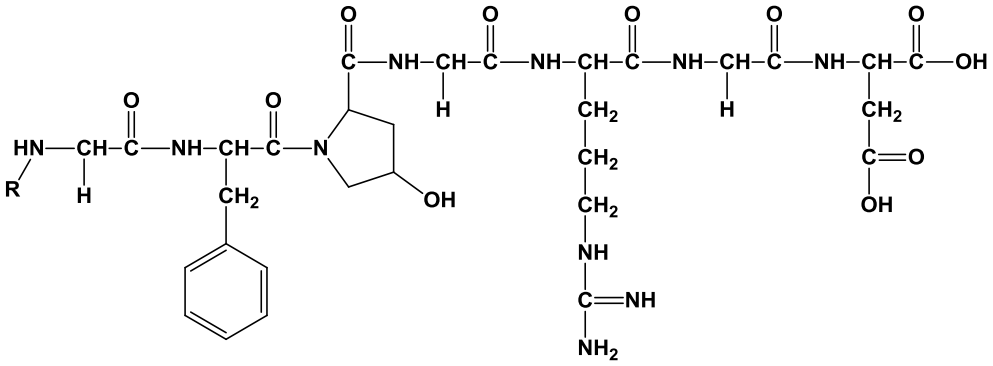
The next amino acid coupled to the resin-bound glycine was Fmoc-Phe (0.78 g, 0.2 M). The amino acid (5 mL) was added to the resin along with the coupling reagent HBTU (5.00 mL) and DIPEA (5 mL) from their stock solutions and bubbled for 45 min. This was followed by another washing which leaves the resin-bound peptide ready for another coupling cycle. The amino acids used to complete the cycle were Fmoc-Hyp (0.82 g, 0.2 M), Fmoc-Gly (0.60 g, 0.2 M), Fmoc-Arg (1.29 g, 0.2 M), Fmoc-Gly (0.60 g, 0.2 M) and Fmoc-Asp (0.83 g, 0.2 M), sequentially. The coupling and washing procedures were the same as the one described above. All the protecting groups were then deprotected and the resin-bound peptide cleaved from the resin (as described below) to afford **60a**. The compounds obtained by replacing phenylalanine with β-aromatic amino acids were **61a**, **61d** and **61g**.

The resin-bound peptides were modified by attaching adamantane and palmitic acid. The palmitic acid (0.512 g, 0.2 M) and adamantane (0.36 g, 0.2 M) were dissolved in DMF (10 mL). These solutions were added to the resin-bound peptides followed by HBTU (5 mL) and DIPEA (5 mL) to afford **60b**, **61b**, **61e**, **61h** and **60c, 61c, 61f, 61i**. The deprotection and washing procedures were similar to the one above.

The cleavage of the peptide from the resin was performed by adding a solution containing 95% TFA, 2.5 % water and 2.5 % TIS, and left to shake overnight. The resin was first vacuum dried before being transferred to a tube containing a 10 mL TFA solution. The resin was filtered, and cold ether was poured into the filtered solution. The solution was centrifuged for five minutes at 5000 rpm and the liquid was transferred into waste leaving a precipitate. The precipitate was centrifuged with ether an additional three times leaving the cleaved peptide which was analysed using mass spectroscopy. The precipitated peptides were filtered and small amounts of each peptide were dissolved in acetonitrile and a few drops of formic acid for the mass spectral analysis by HRMS. The following peptides were synthesised:

2.9.1 α-Peptides 60

The peptide was purified by HLPC yielding **60a** (10%). **HRMS *m/z***: calculated for $C_{30}H_{45}N_{10}O_{11}$: 721.3225, observed: $[M+H]^+$ 721.2547 *m/z*. To a resin-bound peptide **60a** was coupled palmitic acid (0.51 g, 0.2 M) resulting in **60b**. **HRMS *m/z***: calculated for $C_{46}H_{75}N_{10}O_{12}$: 959.5521, observed: $[M+H]^+$ 959.5733 *m/z*. To a resin-bound peptide **60a** was coupled adamantane (0.36 g, 0.2 M) resulting in **60c**. **HRMS *m/z***: calculated for $C_{41}H_{59}N_{10}O_{12}$: 883.4269, observed: $[M+H]^+$ 883.4365 *m/z*.



60

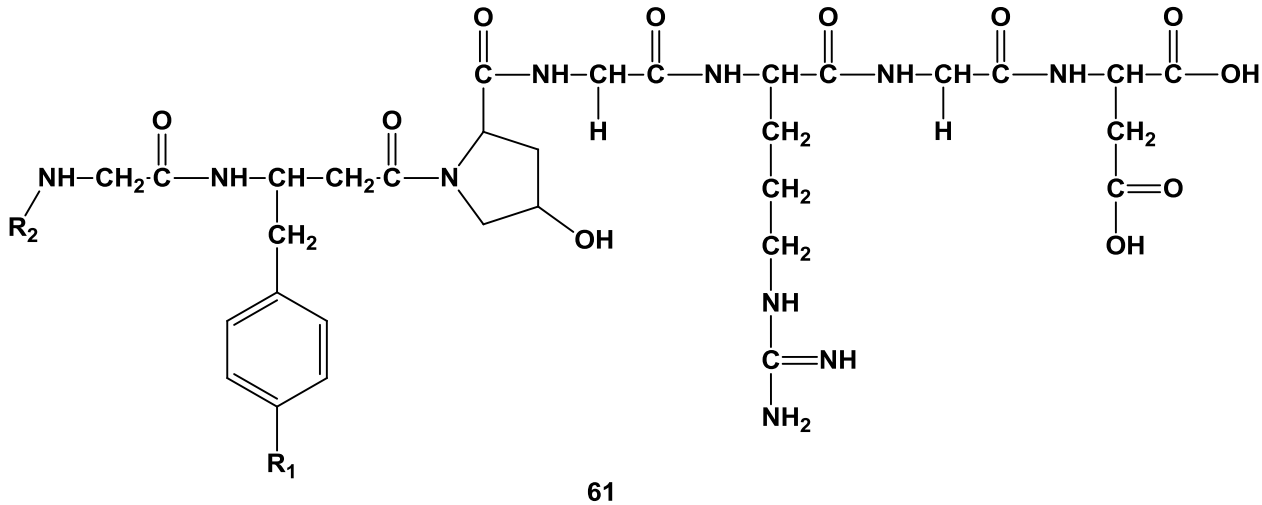
Table 1. The α-peptides derivatives along with their observed masses and yields

Compound	Sequence	R	Calculated mass	Observed mass (*m/z*)	Molecular ion	Yield
60a	G-F-O-G-R-G-D	H	721.3225 $C_{30}H_{45}N_{10}O_{11}$	721.2547	$[M+H]^+$	10%
60b	G-F-O-G-R-G-D-Pal	Palmitic	959.5521 $C_{46}H_{75}N_{10}O_{12}$	959.5733	$[M+H]^+$	-
60c	G-F-O-G-R-G-D-Ada	Adamantane	883.4269 $C_{41}H_{59}N_{10}O_{12}$	883.4365	$[M+H]^+$	-

(-) = Yields not available because peptide was not purified

2.9.2 β-Peptides 61

The synthesis of the rest of the β-peptides and coupling of adamantane and palmitic followed similar procedure as in Section 2.9.1.



61

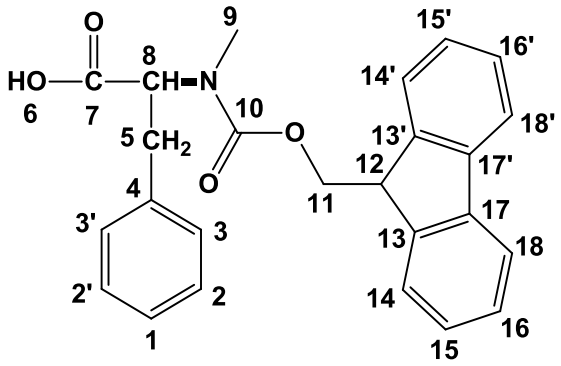
Table 2. The β-amino acid containing peptides derivatives along with their observed mass and yields

Compound	Sequence	R_1	R_2	Calculated mass	Observed mass (*m/z*)	Molecular ion	Yield (%)
61a	G-βPhe-O-G-R-G-D	H	H	735.3381 $C_{31}H_{47}N_{10}O_{11}$	677.3221	[M-Glycine]$^+$	-
61b	G-βPhe-O-G-R-G-D-Pal	H	Palmitic	973.5678 $C_{47}H_{77}N_{10}O_{12}$	973.5709 and 973.5734	$[M+H]^+$	17
61c	G-βPhe-O-G-R-G-D-Ada	H	Adamantane	897.4426 $C_{42}H_{61}N_{10}O_{12}$	897.4424	$[M+H]^+$	13
61d	G-β(Me)Phe-O-G-R-G-D	Me	H	749.3538 $C_{32}H_{49}N_{10}O_{11}$	749.3552	$[M+H]^+$	20

61e	G-β(Me)Phe-O-G-R-G-D-Pal	Me	Palmitic	987.5834 $C_{48}H_{79}N_{10}O_{12}$	987.5906	$[M+H]^+$	-
61f	G-β(Me)Phe-O-G-R-G-D-Ada	Me	Adamantane	911.4582 $C_{43}H_{63}N_{10}O_{12}$	911.4675	$[M+H]^+$	-
61g	G-β(Flu)Phe-O-G-R-G-D	Flu	H	753.3287 $C_{31}H_{46}FN_{10}O_{11}$	753.3288 and 753.3254	$[M+H]^+$	18
61h	G-β(Flu)Phe-O-G-R-G-D-Pal	Flu	Palmitic	991.5584 $C_{47}H_{76}FN_{10}O_{12}$	991.5626	$[M+H]^+$	-
61i	G-β(Flu)Phe-O-G-R-G-D-Ada	Flu	Adamantane	915.4332 $C_{42}H_{60}FN_{10}O_{12}$	961.4468	[M+formic acid+ H]$^+$	-

(-) = Yields not available because peptide was not purified, βPhe = 3-amino-4-phenylbutanoic acid; β(Me)Phe = 3-amino-4-(p-tolyl)butanoic acid; β(Flu)Phe = 3-amino-4-(4-fluorophenyl)butanoic acid; Flu = Fluorine

2.10 Synthesis of 2-((((9H-fluoren-9-yl)methoxy)carbonyl)(methyl)amino)-3-phenylpropanoic acid (Fmoc-*N*-α-MePhe-OH) 62



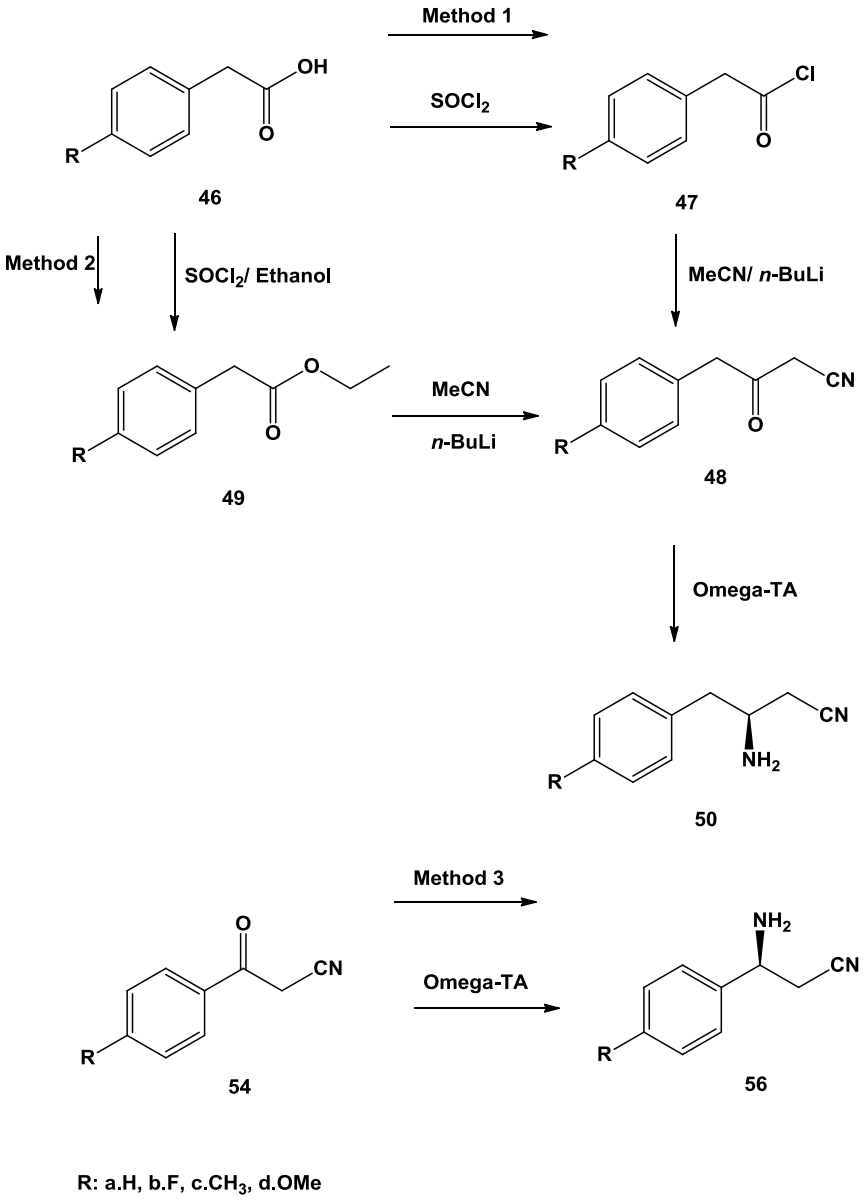
Fmoc-α-Phe-OH (4.67 g, 12.04 mmol) was added to a solution of toluene (40 mL) with paraformaldehyde (2.40 g, 79.92 mmol) and PTSA (0.12 g, 0.69 mmol). The mixture was refluxed for 35 min using a dean stark apparatus. After cooling the solution, was washed with 1M $NaHCO_3$ (3 × 15 mL) and dried using $MgSO_4$. The dried solution (oxazolidinone) was concentrated on the rotary evaporator. The oxazolidinone was dissolved in dry DCM (18 mL), and TFA (18 mL) and TIS (3 mL) were added. The solution was stirred for 24 h under room temperature followed by concentration under reduced pressure to an oil. The TLC (1: 3/2 hexane: ethyl acetate) was used to confirm completion of reaction. The oil was dissolved in ether and concentrated three times. The crude product was purified by silica gel column chromatography yielding Fmoc-*N*-*α*-(Me)PHe-OH **62** (3.62 g, 75%) as a yellow oil. The resulting product Fmoc-*N*-α-(Me)Phe-OH was dissolved in acetonitrile for mass spectral analysis. **^{1}H NMR (300 MHz, $CDCl_3$):** δ 11.19 (1H, s, H6), 7.83 – 7.72 (2H, m, H18 and H18'), 7.53 (2H, m, H14 and H14'), 7.41 (2H, m, H2 and H2'), 7.25 (6H, m, H3 , H3', H16 and H16', H18 and H18'), 6.99 (1H, m, H1), 5.01 (1H, dd, *J* = 711.50 Hz, H8), 4.62 (1H, d, *J* = 19.1 Hz, H11), 4.39 (2H, t, *J* = 6.72 Hz, H12), 3.46 - 3.13 (2H, m, H5), 2.85 (3H, s, H9). **^{13}C NMR (75 MHz, $CDCl_3$):** δ 175.7 (C-7), 156.4 (C-10), 143.6 (C-13 and C-13'), 140.9 (C-17 and C-17'), 136.5 (C-4), 128.4 (C-2 and C-2'), 127.3 (C-3 and C-3'), 126.7 (C-16 and C-16'), 126.7 (C-18 and C-18'), 126.5 (C-1), 124.7 (C-15 and C-15'), 119.6 (C-14 and C-14'), 67.5 (C-8), 67.2 (C-11), 46.7 (C-12), 34.3 (C-5), 31.9 (C-9) (lit. Di Gioia *et al*).[116] **HRMS *m/z***: calculated for $C_{25}H_{24}NO_4$: 402.1661, observed: $[M+H]^+$ 402.1670.

3. RESULTS AND DISCUSSION

The aim of this project was to synthesise enantiopure β-amino acids for incorporation into peptides, thereby moderating their activity as well as their stability to cellular proteases. These peptides have potential for wound healing activity. The approach followed asymmetric biotransformation of the corresponding ketone substrates into enantiopure β-amino acids. The β-ketonitrile substrates were used instead of β-keto acids to eliminate the decarboxylation problem.

3.1 Approach towards synthesis of β-aminonitriles

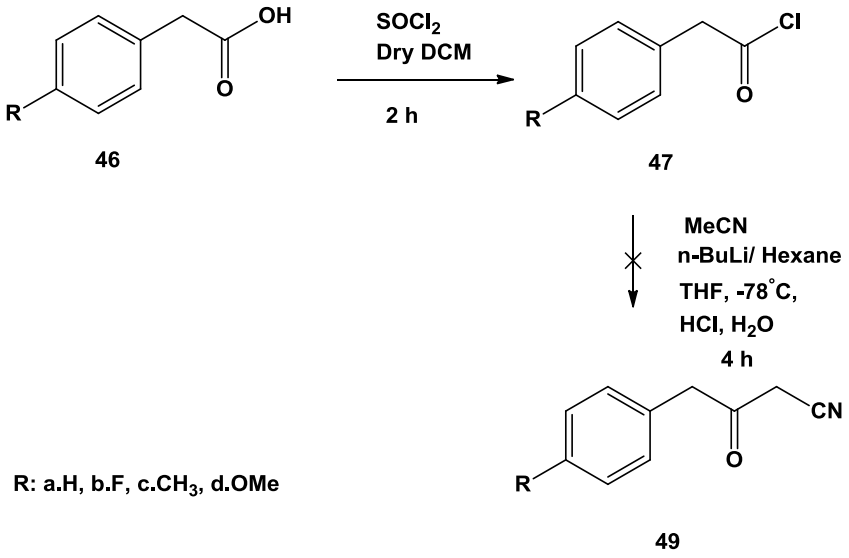
There were three proposed approaches towards the synthesis of the β-amino-nitriles (**Scheme 15**).



Scheme 15. Planned approach towards the synthesis of β-aminonitriles

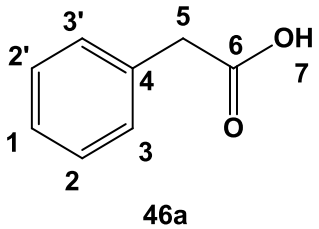
These approaches involved conversion of a carboxylic acid starting material into the corresponding acyl chloride or ester, followed by reaction with acetonitrile in the presence of *n*-BuLi to give the β-ketonitriles. The β-keto-nitrile substrates could then be converted into the corresponding β-amino-nitriles through a reductive amination process using transaminases (**Scheme 15**).

3.1.1 Attempted synthesis of β-ketonitriles via acyl chloride (*Method 1*)



Scheme 16. Proposed synthesis of *beta*-ketonitriles via acyl chloride.

The first proposed synthesis involved conversion of the carboxylic acid **46** into the corresponding acyl chloride **47**, followed by reaction with acetonitrile to give *beta*-ketonitrile **49** (**Scheme 16**). The application of $SOCl_2$ in the conversion of carboxylic acids **46** into acid chlorides **47** is commonly applied methodology.[117] Thionyl chloride was added to aromatic carboxylic acid 2-phenylacetic acid **46a** in dry DCM. The reaction was stirred at room temperature to yield the aromatic acyl chloride 2-phenylacetyl chloride **47a**, which was used without further purification. The purification was not performed to prevent the acid chloride undergoing hydrolysis due to the presence of water. The aromatic acyl chloride **47a** in dry THF was added to a solution of *n*-BuLi and acetonitrile at -78°C and the reaction mixture was stirred for 4 h. The lithiated acetonitrile should have acted as a nucleophile towards the acid chloride. However only the carboxylic acid **46a** was recovered in (0.87 g, 87%) and the reaction did not yield the product of interest **49a**.



46a

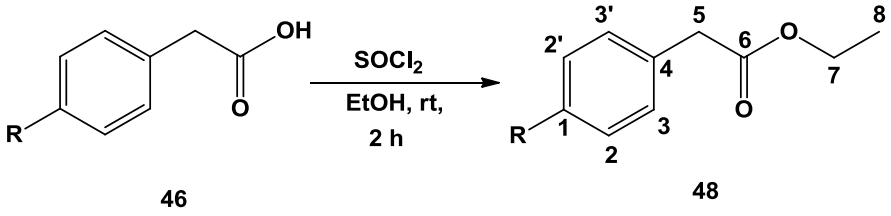
The undesired hydrolysis reaction was envisaged to have proceeded by the following steps. The HCl by-product, formed during the conversion of the aromatic carboxylic acid, reacted with the nucleophile generated through deprotonation of acetonitrile by *n*-BuLi

thereby preventing the conversion of the aromatic acyl chloride into the β-ketonitrile. In the work-up step the aromatic acyl chloride was then hydrolysed as water reacted with the highly electrophilic acyl carbonyl group to substitute the good leaving group, the chloride ion, to generate the carboxylic acid. The other plausible reason as to why the reaction did not work as expected could be that, a small amount base (usually DMF) was supposed to be added in the reaction and refluxed or stirring the carboxylic acid in neat $SOCl_2$ at room temperature.

Two aromatic signals were observed in the ^{1}H NMR spectrum of **46a**; a multiplet signal in the aromatic region between 7.36 and 7.21 ppm integrating for five protons that was assigned to H1, H2 and H3. The one singlet signal integrating for two protons, corresponding to a $-CH_2-$, that was assigned to H5 was observed in the aliphatic region at 3.64 ppm. The ^{13}C NMR spectrum of the starting material **46a** showed six signals in total as expected. The four signals observed in the aromatic region between 133.3 and 127.3 ppm belonged to C-1, C-2, C-3 and C-4. The peak observed at 177.9 ppm was assigned to the carbonyl carbon (C-6) and one singlet signal of $–CH_2-$ in the aliphatic region at 41.1 ppm was assigned to the C-5. Our results were in agreement with the results reported by Zhou *et al*.[118] However since method 1 did not yield the desired product, this approach was abandoned and an alternative route was developed.

3.1.2 Synthesis of β-ketonitriles via esters (*Method 2*)

3.1.2.1 Synthesis of esters from carboxylic acids



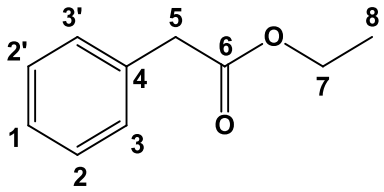
46 48

R: a.H (85%), b.F (89%), c.CH_3, (85%) d.OMe (80%)

Scheme 17. Esterification of aromatic carboxylic acids using thionyl chloride/ethanol

Having established that Method 1 did not yield the desired product, Method 2 was attempted for the synthesis of beta-ketonitriles via the ester substrates. One possible esterification method uses catalytic sulphuric acid in methanol/ethanol under reflux, however sometimes the yields are poor with this method.[119] We decided to use catalytic amounts of thionyl chloride in the presence of ethanol to convert carboxylic acids into corresponding esters (**Scheme 17**), following a known procedure reported by Jiabo *et al*.[120] Thionyl chloride was added to a solution of the aromatic carboxylic acid 2-

phenylacetic acid **46a** in ethanol. The reaction was allowed to stir at room temperature for 2 hours and was monitored by TLC. After the complete conversion, the crude product was purified yielding ethyl-2-phenylacetate **48a** (1.03 g, 85%).



48a

Our ^{1}H NMR data were in agreement with the data reported by Liu *et al*.[109] Four signals were observed in the ^{1}H NMR spectrum of **48a**. The multiplet signal in the aromatic region between 7.37 and 7.19 ppm was assigned to H1, H2 and H3. The three signals in the aliphatic region were observed as; a quartet signal integrating for two protons at 4.13 ppm assigned to H7, a singlet signal integrating for two protons at 3.59 ppm assigned to H5 and a triplet signal integrating for three protons at 1.23 ppm assigned to H8, a characteristic of methyl protons of the group. Eight signals were observed in the ^{13}C NMR spectrum of **48a** as expected. The four signals observed in the aromatic region between 134.2 and 127.0 ppm and one alkyl carbon (C-5) signal at 41.4 ppm resonated at similar chemical shifts as in the starting material. The signals at 60.80 ppm and 14.17 ppm were assigned to C-7 and C-8, respectively. The carbonyl signal was observed at 171.54 ppm, which was more upfield than in the starting material due to the electron donor ethoxy-functional group. These three signals confirmed the successful esterification of the aromatic acid **46a** using thionyl chloride in the presence of ethanol.

The other three analogues; ethyl 2-(*p*-fluorophenyl)acetate **48b**, ethyl 2-(*p*-tolyl)acetate **48c** and ethyl 2-(*p*-methoxyphenyl)acetate **48d** were prepared in a similar manner (**Scheme 17**). The ^{1}H NMR and ^{13}C NMR spectra of the products are similar. Therefore the important signals for the products are tabulated in **Table 3** and **4** below.

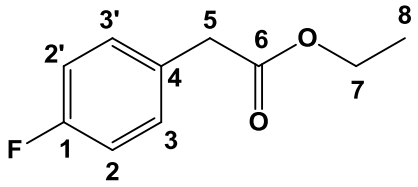
Table 3. Important signals in the ^{1}H NMR spectra of esters **48b-d**

Compound	Aromatic region (ppm)	Aliphatic region –CH_2- (ppm)	Aliphatic region –CH_3 (ppm)
48b	7.25 (2H, dd, *J* = 8.7, 5.4 Hz H3 and H3'), 7.01 (2H, t, *J* = 8.7 Hz H2 and H2')	4.16 (2H, q, *J* = 7.1 Hz, H7)	1.25 (3H, t, *J* = 7.1 Hz, H8)

48c	7.13 (2H, d, *J* = 6.6 Hz, H4 and H4'), 7.06 (2H, d, *J* = 7.1 Hz, H3 and H3')	4.08 (2H, q, *J* = 7.1 Hz, H8)	1.18 (3H, t, *J* = 7.2 Hz, H9)
48d	7.18 (2H, d, *J* = 8.7 Hz, H4 and H4'), 6.84 (2H, d, *J* = 8.7 Hz, H3 and H3')	4.12 (2H, q, *J* = 7.1 Hz, H8)	1.23 (3H, t, *J* = 7.1 Hz, H9)

Table 4. Important signals in the ^{13}C NMR spectra of esters **48b-d**

Compound	Carbonyl carbon (ppm)	Methylene carbon (ppm)	Methyl carbon (ppm)
48b	171.8 (C-6)	61.3 (C-7)	14.5 (C-8)
48c	171.8 (C-7)	60.8 (C-8)	14.3 (C-9)
48d	171.1 (C-7)	59.9 (C-8)	13.4 (C-9)

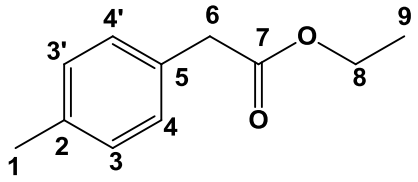


48b

In the ^{1}H NMR spectrum of **48b**, two signals were observed in the aromatic region; a doublet of doublets integrating for two protons at 7.13 ppm assigned to H3 and a triplet signal integrating for two protons at 7.01 ppm assigned to H2 (**Table 3**). The ^{1}H NMR data matched those reported by Song *et al*.[111] For example, the doublet of doublets and triplet signals were also observed by Song and co-workers. These signals were due to the hydrogen-fluorine coupling,[121] whereby the H3 proton at the *meta*-position to the fluorine and *ortho*-position to H2 was split into a doublet of doublets. The H2 proton in the *ortho*-position to the fluorine was spilt into a triplet (**Table 3**). The two signals observed in the aliphatic region at 4.16 ppm and 1.25 ppm (**Table 3**), confirmed the successful esterification reaction of the carboxylic acid into ethyl 2-(*p*-fluorophenyl)acetate **48b**. The two aliphatic carbon signals in the ^{13}C NMR spectrum also validated the successful synthesis of the ester compound **48b** (1.09 g, 89%). The methylene carbon signal was observed at 61.3 ppm assigned to C-7 and the methyl carbon signal was also observed at 14.5 ppm (**Table 4**). Our spectroscopic (^{13}C NMR)

data also match those reported by Songs *et al*.[111] The ester carbonyl carbon we observed at 171.8 ppm assigned to C-6 it was in agreement with the ^{13}C NMR data reported by Songs and co-workers.

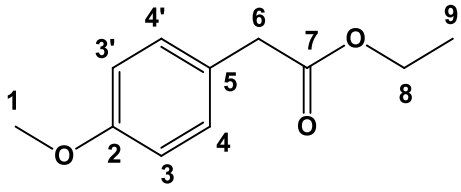
After the successful synthesis of **48b**, the substrate where the aromatic substituent is a methyl-group was used in the synthesis of ethyl 2-(*p*-tolyl)acetate **48c** (1.00 g, 85%).



48c

In the ^{1}H NMR spectrum of **48c**, two signals were observed in the aliphatic region. The quartet signal at 4.08 ppm integrating for two protons was assigned to H8 and the triplet signal at 1.18 ppm integrating for three protons was assigned to H9 (**Table 3**). The successful synthesis of **48c** was also confirmed by ^{13}C NMR spectroscopy, whereby two signals were observed in the aliphatic region. The aliphatic methylene carbon signal was observed at 60.8 ppm and assigned to C-8. The methylene carbon at C-8 is bonded directly to the oxygen atom whereas the methylene carbon at C-6 is bonded to the carbonyl carbon. Therefore, the C-8 signal would be more downfield at 60.8 ppm than the methylene carbon at 41.1 ppm assigned to C-6 due to the electron-withdrawing oxygen atom (**Table 4**). These spectroscopic NMR data were in agreement with the literature data reported by Song and co-workers.[111]

The last ester compound synthesised was **48d** (0.93 g, 80%), where the aromatic substituent was a methoxy-group (an electron donating group).



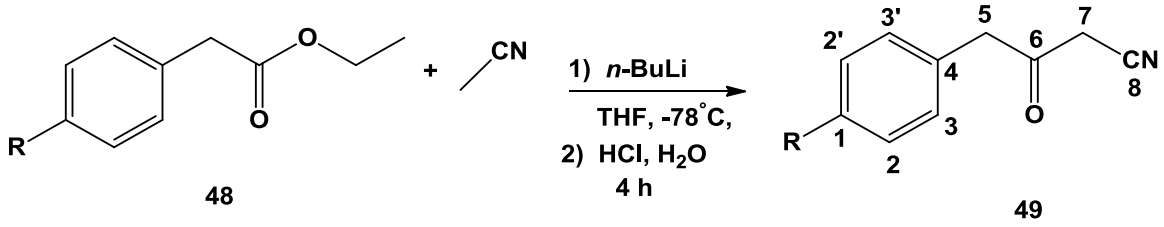
48d

Two signals were observed in the aliphatic region from the ^{1}H NMR spectrum of **48d**. The quartet signal at 4.12 ppm integrating for two protons was assigned to H8 and the triplet signal at 1.23 ppm integrating for three protons was assigned to H9 (**Table 3**). In the ^{13}C NMR spectrum of **48d**, two signals were observed in the aliphatic region at 59.9 ppm (a characteristic of methylene carbon) and at 13.4 ppm (a characteristic of methyl

carbon) assigned to C-8 and C-9, respectively (**Table 4**). These NMR data match those reported by Song and co-workers.[111]

The ester products **48a-d** were successfully synthesised and isolated in good yield, therefore the second step was performed where acetonitrile would be reacted with **48a-d** in the presence of *n*-BuLi to give the β-ketonitriles **49a-d**.

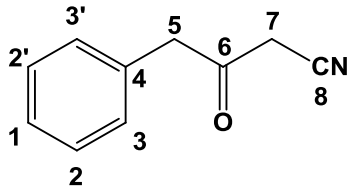
3.1.2.2 Synthesis of *beta*-ketonitriles from esters



R: a.H (78%), b.F (82%), c.CH_3 (73%), d.OMe (79%)

Scheme 18. Synthesis of β-ketonitriles from ester precursors

The esters (**48a-d**) obtained were used in the synthesis of the nitriles **49a-d** in the presence of lithitated acetonitrile. The reaction of ester **48a** using *n*-butyllithium in the presence of dry acetonitrile yielded the β-ketonitrile **49a** (**Scheme 18**). The reaction was conducted under nitrogen atmosphere for 4 h. The reaction required constant monitoring to keep the temperature at -78°C because at elevated temperatures, the formation of the lithiated acetonitrile is difficult. The nucleophilic carbon attached to the lithium metal reacts strongly with the nitrile group, thereby generating by-products.[122] The reaction was quenched by addition of HCl/H_2O to the reaction mixture. The crude product was purified by silica gel column chromatography to yield 3-oxo-4-phenylbutanenitrile **49a** (0.61 g, 78%).



49a

In the ^1H NMR spectrum of product **49a**, there were significant differences observed as compared to the starting material **48a**. The quartet and triplet signals due to the

methylene and methyl group, respectively, which were observed in the starting material were not observed in the ^{1}H NMR spectrum of the product **49a** NMR. Two signals were observed in the aromatic region; a multiplet signal at 7.35 – 7.25 ppm was assigned to H1 and H2, and a doublet signal at 7.15 ppm was assigned to H3. The new singlet signal integrating for two protons observed at 3.77 ppm was assigned to H7. The singlet signal at 3.46 ppm was assigned to H5.

The two methyl-group carbon signals were not observed in the ^{13}C NMR spectrum of the product, indicating that the ester was no longer present. The successful synthesis of **49a** was further confirmed when two new carbon signals were observed at 31.7 ppm and at 114.4 ppm assigned to C-7 and C-8 which corresponded to the methylene carbon (–**C**H_2-CN) and the nitrile-group, respectively. There was a significant shift of the carbonyl carbon signal from 171.54 ppm to 196.21 ppm assigned to C-6 and a shift of the methylene carbon (Ar-CH_2-) from 41.43 ppm to 49.33 ppm assigned to C-5. The carbonyl was now a ketone signal, rather than an ester carbonyl. Our spectroscopic NMR data are in agreement with those reported by Foehlisch and co-workers.[112] The IR spectrum was also used to confirm the successful synthesis of the product with the C≡N stretching band visible at 2225 cm^{-1}.

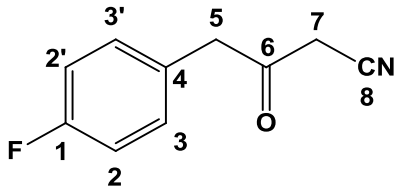
The other three analogues; 4-(4-fluorophenyl)-3-oxobutanenitrile **49b**, 3-oxo-4-(*p*-tolyl)butanenitrile **49c** and 4-(*p*-methoxyphenyl)-3-oxobutanenitrile **49d** were prepared in a similar manner (**Scheme 18**). The products' ^{1}H NMR and ^{13}C NMR spectra were similar. Therefore the key signals are tabulated in **Tables 5** and **6** below.

Table 5. Important signals in the ^{1}H NMR spectra of *beta*-ketonitriles **49b-d**

Compound	Ar-C**H_2**- (ppm)	-C**H_2**-CN (ppm)
49b	3.53 (2H, s, H5)	3.82 (2H, s, H7)
49c	3.73 (2H, s, H8)	3.47 (2H, s, H6)
49d	3.74 (2H, s, H8)	3.49 (2H, s, H6)

Table 6. Important signals in the ^{13}C NMR spectra of *beta*-ketonitriles **49b-d**

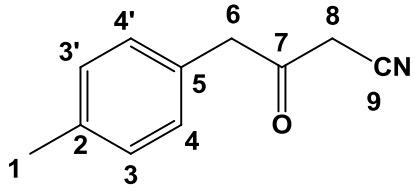
Compound	Carbonyl carbon (ppm)	CN (ppm)	Ar-**C**H_2- (ppm)	-**C**H_2-CN (ppm)
49b	195.1 (C-6)	113.4 (C-8)	47.6 (C-5)	31.0 (C-7)
49c	196.5 (C-7)	114.5 (C-9)	48.9 (C-6)	31.5 (C-8)
49d	195.7 (C-7)	114.1 (C-9)	47.8 (C-6)	30.7 (C-8)



49b

A new singlet signal was observed in the ^{1}H NMR spectrum of **49b**. This signal was due to the methylene protons at 3.82 ppm integrating for two protons assigned to H7 (**Table 5**). The ^{13}C NMR spectrum of **49b** validated the successful substitution of the ethoxy group with the nucleophilic lithiated acetonitrile, as the CN signal was observed at 113.4 ppm assigned to C-8 (**Table 6**). A new signal was also observed at 31.0 ppm assigned to C-7, a characteristic of the methylene carbon (-CH_2-CN) (**Table 6**). The stretching band at 2220 cm^{-1} in the IR spectrum, shows the presence of the nitrile group, therefore confirming the successful synthesis of **49b** (0.64 g, 82%).

The next β-ketonitrile synthesised was 3-oxo-4-(*p*-tolyl)butanenitrile **49c** (0.57 g, 73%) with the fluorine now replaced by a methyl group.

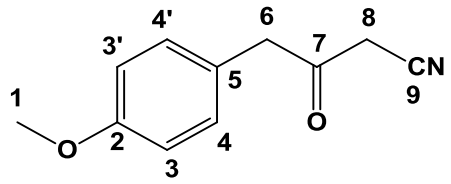


49c

Similarly for **49c**, the quartet and triplet signal in both ^{1}H NMR and ^{13}C NMR spectra had disappeared. A new singlet signal was observed in the ^{1}H NMR spectrum at 3.47 ppm (**Table 5**), a characteristic of the H8 methylene protons (-CH_2-CN). Just as in the ^{13}C NMR spectra of **49a** and **49b**, both the carbonyl carbon and methylene carbon (Ar-CH_2-)

shift downfield to 196.5 ppm and 48.9 ppm, respectively (**Table 6**). The new signal observed at 114.5 ppm, is characteristic of the nitrile group (C-9). The IR spectrum confirmed the success of the reaction as the CN stretching band was observed at 2210 cm^{-1}.

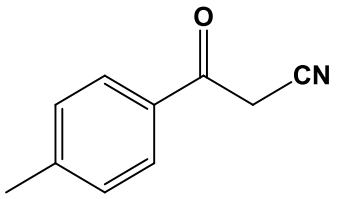
Lastly, the 4-(*p*-methoxyphenyl)-3-oxobutanenitrile **49d** (0.66 g, 79%) was prepared in a similar manner where the aromatic substituent was now a methoxy group.



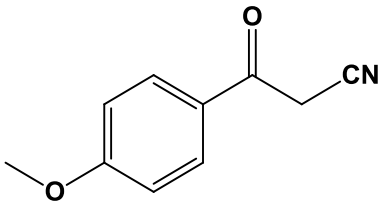
49d

In the ^{1}H NMR spectrum of **49d**, a singlet signal was observed in the aliphatic region at 3.49 ppm integrating for two protons assigned to H8. Similarly for product **49d**, both the ketone carbonyl and the methylene carbon (Ar-CH_2-) signals shift downfield to 195.7 and 47.8 ppm, respectively. The new signal at 114.1 ppm assigned to C-9 was due to the nitrile carbon whereas the other new signal at 30.7 ppm was due to the methylene carbon at C-8 (-**C**H_2-CN). Our NRM spectroscopic data match those reported by Katritzky and co-workers.[113] The absorption band at 2222 cm^{-1}, was observed in the IR spectrum.

These substrates (β-ketonitriles) have been reported in the literature. Only the methyl derivative seems to be missing from the literature, the other 3 have all been synthesised before. However, herein the successful synthesis of the β-ketonitriles was reported. The substrates specificity of the omega-transaminases was determine by the purchased β-ketonitriles **54c** and **54d** where the carbonyl carbon is adjacent to the aromatic ring.



54c

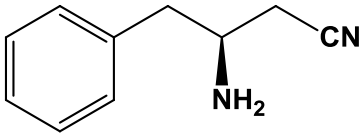


54d

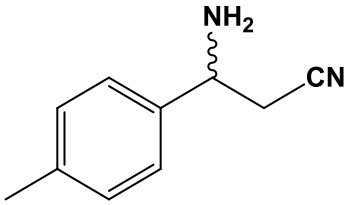
At this stage, the next step to be performed was the reductive amination of these substrates into β-aminonitriles using transaminases. However, the β-aminonitrile standards had to be prepared to be used as a control for biotransformation reactions.

3.2 Synthesis of racemic *beta*-aminonitrile standards

Different known methods were attempted for the synthesis of the standard *beta*-aminonitriles (**50a** and **56**). In the first approach, Boc-Phenylalanine was used as the starting material in attempting the synthesis of 3-amino-4-phenylbutanenitrile **50a**. This route was abandoned due to the low yields of the intermediate required to continue to the next step, therefore we decided to use an alternative approach. In the second attempted approach, we used the readily available 4-methylbenzonitrile as the starting material in the synthesis of the second types of *beta*-aminonitriles where the amine group would be adjacent to the aromatic ring; 3-amino-3-(*p*-tolyl)propanenitrile **56c**. The proposed schemes and routes are explained in the subsections below, respectively.



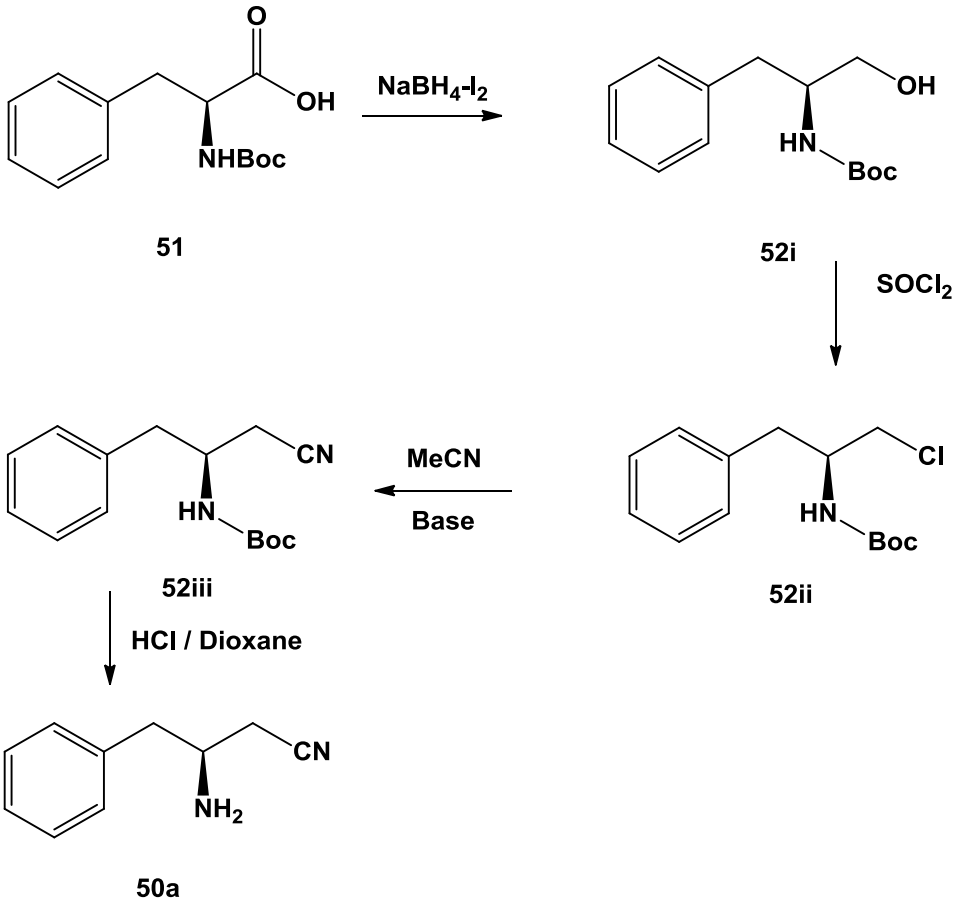
50a



56c

3.2.1 First attempted approach towards *beta*-aminonitrile standards 50a

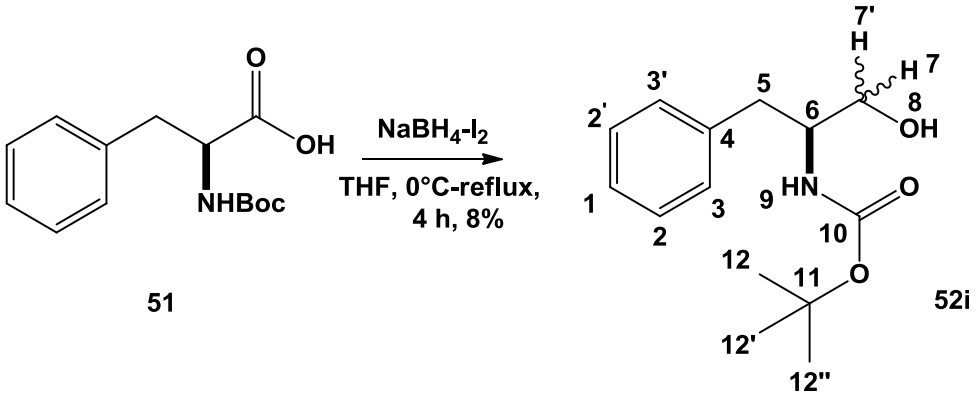
The first proposed route for the synthesis of 3-amino-4-phenylbutanenitrile **50a** used Boc-phenylalanine as the starting material (**Scheme 19**).



Scheme 19. Proposed route for the synthesis of 3-amino-4-phenylbutanenitrile **50a**

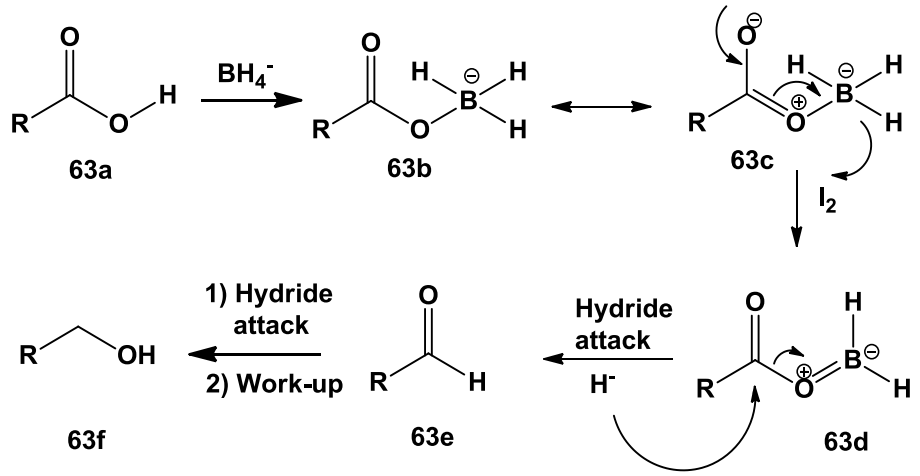
The choice of this starting material was thought to be better since it contains a single enantiomer, hence the product would also contain a single enantiomer which would be used as a standard control for chiral analysis of the biotransformation reactions. The first step involves a reduction of acid into alcohol intermediate **52i** (**Scheme 19**). The alcohol would then be subjected to thionyl chloride for the substitution of the hydroxyl group with chlorine resulting in the chlorine intermediate **52ii**, followed by reaction with the lithiated acetonitrile which would undergo a nucleophilic substitution towards the chlorine intermediate **52ii** to give the nitrile product **52iii**. The last step would involve acid catalyzed Boc-deprotection to yield enatiopure β-aminonitrile **50a**.

3.2.1.1 Synthesis of *tert*-butyl (1-hydroxy-3-phenylpropan-2-yl)carbamate 52i



Scheme 20. Reduction of Boc-phenylalanine using $NaBH_4$-I_2, 8% yield.

The proposed approach towards synthesis of the β-amino acid was to reduce the Boc-phenylalanine using sodium borohydride/iodine into the corresponding alcohol (**Scheme 20**), following the known procedure reported by Prasad *et al*.[123] Previous work has reported that sodium borohydride does not reduce carboxylic acids into alcohols due to its low reactivity.[123] However, in the presence of the electrophile (iodine) it does reduce the carboxylic acids into alcohols.[123] The reaction between $NaBH_4$-I_2 and Boc-phenylalanine yielded the corresponding alcohol **52i** (0.15 g, 8%). The proposed mechanism involving $NaBH_4$-I_2 is shown in **Scheme 21** below.



Scheme 21. Proposed mechanism involving $NaBH_4$-I_2

The intermediate **63c** reacts with the electrophile I_2 to produce highly activated intermediate **63d** (**Scheme 21**).[124] Boron withdraws electrons from the oxygen in **63d** thereby increasing the electrophilicity of the carbonyl carbon. This electron deficiency encourages the nucleophilic attack by hydride, substituting the oxoborane to produce the aldehyde **63e**. A second attack by hydride on **63e** followed by work-up produces the

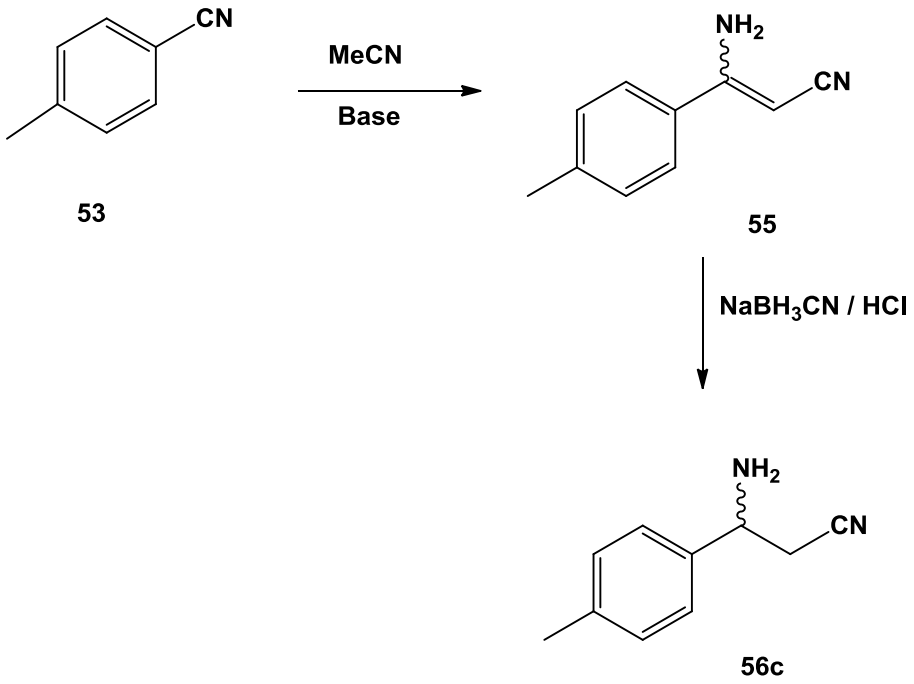
primary alcohol **63f** (**Scheme 21**).[124] However, in our case the alcohol **52i** was produced in very low yield which prevented the next step for the synthesis of the desired product **50a**. This could be due to the presence of iodine since Boc-protecting group is not stable in the presence of an acid, resulting into the formation of amino alcohol, hence the low yield of the product of interest **52i** (0.15 g, 8%). However, the spectroscopic (NMR) data for the isolated intermediate **52i** were obtained.

In the ^{1}H NMR spectrum of **52i**, seven signals were observed. The multiplet signal in the aromatic region between 7.47 and 7.05 ppm was assigned to H1, H2 and H3. The broad singlet signal at 5.58 ppm was assigned to H8, a characteristic of the OH-group. The multiplet signal at 5.54 – 5.34 ppm integrating for one proton was assigned to H6. The multiplet signal at 4.50 – 4.25 and 3.94 – 3.70 ppm integrating for one proton each were assigned to H7 and H7', respectively. The multiplet signal at 3.27 – 2.56 ppm was due to H5 integrating for two protons. The singlet signal at 1.31 ppm integrating for nine protons was assigned to the methyl protons H12, H12' and H12'' all in the same environment. In the ^{13}C NMR spectrum of **52i**, the most significant difference observed from compound **46a** was the disappearance of the carboxylic carbonyl carbon at 177.89 ppm and the new alcohol carbon signal observed at 63.07 ppm that was assigned to C-7. Our spectroscopic (NMR) data match those reported by Nagendra *et al*.[114]

The intermediate **52i** being recovered in low yield, was attributed to the carboxylic acid's carbon of the starting material which is less reactive to the nucleophilic addition reaction as compared to the carbonyl carbon atom of aldehydes or ketones.[110] The acidic proton in the starting material can react with sodium borohydride to produce salt and hydrogen gas, hence hindering the reductive nucleophilic addition forward reaction. This would lead to low yields of the intermediate **52i**. Therefore this approach was abandoned and an alternative route was sought.

3.2.2 Second approach towards *beta*-aminonitrile standards 56c

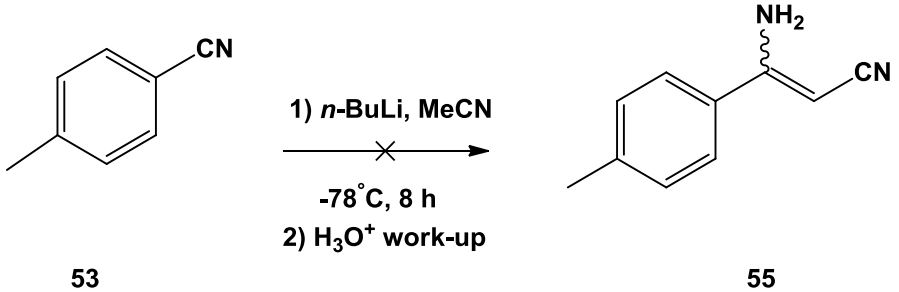
The first attempted approach suffered from low yields of the intermediate, therefore posed difficulties in synthesising the amine standards **50** which would have been used as controls for the transaminase reactions. Therefore an alternative route was developed to synthesise a different amine standard **56c**, since it has been synthesised previously here at the University of the Witwatersrand in the organic research group using a 4-methylbenzonitrile **53** as a starting material.[44] Then similar conditions reported by Chhiba and co-workers were adopted to synthesise the standard amine **56c** (**Scheme 22**).



Scheme 22. Planned approach towards synthesis of 3-amino-3-(*p*-tolyl)propanenitrile **56c**

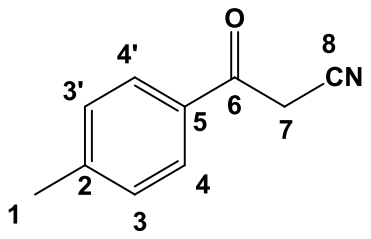
This second approach would involve the use of a base for the deprotonation of acidic acetonitrile protons to give a lithiated acetonitrile (**Scheme 22**). Since the lithiated acetonitrile has a strong affinity for cyano group containing compounds, it would perform a nucleophilic attack on the cyano carbon to give 3-amino-3-(*p*-tolyl)acrylonitrile **55**. The resulting product **55** would then be subjected to reducing conditions sodium cyanoborohydride in the presence hydrochloric acid to give the desired product 3-amino-3-(*p*-tolyl)propanenitrile **56c**.

3.2.2.1 Attempted synthesis of 3-amino-3-(*p*-tolyl)acrylonitrile 55



Scheme 23. Synthesis of the enamine using *n*-BuLi

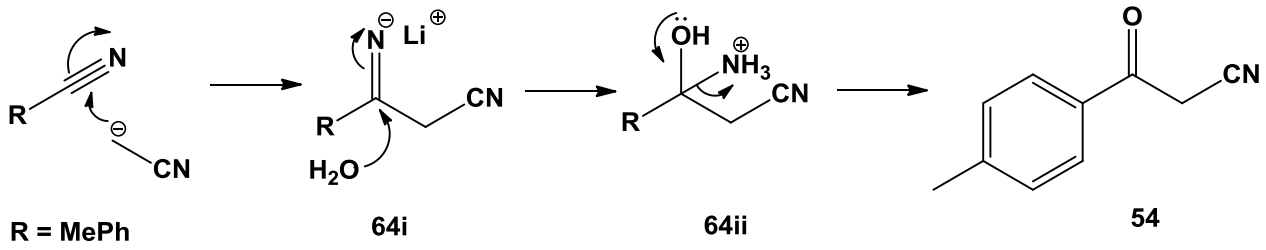
The 4-methylbenzonitrile **53** was used as the starting material in the approach to synthesise a *beta*-aminonitrile (**Scheme 23**), following a known procedure reported by Sohda *et al*.[125] The starting material was dissolved in dry THF and added to the solution of *n*-butyllithium containing the deprotonated acetonitrile, which then act as a nucleophile at the carbon of the nitrile group in the starting material (**Scheme 23**). The reaction was conducted at -78°C under nitrogen atmosphere for 8 h. HCl (2M) was added to the reaction mixture followed by extraction with ethyl acetate. The resulting crude product was purified by silica gel column chromatography yielding 3-oxo-3-(*p*-tolyl)propanenitrile **54c** which was inadvertently generated instead of the anticipated product.



54c

Four signals were observed in the ^{1}H NMR spectrum of **54c**. The two doublet signals in the aromatic region were assigned to H3 at 7.82 ppm and H4 at 7.32 ppm, both integrating for two protons. The singlet signal at 4.05 ppm integrating for two protons was assigned to H7. The singlet signal at 2.44 ppm integrating for three protons was assigned to H1. Eight signals were observed in the ^{13}C NMR spectrum for **54c**. Four signals were observed in the aromatic region between 145.7 and 128.3 ppm. The presence of the carbonyl carbon signal at 186.31 ppm assigned to C-6, confirmed the formation of undesired product **54c**. The nitrile carbon signal appeared at 113.61 ppm. The two signals observed in the alkyl region were at 28.9 and 21.5 ppm assigned to C-7 and C-1, respectively. Our NMR data were in agreement with those reported by Katritzky *et al*.[115]

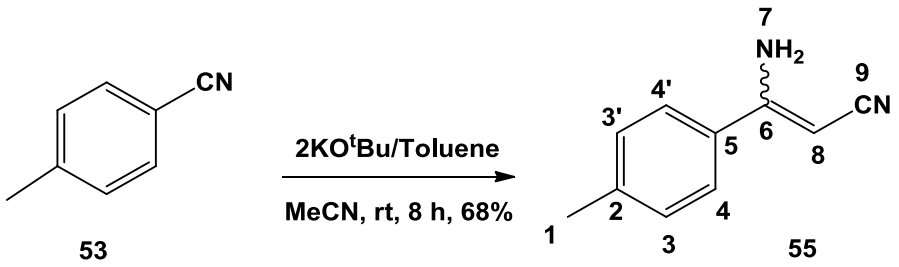
It has been established in previous work that imines rapidly undergo hydrolysis under acidic conditions.[126] Therefore, a plausible explanation for the formation of the ketone product would be, since *n*-BuLi was added in excess to a nitrile it resulted in the formation of the lithium-stabilised iminium N-anion **64i**, which then hydrolysed to ketone **54c** immediately (**Scheme 24**).



Scheme 24. Proposed mechanism for the formation of ketone during work-up

Therefore 3-oxo-3-(*p*-tolyl)propanenitrile **54c** was recovered instead of the product 3-amino-3-(*p*-tolyl)acrylonitrile **55,** possibly due to this hydrolysis during the work-up step. An alternative route was then attempted where the potassium *tert*-butoxide was used and the work-up step or any presence of acidic conditions was eliminated.

3.2.2.2 Synthesis of 3-amino-3-(*p*-tolyl)acrylonitrile 55



Scheme 25. Synthesis of enamine using KO^{t}Bu/toluene

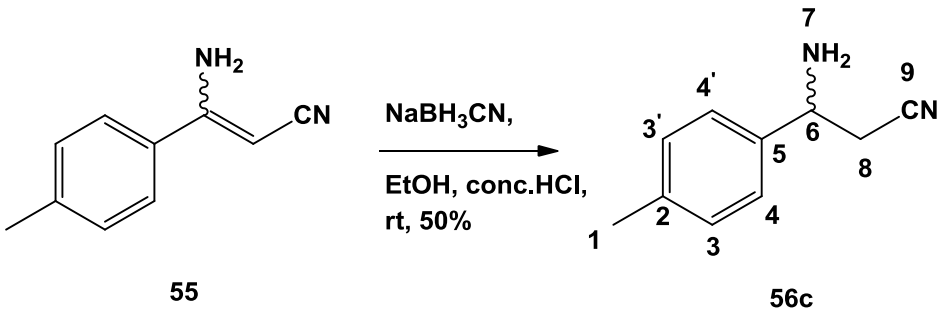
The starting material 4-methylbenzonitrile **53** was dissolved in dry toluene and added to the solution of potassium *tert*-butoxide containing acetonitrile at room temperature (**Scheme 25**), following a known synthetic procedure reported by Chhiba *et al*.[44] The reaction was monitored by TLC. The crude product was purified by chromatography on a silica gel column yielding 3-amino-3-(*p*-tolyl)acrylonitrile **55** (68%).

Five signals were observed in the ^{1}H NMR spectrum for **55**. Two doublet signals in the aromatic region were assigned to H3' at 7.38 ppm and H4' at 7.20 ppm. The singlet signal at 5.07 ppm integrating for two protons was assigned to the H7, the NH_2 protons. The singlet signal at 4.16 ppm integrating for one proton was assigned to H8, the alkene proton. The singlet signal at 2.35 ppm integrating for three protons was assigned to the methyl protons (H1). Eight signals were observed in the ^{13}C NMR spectrum for **55**. Four signals were observed in the aromatic region between 141.9 and 125.8 ppm. The signal at 161.8 ppm was assigned to the enamine carbon assigned to C-6. The signal at 119.9 ppm was due to the nitrile carbon assigned to C-9. The signal at 62.35 ppm was

assigned to the C-8 enamine α-carbon. The signal at 21.3 ppm was allocated to the C-1 methyl carbon. Our spectroscopic (NMR) data are in agreement with those reported by Chhiba and co-workers.[44] In contrast, we observed a singlet signal for the alkene proton, whereas in literature they reported a triplet signal.[44] The N-H stretching band visible at 3350 cm^{-1}, the C≡N stretching band visible at 2230 cm^{-1} and C-N stretching band visible at 1100 cm^{-1} in the IR spectrum confirmed the identity of the product **55**.

The reaction was successful because potassium is much poorer at coordinating hard anions (such as iminium anion) compared to lithium, hence no hydrolysis occurred. Having obtained 3-amino-3-(*p*-tolyl)acrylonitrile **55** (68%), led to the final step of synthesising the desired standard racemic 3-amino-3-(*p*-tolyl)propanenitrile **56c**.

3.2.3 Synthesis of 3-amino-3-(*p*-tolyl)propanenitrile 56c



Scheme 26. Synthesis of 3-amino-3-(*p*-tolyl)propanenitrile **56c** using $NaBH_3CN$

Reduction of the alkene in the starting material was achieved by subjecting 3-amino-3-(*p*-tolyl)acrylonitrile **55** to sodium cyanoborohydride and hydrochloric acid (**Scheme 26**). The concentrated HCl was added to activate the alkene carbon so that the nucleophilic hydride could attack the electrophilic carbon leading to the generation of 3-amino-3-(*p*-tolyl)propanenitrile **56c** (50%). Following a known procedure reported by Chhiba *et al*.[44]

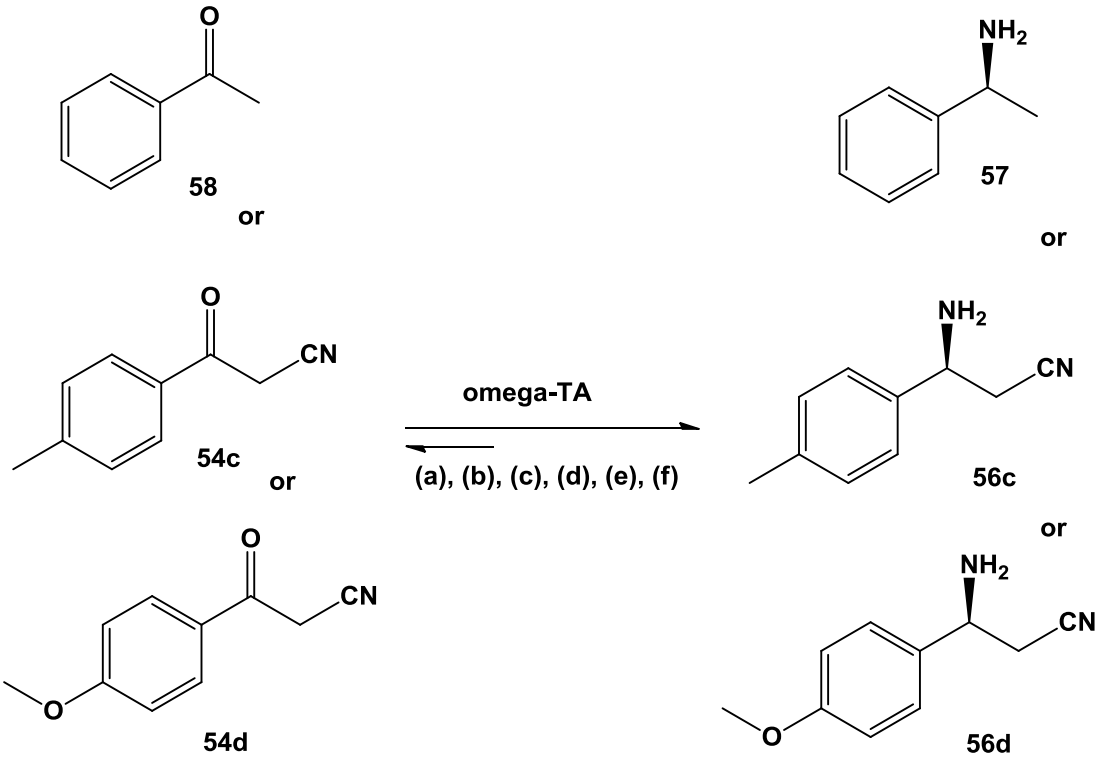
Six signals were observed in the ^{1}H NMR spectrum for **56c**. Two signals were observed in the aromatic region; a doublet at 7.25 ppm that was due to H3 and a doublet signal at 7.16 ppm was due to H4. The multiplet signal at 4.30 – 4.22 ppm integrating for one proton was allocated to H6. The doublet of doublets signal integrating for two protons resonating at 2.62 ppm was assigned to H8. The singlet at 2.33 ppm integrating for two protons was assigned to H7 of the amine protons. The singlet at 1.71 ppm integrating for three protons was assigned to the methyl protons (H1). The eight peaks observed in the ^{13}C NMR spectrum for **55** confirmed the success of the reaction. Four peaks were observed in the aromatic region between 139.1 and 125.4 ppm. The upfield shift from 119.9 ppm to 117.36 ppm of the nitrile carbon (C-9) was observed. Two peaks observed

in the alkyl region were the peak at 51.9 ppm that was assigned to C-6, a characteristic of the –**C**H_2-NH_2 and the one at 28.0 ppm assigned to C-8 of the methylene carbon (-**C**H_2-CN). The identity of the product was also confirmed by the disappearance of the enamine carbon as the shift from 161.8 ppm. Instead, a new carbon signal at 51.9 ppm was observed. The upfield shift from 62.4 ppm to 28.0 ppm indicated the successful reduction of the enamine alkene to the alkyl chain. These NMR data match those reported by Chhiba *et al*.[44] The mass of the product observed in the HMRS of 161.1067 m/z for $[M+H]^+$ was similar to the calculated mass of 161.1035 m/z for $[M+H]^+$. Chiral analysis of the standard product 3-amino-3-(*p*-tolyl)propanenitrile conducted on Chiral-HPLC showed 50 percent presence for each enantiomer indicating that the product was a racemic mixture as expected.

Having obtained the amine standard **56c** and purchased MBA **57**, their corresponding ketones **54c** and acetophenone **58** were then used as substrates for screening the omega-transaminase activity. The standards **56c** and **57** would be used as controls to give better indication as whether the transaminase reactions have activity towards their corresponding ketone substrates in the reductive amination reactions. If the ω-TA shows good activity towards **54c**, then the β-ketonitriles **49** substrates would be tested against the transaminases that showed good activity with good yields of the amine product **56c**.

3.3 Transaminase activities

The omega-transaminase reactions have attracted a great deal of attention due to their enantioselectivity and complete conversion of the ketone substrates. However, there are a number of things that can affect the transaminase reaction; some of them are substrate and product inhibition, diamine donor, the unfavourable equilibrium of the formation of amine product and the removal of the co-product generated during the reductive amination.



Scheme 27. Biotransformation of β-ketonitriles using omega-transaminase; (a) and (b) Screening of transaminase activity using **57** and **58**.(c) and (d) Investigating substrate and product inhibition using **57** and **58**. (e) Displacing unfavourable equilibrium by testing LDH system and different amine donors on **58**. (f) Asymmetric synthesis of β-aminonitriles using diamine donor on **58**, **54c** and **54d**.

Different methods were attempted to find better and optimized reaction conditions for the omega-transaminase from the Enzymicals AG (omega-TA ECS kit) (Germany), Prozomix-TA's kit from Prozomix Limited (UK) and *Aspergillus fumigatus* omega-TA (Sigma Aldrich) (**Scheme 27**). The first thing attempted was to assess whether the enzymes from three different kits were active or not. The most common substrate MBA **57** was used to screen the enzyme activities. The substrate and product inhibition of the transaminase reaction by acetophenone and MBA was investigated, as these reactions are prone to substrate and product inhibition. The inhibition was investigated at various concentrations of acetophenone **58** and methylbenzylamine **57** using L-alanine (amine donor) and pyruvate (amine acceptor), respectively (**Scheme 27**). Thermodynamic equilibrium in reductive amination reaction using transaminase is one of the major drawbacks, as the ketone substrate is more favourable than the amine product, therefore the suitable amine donor or a system for the removal of the co-product to drive the equilibrium towards the amine product would be determined (**Scheme 27**). Finally, after finding suitable system or amine donor, the reductive amination reactions on β-

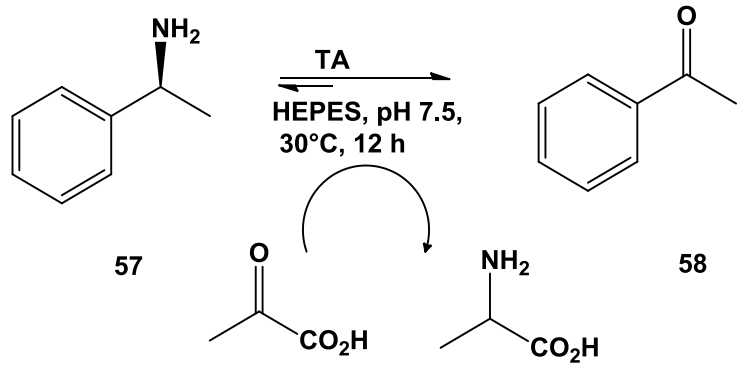
ketonitriles substrates **54c** and **54d** would be conducted. The results would be discussed in detail in the following subsections.

3.3.1 LC-HRMS analysis of the standards 57 and 58

Before the screening of the enzymes, the standards were analysed through LC-MS using a high resolution MS (HRMS) which were used as the controls for indicating the enzyme activity in the biotransformation reactions. MBA **57** and acetophenone **58** were used as the substrate standards. The peak of the standard **57** was observed in the LC-MS at 0.61 min and 1.88 min retention times. The observed mass for **57** at 0.61 min was 122.0965 *m/z* and at 1.88 min was 122.0963 *m/z* with the molecular formula of $C_8H_{12}N$ (**Appendix, Figure A1**). Often amines are not well retained by the column and results may be affected by different ionic forms of the compound. The standard acetophenone **58** was also analysed using LC-MS, however the peak for **58** was not intense in the LC-MS chromatogram (**Appendix, Figure A2**), possibly due to weak ionisability of the compound **58** compared to MBA **57**. The peak of **58** was observed in the UV-Chromatogram 254 nm at 5.53 min retention time with the observed mass of 121.0645 *m/z* for C_8H_9O, for LC-MS data see **Appendix Figure A2**. Having confirmed the retention times and the corresponding masses of the standards in the LC-MS, the enzyme activities were then screened using these LC-MS data as controls for the transaminase reaction.

3.3.1.1 Screening of the transaminase using 57

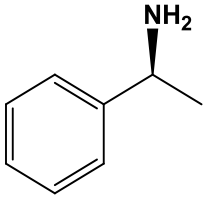
It has been reported that the most abundant ω-TA's are *S*-selective while the *R*-selective ones have been barely explored.[127] Therefore, since methylbenzylamine is the most commonly used substrate with pyruvate as the amine acceptor, the *S*-MBA **57** was used for screening of the transaminase activities (**Scheme 28**).



Scheme 28. Deamination of methylbenzylamine using pyruvate

Screening of enzyme activities was conducted using the equilibrium favourable forward reaction; the formation of a ketone product. Transaminase from the Enzymicals (omega-TA ECS kit), Prozomix-TA's kit and omega-TA's *Aspergillus fumigatus,* with the co-factor PLP were rehydrated in HEPES buffer at pH 7.5. Since most of the substrates have low solubility in buffer solution, it has been demonstrated that 15% v/v DMSO is the co-solvent that has significant benefits in substrate conversion as well as enhancing stereoselectivity.[92] The substrate MBA **57** (50 mM)**,** dissolved in DMSO, and pyruvate (10 mM) were added to the enzyme solution at 30°C. TLC and LC-MS were used to monitor the generation of acetophenone to indicate enzyme activity. The enzymes screened are shown in **Table 7** below.

Table 7: Deamination of methylbenzylamine using different transaminases

Substrate	Enzyme Code	Activity
 **57**	Prozomix-TA016-62	√
	Prozomix-TA030-66	√
	Prozomix-TA037-64	√
	Prozomix-TA045-52	√

(a) Tick (√) indicate that the enzyme is active.

Two spots were observed on the TLC plate for all transaminase reactions, for TLC data see (**Appendix, Figure A3**). The TLC analysis showed that all four transaminases had activity towards **57** (**Table 7**), with product **58** generated from the reactions being observed at R_f = 0.70, a similar retention factor (R_f) as for the standard (**Appendix, Figure A3**). The MBA substrate was observed with a retention of R_f = 0.15, similar to that of the standard. One of the reactions was followed using LC-MS and analysed in detail, and the other results are based on this one; in this reaction the ω-transaminase Prozomix-TA045 was used. The product was not isolated as the reaction gave a low yield (< 1 mg), and therefore the structure of the product could not be confirmed by the NMR techniques. The crude reaction mixture was monitored using LC-MS for the analysis of this biotransformation reaction and our conclusions were based on these LC-MS and TLC data.

The two spots observed on the TLC showed the incomplete conversion of **57** into the corresponding acetophenone **58**. LC-MS also seemed to validate this observation; as the **57** peak was observed in the chromatogram spectrum at 1.86 min with the observed mass of $[M+H]^+$ 122.0961 *m/z* for $C_8H_{12}N$ (**Appendix Figure A4**). These observed LC-MS data matched those observed in the standard **57**, therefore confirming presence of

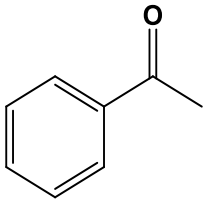
57 in the reaction mixture, indicating the incomplete conversion. As for the LC-MS of the standard **58**, the molecular peak of the generated acetophenone was not observed in the chromatogram, however in the UV-Chromatogram 254 nm it was observed at 5.55 min with a mass of $[M+H]^+$ 121.0656 *m/z* for C_8H_9O (**Appendix Figure A4**) in agreement with the LC-MS data of the standard **58**. This confirms the successful generation of the acetophenone **58** product, hence indicating that the transaminase Prozomix-TA045 was active. Knowing that most of the enzymes from different tested kits are active, it was then decided that the next step would be to find a suitable enzyme for the reaction of interest; a reverse reaction which is a reductive amination of acetophenone.

3.3.1.2 Screening of the transaminase using 58

Employing a ketone substrate for screening of the transaminase would be advantageous as it would shed some insight on the reductive amination reaction and if the reaction conditions should be improved. To find a suitable enzyme, 40 commercially available ω-transaminases were tested using similar reaction conditions in **Scheme 27**, except that now the substrate employed was acetophenone at 5 mM with the amine donor L-alanine at 0.5 equiv (2.5 mM) (**Table 8**).

Table 8. Reductive amination of acetophenone using different transaminases

Substrate	Enzyme code	Activity
	ECS-TA01	√
	ECS-TA02	√
	ECS-TA03	√
	ECS-TA04	√
	ECS-TA05	√
	ECS-TA06	√
	ECS-TA07	√
	ECS-TA08	√
	Aspergillus fumigatus TA	√
	Prozomix-TA001	√
	Prozomix-TA002	√

 58	Prozomix-TA003	√
	Prozomix-TA004	√
	Prozomix-TA005	√
	Prozomix-TA006	√
	Prozomix-TA007	√
	Prozomix-TA009	√
	Prozomix-TA010	√
	Prozomix-TA011	√
	Prozomix-TA018	x
	Prozomix-TA016	√
	Prozomix-TA020	x
	Prozomix-TA022	√
	Prozomix-TA023	x
	Prozomix-TA024	√
	Prozomix-TA025	x
	Prozomix-TA027	x
	Prozomix-TA030	√
	Prozomix-TA032	√
	Prozomix-TA033	√
	Prozomix-TA035	√
	Prozomix-TA037	√
	Prozomix-TA038	√
	Prozomix-TA040	√
	Prozomix-TA041	√

	Prozomix-TA042	√
	Prozomix-TA045	√
	Prozomix-TA046	√
	Prozomix-TA048	√
	Prozomix-TA049	√
	Prozomix-TA050	X

(a) Tick (√) indicate that the enzyme is active.
(b) Cross (X) indicate that the enzyme is not active

All 40 reductive amination reactions for screening of the transaminase activity were monitored by TLC, and only two reactions for Prozomix-TA022 and Prozomix-TA024 were analysed in detail using LC-MS. All the other results are based on these two reactions. Three spots were observed on the TLC plate for all the enzymes in **Table 8**, except for six transaminases Prozomix-TA018-93, Prozomix-TA020-80, Prozomix-TA023-89, Prozomix-TA025-90, Prozomix-TA027-91, and Prozomix-TA050-94 which showed only the starting material, for TLC data see **Appendix Figure A5**. The acetophenone starting material was observed with a retention similar to the standard at Rf = 0.78. One of these six transaminase reactions (Prozomix-TA018) was analysed in detail using LC-MS and only the starting material was observed in the LC-MS spectrum (**Appendix Figure A6**). These results confirmed that the enzyme was not active as the product MBA was not observed. On this basis, it was concluded that the other five enzymes which showed only the starting material by TLC analysis were also not active on this substrate.

Of the transaminase reactions that showed three spots in the TLC, two reactions involving ECS-TA02 and Prozomix-TA024 were analysed in detail by LC-MS. Compounds have R_f values similar to the standards reported above for the forward reaction. However the peak of the third spot observed on the TLC at R_f = 0.15 was not observed in the LC-MS chromatograms of both the ECS-TA02 and Prozomix-TA024 reactions. Therefore the by-product formed at this third spot was not identified. The peaks of the other two spots were observed in the LC-MS chromatograms of both reactions. In the LC-MS data of the reaction involving transaminase ECS-TA02, the molecular peak of the starting material was observed in the UV-Chromatogram 254 nm at 5.53 min with the accurate mass of $[M+H]^+$ 121.0653 *m/z* for C_8H_9O corresponding to the mass of the standard acetophenone reported above (**Appendix, Figure A7**). The molecular peaks of the generated MBA were observed in similar manner as the standard at 0.60 min and 1.88 min with their accurate masses of $[M+H]^+$ 122.0966 *m/z*

and 122.0966 *m/z* for $C_8H_{12}N$, respectively. These observed masses were consistent with the mass of the analysed standard MBA. This result therefore seemed to validate the successful reductive amination of acetophenone. The LC-MS data for reductive amination reaction involving the transaminase Prozomix-TA024 is shown in **Appendix Figure A8**. These LC-MS data match the data of the reaction involving transaminase ECS-TA02.

Based on the TLC and LC-MS data obtained, the analysis seemed to show that amine product was generated successfully from the ketone substrate. This brought the work closer to the first aim of the study of the reductive amination of the ketone. For the preparative scale the substrate concentration at which the transaminase activity is drastically inhibited needs to be determined. Therefore we decided to investigate the substrate's and product's concentrations which inhibit the enzyme activity.

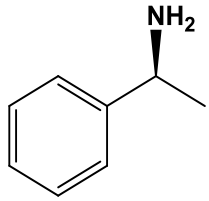
3.3.2 Substrate and product inhibition

3.3.2.1 Determining product inhibition by amine product 57

The use of omega-transaminases in the industry has been limited by substrate and product inhibition despite their natural advantages in synthesising enantiopure unnatural amino acids.[128] Substrate and product inhibition has a significant role in enzymes' efficiency in the biocatalytic reactions. Since most transaminases screened showed activity towards the amino acceptor (pyruvate), it was then used as the amino acceptor for investigating the product inhibition by *S*-MBA **57** as it is the common ideal substrate for ω-TA (**Scheme 27**).[75,128] Deamination reaction was conducted in HEPES buffer at pH 7.5 at 30°C using selected active enzymes including transaminase ECS-TA03, Prozomix-TA002, Prozomix-TA016, Prozomix-TA045 and *Aspergillus fumigatus* TA to determine product inhibition by *S*-MBA employing various concentrations in the presence of pyruvate (10 mM) as the amine acceptor (**Table 9**).

Table 9. Transaminase tested on different MBA concentrations

Substrate	ω-TA code (5 mg)	Substrate [C] (mM)	Activity
	ECS-TA-03	50	√
	Prozomix-TA016	50	√
	Prozomix-TA002	100	√
	Prozomix-TA045	100	√
	ECS-TA03	250	x

 57	Prozomix-TA041	250	√
	Prozomix-TA045	250	x
	Aspergillus fumigatus TA	250	x

The transaminases showed activity up to the substrate concentration of 100 mM (**Table 9**). The concentrations of 100 mM to 250 mM were used to determine the maximum concentration at which the amine product inhibits the reaction. The TLC and LC-MS were used to determine the enzymes activity. All enzymes showed identical results by TLC analysis for the substrate concentrations of 50 and 100 mM (**Appendix Figure A9**). No activity was observed at 250 mM except for Prozomix-TA041. The transaminase Prozomix-TA041 did show activity at a substrate concentration of 250 mM since the acetophenone generated in the reaction, was observed with a retention time similar to the standard at R_f = 0.8 (**Appendix, Figure A9**). The transaminases ECS-TA03, Prozomix-TA045 and *Aspergillus fumigatus* TA did not show any activity towards 250 mM, this was confirmed by the LC-MS analysis of the reaction involving Prozomix-TA0045 as only the starting material was observed at 0.60 min and 1.88 min with the observed mass corresponding with the standard and no peak for the product observed (**Appendix, Figure A10**).

It has been reported that the substrate inhibition by *S*-MBA often occurs at concentration above 200 mM.[128,129] In our studies, it was observed that transaminases did not show activity at 250 mM, therefore these results were in agreement with the results reported by Mathew *et al*,[129] where they observed activity at substrate concentration up to 100 mM. The choice of pyruvate's concentration (10 mM) was influenced by the reported findings that the highest transaminases activity was observed at 25 mM pyruvate.[129]

3.3.2.2 Investigating substrate inhibition by 58

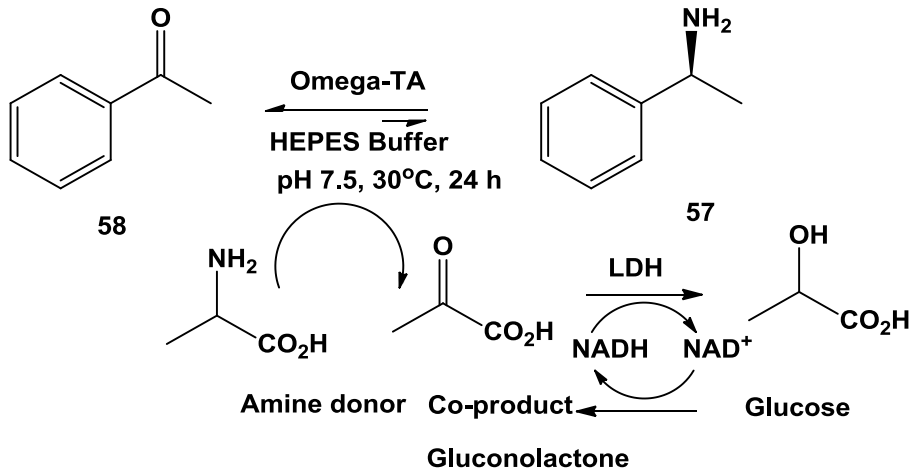
Additionally, the substrate inhibition by acetophenone was also determined, as this was our reaction of interest using three transaminases namely Prozomix-TA022, Prozomix-024 and Prozomix-038. For the reaction involving ω-TA Prozomix-TA022, with L-alanine concentration kept the same at 250 mM and acetophenone concentration reduced to 25 mM, it was observed that the enzyme was still active as the amine product was detected by TLC and LC-MS (**Appendix, Figures A11-12**). Similar results were observed for Prozomix-024, with L-alanine concentration at 250 mM and 50 mM of acetophenone (See **Appendix Figures A13-14**). However the activity was lost when

the acetophenone concentration was increased beyond 50 mM for the reaction involving ω-transaminase Prozomix-TA038, L-alanine (250 mM) and acetophenone concentration doubled to 100 mM. Only the starting material was observed on the TLC and LC-MS analysis, no product was detected indicating that the ketone substrate inhibit the transaminase reaction at concentrations higher than 50 mM (**Appendix, Figures A15-16**). Mathew and co-workers also reported that vast activity is lost at acetophenone concentration beyond 20 mM.[128] Therefore the tested transaminases are susceptible to acute ketone substrate inhibition as well as amine product inhibition at concentrations beyond 100 mM. The reactions still suffered low yield when L-alanine was employed as an amine donor, leading to the investigation of a better amine donor and pyruvate removal system to displace the unfavourable equilibrium towards the amine.

3.3.3 Displacing the unfavourable equilibrium

3.3.3.1 Employing LDH pyruvate removal system

The application of ω-transaminases in asymmetric synthesis is challenging since the equilibrium favours formation of the substrate (ketone, L-alanine) and not the desired product (amine, pyruvate).[58,62] Previously, we employed L-alanine in the absence of the system for the removal of the co-product pyruvate. Initially, we examined whether six selected active enzymes ECS-TA05, Prozomix-TA003, Prozomix-TA005, Prozomix-TA016, Prozomix-TA045, and *Aspergillus fumigatus* TA were applicable to the asymmetric reductive amination of the ketone substrates to the corresponding amine product using lactate dehydrogenase (LDH) pyruvate removal mixture to drive the equilibrium towards the amine product. The LDH mixture was employed in a coupled reaction with each of the six transaminase to shift the equilibrium towards the amine product by reducing the product inhibition due to the generated pyruvate (**Scheme 29**).



Scheme 29. Reductive amination of acetophenone using LDH mixture

The amine donor L-alanine was added to the reaction mixture of transaminase and PLP in HEPES buffer at pH 7.5 and allowed to equilibrate for 2 h. Having established that the acetophenone undergoes substrate inhibition at concentrations beyond 50 mM, then similar concentration of **58** (50 mM) was dissolved **58** at in DMSO and added it to the enzyme solution along with the LDH mixture to remove the generated pyruvate which inhibit the product generation. The generation of the amine product was monitored by TLC (**Scheme 29**). The ω-TA ECS-TA05, Prozomix-TA016, Prozomix-TA045, and *Aspergillus fumigatus* were tested on acetophenone substrate at 50 mM, and the spot of the product **57** generated was observed at similar R_f = 0.53 (60% EtoAc/hexane) by all four enzymes with a better intensity on the TLC plate (**Appendix, Figure A17**). In case of ECS-TA05, the spot of the MBA generated was observed at R_f = 0.35 (**Figure A17**). However this result was not confirmed by LC-MS. The TLC of the MBA generated in the tested reactions for substrate inhibition by acetophenone at 50 mM (Section 3.3.1) showed weaker intensity than when the LDH system was employed at similar substrate concentration. Therefore LDH mixture plays an important role in reductive amination reaction as it removes the co-product from the reaction mixture thereby avoiding product inhibition by pyruvate and increased the formation of the amine product.

The LDH/GDH system demonstrated that removal of the co-product plays an important role in transaminases biotransformation of the ketones into the corresponding amine product. However, the drawback of this approach is that it requires expensive co-factors NAD, GDH and LDH for pyruvate removal to drive the equilibrium to the product side.[99] Hence it is used for small scale reactions. Therefore, this method was abandoned, and decided to explore different amine donors which would drive the equilibrium towards the amine product.

3.3.3.2 Employing isopropyl as amine donor

To date, the current method widely used involves the application of amine donor isopropyl amine in larger excess instead of L-alanine in the reductive amination of the ketone substrate where the generated co-product (acetone) is easily removed by evaporation.[99] On this basis, we decided to employ isopropyl amine in large excess at 250 mM as amine donor in the reductive amination of the ketone substrate. The transaminase tested on different acetophenone concentrations using this system are listed in **Table 10** below.

Table 10. Reductive amination of ketone using isopropyl amine as the amine donor

Substrate	ω-TA code	Substrate [C] (mM)	Activity
58	Prozomix-TA046	10	x
58	Prozomix-TA048	10	x
58	Prozomix-TA048	50	x
58	Prozomix-TA049	50	x

The amine donor isopropyl amine was employed at similar concentration as before at 250 mM, and added to the rehydrated omega-transaminase Prozomix-TA046, Prozomix-TA048, Prozomix-TA049 and PLP in HEPES buffer at pH 7.5 and then allowed the reaction to equilibrate for 2 h to prevent the direct reaction between acetophenone and isopropyl amine. The ketone substrate acetophenone was employed at different concentrations ranging from 10 mM to 50 mM in DMSO and added to the enzyme solution, followed by incubation at 30°C for 24 h (**Table 10**). Most of the biocatalysis reactions are conducted between room temperature and 37°C so that the stability of the enzymes would not be compromised by thermal denaturation.[130] The use of isopropyl amine as amine donor was preferred as the transaminase reaction was conducted at 30°C and the boiling point of isopropyl amine is 34°C. At 30°C, the isopropyl amine donor would not evaporate. However, no bioconversion was observed in all the reactions, as no desired product was detected.

The transaminase reaction mechanism described in the Introduction (Scheme 5, Section 1.3.1), showed that the co-product (acetone in this case) and the PMP are generated during the equilibration between internal aldimine and amine donor before the addition of the amino accepter (acetophenone), hence the desired amine product could only be generated after the acetone and PMP are generated. This suggests that the bioconversion relies on, but is not limited to the affinity between the PMP and the substrate (acetophenone) as well as the generated acetone (which could potentially inhibit the reaction between the substrate and the PMP).

It has been reported that acetone could also be removed at slightly raised temperatures or under reduced pressure.[130] Therefore, the reaction temperature was gradually raise from 30°C to 60°C so that the possibly generated acetone could evaporate and shift the reaction equilibrium towards amine product. The reaction progression was monitored by TLC (**Appendix, Figure A18**) and LC-MS. Herein, one of the reactions was analysed in details involving Prozomix-TA048 at substrate (10 mM) using LC-MS (**Appendix, Figure A19**), and no product was detected even after increasing the reaction temperature. Only the starting material was recovered and its molecular peak was observed at 5.56 min with the observed mass of 121.0648 *m/z* in agreement with the mass of the standard of 121.0645 *m/z*. The other two peaks observed at 0.61 min and 2.00 min with the detected mass of $[M+H]^+$ 162.1274 *m/z* were possibly due to the imine by-product formed by reaction between the isopropyl amine and acetophenone, for mechanism and by-product generated see **Appendix Figure A20**.

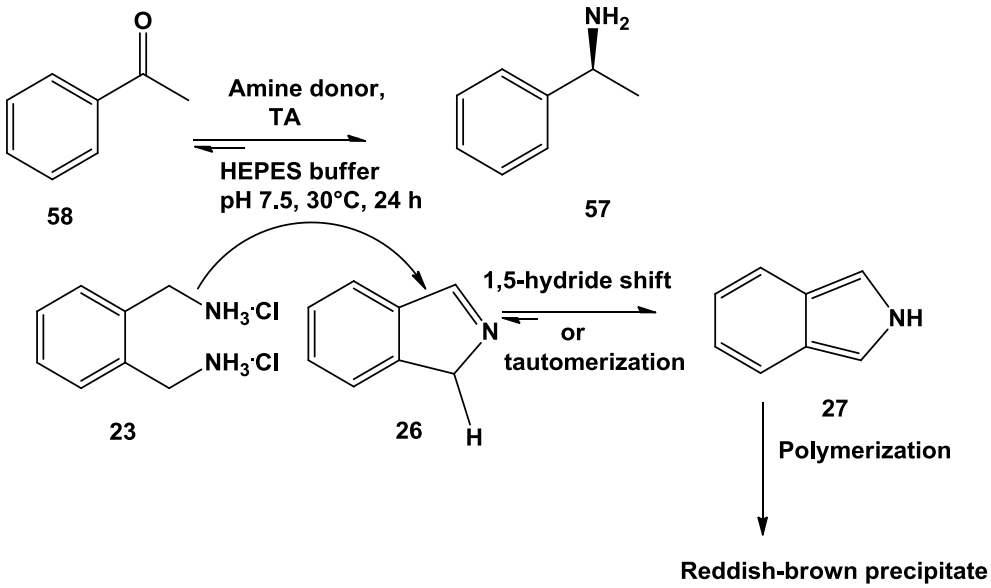
Based on literature, usually to prevent the direct reaction of acetophenone and the amine donor, the reaction is allowed to equilibrate for 1-2 hours to form the Schiff base, PMP and acetone before adding the ketone substrate.[131] Therefore, a similar procedure was adopted and the PLP-bound enzyme was allowed to dissolve and form the Schiff base with the amine donor for 2 h. Having to presume that after 2 h, all the amine donor would be in the form of Schiff base, we then added acetophenone as the amine acceptor. But unfortunately in this case, it seems that the equilibration did not occur, therefore the isopropyl amine and acetophenone were free to react with each other.

The high temperature also probably posed a negative impact on the enzymes stability and consequently, compromising the conversion of the ketone substrate into the amine product. Kelefiotis-Stratidakis and coworkers demonstrated that transaminases reactions that are conducted at high temperature show dismal conversion percentages due to compromised stability of the enzyme.[130] Therefore, lower temperatures are preferred for biocatalysis reactions in order to preserve the enzyme activity.

The ω-transaminase Prozomix-TA046, Prozomix-TA048 and Prozomix-TA049 showed no activity towards isopropyl amine as amine donor, hence applicable advantages of isopropyl amine in amine synthesis are questionable as the ketone substrate seemed to be reactive towards the isopropyl amine and the removal of the acetone is very challenging (assuming that the PMP and the acetone were generated).[131] Then it was suggested that the application of isopropyl amine as amine donor has to be discontinued and explore the diamine donor xylylenediamine dihydrochloride as it has been reported by researchers in Tuner's lab, that drives the reaction towards the amine product due to its tautomerisation into isoindole which then polymerises into a reddish-brown precipitate indicating that the transaminase reaction has worked.[99]

3.3.3.3 Employing xylylenediamine dihydrochloride diamine donor

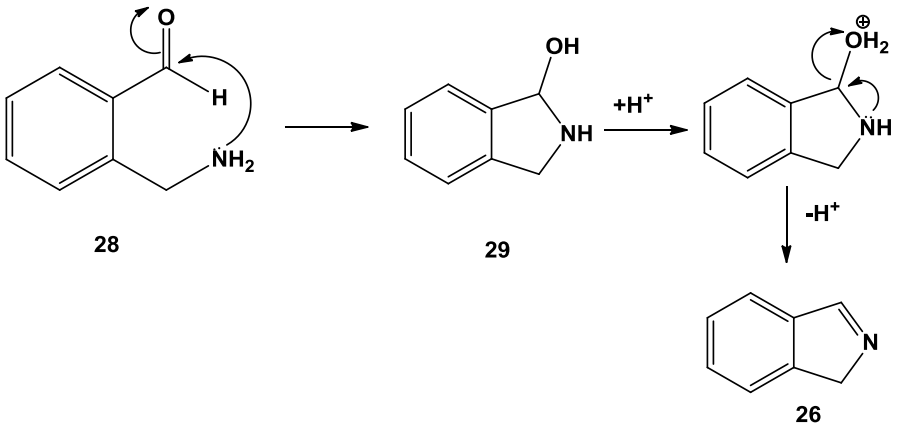
The lack of a convenient and simple method for high-throughput screening of transaminase reactions poses a great challenge in developing the efficient ω-transaminases for asymmetric synthesis of amine products. Turner and coworkers recently demonstrated the use of a low-cost, achiral xylylenediamine dihydrochloride diamine donor that provides a high-throughput screening method and significantly shifts the equilibrium towards the amine product.[99] This high-throughput screening method is colorimetric based and it is extremely desirable for the development of new omega-transaminases, optimization of transaminase properties through genetic engineering or directed evolution.[99,132] In light of this high-throughput method, xylylenediamine amine donor was employed as the source of amine for asymmetric synthesis of MBA under the reaction conditions described by Green *et al*[99] (**Scheme 30**).



Scheme 30. Synthesis of MBA using diamine donor

Only one transaminase (ECS-TA06) was tested using acetophenone in the presence of the diamine donor **23**. The active ECS-TA06 solution containing the 0.5 equivalent of PLP and diamine donor (1.1 equiv) was allowed to equilibrate for 2 h to generate the Schiff base. Then the common model substrate acetophenone was dissolved in DMSO and added to the enzyme solution (**Scheme 30**), followed the method reported by Turner and co-workers.[99] The reddish-brown precipitates formed gradually as shown in **Appendix Figure A21**, and was possibly due to the spontaneous polymerization of isoindole **27**.[99] The formation of the reddish-brown precipitates indicates that the diamine donor **23** successfully transferred one of its amino group to the PLP cofactor to produce the 2-(aminomethyl)benzaldehyde **28** and the intermediate pyridoxamine-5'-phosphate (PMP) which is required to react with the amine acceptor acetophenone. The

deamination of **23** led to the formation of the intermediate aldimine **26** through the remaining primary amine cyclisation of the 2-(aminomethyl)benzaldehyde **28** (**Scheme 31**).



Scheme 31. 5-exo-trig cyclisation of 2-(aminomethyl) benzaldehyde

Cyclisation of 2-(aminomethyl)benzaldehyde **28** through 5-exo-trig mechanism into isoindolin-1-ol **29** removes the co-product **28** from the reaction mixture thereby shifting the unfavorable equilibrium towards the amine product (**Scheme 31**).[99] The elimination of water from the isoindolin-1-ol led to the formation of aldimine **26** which tautomerised or undergoes a 1,5-hydride shift into isoindole **27** followed by precipitation, demonstrating the extensive efficacy of this xylylenediamine dihydrochloride as amine donor for the asymmetric synthesis of the enantiopure amines. The aldimine **26** tautomerised into isoindole **27** which further polymerised to give a coloured precipitate (**Scheme 30**).

In light of these advantages, the Turner's method,[99] was used for the reductive amination of **58** into **57** using ω-TA ECS-TA06. The generation of **57** was monitored using TLC and LC-MS. Three spots were also observed on the TLC plate as in the above reductive amination reactions of **58** with similar R_f values. The analysis of the standards MBA **57** and acetophenone **58** were performed using the C_{18} column, however the MBA **57** also came out with the unretained peak (at approximately the void volume value) at 0.61 min with the accurate mass of 122.0965 *m/z* (**Appendix, Figure A1**) leading to the use of an alternate column: a Hilic column. Therefore, this reaction was analysed in detail using LC-MS and the Hilic column to retain the amine product better than the previously used C_{18} column. The peak of the product **57** was observed at 6.32 min with the accurate mass of 122.1150 *m/z* for $[M+H]^+$, which is in agreement with the mass of the standard for $C_8H_{12}N$ of 122.1144 *m/z* (**Appendix, Figure A22**). This reaction also gave incomplete conversion as the peak of the starting material was

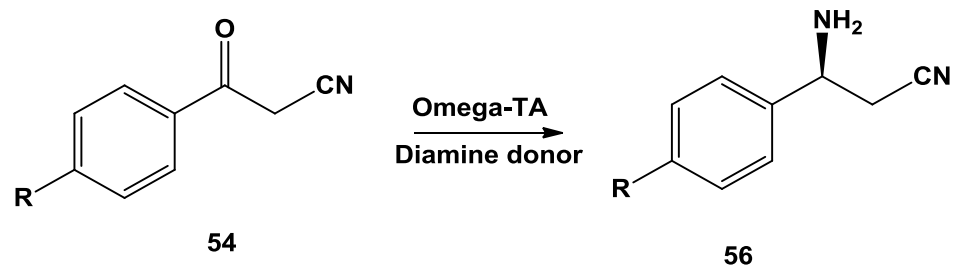
observed in the LC-MS at 10.49 min with the mass of 121.0830 *m/z* matching the mass of the standard (**Appendix, Figure A22**).

Prior to the addition of acetophenone into the reaction, the transaminase solution was yellow in colour, and upon addition of diamine donor (1.1 equiv) the colour changed to green (evidence or picture not captured). It was also demonstrated in the previous work that the colour changed to green after the addition of diamine donor into the transaminase solution.[99] This was probably due to conversion of the PLP into PMP.[99] A tremendous change in colour was observed from the transaminase solution upon addition of the amine acceptor acetophenone (10 mM, 1.0 equiv) after 1 h. The dark reddish-brown precipitates were observed after the reaction mixture was incubated for 12 h at 30°C, as it can be seen in **Appendix Figure A21**. Since the LC-MS seemed to show that the transaminase was active towards diamine donor, it was important to test Turner's method on the β-ketonitrile substrates required for the synthesis of β-beta-amino acids. Additionally, the diamine donor seemed to be a better source of amino group as this method gave a high-throughput screening method with the colour change upon addition of a ketone, therefore similar reaction conditions would be employed in the reductive amination reactions using β-ketonitrile substrates **54c** and **54d**.

3.4 Asymmetric synthesis of *beta*-aminonitriles

The diamine donor xylylenediamine dihydrochloride has shown to be acceptable by numerous *S* and *R*-selective omega-transaminases.[99,133,134] The screening of variants of omega-transaminases and large substrates using diamine donor **23** was demonstrated by Turner and coworkers.[99] The natural substrates for the synthesis of β-amino acids using omega-transaminases are known to be β-keto acids.[54,135] However asymmetric synthesis of β-amino acids from β-keto acids substrates was not ideal as these substrates undergo decarboxylation in buffer solution through a cyclic transition state mechanism to give the more stable acetophenone and carbon dioxide.[54] On this basis, we decided to use stable β-ketonitriles for asymmetric synthesis of β-aminonitriles using active omega-transaminases.

In this study, the approach to circumvent the decarboxylation was attempted by conducting a reaction cascade which involved the reductive amination of the β-ketonitrile into β-aminonitriles. The synthesis of β-aminonitriles from larger ketone substrates using xylylenediamine **23** as the source of amino group was explored. The stable β-ketonitrile substrates **54** were then converted into β-aminonitriles **56** through reductive amination using transaminases in the presence of diamine donor **23** (**Figure 13**).



54 **56**

R: a.H, b.F, c.CH_3, d.OMe

Figure 13. Biotransformation of *beta*-ketonitriles using omega-transaminases

Having β-ketonitriles at our disposal, tω-TA *Aspergillus fumigatus*, Prozomix-TA005, Prozomix-TA010, Prozomix-TA011, Prozomix-TA037, Prozomix-TA040, and Prozomix-TA042 were tested in reductive amination of β-aminonitriles using diamine donor **23**. The transaminase was rehydrated in HEPES buffer at pH 7.5 with the PLP co-factor. The ketone **54c** in DMSO was added to the transaminase solution and the reaction mixture was incubated at 30°C for 24 h. The generation of the amine product **56** was monitored by TLC and LC-MS. The method reported by Turner and co-workers was followed.[99] The transaminases tested on different substrates are listed in **Table 11** below.

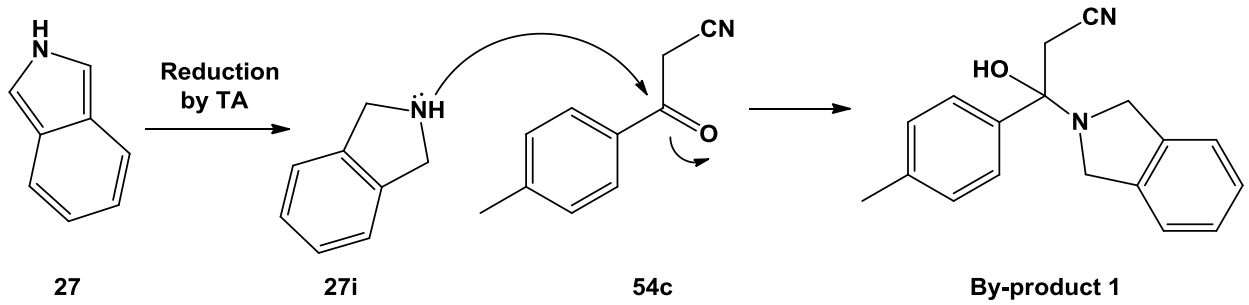
Table 11. Reductive amination of β-ketonitriles using different transaminases

Substrate	ω-TA code	Substrate [C] (mM)	Activity
54c	Prozomix-TA005	10	√
54c	Prozomix-TA010	10	√
54c	Prozomix-TA011	10	√
54d	Prozomix-TA011	10	√
54c	Prozomix-TA040	10	√
54c	Prozomix-TA042	10	√
54d	Prozomix-TA046	10	√
54d	*Aspergillus fumigatus* TA	10	√

All the transaminases tested showed activity towards **54c-d** at substrate concertation of 10 mM (**Table 11**). More than three spots were observed on the TLC for all the transaminases tested on **54c-d**, indicating that there were more by-products generated. Since the previous column used did not retain the amine product or standards sufficiently, the Hilic column was used in the analysis for the reductive amination reactions of **54c-d** (**Table 11**). The standards were first analysed on LC-MS using a solvent gradient 5-95% acetonitrile. In the LC-MS analysis of **54c**, the peak of the standard was observed at 10.65 min with the mass $[M+H]^+$ of 160.0752 *m/z* for $C_{10}H_{10}NO$ (**Appendix, Figure A23**). In the LC-MS of the amine standard **56c**, the peak of **56c** was observed at 6.71 min with the mass of $[M+H]^+$ 161.1067 *m/z* for $C_{10}H_{13}N_2$ (**Appendix, Figure A24**).

The TLC of the biotransformation reactions of **54c** involving Prozomix-TA005, Prozomix-TA010, Prozomix-TA011, and Prozomix-TA040 showed identical results with the amine product observed at R_f = 0.65 , which is very close to the amine standards R_f value of 0.64 (**Appendix, Figure A25**). The other spots are possibly due to the side reactions.

Herein, one of the reactions is reported which was analysed in detail involving Prozomix-TA042 in the reductive amination of **54c**. The product was not isolated due to the low yields, hence only the TLC and LC-MS were used to monitor the generation of the amine product. The generated product **56c** was observed with a retention time similar to the standard at R_f = 0.30, while the starting material was observed with a retention time similar to the standard at R_f = 0.8. In contrast, the LC-MS did not show the mass of the starting material, indicating that something happened to the starting material observed by the TLC (**Appendix, Figure A25**). A major peak observed at 8.2 min with the observed mass of 279.1490 *m/z* corresponded well with the calculated mass of 279.1453 *m/z* (**Appendix, Figure A26**), was identified to be a potential by-product 1 (**Scheme 32**).

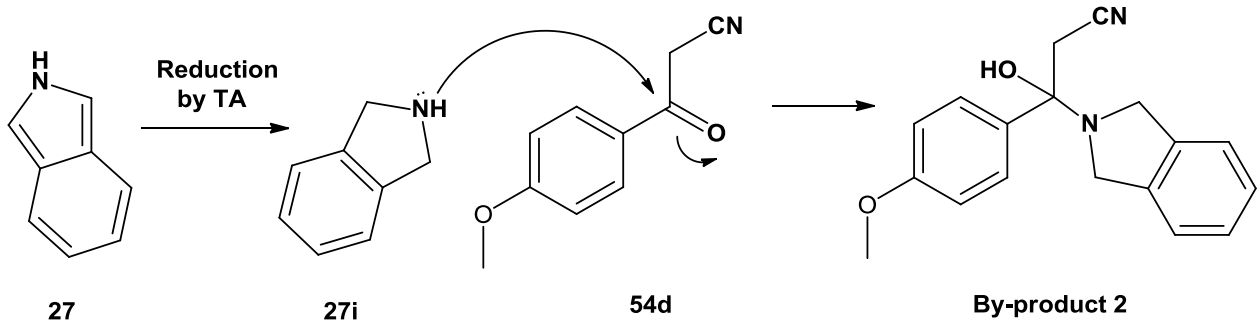


Scheme 32. Mechanism of the side-reaction between starting material **54c** and the isoindole

To obtain by-product 1, the reaction must have proceeded to some extent, otherwise the isoindole **27** would not have been formed. The generated **27** was then reduced by transaminase in to the very stable, highly basic isoindoline **27i**, which then readily forms a hemiaminal through that basic nitrogen with **54c** to generate by-product 1. Therefore, reducing the substrate's concentration from the reaction. The peak of the generated **56c** was observed at 6.90 min (similar retention time as the standard) with the accurate mass of 161.1075 *m/z* for $C_{10}H_{13}N_2$ in agreement with the mass of the amine standard 161.1034 *m/z* (**Appendix, Figure A26**).

The second substrate was now examined to investigate if a similar by-product 1 would be generated. Firstly, the standard **54d** was analysed with LC-MS. The LC-MS of the standard **54d**, showed the peak of the standard substrate **54d** at 5.62 min with the mass of 176.0703 *m/z* for $C_{10}H_{10}NO_2$ (**Appendix, Figure A27**). Then ω-transaminase Prozomix-TA011, Prozomix-TA046 and *Aspergillus fumigatus* TA were tested on a different substrate **54d** following similar reaction procedures and conditions above (**Table 11**). In contrast to the reaction involving ω-TA *Aspergillus fumigatus* TA, the starting material was not observed on the TLC of the reaction involving ω-TA Prozomix-TA011. There were two spots observed at R_f = 0.21 and R_f = 0.35 (**Appendix, Figure A28**). The LC-MS was then used to determine if the reaction was successful. In the LC-MS of 3-amino-3-(*p*-methoxyphenyl)propanenitrile **56b**, the peak of the possibly generated **56d** was observed at 2.01 min with the mass of 177.1023 *m/z* for $[M+H]^+$ which was consistent with the calculated mass for $C_{11}H_{13}N_2O$; 177.0983 *m/z* (**Appendix, Figure A29**).

Similarly, a significant major peak was observed at 3.93 min with the mass of 295.1469 *m/z* in agreement with the calculated mass of 295.1402 *m/z* for $C_{18}H_{18}N_2O_2$; designated by-product 2 in **Scheme 33**.



Scheme 33. Mechanism of the side-reaction between starting material **54d** and the isoindole

Since there were some other peaks observed in the LC-MS, it is possible that the diamine donor underwent other side-reaction with the starting material in similar manner as with **54c**. On the other hand, ω-TA Prozomix-046, showed low activity towards **54d** since the starting material on the TLC was observed with a retention time similar to the standard at R_f = 0.7 (**Appendix, Figure A28**).

The transaminases were found to be active towards different substrates, however the reaction did not work out as expected. Interestingly, the major product obtained was in fact not the desired product, instead it were the by-products shown in **Scheme 32** and **33**. But it indicated that some of the product must have been formed, because the by-products had to be formed from the isoindoline intermediate **27i** (**Scheme 33**), therefore some percentage of the amine product must have been generated successfully. But unfortunately, the reactivity of the carbonyl carbon of the β-ketonitriles **54c** and **54d**, possibly because of the strongly electron withdrawing nitrile group, made it highly reactive towards the basic isoindoline **27i** generating the by-products 1 and 2. In light of these low yields and side-reactions, it was decided not to expand the library to consider the other set of β-ketonitriles **49**. Instead, the possible side reactions that might be happening in the reaction preventing the generation of the amine product in good yield were investigated.

3.5 Reaction controls using 54c and 56c

The poor yields of the biotransformation reactions were probably due to the side reactions involving the starting material and other components in the reaction mixture. Therefore reaction controls were conducted employing **54c** and **56c** to investigate these possible side reactions. Several reaction controls were conducted to determine which of the components were involved in side reactions leading to formation of by-products (**Table 12**).

Table 12. Reaction controls for biotransformation of 3-oxo-4-(*p*-tolyl)butanenitrile

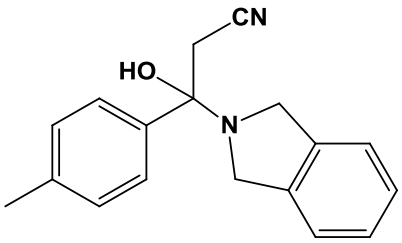
Entry	1	2	3	4
ω-TA	√			
PLP	√	√	√	
Diamine Donor	√	√	√	√
Substrate	√	√		√
Buffer	√	√	√	√

DMSO	√	√		√
By-product 1 (See structures in **Table 13**)	Observed	Not observed	Not observed	Not observed

(a) Tick (√) indicate components involved in reaction

The by-product 1 resulting from reaction control 1 in **Table 12** was observed in the LC-MS of which its mass and structural representation are tabulated below (**Table 13**).

Table 13. By-products generated from reaction controls

By-products	Structures for by-products	Calculated mass $[M+H]^+$	Observed mass $[M+H]^+$	Retention time (min)
1		279.1453 $C_{18}H_{18}N_2O$	279.1490	8.2

The main reaction control 1 involved all the necessary components required for reductive amination of 3-oxo-4-(*p*-tolyl)butanenitrile **54c** (**Table 12**) and the by-product 1 was detected on the LC-MS (**Table 13**). Then different reaction controls were conducted in order to investigate if this by-product could be generated in the absence of enzyme and where one component was omitted per control (**Table 12**). The by-product 1 was not detected in the absence of the transaminase (**Table 12,** entry 2, 3 & 4), indicating that the biotransformation reaction was catalysed by the enzyme. The starting material was found to be directly reacting with the diamine donor in controls 2, 3 and 4 (**Table 12**), therefore reducing the substrate concertation from the reaction mixture, resulting in extreme low yields.

β-Ketonitriles were also reported to be potential substrates for synthesis of the β-amino acids whereby nitrilase from *Bradyrhizobium japonicum* (NitBJ) USDA 110 was employed to hydrolyse these substrates into β-keto acids followed by *in-situ* amination

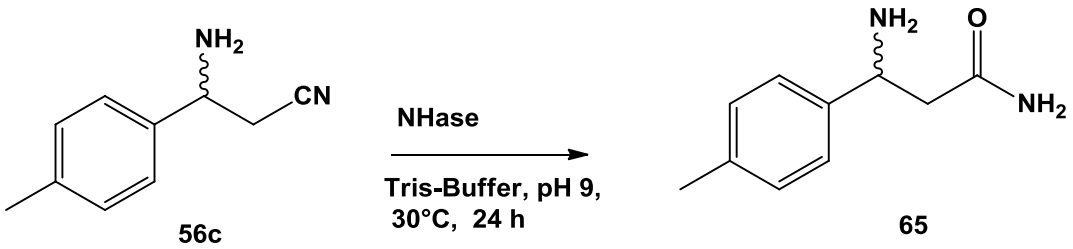
into β-amino acids using β-amino acid dehydrogenase, NADPH and glucose dehydrogenase recycling enzymes.[133] This suggests that carboxylic acid in the transaminase substrates is required to enhance the reaction efficiency of asymmetric reductive amination by ω-TA. The novel β-ketonitrile substrates used in the current study do not bear the carboxylic acid. This might be the reason why the reactions gave poor yields since the substrates were probably not recognised in the ω-TA's active site.

Until now, natural existing omega-transaminases that accept β-ketonitrile as amino acceptors are unknown. More focus should therefore be on engineering of variants omega-transaminases that accepts β-ketonitriles as precursors.

3.6 Hydrolysis of nitrile substrates using nitrile hydratase

Once the β-aminonitriles have been synthesised, they need to be converted to a form that can be incorporated into the peptides. This can be achieved stereoselectively using biocatalysis. Nitrile hydratase/amidase are mainly known to hydrolyse aliphatic nitriles whereas nitrilases generally hydrolyse aromatic nitriles substrates.[105] However it was reported that *Rhodococcus rhodochrous* ATCC BAA-870 has activity towards aromatic nitriles, aliphatic nitrile, benzonitrile and 3-hydroxy-3-phenylpropionitrile substrates.[44,105] Some nitriles act as inhibitors instead of being substrates, for example; isobutyronitrile and α-hydroxynitriles inhibit *Rhodococcus* R312 and *Corynebacterium nitrilophilus* nitrile hydratases whereas benzonitrile inhibits nitrile hydratase from *Bacillus pallidus* Dac521.[105] Therefore, isolated nitrile hydratase from *Rhodococcus rhodochrous* ATCC BAA-870 was tested for activity against β-ketonitriles and β-aminonitriles as they are important substrates for the synthesis of the β-amino acids.

3.6.1. Hydrolysis of β-aminonitrile



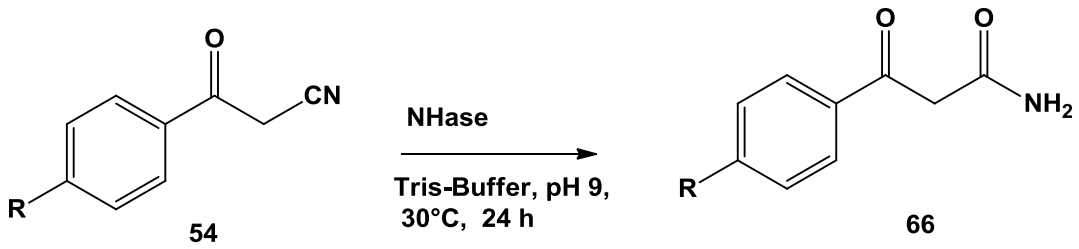
Scheme 34. Hydrolysis of β-aminonitrile **56c** using NHase

The hydrolysis of **56c** was conducted using isolated NHase from *Rhodococcus rhodochrous* ATCC BAA-870 in Tris-buffer at pH 9 (**Scheme 34**), following a method

reported by Chhiba and co-workers.[44] Two spots were observed on TLC; the starting material was observed at similar R_f with the standard at R_f = 0.14, while the other spot was observed at R_f = 0.07 (**Appendix, Figure A39**). In this reaction, the product was not isolated since it was conducted as a test reaction on a small scale, therefore LC-MS was used to monitor the synthesis of 3-amino-3-(*p*-tolyl)propanamide **65**. The molecular peak of the product **65** was observed in the chromatogram at 1.70 min with the mass of $[M+H]^+$ 179.1171 *m/z*, which was in good agreement to both the calculated mass of 179.1140 *m/z* for $C_{10}H_{15}N_2O$ and that observed by Chhiba and co-workers (**Appendix, Figure A31**). The incomplete conversion was confirmed by the peak of the starting material that was observed at 2.25 min with the observed mass of 161.1070 *m/z*, which is consistent with the mass of the standard (**Appendix, Figure A31**). The racemic substrate **56c** was not converted completely to the amide product, which was possibly due to enantioselectivity of the nitrile hydratase.[44]

It has been demonstrated that nitrile hydratase containing cobalt in the active site of *Rhodococcus rhodochrous* ATCC BAA-870, hydrolyse β-aminonitriles into enantiopure β-amino amides.[44] They also showed enantioselectivity towards α-aminonitriles compared to the iron-containing nitrile hydratase counterparts.[44] Therefore this maybe one of the reason why two spots were observed for starting material and product on the TLC, hence incomplete conversion. Based on the findings of Chhiba and co-workers, NHase might kinetically resolved (hydrolysis of one enantiomer over the other) the racemic starting material **56c**. Therefore, it is important to synthesise enantiopure *R* and *S*-β-aminonitriles using ω-transaminases so that the reaction can go to completion depending on the enantiospecificity of the *Rhodococcus rhodochrous* ATCC BAA-870 nitrile hydratase. Having observed that *Rhodococcus rhodochrous* ATCC BAA-870 is active towards β-aminonitrile, it was then decided to also test *Rhodococcus rhodochrous* ATCC BAA-870 against β-ketonitrile for substrate specific and investigate if it could convert these substrates into β-Keto amides.

3.6.2 Hydrolysis of β-ketonitriles



R: (c) Me, (d) OMe

Scheme 35. Hydrolysis of β-ketonitriles **66** using NHase

The high electrophilicity of the carbonyl carbon seemed to make it difficult to synthesise enantiopure β-aminonitriles since diamine donor seemed to attack the β-ketonitrile starting material. Therefore it was deemed necessary to conduct the asymmetric hydrolysis conversion of β-ketonitriles into β-keto amides which would be potential novel substrates for asymmetric reductive amination using ω-TA. Using similar procedure as above, β-ketonitriles 3-oxo-3-(*p*-tolyl)propanenitrile **54c** and 3-(*p*-methoxyphenyl)-3-oxopropanenitrile **54d** substrates were hydrolysed by *Rhodococcus rhodochrous* ATCC BAA-870 nitrile hydratase into β-ketoamides 3-oxo-3-(*p*-tolyl)propanamide **66c** and 3-(*p*-methoxyphenyl)-3-oxopropanamide **66d**, respectively (**Scheme 35**). Only one spot at R_f = 0.64 for reaction involving hydrolysis of **54c** and also at R_f = 0.61 for hydrolysis of **54d**, was observed on the TLC suggesting the complete conversion of the hydrolysis reactions (**Appendix, Figure A30**).

No 3-oxo-3-(*p*-tolyl)propanenitrile **54c** peak observed in the LC-MS spectrum of the hydrolysis reaction. Only the peak of the product 3-oxo-3-(p-tolyl)propanamide **66c** at 4.15 min with the observed mass of $[M+H]^+$ 178.0861 *m/z* which is in agreement with the calculated mass for $C_{10}H_{12}NO_2$: 178.0823 *m/z* (**Appendix, Figure A32**). The absence of the starting material in both TLC and LC-MS indicates complete conversion. However some carbonyl containing compounds do not ionize easily. When 3-(*p*-methoxyphenyl)-3-oxopropanenitrile **54d** was used as the starting material, similar pattern was observed as in **54c** substrate. In the LC-MS of the hydrolysis of **54d**, the peak of **66d** was observed at 3.65 min with the observed mass of **66d** $[M+H]^+$ 194.010 *m/z* corresponding to the calculated mass of 194.0772 *m/z* for $C_{10}H_{12}NO_3$ (**Appendix, Figure A42**).

Nitrile hydratase *Rhodococcus rhodochrous* ATCC BAA-870 gave complete hydrolysis conversion of the β-ketonitriles into β-keto amides as compared to the β-aminonitriles. Therefore we demonstrated that *Rhodococcus rhodochrous* ATCC BAA-870 has high activity towards aromatic β-ketonitriles.

It can be suggested that the preparative scale can be used to prepare more β-ketoamides that can possibly then be used for asymmetric synthesis of β-amino acids using ω-transaminases and subsequent hydrolysis of amide group using amidase into β-amino acid for incorporation into wound healing peptides synthesis. This will be evaluated in future work.

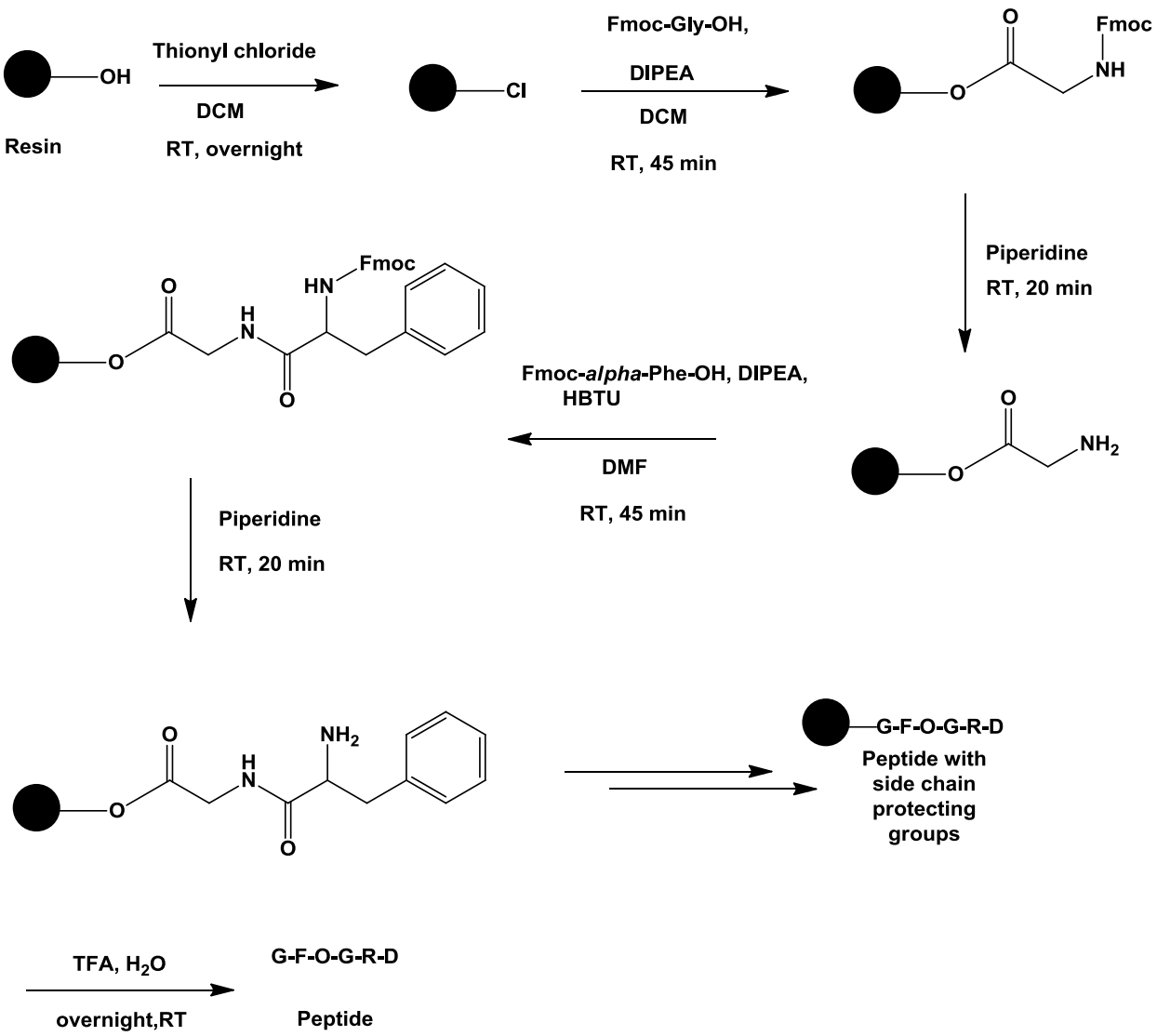
In summary, we synthesized the starting material, screened the enzyme kits, generated trace amounts of *beta*-aminonitriles (low yields probably due to a combination of the substrate not being the best substrate, low enzyme activity and by-product formation). In future yields could be improved by varying reaction conditions or by enzyme engineering. The racemic product was synthesized in sufficient yields to demonstrate a biocatalysis reaction to convert them to the amides. These could then be hydrolysed by an amidase in the future research.

As the β-aminonitriles were synthesised in poor yields, therefore the desired β-amino acids were not synthesised as expected. Since the required amount of each amino acid is approximately 0.5 g, then the enantiopure β-amino acids were purchased to demonstrate the next step.

3.7 Approach towards synthesis of wound healing peptides

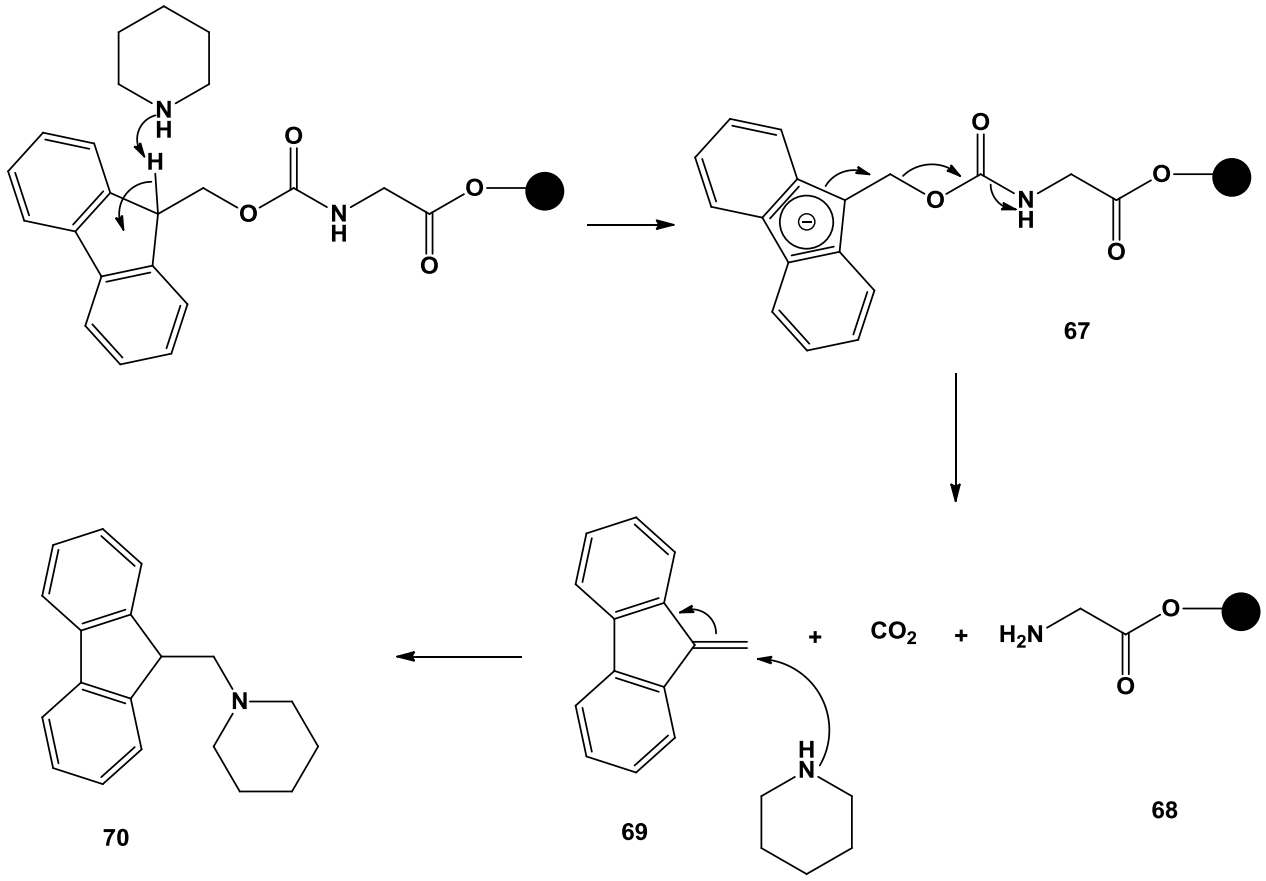
3.7.1 Synthesis of *alpha*-peptides

The choice of resin, linker (chemical compound which link the peptide to the resin), coupling reagents, protected amino acids and peptide cleaving condition, play an important role in the successful synthesis of peptides using the solid-phase peptide synthesis technique (SPPS).[136] The peptides were designed with a carboxylic acid C-terminus since the carboxylates negative charge stabilise the triple-helix structure of the collagen mimetic peptides (CMPs) better than the ammonium positive charge of the amide motif.[137] Thus, a 2-chlorotrityl resin was used as the solid support in the peptide synthesis. Manual and automated SPPS were carried out under inert nitrogen gas atmosphere (**Scheme 33**).



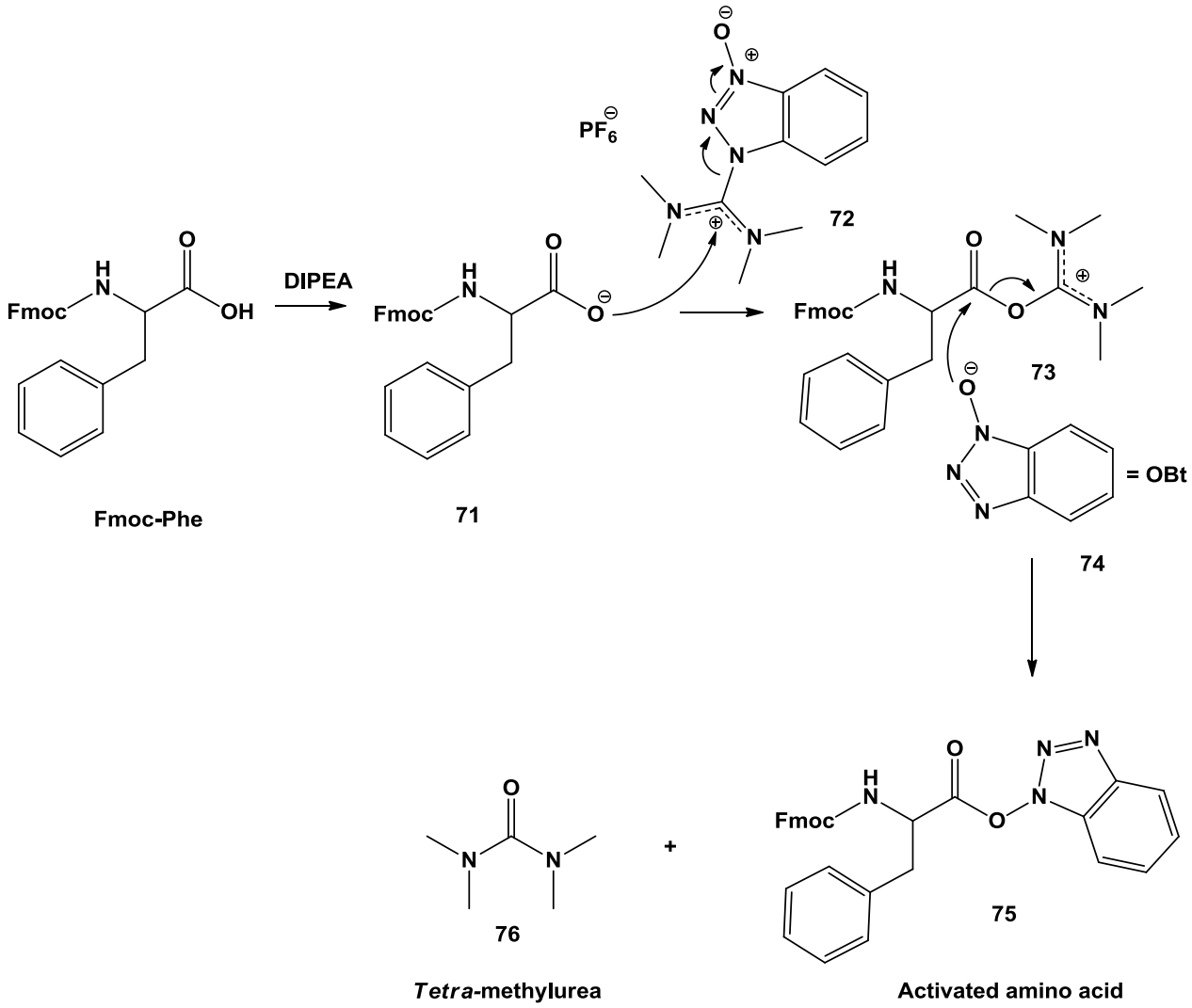
Scheme 33. Synthesis of wound healing peptides

The procedures reported by APPTEC,[138] was adopted and modified for the activation of the 2-chlorotrityl resin. The resin grains were soaked in dry DCM in the presence of thionyl chloride overnight to substitute the hydroxyl group on the resin with a chlorine group (**Scheme 33**). The first amino acid, Fluorenylmethyloxycarbonyl-Glycine (Fmoc-Gly (G)) was coupled to the resin using a base *N,N*-Diisopropylethylamine (DIPEA) to deprotonate the carboxylic proton of the amino acid which then undergoes a nucleophilic substitution with the chlorine group on the resin. The amine protecting group (Fmoc) of the amino acid is then deprotected to give a free amine (NH_2) (**Scheme 34**).



Scheme 34. Fmoc-deprotection mechanism using piperidine.[139]

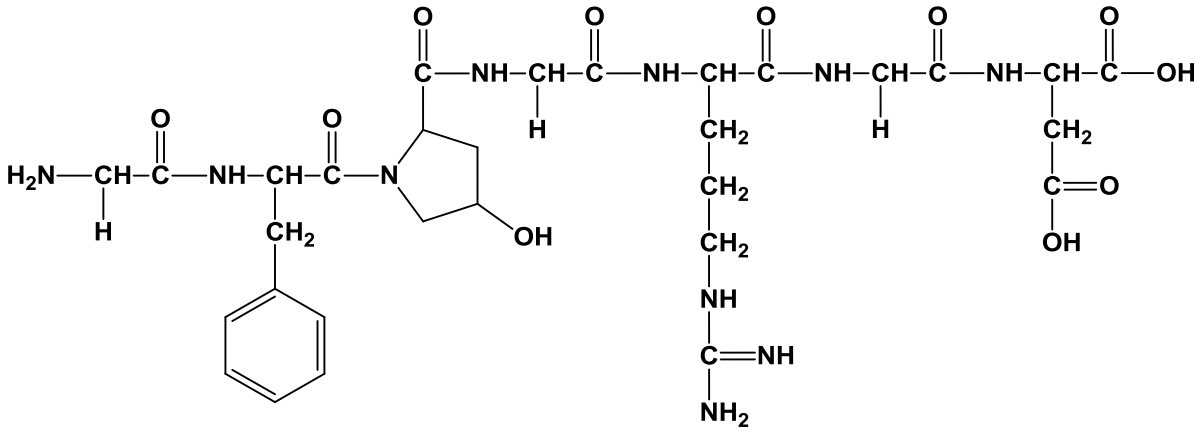
The added secondary amine (piperidine) deprotonates the acidic proton of the Fmoc ring followed by β-elimination of **67** that leads to the formation of a free NH_2 glycine-bound to the resin **68** and dibenzofulvene **69** which is trapped by piperidine to generates by-product **70** (**Scheme 34**).[139] The Fmoc was used to protect the amino group (N-terminal group) to prevent the intramolecular interaction within the peptide.[138,140] The glycine-bound to the resin was washed to remove the excess reagents and byproducts. The second amino acid that was coupled to the resin bound-glycine was Fmoc-α-Phenylalanine (Fmoc-Phe (F)). A coupling reagent 2-(1H-benzotriazol-1-yl)-1,1,3,3-tetramethyluronium hexafluorophosphate (HBTU) was used to activate the carbonyl carbon of the Fmoc-α-Phe at the C-terminal (**Scheme 35**).[140]



Scheme 35. The activation of amino acid using HBTU[140]

Then a base DIPEA was added, which deprotonates the carboxylic acid proton resulting in a carboxylate anion **71** which then attacks the cation carbodiimide carbon of the HBTU **72** to form the ester **73** and triazine **74**. The generated triazine **74** attacks the carbonyl carbon of the ester **73** resulting in the formation of the activated carbonyl carbon of Fmoc-α-Phe **75**. Hydroxybenzotriazole (HOBt) **74** is a better leaving group than the hydroxyl group and *tetra*-methylurea **76** (**Scheme 35**). The amino group of the deprotected glycine-bound resin attacks the carbonyl carbon of the activated amino acid substituting the better leaving group HOBt **74** leading to the extension of the peptide chain. After coupling the Fmoc-α-Phe, the resin bound-peptide was washed followed by Fmoc-deprotection using 20% piperide/DMF preparing it for the next coupling cycle. The next amino acids coupled to the peptide-bound resin to complete the peptide sequence were Fmoc-Hydroxyproline (Fmoc-Hyp (O)), Fmoc-Gly (G), Fmoc-Arginine (Fmoc-Arg (R)), Fmoc-Gly (G) and Fmoc-Aspartic acid (Fmoc-Asp (D)), sequentially. The coupling,

deptotection and washing procedures were reported in Section 2.9. After the cycle was complete, all the protecting groups were removed along with the resin followed by purification using the HPLC to give **60a** α-peptide G-F-O-G-R-G-D (**Figure 16**).



60a

Figure 16. Structural representation of α-peptide G-F-O-G-R-G-D

The successful coupling of each amino acid was monitored by LC-MS. For example, after an amino acid coupling and Fmoc-deprotection, a few resin grains were taken out and cleaved. The LC-MS analysis was used to confirm the successful coupling of Fmoc-Hyp (O), Fmoc-Gly (G), Fmoc-Arg (R), Fmoc-Gly (G) and Fmoc-Asp (D) (**Table 9**). The observed masses were consistent with the calculated masses of the peptides (**Table 14**), for the LC-MS analysis see **Appendix Figure A34-38**.

Table 14. LC-MS data analysis of each amino acid coupled

Entry	Sequence	Amino acid coupled	Calculated mass (*m/z*) $[M+H]^+$	Observed mass $[M+H]^+$	Retention time (min)
1	G-F-O	O	336.1515 $C_{16}H_{22}N_3O_5$	336.1383 and 336.1381	8.27 and 8.37
2	G-F-O-G	G	393.1729 $C_{18}H_{25}N_4O_6$	393.1556 and	8.38 and

				393.1567	8.46
3	G-F-O-G-R	R	549.2741 $C_{24}H_{37}N_8O_7$	549.2763	5.79
4	G-F-O-G-R-G	G	606.2955 $C_{26}H_{40}N_9O_8$	606.2712 and 606.2713	5.73 and 5.77
5	G-F-O-G-R-G-D	D	721.3225 $C_{30}H_{45}N_{10}O_{11}$	721.2868 and 721.2869	8.19 and 8.21

m/z = Mass-to-Charge Ratio

Table 14 showed that the observed mass was increasing with the coupling of each amino acid leading to the extension of the peptide chain. After coupling the last amino acid Fmoc-Asp (D) entry 5 (**Table 14**), the peptide was cleaved from the resin. The peptide was purified by HPLC yielding peptide **60a** G-F-O-G-R-G-D and the LC-MS analysis confirmed the successfully synthesis of our desired peptide **60a** (**Appendix, Figure 39**), since the split peak at 8.22 and 8.27 min with the observed masses of 721.2537 *m/z* and 721.2547 *m/z,* respectively were consistent with the calculated mass 721.3325 *m/z* for $C_{30}H_{45}N_{10}O_{11}$ (**Table 14**).

The LC-MS analysis showed the split peaks after the coupling of hydroxyproline. It was first presumed that these double peaks were due to the impurities from the unpurified peptides (**Table 14**). However previous work have reported that peptides containing proline residue can exhibit conformational isomers (*cis* and *trans*) resulting in the formation of a peak shoulder.[141,142] These conformational isomers are due to the inversion of the imide nitrogen lone pair relative to the **C_a-H** of the proline residue, which results from the amide-imidate tautomerisation (**Figure 17**).[143,144]

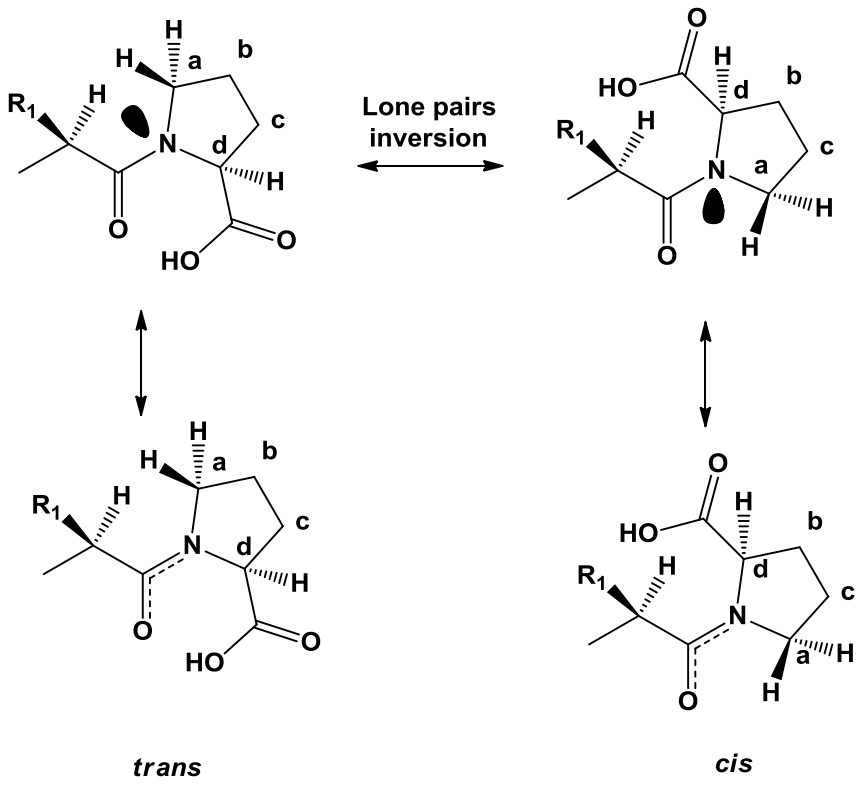


Figure 17. Conformational isomers of peptide containing proline.[143,144]

Our peptide contains hydroxyproline instead of proline, however the only difference is the presence of a hydroxyl-group which doesn't have a significant role in nitrogen lone pair inversion. Therefore, based on the previous findings (**Figure 17**) and the observed results after the purification of the hydroxyproline-containing peptide **60a**, it is suggested that the split peaks observed from the LC-MS chromatogram at 8.22 and 8.25 min retention times that have similar mass (**Appendix, Figure A39**) were possibly due to the *cis-trans* conformational isomers. These kinds of isomers were separated by Kalman and co-workers, using reverse-phase chromatography at low temperatures.[142] The *cis-trans* conformers have a slight difference in retention times which makes it difficult to separate, however the slow interconversion between the *cis-trans* conformers enabled them to be separated at low temperatures.[141,142] On this basis, in the future we will adopt a similar approach to separate these conformers.

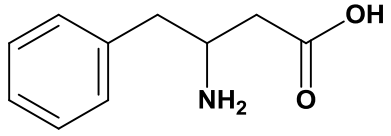
It has been reported that lipophilic peptides (lipopeptides) are important for cell membrane permeability, therefore it is vital for the peptides to have a hydrophobic side chain to facilitate the membrane fusion.[145] Previous studies have reported that palmitic acid and adamantane can be attached to peptides to provide the necessary lipophilicity, thereby improving their pharmacokinetics.[146,147] Having to successfully synthesised the standard α-peptide **60a** GFOGRGD, then **60a** was modified for membrane permeability by attaching palmitic acid (Pal) and adamantine (Ada) at the N-terminus. The coupling,

washing and cleavage followed the same protocol as described before (Section 2.9) to give **60b** and **60c** (**Appendix, Figure A49-50**). These peptides were not purified due to time constrain, however the purification will be done in the future. The LC-MS analysis showed the successful coupling of palmitic moiety where the observed mass of 959.5737 *m/z* for $[M+H]^+$ was consistent with the calculated mass 959.5521 *m/z* for $C_{46}H_{75}N_{10}O_{12}$ (**Appendix, Figure A40**). The successful coupling of adamantane was confirmed by LC-MS whereby the observed mass of 883.4365 *m/z* for $[M+H]^+$ was also consistent with the calculated mass 883.4269 *m/z* for $C_{41}H_{59}N_{10}O_{12}$ (**Appendix, Figure A41**).

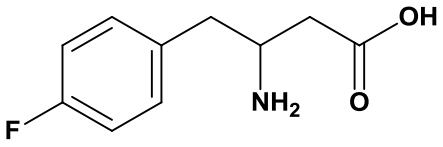
The purification and potency of these lipopeptides will be evaluated in future work. Since *alpha*-peptides are known to be susceptible to proteases as indicated in chapter 1, therefore it was then decided to purchase and incorporate enantiopure β-amino acid in our peptides.

3.7.2 Synthesis of *beta*-peptides

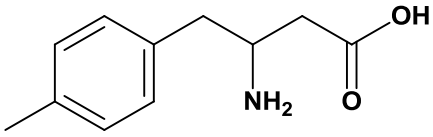
The reductive amination of the β-ketonitriles reaction cascade gave very low yields for β-amino acid (Section 3.5), we then decided to purchase these β-aromatic amino acids; 3-amino-4-phenylbutanoic acid, 3-amino-4-(*p*-tolyl)butanoic acid and 3-amino-4-(4-fluorophenyl)butanoic acid (**Figure 18**), to demonstrate that they can be incorporated into peptide sequences. The phenylalanine was replaced by the purchased β-aromatic amino acid to give the β-peptides. These modifications would increase the hydrophobic interaction of the peptide with the integrin active site thereby improving the formation of fibers and platelets aggregation.



3-amino-4-phenylbutanoic acid



3-amino-4-(4-fluorophenyl)butanoic acid



3-amino-4-(*p*-tolyl)butanoic acid

Figure 18. Purchased aromatic β-amino acids

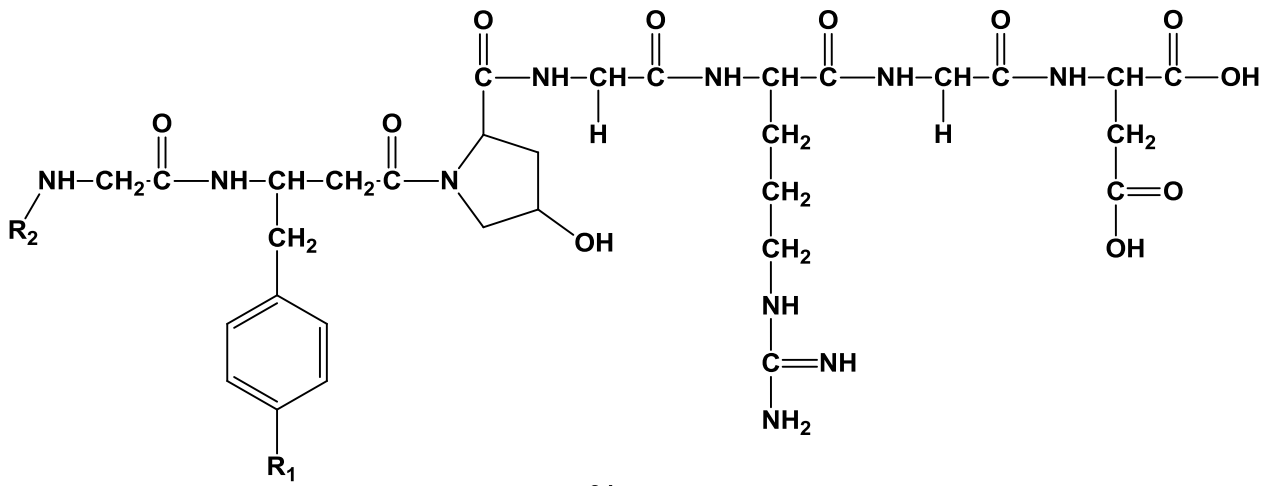
The synthesis of the β-peptides followed similar coupling cycles as described in the synthesis of the α-peptides (in Section 2.9). The phenylalanine was replaced with 3-amino-4-phenylbutanoic acid, 3-amino-4-(*p*-tolyl)butanoic acid and 3-amino-4-(4-fluorophenyl)butanoic acid, to give **61a**, **61d** and **61g**. We only monitored the coupling progress of peptide **61d** by LC-MS to investigate if the β-aromatic amino acids could be incorporated into the wound healing peptide sequence. The monitoring method followed the one described in 3.7.1 and the LC-MS analysis confirmed the successful coupling of amino acids used to complete the peptide sequence G-β(Me)Phe-O-G-R-G-D (**Table 15**). For mass spectra see **Appendix Figure A42-46**.

Table 15. LC-MS analysis of reaction progress for assembling peptide **61d**

Entry	Sequence	Amino acid coupled	Calculated mass (*m/z*) $[M+H]^+$	Observed mass $[M+H]^+$
1	G-β(Me)Phe-O	O	364.1828 $C_{18}H_{26}N_3O_5$	364.1850
2	G-β(Me)Phe-O-G	G	421.2042 $C_{20}H_{29}N_4O_6$	421.2051
3	G-β(Me)Phe-O-G-R	R	577.3054 $C_{26}H_{41}N_8O_7$	577.3081
4	G-β(Me)Phe-O-G-R-G	G	634.3268 $C_{28}H_{44}N_9O_8$	634.3283
5	G-β(Me)Phe-O-G-R-G-D	D	749.3538 $C_{30}H_{45}N_{10}O_{11}$	749.3656

β(Me)Phe = 3-amino-4-(p-tolyl)butanoic acid

There is a correlation between **Table 14** and **Table 15** as the accurate masses were consistent with the amino acid coupled per cycle. These free NH_2 β-peptides **61a**, **61d** and **61g** were modified by coupling palmitic acid and adamantane, respectively to give **61b**, **61c**, **61e**, **61f**, **61h** and **61i** (**Table 16**). For LC-MS analysis see the **Appendix Figure A47-55**.



61

Table 16. The β-peptides containing β-aromatic amino acid derivatives

Compound	Sequence	R_1	R_2	Calculated mass	Observed mass	Molecular ion
61a	G-βPhe-O-G-R-G-D	H	H	735.3381 $C_{31}H_{47}N_{10}O_{11}$	677.3221	[M-Glycine]$^+$
61b	G-βPhe-O-G-R-G-D-Pal	H	Palmitic	973.5678 $C_{47}H_{77}N_{10}O_{12}$	973.5709 and 973.5734	$[M+H]^+$
61c	G-βPhe-O-G-R-G-D-Ada	H	Adamantane	897.4426 $C_{42}H_{61}N_{10}O_{12}$	897.4424	$[M+H]^+$
61d	G-β(Me)Phe-O-G-R-G-D	Me	H	749.3538 $C_{32}H_{49}N_{10}O_{11}$	749.3552	$[M+H]^+$
61e	G-β(Me)Phe-O-G-R-G-D-Pal	Me	Palmitic	987.5834 $C_{48}H_{79}N_{10}O_{12}$	987.5906	$[M+H]^+$
61f	G-β(Me)Phe-O-G-R-G-	Me	Adamantane	911.4582 $C_{43}H_{63}N_{10}O_{12}$	911.4675	$[M+H]^+$

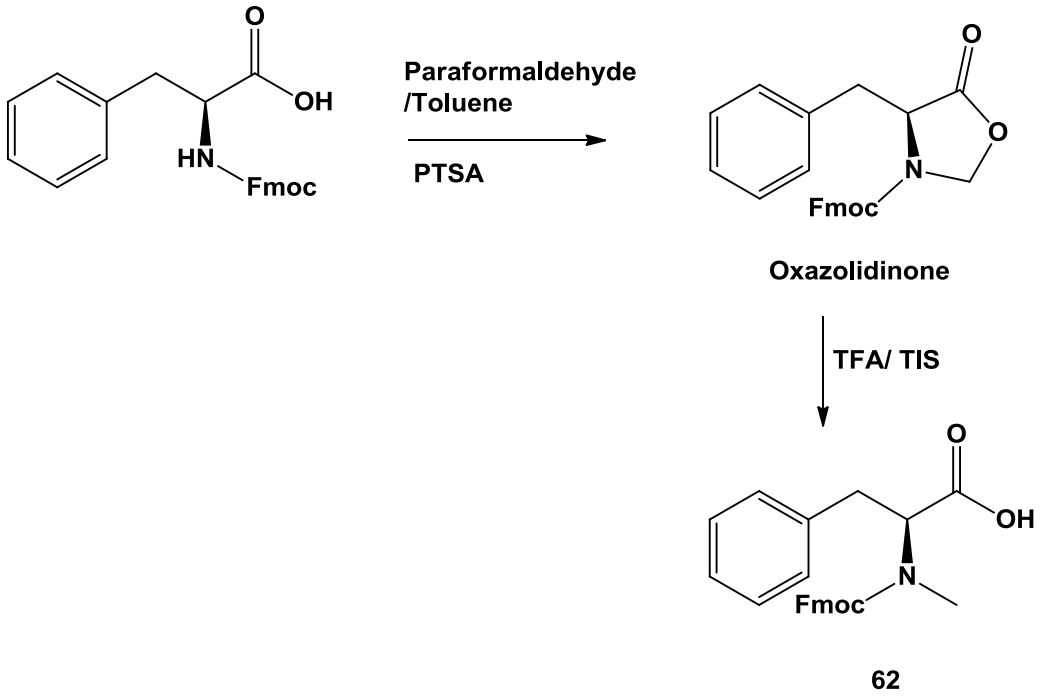
	D-Ada					
61g	G-β(Flu)Phe-O-G-R-G-D	Flu	H	753.3287 $C_{31}H_{46}FN_{10}O_{11}$	753.3288 and 753.3254	$[M+H]^+$
61h	G-β(Flu)Phe-O-G-R-G-D-Pal	Flu	Palmitic	991.5584 $C_{47}H_{76}FN_{10}O_{12}$	991.5626	$[M+H]^+$
61i	G-β(Flu)Phe-O-G-R-G-D-Ada	Flu	Adamantane	915.4332 $C_{42}H_{60}FN_{10}O_{12}$	961.4432	[M+ Formic acid+H]$^+$

βPhe = 3-amino-4-phenylbutanoic acid; β(Me)Phe = 3-amino-4-(p-tolyl)butanoic acid; β(Flu)Phe = 3-amino-4-(4-fluorophenyl)butanoic acid, Flu = Fluorine

The HPLC was used to purify peptide **61b**, **61c**, **61d** and **61g** (**Table 16**). The rest of the peptides were not purified due to time constrain. However LC-MS analysis for all the peptides confirmed the successful synthesis of the desired β-peptides as the observed masses were consistent with the calculated masses (**Table 16**). Previous studies have reported that lipopeptides that are more hydrophobic tend to have greater membrane permeability.[147] Therefore the attachment of adamantane and palmitic acid to these β-peptides would improve their hydrophobicity, hence increase membrane permeability. The membrane permeability of α-peptides was also attempted to be improved by the *N*-methylation of phenylalanine.

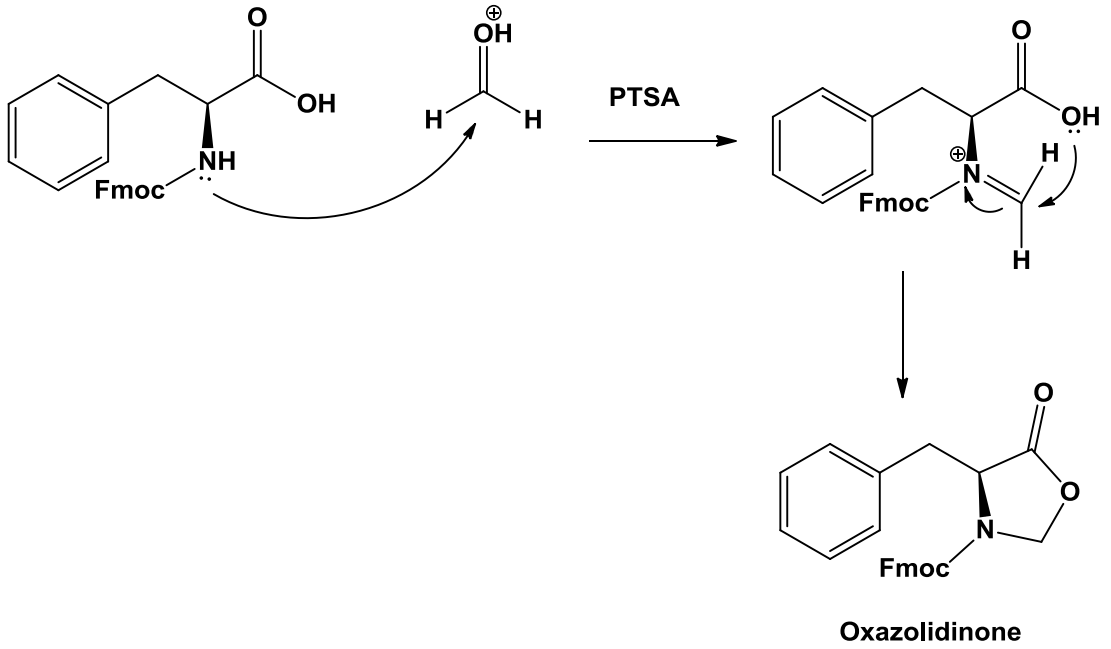
3.7.3 *N*-methylation of α-phenylalanine

Previous studies have reported that peptides which are N-methylated get degraded less than normal peptides and they also have an improved conformational rigidity.[31] On this basis, the *N*-methylation on phenylalanine was attempted so that it can be incorporated into collagen mimetic peptides (**Scheme 36**).



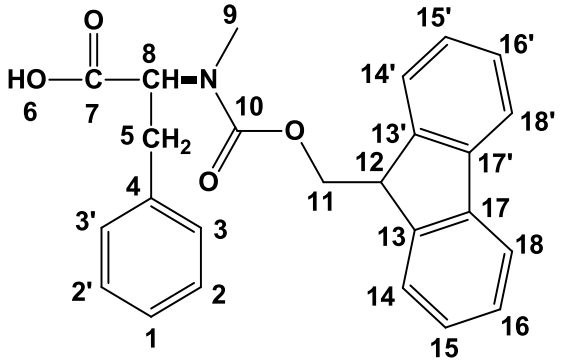
Scheme 36. Synthesis of *N*-methylated phenylalanine **62**

Fmoc-α-Phenylalanine was subjected to paraformaldehyde in the presence of PTSA yielding oxazolidinone (**Scheme 36**). PTSA was added to activate the carbonyl carbon of paraformaldehyde followed by nucleophilic attack by the nitrogen to the activated carbonyl and dehydration resulting into an imine.The hydroxyl group of the carboxylic acid then attacks the imine to give oxazolidinone (**Scheme 37**). Subsequent reaction of oxazolidinone with TFA and TIS gave *N*-methylated α-phenylalanine **62** (**Scheme 36**).



Scheme 37. Proposed mechanism of the formation of oxazolidinone

The cleaving mixture added to the oxazolidinone opened the five-membered ring yielding **62**.



62

Eleven signals were observed in the ^{1}H NMR spectrum of **62**, with five signals in the aromatic region between 7.83 and 6.99 ppm integration for thirteen protons, indicating the presence of Fmoc protecting group as well as the aromatic ring of the *N*-methylated phenylalanine. The singlet signal observed at 11.19 ppm integrating for one proton was assigned to H6, a characteristic of hydroxyl group. Therefore confirming the successful ring opening of the oxazolidinone. A singlet signal observed at 2.85 ppm integrating for three protons assigned to H9, was due to the methyl protons (-N-C**H**$_3$). Therefore suggesting successful *N*-methylation of the phenylalanine **62**. The ^{13}C NMR spectrum

also confirmed the success of the reaction as the methyl carbon (-N-**C**H_3) was observed at 31.9 ppm. Our NMR data match those reported by Di Gioia and co-workers.[116] The successful synthesis of **62** was also confirmed by LC-MS as the observed mass of 402.1670 *m/z* for $[M+H]^+$ was consistent with the calculated mass of 402.1661 *m/z* for $C_{25}H_{24}NO_4$.

The *N*-methylated α-phenylalanine **62** was not incorporated into the peptides, due to time constraints.

4. CONCLUSION AND FUTURE WORK

4.1 Conclusion

The main aim of this project was to synthesise enantiopure β-amino acids from corresponding β-ketonitrile substrates using the combination of ω-transaminases and nitrilase or nitrile hydratases/amidase reaction cascades. The β-ketonitrile substrates were successfully synthesized from aromatic carboxylic acids through esterification in ethanol followed by nucleophilic substitution with acetonitrile in *n*-BuLi solution. The racemic standard β-aminonitrile **56c** was also synthesised through conventional methods using a commercially available 4-methylbenzonitrile as the starting material in the presence of potassium *tert*-butoxide as a base for deprotonating acetonitrile, resulting into 3-amino-3-(*p*-tolyl)acrylonitrile **55**. Subsequent reduction of **55** in sodium cyanoborohydride yielded 3-amino-3-(*p*-tolyl)propanenitrile **56c**. The synthesised compounds were characterised and analysed by spectroscopic NRM, IR and LC-MS techniques.

ω-Transaminase kits were screened against different substrates with acetophenone being the standard substrate for screening most of the enzymes. It was observed that most of the ω-transaminases were showing activity towards the ketone substrates except for ω-TA Prozomix-TA008, Prozomix-TA018, Prozomix-TA020, Prozomix-TA023, Prozomix-TA025, Prozomix-TA027, and Prozomix-TA043. The concentrations at which the ketone substrate inhibits the transaminase were also investigated. The ω-TA's were observed to be susceptible to inhibition at substrate concentrations beyond 50 mM.

A better amino donor was also investigated for reductive amination of β-ketonitrile substrates. It was observed that, L-alanine was a better amine donor in the presence of pyruvate removal system (LDH mixture), however this system is not applicable in larger scale due to the costly enzyme co-factors. On the other hand, there were drawbacks using the Turner protocol as by-products were generated involving diamine donor and β-ketonitrile substrate, therefore reducing substrate concentration in the reaction mixture. However, the β-aminonitrile products were successfully generated in trace amounts. It can be argued that the ω-transaminase possibly had low activity since low

yields were recovered in all the amine donors tested. The synthesised β-aminonitrile standard was used as a control and analytical tools (TLC and LC-MS) were used to detect the generation of the amine product. The plan was to use the Mosher's amides to determine the stereochemistry of the enantiopure β-aminonitriles. This was not achieved because the β-aminonitriles were generated in very low yields.

The nitrile hydratase was also employed as a test reaction in the hydrolysis of the β-aminonitriles using racemic 3-amino-3-(*p*-tolyl)propanenitrile **56c** as it is one of the important steps in synthesising β-amino acids. Based on the LC-MS data, it was concluded that **56c** was successfully hydrolysed into β-amino amide **65aii**. The substrate specificity for *Rhodococcus rhodochrous* ATCC BAA-870 ntrile hydratase was also investigated with two different β-ketonitrile substrates **65bi** and **65bii**. The hydrolysis of **65bi** and **65bii** gave the highest conversion (as only one spot of the product was observed on the TLC) compared to the hydrolysis of the racemic **56c**. Therefore *Rhodococcus rhodochrous* ATCC BAA-870 nitrile hydratase showed higher preference for β-ketonitrile substrates than β-aminonitriles.

Having recovered the β-aminonitriles in low yields, the enantiopure β-amino acids were purchased. They were used to investigate if they could be incorporated into wound healing peptides. LC-MS data confirmed that β-amino acids were successfully incorporated into peptides. The hydroxyproline in the peptides was observed to cause the peak splitting due to *cis-trans* conformational isomers generated through the rotational peptidyl-bond. The lipophilicity of these peptides was also increased through attachment of adamantane, palmitic acid and *N*-methylation. The adamantane and palmitic acid were also successfully attached to the α and β-peptides to improve their membrane permeability. The *N*-methylation was performed on phenylalanine for incorporation into peptides. Based on the NMR and LC-MS data, the *N*-methylated phenylalanine was successfully synthesised

To sum up, the β-ketonitrile substrates were synthesised, demonstrated that ω-transaminase can generate the β-aminonitrile in detectable quantities, it was also shown that nitrile can be converted into the amide intermediate, and incorporate the β-aminoacid into a peptide. Improvements in the individual steps may result in a viable method for therapeutic peptide production.

4.2 Future work

The transaminase reaction needs to be improved, with purer enzyme preparations with higher activity, screening of different substrates, and amine donors and optimization of reaction conditions to improve the yields. The Mosher's amides should be used to identify the stereochemistry of β-amino acids. Nitrilase should be evaluated for the hydrolysis of nitrile group (now that induction of this enzyme in our strains has recently

been demonstrated by Chhiba-Govindjee) or amidase used in conjunction with the successful nitrile hydratase to form the β-amino acid. The β-amino acid (N-methylated β-phenylalanine) will also be incorporated into peptides. The rest of the peptides will be purified and sent for biological testing. The NMR for peptides must also be obtained for the characterization of the peptides to determine the conformation and shape (3D structure) for computational studies and to determine how it will fit in the integrin's receptor. The ROESY NMR will be used since it can detect medium sized molecules such peptides.

References

1. Liskamp, R. M. J.; Rijkers, D. T. S.; Kruijtzer, J. A. W.; Kemmink, J., Peptides and proteins as a continuing exciting source of inspiration for peptidomimetics. *ChemBioChem* **2011,** *12* (11), 1626-1653.
2. Hruby, V. J., Conformational and topographical considerations in the design of biologically active peptides. *Biopolymers* **1993,** *33* (7), 1073-1082.
3. (a) Waingeh, V. F.; Ngassa, F. N.; Song, J., A theoretical study of β-amino acid conformational energies and solvent effect. *Open Journal of Physical Chemistry* **2015,** *5* (04), 122; (b) Chow, D.; Nunalee, M. L.; Lim, D. W.; Simnick, A. J.; Chilkoti, A., Peptide-based biopolymers in biomedicine and biotechnology. *Materials Science and Engineering: R: Reports* **2008,** *62* (4), 125-155.
4. Bestian, H., Poly-β-amides. *Angewandte Chemie International Edition in English* **1968,** *7* (4), 278-285.
5. Applequist, J.; Glickson, J. D., Conformation of poly-.beta.-alanine in aqueous solution from proton magnetic resonance and deuterium exchange studies. *Journal of the American Chemical Society* **1971,** *93* (13), 3276-3281.
6. Dreifke, M. B.; Jayasuriya, A. A.; Jayasuriya, A. C., Current wound healing procedures and potential care. *Materials Science and Engineering: C* **2015,** *48*, 651-662.
7. Gainza, G.; Villullas, S.; Pedraz, J. L.; Hernandez, R. M.; Igartua, M., Advances in drug delivery systems (DDSs) to release growth factors for wound healing and skin regeneration. *Nanomedicine: Nanotechnology, Biology and Medicine* **2015,** *11* (6), 1551-1573.
8. Austin, D.; Santamaria, N., *Wound imaging and people with chronic wounds: what happened to hexis?* 2004; Vol. 11, p 12-19.
9. Schreml, S.; Szeimies, R.-M.; Prantl, L.; Landthaler, M.; Babilas, P., Wound healing in the 21st century. *Journal of the American Academy of Dermatology* **2010,** *63* (5), 866-881.
10. Schmitz, M., *German S3-Clinical Practice Guideline: Topical treatment of chronic wounds at patients with the risks of occlusive arterial disease, diabetes mellitus, chronic venous insufficiency: Importance and consequences for wound management*. 2013; Vol. 1, p 37–40.
11. Kasuya, A.; Tokura, Y., Attempts to accelerate wound healing. *Journal of Dermatological Science* **2014,** *76* (3), 169-172.
12. Greaves, N. S.; Ashcroft, K. J.; Baguneid, M.; Bayat, A., Current understanding of molecular and cellular mechanisms in fibroplasia and angiogenesis during acute wound healing. *Journal of Dermatological Science* **2013,** *72* (3), 206-217.
13. Erfurt-Berge, C.; Renner, R., Chronic wounds – Recommendations for diagnostics and therapy. *Reviews in Vascular Medicine* **2015,** *3* (1), 5-9.
14. Chan, T. R.; Stahl, P. J.; Li, Y.; Yu, S. M., Collagen–gelatin mixtures as wound model, and substrates for VEGF-mimetic peptide binding and endothelial cell activation. *Acta Biomaterialia* **2015,** *15*, 164-172.
15. Lin, Y.-J.; Lee, G.-H.; Chou, C.-W.; Chen, Y.-P.; Wu, T.-H.; Lin, H.-R., Stimulation of wound healing by PU/hydrogel composites containing fibroblast growth factor-2. *Journal of Materials Chemistry B* **2015,** *3* (9), 1931-1941.
16. CHEN, E. Y.; SEEBURG, P. H., Supercoil sequencing: a fast and simple method for sequencing plasmid DNA. *DNA* **1985,** *4* (2), 165-170.
17. Gil, E. S.; Panilaitis, B.; Bellas, E.; Kaplan, D. L., Functionalized silk biomaterials for wound healing. *Advanced Healthcare Materials* **2013,** *2* (1), 206-217.
18. Yamazaki, C. M.; Nakase, I.; Endo, H.; Kishimoto, S.; Mashiyama, Y.; Masuda, R.; Futaki, S.; Koide, T., Collagen-like cell-penetrating peptides. *Angewandte Chemie International Edition* **2013,** *52* (21), 5497-5500.
19. Emsley, J.; Knight, C. G.; Farndale, R. W.; Barnes, M. J.; Liddington, R. C., Structural basis of collagen recognition by integrin α2β1. *Cell* **2000,** *101* (1), 47-56.

20. Fallas, J. A.; O'Leary, L. E. R.; Hartgerink, J. D., Synthetic collagen mimics: self-assembly of homotrimers, heterotrimers and higher order structures. *Chemical Society Reviews* **2010,** *39* (9), 3510-3527.
21. White, D. J.; Puranen, S.; Johnson, M. S.; Heino, J., The collagen receptor subfamily of the integrins. *The International Journal of Biochemistry & Cell Biology* **2004,** *36* (8), 1405-1410.
22. Niu, G.; Chen, X., Why integrin as a primary target for imaging and therapy. *Theranostics* **2011,** *1*, 30-47.
23. Humphries, M. J.; McEwan, P. A.; Barton, S. J.; Buckley, P. A.; Bella, J.; Paul Mould, A., Integrin structure: heady advances in ligand binding, but activation still makes the knees wobble. *Trends in Biochemical Sciences* **2003,** *28* (6), 313-320.
24. Emsley, J.; King, S. L.; Bergelson, J. M.; Liddington, R. C., Crystal structure of the I domain from integrin α2β1. *J. Biol. Chem.* **1997,** *272* (45), 28512-28517.
25. Lee, J.-O.; Bankston, L. A.; Robert C Liddington, M. A. A. a., Two conformations of the integrin A-domain (I-domain): a pathway for activation? *Structure* **1995,** *3* (12), 1333-1340.
26. Knight, C. G.; Morton, L. F.; Peachey, A. R.; Tuckwell, D. S.; Farndale, R. W.; Barnes, M. J., The collagen-binding a-domains of Integrins α1β1 and α2β1Recognize the same specific amino acid sequence, GFOGER, in native (triple-helical) collagens. *Journal of Biological Chemistry* **2000,** *275* (1), 35-40.
27. Bellis, S. L., Advantages of RGD peptides for directing cell association with biomaterials. *Biomaterials* **2011,** *32* (18), 4205-4210.
28. Kritzer, J. A.; Stephens, O. M.; Guarracino, D. A.; Reznik, S. K.; Schepartz, A., β-Peptides as inhibitors of protein–protein interactions. *Bioorganic & Medicinal Chemistry* **2005,** *13* (1), 11-16.
29. Cabrele, C.; Martinek, T. A.; Reiser, O.; Berlicki, Ł., Peptides containing β-amino acid patterns: challenges and successes in medicinal chemistry. *Journal of Medicinal Chemistry* **2014,** *57* (23), 9718-9739.
30. Ding, J.; Takamoto, D. Y.; von Nahmen, A.; Lipp, M. M.; Lee, K. Y. C.; Waring, A. J.; Zasadzinski, J. A., Effects of lung surfactant proteins, SP-B and SP-C, and palmitic acid on monolayer stability. *Biophysical Journal* **2001,** *80* (5), 2262-2272.
31. Zhang, S.; Govender, T.; Norström, T.; Arvidsson, P. I., An Improved synthesis of Fmoc-N-methyl-α-amino Acids. *The Journal of Organic Chemistry* **2005,** *70* (17), 6918-6920.
32. Kovacs, J.; Ballina, R.; Rodin, R. L.; Balasubramanian, D.; Applequist, J., Poly-β-L-aspartic acid. Synthesis through pentachlorophenyl active ester and conformational studies. *Journal of the American Chemical Society* **1965,** *87* (1), 119-120.
33. (a) Appella, D. H.; Christianson, L. A.; Karle, I. L.; Powell, D. R.; Gellman, S. H., Synthesis and characterization of trans-2-aminocyclohexanecarboxylic acid oligomers: an unnatural helical secondary structure and implications for β-peptide tertiary structure. *Journal of the American Chemical Society* **1999,** *121* (26), 6206-6212; (b) Appella, D. H.; Christianson, L. A.; Klein, D. A.; Richards, M. R.; Powell, D. R.; Gellman, S. H., Synthesis and structural characterization of helix-forming β-peptides: trans-2-aminocyclopentanecarboxylic acid oligomers. *Journal of the American Chemical Society* **1999,** *121* (33), 7574-7581; (c) Barchi, J. J.; Huang, X.; Appella, D. H.; Christianson, L. A.; Durell, S. R.; Gellman, S. H., Solution Conformations of helix-forming β-amino acid homooligomers. *Journal of the American Chemical Society* **2000,** *122* (12), 2711-2718.
34. Raguse, T. L.; Porter, E. A.; Weisblum, B.; Gellman, S. H., Structure−activity studies of 14-helical antimicrobial β-peptides: probing the relationship between conformational stability and antimicrobial potency. *Journal of the American Chemical Society* **2002,** *124* (43), 12774-12785.
35. Wu, Y.-D.; Han, W.; Wang, D.-P.; Gao, Y.; Zhao, Y.-L., Theoretical analysis of secondary structures of β-peptides. *Accounts of Chemical Research* **2008,** *41* (10), 1418-1427.

36. Horne, W. S.; Gellman, S. H., Foldamers with heterogeneous backbones. *Accounts of Chemical Research* **2008,** *41* (10), 1399-1408.
37. Hill, D. J.; Mio, M. J.; Prince, R. B.; Hughes, T. S.; Moore, J. S., A Field guide to foldamers. *Chemical Reviews* **2001,** *101* (12), 3893-4012.
38. Gung, B. W.; Zou, D.; Miyahara, Y., Synthesis of a hybrid peptide with both α- and β-amino acid residues: toward a new β-sheet nucleator. *Tetrahedron* **2000,** *56* (50), 9739-9746.
39. Porter, E. A.; Wang, X.; Lee, H.-S.; Weisblum, B.; Gellman, S. H., Non-haemolytic β-amino-acid oligomers. *Nature* **2000,** *404*, 565.
40. Porter, E. A.; Weisblum, B.; Gellman, S. H., Mimicry of host-defense peptides by unnatural oligomers: antimicrobial β-peptides. *Journal of the American Chemical Society* **2002,** *124* (25), 7324-7330.
41. Cardillo, G.; Tomasini, C., Asymmetric synthesis of ß-amino acids and α-substituted β-amino acids. *Chemical Society Reviews* **1996,** *25* (2), 117-128.
42. Chen, Y. K.; Lurain, A. E.; Walsh, P. J., A general, highly enantioselective method for the synthesis of d and l α-amino acids and allylic amines. *Journal of the American Chemical Society* **2002,** *124* (41), 12225-12231.
43. DeGrado, W. F.; Schneider, J. P.; Hamuro, Y., The twists and turns of β-peptides. *The Journal of Peptide Research* **1999,** *54* (3), 206-217.
44. Chhiba, V.; Bode, M. L.; Mathiba, K.; Kwezi, W.; Brady, D., Enantioselective biocatalytic hydrolysis of β-aminonitriles to β-amino-amides using *Rhodococcus rhodochrous ATCC BAA-870*. *Journal of Molecular Catalysis B: Enzymatic* **2012,** *76*, 68-74.
45. March, T. L.; Johnston, M. R.; Duggan, P. J.; Gardiner, J., Synthesis, structure, and biological applications of α-fluorinated β-amino acids and derivatives. *Chemistry & Biodiversity* **2012,** *9* (11), 2410-2441.
46. Boddeti, G.; Bhagavathula, D.; Murthy L. N. Y., *A brief review on synthesis & applications of β-enamino carbonyl compounds*. 2012; Vol. 5, p 105-119.
47. Rudat, J.; Brucher, B. R.; Syldatk, C., Transaminases for the synthesis of enantiopure beta-amino acids. *AMB Express* **2012,** *2* (1), 11.
48. Gerfaud, T.; Chiang, Y.-L.; Kreituss, I.; Russak, J. A.; Bode, J. W., Enantioselective, chromatography-free synthesis of β3-amino acids with natural and unnatural side chains. *Organic Process Research & Development* **2012,** *16* (4), 687-696.
49. Li, S.; Xiao, T.; Li, D.; Zhang, X., First iridium-catalyzed highly enantioselective hydrogenation of β-nitroacrylates. *Organic Letters* **2015,** *17* (15), 3782-3785.
50. Dondoni, A.; Perrone, D.; Merino, P., Chelation- and non-chelation-controlled addition of 2-(trimethylsilyl)thiazole to .alpha.-amino aldehydes: Stereoselective Synthesis of the .beta.-Amino-.alpha.-hydroxy Aldehyde Intermediate for the Preparation of the Human Immunodeficiency Virus Proteinase Inhibitor Ro 31-8959. *The Journal of Organic Chemistry* **1995,** *60* (24), 8074-8080.
51. Uhl, M. K.; Oberdorfer, G.; Steinkellner, G.; Riegler-Berket, L.; Mink, D.; van Assema, F.; Schürmann, M.; Gruber, K., The crystal structure of d-threonine aldolase from alcaligenes xylosoxidans provides insight into a metal ion assisted plp-dependent mechanism. *PLOS ONE* **2015,** *10* (4), e0124056.
52. Turner, N. J., Ammonia lyases and aminomutases as biocatalysts for the synthesis of α-amino and β-amino acids. *Current Opinion in Chemical Biology* **2011,** *15* (2), 234-240.
53. Mathew, S.; Jeong, S.-S.; Chung, T.; Lee, S.-H.; Yun, H., Asymmetric synthesis of aromatic β-amino acids using ω-transaminase: Optimizing the lipase concentration to obtain thermodynamically unstable β-keto acids. *Biotechnology Journal* **2016,** *11* (1), 185-190.
54. Liljeblad, A.; Kanerva, L. T., Biocatalysis as a profound tool in the preparation of highly enantiopure β-amino acids. *Tetrahedron* **2006,** *62* (25), 5831-5854.

55. Kudo, F.; Miyanaga, A.; Eguchi, T., Biosynthesis of natural products containing β-amino acids. *Natural Product Reports* **2014,** *31* (8), 1056-1073.
56. Buß, O.; Jager, S.; Dold, S. M.; Zimmermann, S.; Hamacher, K.; Schmitz, K.; Rudat, J., Statistical Evaluation of HTS Assays for Enzymatic Hydrolysis of β-Keto Esters. *PLOS ONE* **2016,** *11* (1), e0146104.
57. Breuer, M.; Ditrich, K.; Habicher, T.; Hauer, B.; Keßeler, M.; Stürmer, R.; Zelinski, T., Industrial methods for the production of optically active intermediates. *Angewandte Chemie International Edition* **2004,** *43* (7), 788-824.
58. Truppo, M. D.; Turner, N. J.; Rozzell, J. D., Efficient kinetic resolution of racemic amines using a transaminase in combination with an amino acid oxidase. *Chemical Communications* **2009,** (16), 2127-2129.
59. (a) Taylor, P. P.; Pantaleone, D. P.; Senkpeil, R. F.; Fotheringham, I. G., Novel biosynthetic approaches to the production of unnatural amino acids using transaminases. *Trends in Biotechnology* **1998,** *16* (10), 412-418; (b) Höhne, M.; Bornscheuer, U. T., Biocatalytic routes to optically active amines. *ChemCatChem* **2009,** *1* (1), 42-51.
60. Patel, R. N., Microbial/enzymatic synthesis of chiral intermediates for pharmaceuticals. *Enzyme and Microbial Technology* **2002,** *31* (6), 804-826.
61. C. Cole, D., Recent stereoselective synthetic approaches to β-amino acids. *Tetrahedron* **1994,** *50* (32), 9517-9582.
62. Fülöp, F., The chemistry of 2-aminocycloalkanecarboxylic acids. *Chemical Reviews* **2001,** *101* (7), 2181-2204.
63. Sreekanth, B.; Bhaskar Reddy, C. M.; S G Manjunatha, D., *ADVAnced synthetic applications of Semmler-Wolff rearrangement*. 2018; Vol. 8.
64. Martín-Vilà, M.; Muray, E.; Aguado, G. P.; Alvarez-Larena, A.; Branchadell, V.; Minguillón, C.; Giralt, E.; Ortuño, R. M., Enantioselective synthetic approaches to cyclopropane and cyclobutane β-amino acids: synthesis and structural study of a conformationally constrained β-dipeptide. *Tetrahedron: Asymmetry* **2000,** *11* (17), 3569-3584.
65. Wentrup, C.; Bornemann, H., The Curtius Rearrangement of acyl azides revisited – formation of cyanate (R–O–CN). *European Journal of Organic Chemistry* **2005,** *2005* (21), 4521-4524.
66. https://www.brainyresort.com/it/trasposizione-di-curtius-e-hofmann/trasposizione-di-curtius-meccanismo-di-reazione/ 20/05/2018.
67. Patel, R. N., Biocatalysis: Synthesis of key intermediates for development of pharmaceuticals. *ACS Catalysis* **2011,** *1* (9), 1056-1074.
68. Pollard, D. J.; Woodley, J. M., Biocatalysis for pharmaceutical intermediates: the future is now. *Trends in Biotechnology* **2007,** *25* (2), 66-73.
69. Patel, R. N., Biocatalytic synthesis of intermediates for the synthesis of chiral drug substances. *Current Opinion in Biotechnology* **2001,** *12* (6), 587-604.
70. Tao, J.; Xu, J.-H., Biocatalysis in development of green pharmaceutical processes. *Current Opinion in Chemical Biology* **2009,** *13* (1), 43-50.
71. Zheng, G.-W.; Xu, J.-H., New opportunities for biocatalysis: driving the synthesis of chiral chemicals. *Current Opinion in Biotechnology* **2011,** *22* (6), 784-792.
72. Weiner, B.; Szymański, W.; Janssen, D. B.; Minnaard, A. J.; Feringa, B. L., Recent advances in the catalytic asymmetric synthesis of β-amino acids. *Chemical Society Reviews* **2010,** *39* (5), 1656-1691.
73. Muñoz Solano, D.; Hoyos, P.; Hernáiz, M. J.; Alcántara, A. R.; Sánchez-Montero, J. M., Industrial biotransformations in the synthesis of building blocks leading to enantiopure drugs. *Bioresource Technology* **2012,** *115*, 196-207.
74. Nestl, B. M.; Hammer, S. C.; Nebel, B. A.; Hauer, B., New Generation of biocatalysts for organic synthesis. *Angewandte Chemie International Edition* **2014,** *53* (12), 3070-3095.

75. Koszelewski, D.; Tauber, K.; Faber, K.; Kroutil, W., ω-Transaminases for the synthesis of non-racemic α-chiral primary amines. *Trends in Biotechnology* **2010,** *28* (6), 324-332.
76. Fuchs, M.; Farnberger, J. E.; Kroutil, W., The industrial age of biocatalytic transamination. *European Journal of Organic Chemistry* **2015,** *2015* (32), 6965-6982.
77. Koszelewski, D.; Clay, D.; Rozzell, D.; Kroutil, W., Deracemisation of α-chiral primary amines by a one-pot, two-step cascade reaction catalysed by ω-transaminases. *European Journal of Organic Chemistry* **2009,** *2009* (14), 2289-2292.
78. Mathew, S.; Yun, H., ω-Transaminases for the production of optically pure amines and unnatural amino acids. *ACS Catalysis* **2012,** *2* (6), 993-1001.
79. Engelmark Cassimjee, K. ω-Transaminase in biocatalysis : methods, reactions and engineering. doctoral thesis, comprehensive summary, KTH Royal Institute of Technology, Stockholm, 2012.
80. Cassimjee, K. E.; Humble, M. S.; Miceli, V.; Colomina, C. G.; Berglund, P., Active site quantification of an ω-transaminase by performing a half transamination reaction. *ACS Catalysis* **2011,** *1* (9), 1051-1055.
81. Schätzle, S.; Steffen-Munsberg, F.; Thontowi, A.; Höhne, M.; Robins, K.; Bornscheuer, U. T., Enzymatic asymmetric synthesis of enantiomerically pure aliphatic, aromatic and arylaliphatic amines with (r)-selective amine transaminases. *Advanced Synthesis & Catalysis* **2011,** *353* (13), 2439-2445.
82. Thomsen, M.; Skalden, L.; Palm, G. J.; Hohne, M.; Bornscheuer, U. T.; Hinrichs, W., Crystallographic characterization of the (R)-selective amine transaminase from *Aspergillus fumigatus*. *Acta Crystallographica Section D* **2014,** *70* (4), 1086-1093.
83. Humble, M. S.; Cassimjee, K. E.; Håkansson, M.; Kimbung, Y. R.; Walse, B.; Abedi, V.; Federsel, H.-J.; Berglund, P.; Logan, D. T., Crystal structures of the *Chromobacterium violaceum* ω-transaminase reveal major structural rearrangements upon binding of coenzyme PLP. *The FEBS Journal* **2012,** *279* (5), 779-792.
84. Sayer, C.; Martinez-Torres, R. J.; Richter, N.; Isupov, M. N.; Hailes, H. C.; Littlechild, J. A.; Ward, J. M., The substrate specificity, enantioselectivity and structure of the (R)-selective amine : pyruvate transaminase from *Nectria haematococca*. *The FEBS Journal* **2014,** *281* (9), 2240-2253.
85. Wybenga, G. G.; Crismaru, C. G.; Janssen, D. B.; Dijkstra, B. W., Structural determinants of the β-selectivity of a bacterial aminotransferase. *Journal of Biological Chemistry* **2012**.
86. Höhne, M.; Schätzle, S.; Jochens, H.; Robins, K.; Bornscheuer, U. T., Rational assignment of key motifs for function guides in silico enzyme identification. *Nature Chemical Biology* **2010,** *6*, 807.
87. Park, E.-S.; Park, S.-R.; Han, S.-W.; Dong, J.-Y.; Shin, J.-S., Structural determinants for the non-canonical substrate specificity of the ω-transaminase from paracoccus denitrificans. *Advanced Synthesis & Catalysis* **2014,** *356* (1), 212-220.
88. Malik, M. S.; Park, E.-S.; Shin, J.-S., Features and technical applications of ω-transaminases. *Applied Microbiology and Biotechnology* **2012,** *94* (5), 1163-1171.
89. Xie, Y.; Pan, H.; Liu, M.; Xiao, X.; Shi, Y., Progress in asymmetric biomimetic transamination of carbonyl compounds. *Chemical Society Reviews* **2015,** *44* (7), 1740-1748.
90. Kim, M.-J.; Ahn, Y.; Park, J., Dynamic kinetic resolutions and asymmetric transformations by enzymes coupled with metal catalysis. *Current Opinion in Biotechnology* **2002,** *13* (6), 578-587.
91. Fernandes, B. C. M.; Mateo, C.; Kiziak, C.; Chmura, A.; Wacker, J.; van Rantwijk, F.; Stolz, A.; Sheldon, R. A., Nitrile hydratase activity of a recombinant nitrilase. *Advanced Synthesis & Catalysis* **2006,** *348* (18), 2597-2603.
92. Koszelewski, D.; Lavandera, I.; Clay, D.; Rozzell, D.; Kroutil, W., Asymmetric Synthesis of optically pure pharmacologically relevant amines employing ω-transaminases. *Advanced Synthesis & Catalysis* **2008,** *350* (17), 2761-2766.
93. Wohlgemuth, R., Asymmetric biocatalysis with microbial enzymes and cells. *Current Opinion in Microbiology* **2010,** *13* (3), 283-292.

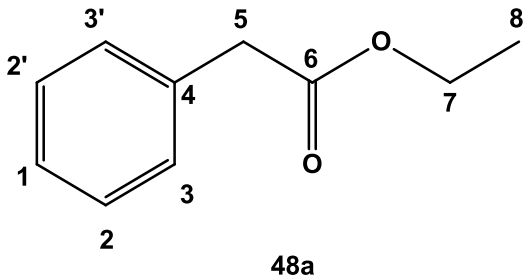
94. García-Urdiales, E.; Alfonso, I.; Gotor, V., Enantioselective enzymatic desymmetrizations in organic synthesis. *Chemical Reviews* **2005,** *105* (1), 313-354.
95. Schulze, B.; Wubbolts, M. G., Biocatalysis for industrial production of fine chemicals. *Current Opinion in Biotechnology* **1999,** *10* (6), 609-615.
96. Hoyos, P.; Fernández, M.; Sinisterra, J. V.; Alcántara, A. R., Dynamic kinetic resolution of benzoins by lipase−metal combo catalysis. *The Journal of Organic Chemistry* **2006,** *71* (20), 7632-7637.
97. Savile, C. K.; Janey, J. M.; Mundorff, E. C.; Moore, J. C.; Tam, S.; Jarvis, W. R.; Colbeck, J. C.; Krebber, A.; Fleitz, F. J.; Brands, J.; Devine, P. N.; Huisman, G. W.; Hughes, G. J., Biocatalytic asymmetric synthesis of chiral amines from ketones applied to sitagliptin manufacture. *Science* **2010,** *329* (5989), 305-309.
98. Schätzle, S. Identification, characterization and application of novel (R)-selective amine transaminases. 2011.
99. Green, A. P.; Turner, N. J.; O'Reilly, E., Chiral amine synthesis using ω-transaminases: an amine donor that displaces equilibria and enables high-throughput screening. *Angewandte Chemie International Edition* **2014,** *53* (40), 10714-10717.
100. Gong, J.-S.; Lu, Z.-M.; Li, H.; Shi, J.-S.; Zhou, Z.-M.; Xu, Z.-H., Nitrilases in nitrile biocatalysis: recent progress and forthcoming research. *Microbial Cell Factories* **2012,** *11* (1), 142.
101. Agarwal, A.; Nigam, V., *Nitrilases-an attractive nitrile degrading biocatalyst*. 2012; Vol. 3, p 232-246.
102. Winkler, M.; Glieder, A.; Klempier, N., Enzyme stabilizer DTT catalyzes nitrilase analogue hydrolysis of nitriles. *Chemical Communications* **2006,** (12), 1298-1300.
103. Novo, C.; Tata, R.; Clemente, A.; Brown, P. R., *Pseudomonas aeruginosa* aliphatic amidase is related to the nitrilase/cyanide hydratase enzyme family and Cys166 is predicted to be the active site nucleophile of the catalytic mechanism. *FEBS Letters* **1995,** *367* (3), 275-279.
104. Kobayashi, M.; Goda, M.; Shimizu, S., The catalytic mechanism of amidase also involves nitrile hydrolysis. *FEBS Letters* **1998,** *439* (3), 325-328.
105. Frederick, J.; Brady, D.; Dirr, H., Characterisation of the nitrile biocatalytic activity of *Rhodococcus rhodochrous ATCC BAA-870*. 2019.
106. Hopmann, K. H., Full reaction mechanism of nitrile hydratase: a cyclic intermediate and an unexpected disulfide switch. *Inorganic Chemistry* **2014,** *53* (6), 2760-2762.
107. Labahn, J.; Neumann, S.; Büldt, G.; Kula, M.-R.; Granzin, J., An alternative mechanism for amidase signature enzymes. *Journal of Molecular Biology* **2002,** *322* (5), 1053-1064.
108. Sigma Aldrich.
109. Liu, C.; He, C.; Shi, W.; Chen, M.; Lei, A., Ni-Catalyzed mild arylation of α-halocarbonyl compounds with arylboronic acids. *Organic Letters* **2007,** *9* (26), 5601-5604.
110. Busto, E.; Gotor-Fernández, V.; Montejo-Bernardo, J.; García-Granda, S.; Gotor, V., First desymmetrization of 1,3-propanediamine derivatives in organic solvent. development of a new route for the preparation of optically active amines. *Organic Letters* **2007,** *9* (21), 4203-4206.
111. Song, B.; Rudolphi, F.; Himmler, T.; Gooßen, L. J., Practical synthesis of 2-arylacetic acid esters via palladium- catalyzed dealkoxycarbonylative coupling of malonates with aryl halides. *Advanced Synthesis & Catalysis* **2011,** *353* (9), 1565-1574.
112. Foehlisch, B.; Wolf, E., Generation of aryl-substituted 1-cyanoallylium-2-olates and their [4 + 3] cycloaddition to furan. *J. Chem. Res., Synop.* **1983,** (7), 166.
113. Katritzky, A. R.; Akue-Gedu, R.; Vakulenko, A. V., C-cyanation with 1-cyanobenzotriazole. *ARKIVOC (Gainesville, FL, U. S.)* **2007,** (3), 5-12.
114. Nagendra, G.; Madhu, C.; Vishwanatha, T. M.; Sureshbabu, V. V., An expedient route for the reduction of carboxylic acids to alcohols employing 1-propanephosphonic acid cyclic anhydride as acid activator. *Tetrahedron Letters* **2012,** *53* (38), 5059-5063.

115. Katritzky, A. R.; Abdel-Fattah, A. A. A.; Wang, M., Expedient acylations of primary and secondary alkyl cyanides to α-substituted β-ketonitriles. *The Journal of Organic Chemistry* **2003,** *68* (12), 4932-4934.
116. Di Gioia, M. L.; Leggio, A.; Liguori, A.; Perri, F., Solid-phase synthesis of N-Nosyl- and N-Fmoc-N-methyl-α-amino acids. *The Journal of Organic Chemistry* **2007,** *72* (10), 3723-3728.
117. Gonec, T.; Kos, J.; Nevin, E.; Govender, R.; Pesko, M.; Tengler, J.; Kushkevych, I.; Stastna, V.; Oravec, M.; Kollar, P.; O'Mahony, J.; Kralova, K.; Coffey, A.; Jampilek, J., Preparation and biological properties of ring-substituted naphthalene-1-carboxanilides. *Molecules* **2014,** *19* (7), 10386-10409, 24 pp.
118. Zhou, G.-B.; Zhang, P.-F.; Pan, Y.-J., A novel method for synthesis of arylacetic acids from aldehydes, N-(2,3,4,6-tetra-O-pivaloylated-D-glucopyranosyl)amine and trimethylsilyl cyanide. *Tetrahedron* **2005,** *61* (23), 5671-5677.
119. Kiss, A. A.; Dimian, A. C.; Rothenberg, G., Solid acid catalysts for biodiesel production –-towards sustainable energy. *Advanced Synthesis & Catalysis* **2006,** *348* (1-2), 75-81.
120. Li, J.; Sha, Y., A Convenient Synthesis of Amino Acid Methyl Esters. *Molecules* **2008,** *13* (5), 1111.
121. Bildsoe, H.; Schaumburg, K., Proton and fluorine-19 NMR spectra of aromatic carbonyl fluorides. CNDO/2 and INDO calculations. *Journal of Magnetic Resonance (1969)* **1974,** *14* (2), 223-234.
122. Yoshida, J. I., Flash chemistry: flow microreactor synthesis based on high-resolution reaction time control. *The Chemical Record* **2010,** *10* (5), 332-341.
123. Prasad, A. S. B.; Kanth, J. V. B.; Periasamy, M., Convenient methods for the reduction of amides, nitriles, carboxylic esters, acids and hydroboration of alkenes using NaBH4/I2system. *Tetrahedron* **1992,** *48* (22), 4623-4628.
124. Simek, J. W.; Tuck, T.; Bush, K. C., Reduction of carboxylic acids with sodium borohydride and an electrophile. *Journal of Chemical Education* **1997,** *74* (1), 107.
125. Sohda, T.; Makino, H.; Baba, A.; Yamane, T. Thienodipyridine derivatives as antiinflammatory and antiarthritis agents. WO9965916A1, 1999.
126. Nematollahi, D.; Shayani-Jam, H.; Alimoradi, M.; Niroomand, S., Electrochemical oxidation of acetaminophen in aqueous solutions: Kinetic evaluation of hydrolysis, hydroxylation and dimerization processes. *Electrochimica Acta* **2009,** *54* (28), 7407-7415.
127. Park, E.-S.; Dong, J.-Y.; Shin, J.-S., Active site model of (R)-selective ω-transaminase and its application to the production of d-amino acids. *Applied Microbiology and Biotechnology* **2014,** *98* (2), 651-660.
128. Mathew, S.; Bea, H.; Nadarajan, S. P.; Chung, T.; Yun, H., Production of chiral β-amino acids using ω-transaminase from Burkholderia graminis. *Journal of Biotechnology* **2015,** *196-197*, 1-8.
129. Mathew, S.; Nadarajan, S. P.; Chung, T.; Park, H. H.; Yun, H., Biochemical characterization of thermostable ω-transaminase from *Sphaerobacter thermophilus* and its application for producing aromatic β- and γ-amino acids. *Enzyme and Microbial Technology* **2016,** *87-88*, 52-60.
130. Kelefiotis-Stratidakis, P.; Tyrikos-Ergas, T.; Pavlidis, I. V., The challenge of using isopropylamine as an amine donor in transaminase catalysed reactions. *Organic & Biomolecular Chemistry* **2018**.
131. Cassimjee, K. E.; Branneby, C.; Abedi, V.; Wells, A.; Berglund, P., Transaminations with isopropyl amine: equilibrium displacement with yeast alcohol dehydrogenase coupled to in situ cofactor regeneration. *Chemical Communications* **2010,** *46* (30), 5569-5571.
132. Green, A. P.; Turner, N. J., Biocatalytic retrosynthesis: Redesigning synthetic routes to high-value chemicals. *Perspectives in Science* **2016,** *9*, 42-48.
133. Buß, O.; Voss, M.; Delavault, A.; Gorenflo, P.; Syldatk, C.; Bornscheuer, U.; Rudat, J., β-Phenylalanine ester synthesis from stable β-keto ester substrate using engineered ω-transaminases. *Molecules* **2018,** *23* (5), 1211.

134. Sun, H.; Zhang, H.; Ang, E. L.; Zhao, H., Biocatalysis for the synthesis of pharmaceuticals and pharmaceutical intermediates. *Bioorganic & Medicinal Chemistry* **2018,** *26* (7), 1275-1284.
135. Kim, J.; Kyung, D.; Yun, H.; Cho, B.-K.; Seo, J.-H.; Cha, M.; Kim, B.-G., Cloning and characterization of a novel β-transaminase from *Mesorhizobium* sp. Strain LUK: A new biocatalyst for the synthesis of enantiomerically pure β-amino acids. *Applied and Environmental Microbiology* **2007,** *73* (6), 1772-1782.
136. Fields, G. B., Introduction to peptide synthesis. *Current protocols in protein science* **2002,** *Chapter 18*, Unit-18.1.
137. Egli, J.; Erdmann, R. S.; Schmidt, P. J.; Wennemers, H., Effect of N- and C-terminal functional groups on the stability of collagen triple helices. *Chemical Communications* **2017,** *53* (80), 11036-11039.
138. AAPPTEC:https://www.peptide.com/custdocs/aapptec%20synthesis%20guide%202-0%20(2).pdf.
139. Luna, O. F.; Gomez, J.; Cárdenas, C.; Albericio, F.; Marshall, S. H.; Guzmán, F., Deprotection reagents in fmoc solid phase peptide synthesis: moving away from piperidine? *Molecules* **2016,** *21* (11), 1542.
140. Pedersen, S. L.; Tofteng, A. P.; Malik, L.; Jensen, K. J., Microwave heating in solid-phase peptide synthesis. *Chemical Society Reviews* **2012,** *41* (5), 1826-1844.
141. Balasubramaniam, A.; Knittel, J. J.; Gill, C.; Andrews, P. C., Detection of conformational isomers of anglerfish peptide YG (aPY) by reversed phase chromatography. *International Journal of Peptide and Protein Research* **1989,** *34* (2), 158-160.
142. Kálmán, A.; Thunecke, F.; Schmidt, R.; Schiller, P. W.; Horváth, C., Isolation and identification of peptide conformers by reversed-phase high-performance liquid chromatography and NMR at low temperature. *Journal of Chromatography A* **1996,** *729* (1), 155-171.
143. Ünal, C. M.; Steinert, M., Microbial peptidyl-prolyl cis/trans isomerases (ppiases): virulence factors and potential alternative drug targets. *Microbiology and Molecular Biology Reviews* **2014,** *78* (3), 544-571.
144. Fischer, S.; Dunbrack, R.; Karplus, M., *Cis-Trans Imide Isomerization of the Proline Dipeptide*. 1994; Vol. 116.
145. Avrahami, D.; Shai, Y., *A* new group of antifungal and antibacterial lipopeptides derived from non-membrane active peptides conjugated to palmitic acid. 2004; Vol. 279, p 12277-85.
146. Wanka, L.; Iqbal, K.; Schreiner, P. R., The lipophilic bullet hits the targets: medicinal chemistry of adamantane derivatives. *Chemical Reviews* **2013,** *113* (5), 3516-3604.
147. Versluis, F.; Voskuhl, J.; van Kolck, B.; Zope, H.; Bremmer, M.; Albregtse, T.; Kros, A., In situ modification of plain liposomes with lipidated coiled coil forming peptides induces membrane fusion. *Journal of the American Chemical Society* **2013,** *135* (21), 8057-8062.

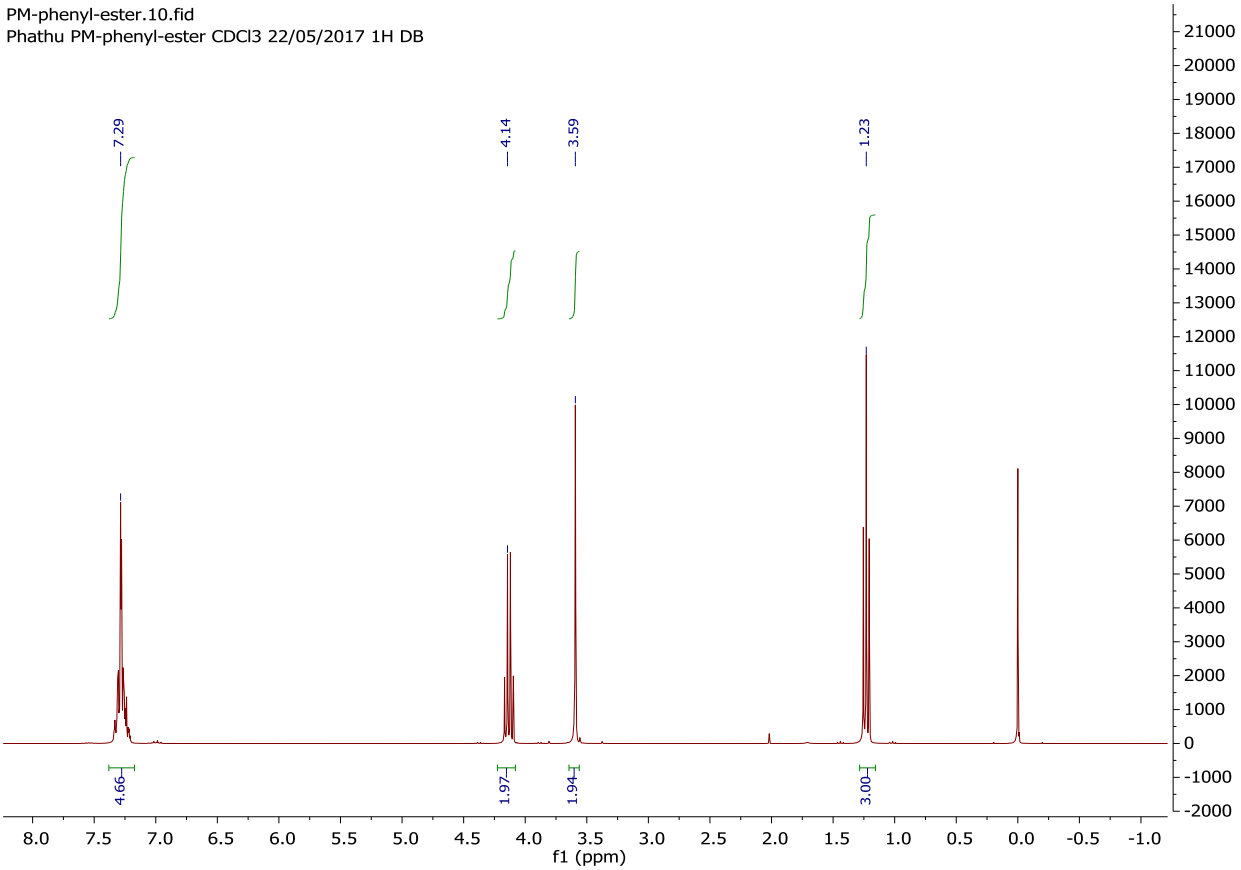
APPENDIX

Spectra of selected compounds:

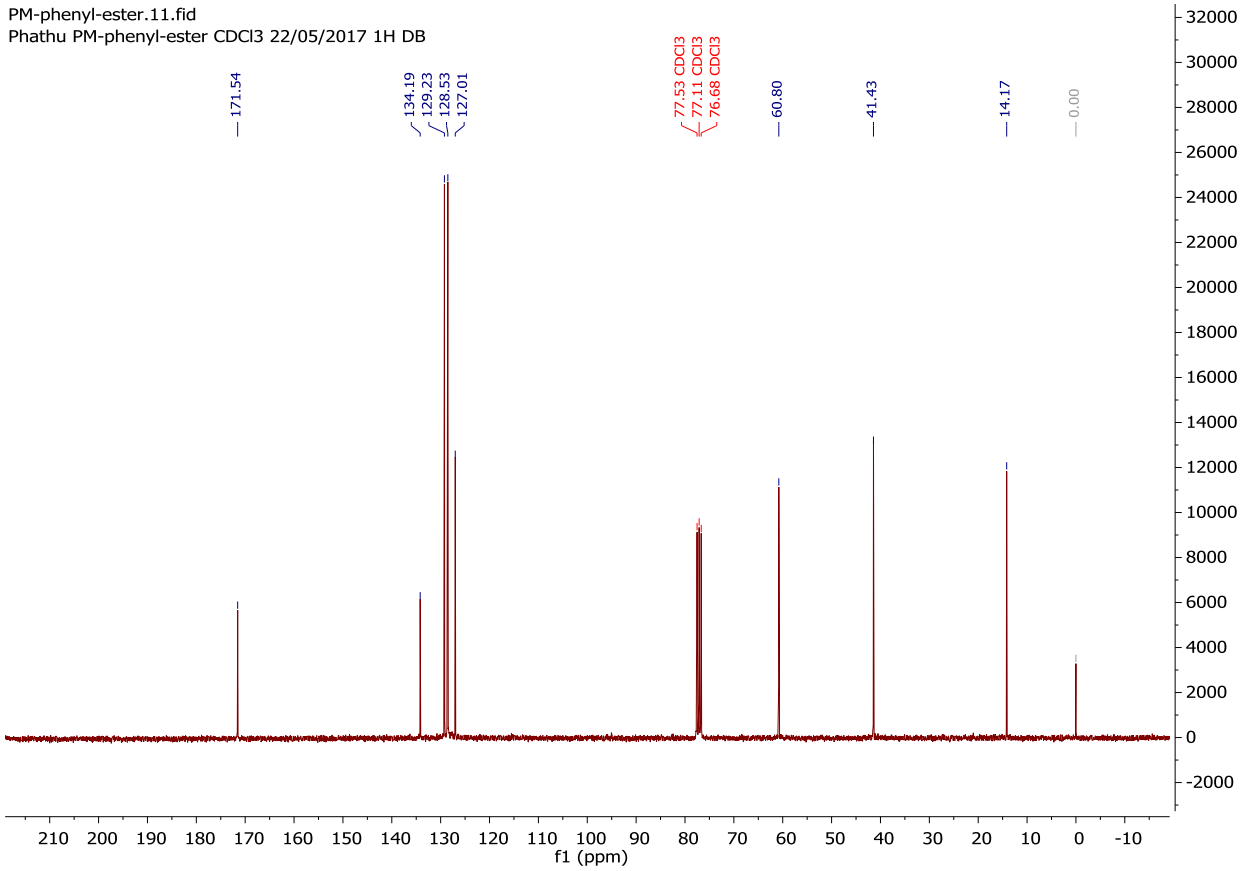


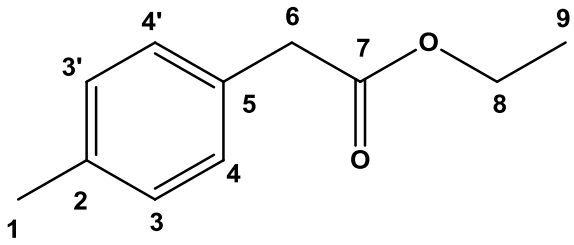
48a

^{1}H NMR of 48a



^{13}C NMR of 48a

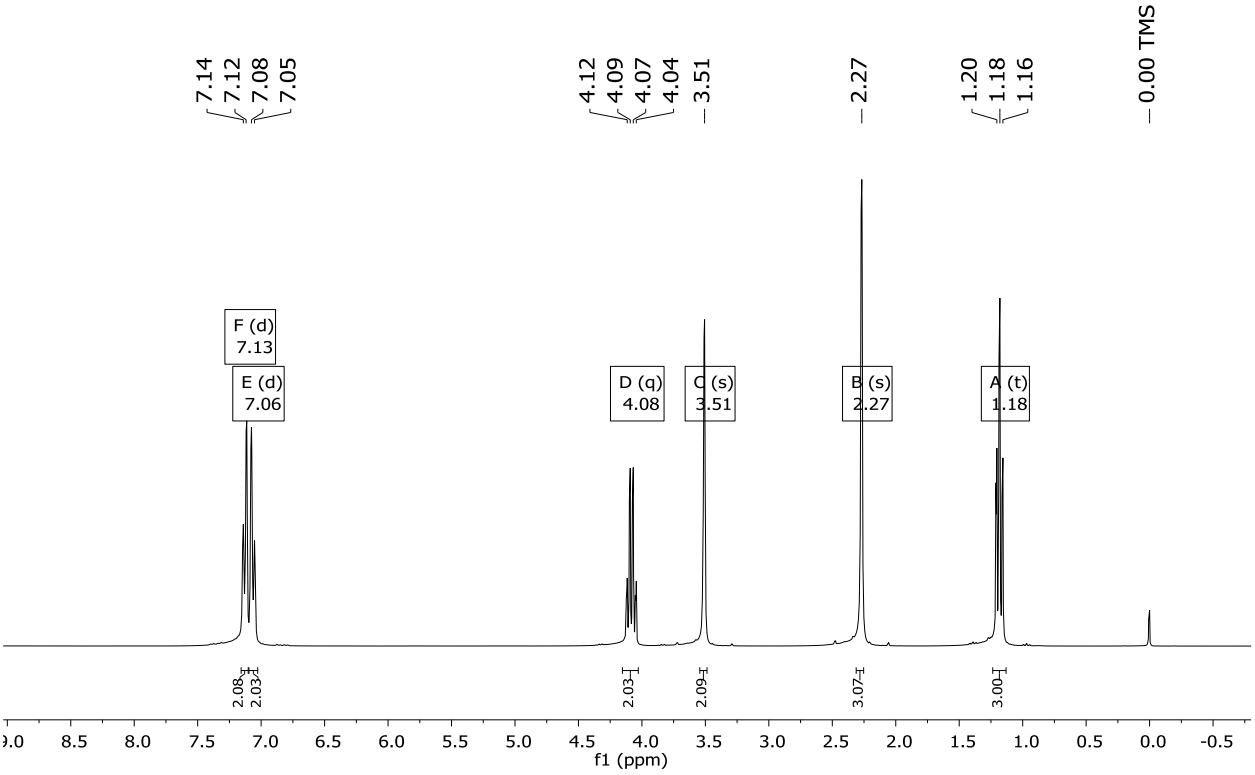




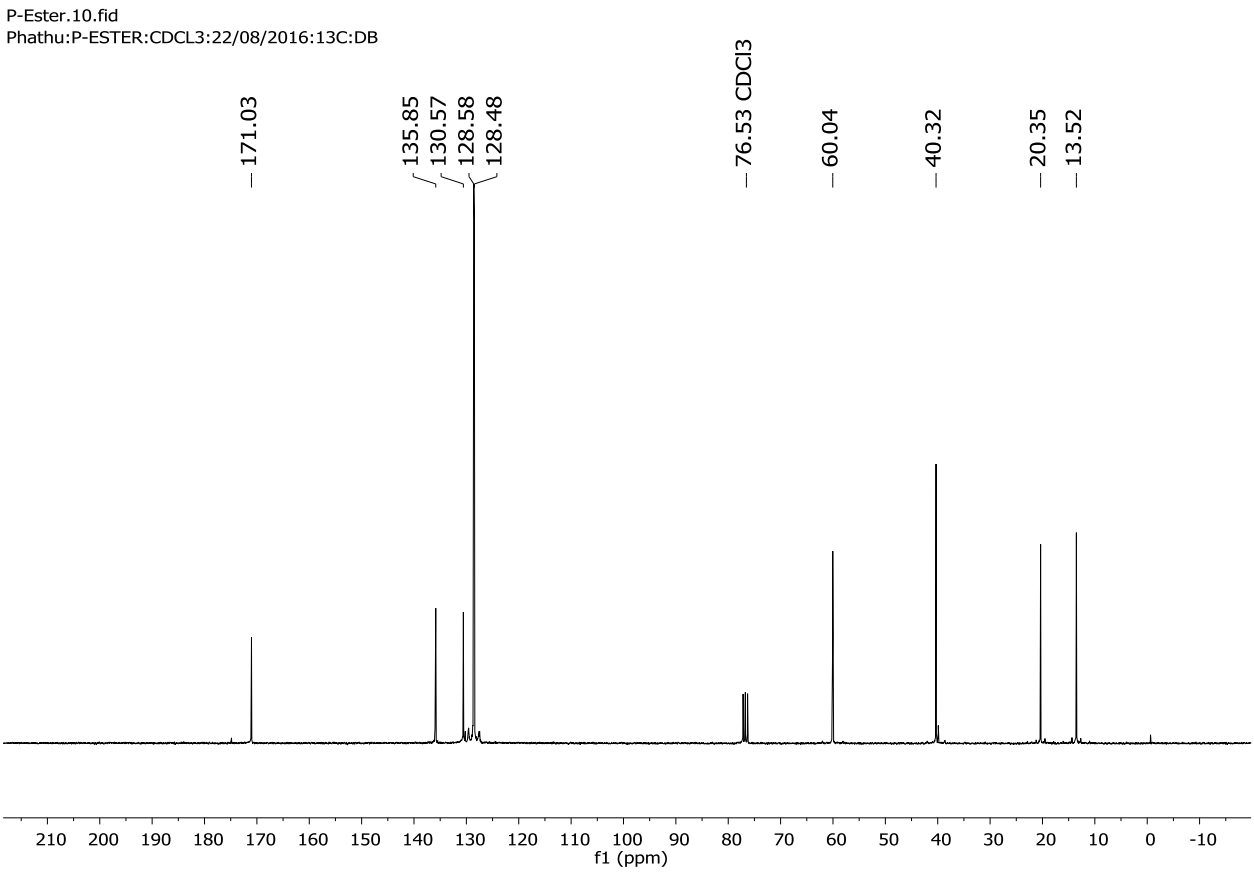
48c

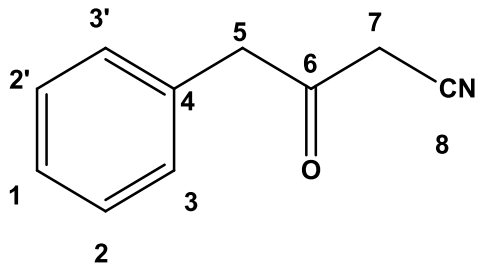
^{1}H NMR of 48c

P-Ester.20.fid
Phathu:P-ESTER:CDCL3:22/08/2016:1H:DB

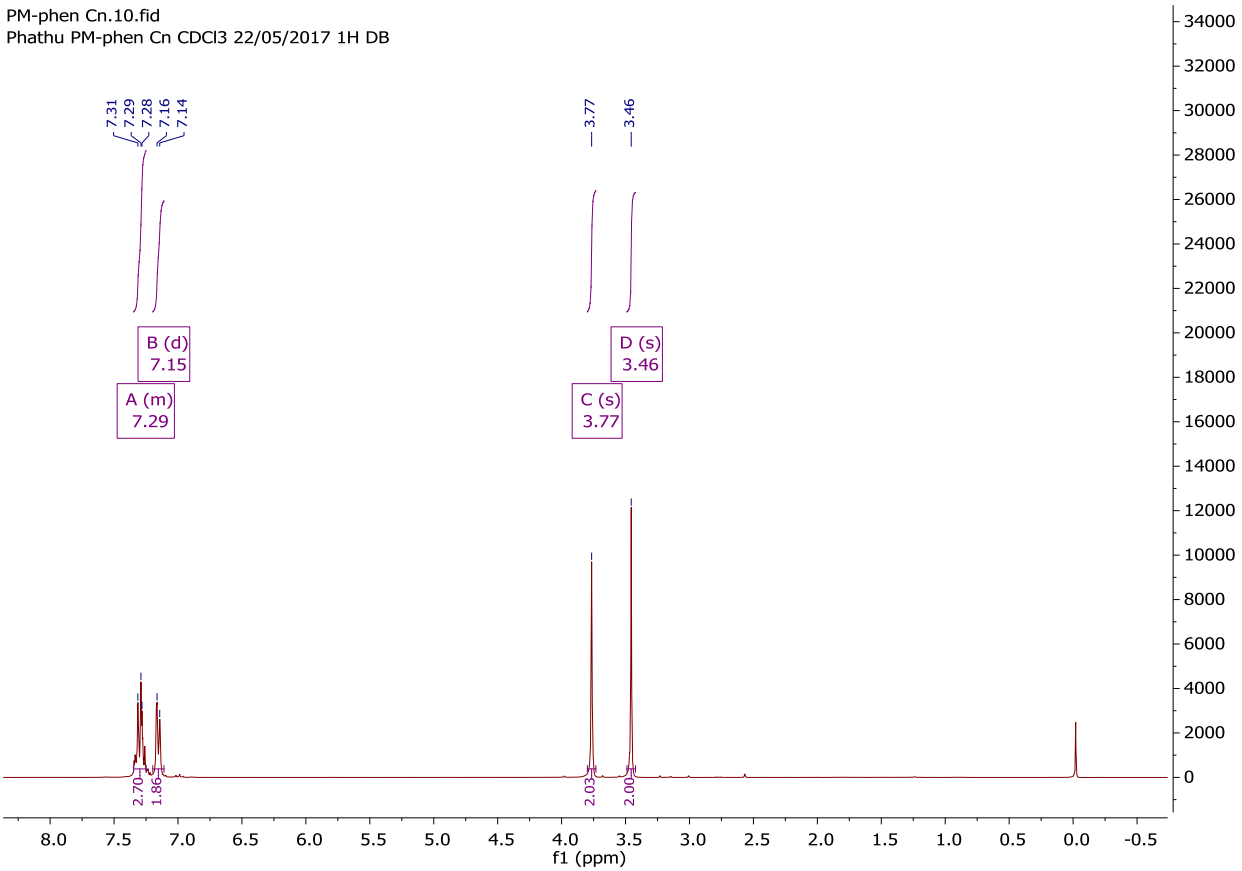


^{13}C NMR of 48c


P-Ester.10.fid
Phathu:P-ESTER:CDCL3:22/08/2016:13C:DB
171.03
135.85
130.57
128.58
128.48
76.53 CDCl3
60.04
40.32
20.35
13.52
210 200 190 180 170 160 150 140 130 120 110 100 90 80 70 60 50 40 30 20 10 0 -10
f1 (ppm)

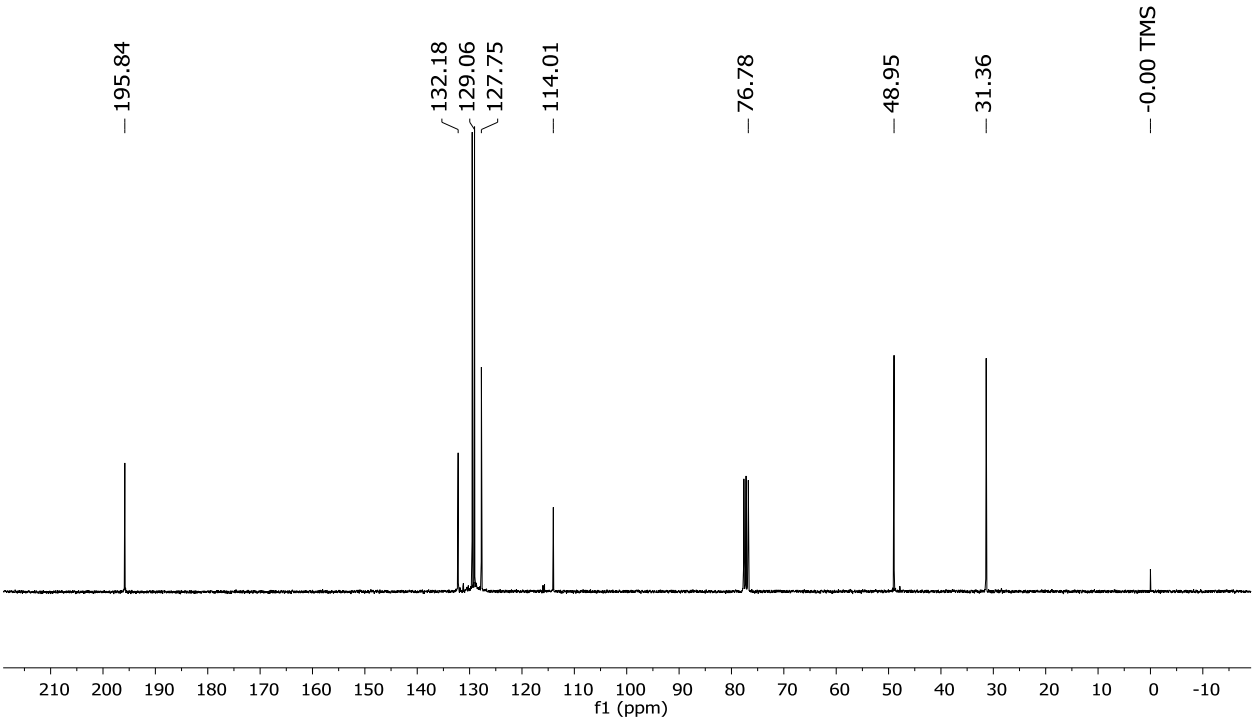

3'
5
7
2'
6
CN
4
8
O
1
3
2

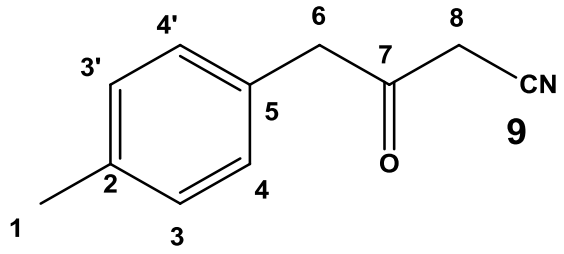
49a



^{13}C NMR of 49a

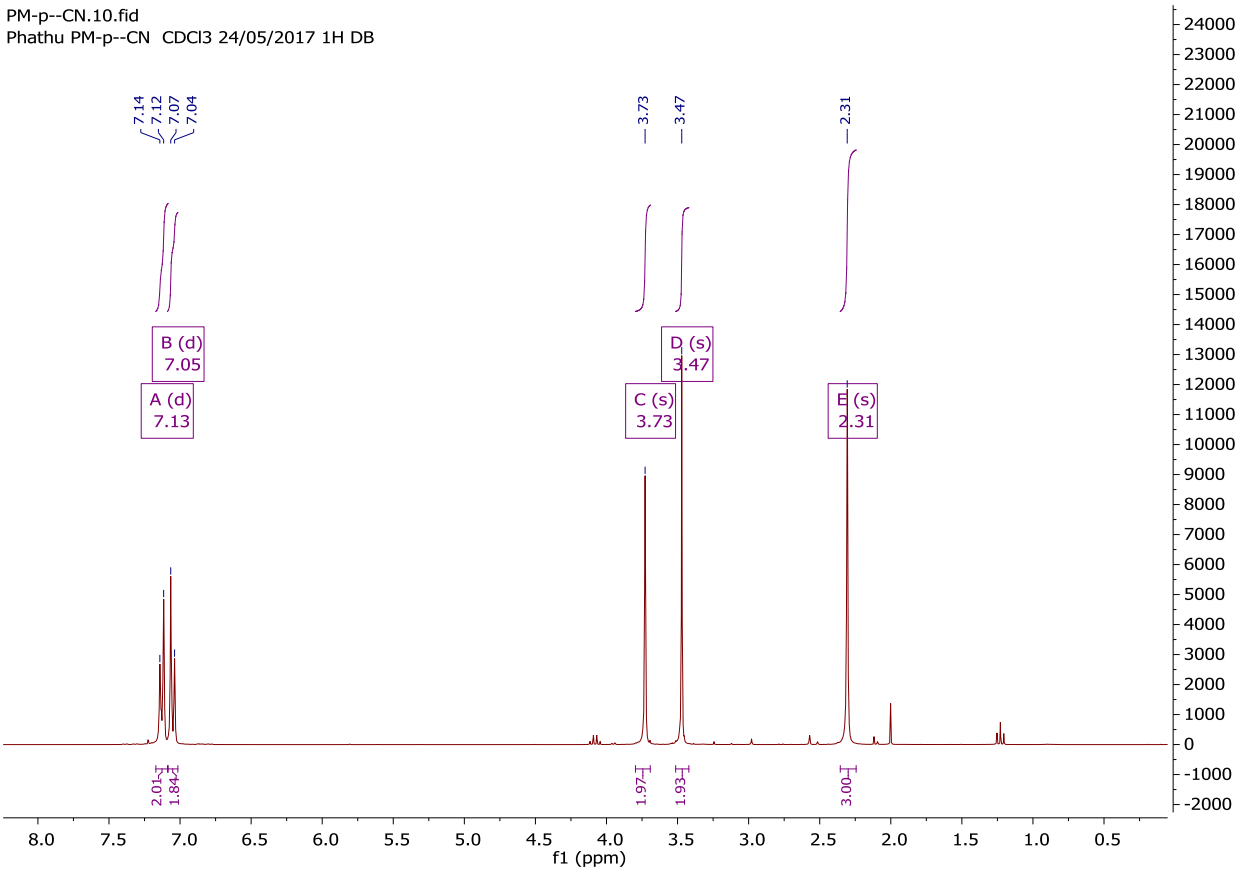
PM-phen Cn.11.fid
Phathu PM-phen Cn CDCl3 22/05/2017 13C DB



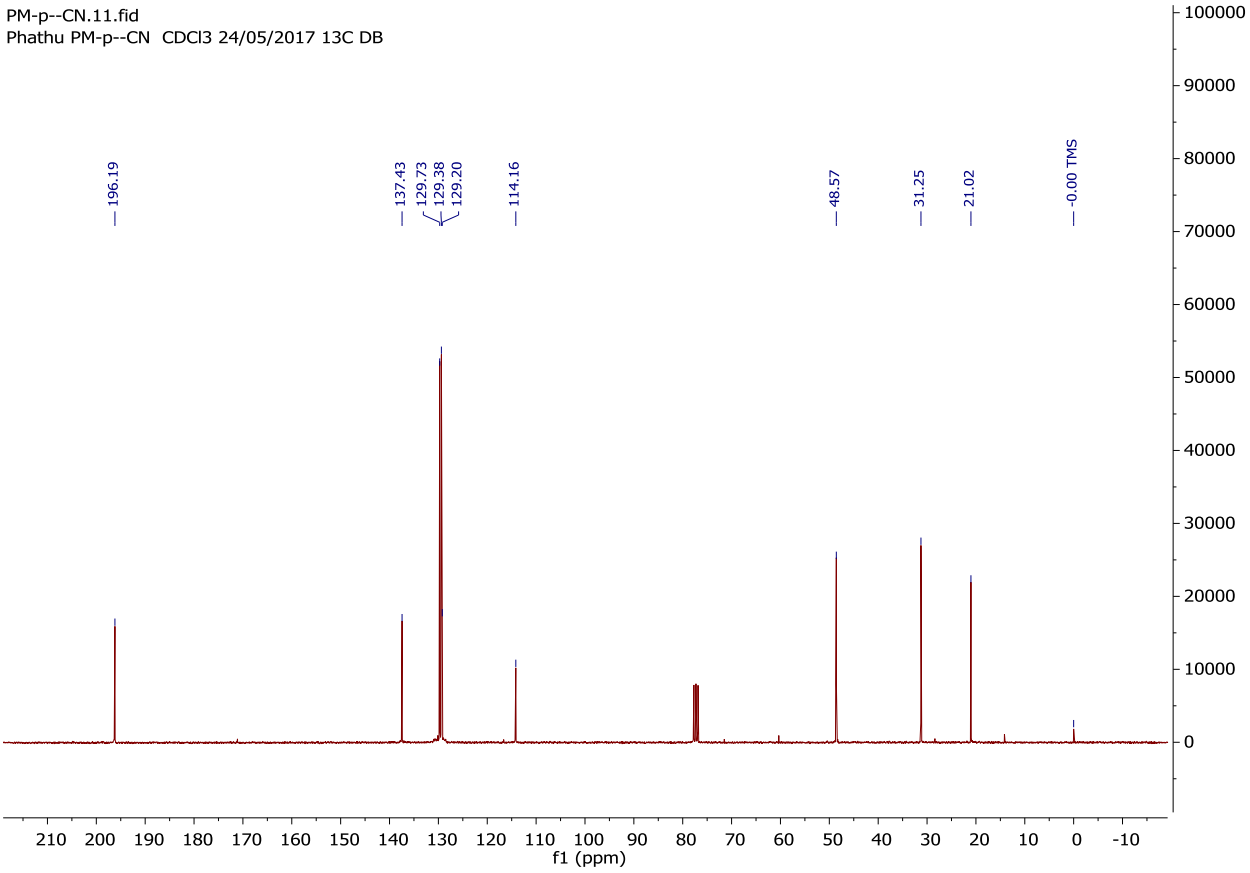


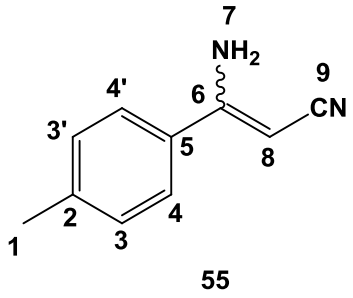
49c

^{1}H NMR of 49c



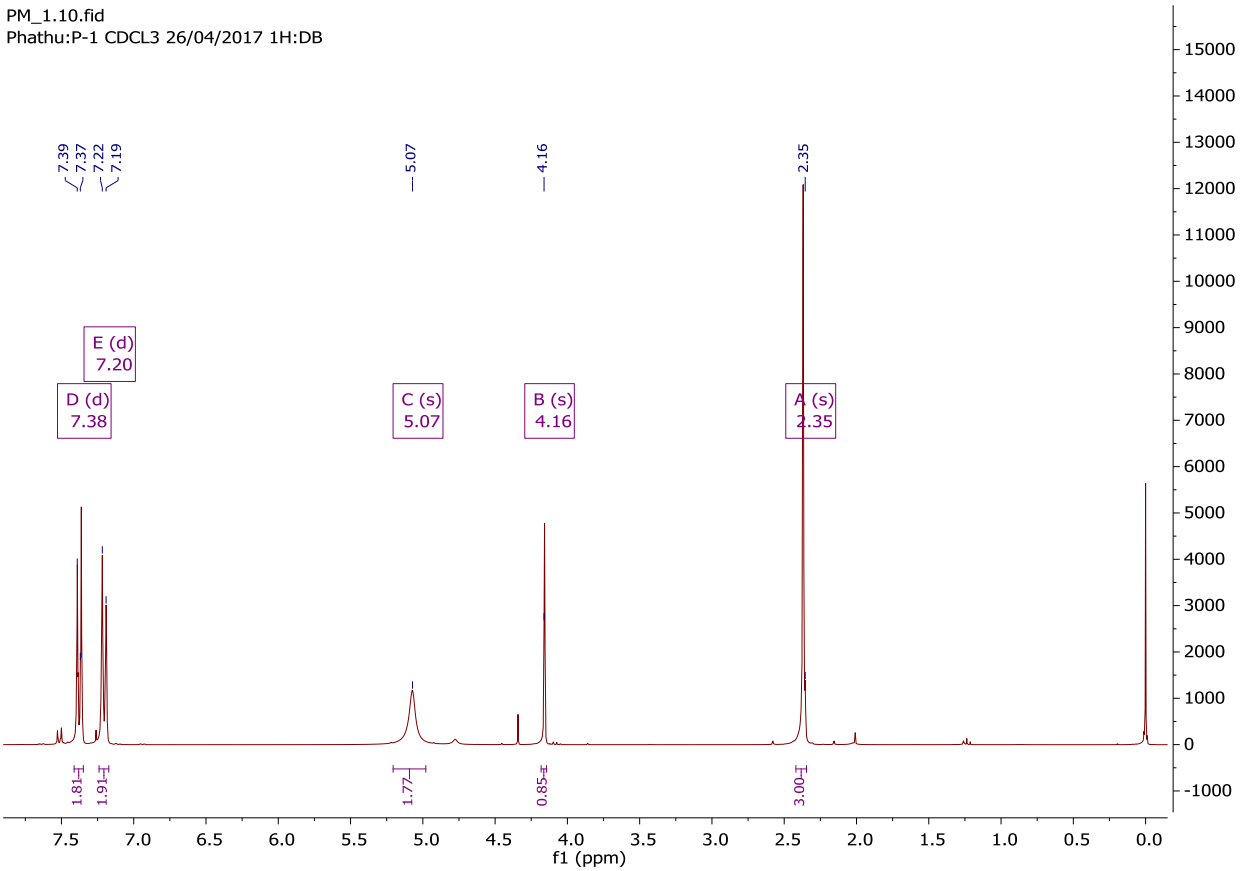
^{13}C NMR of 49c



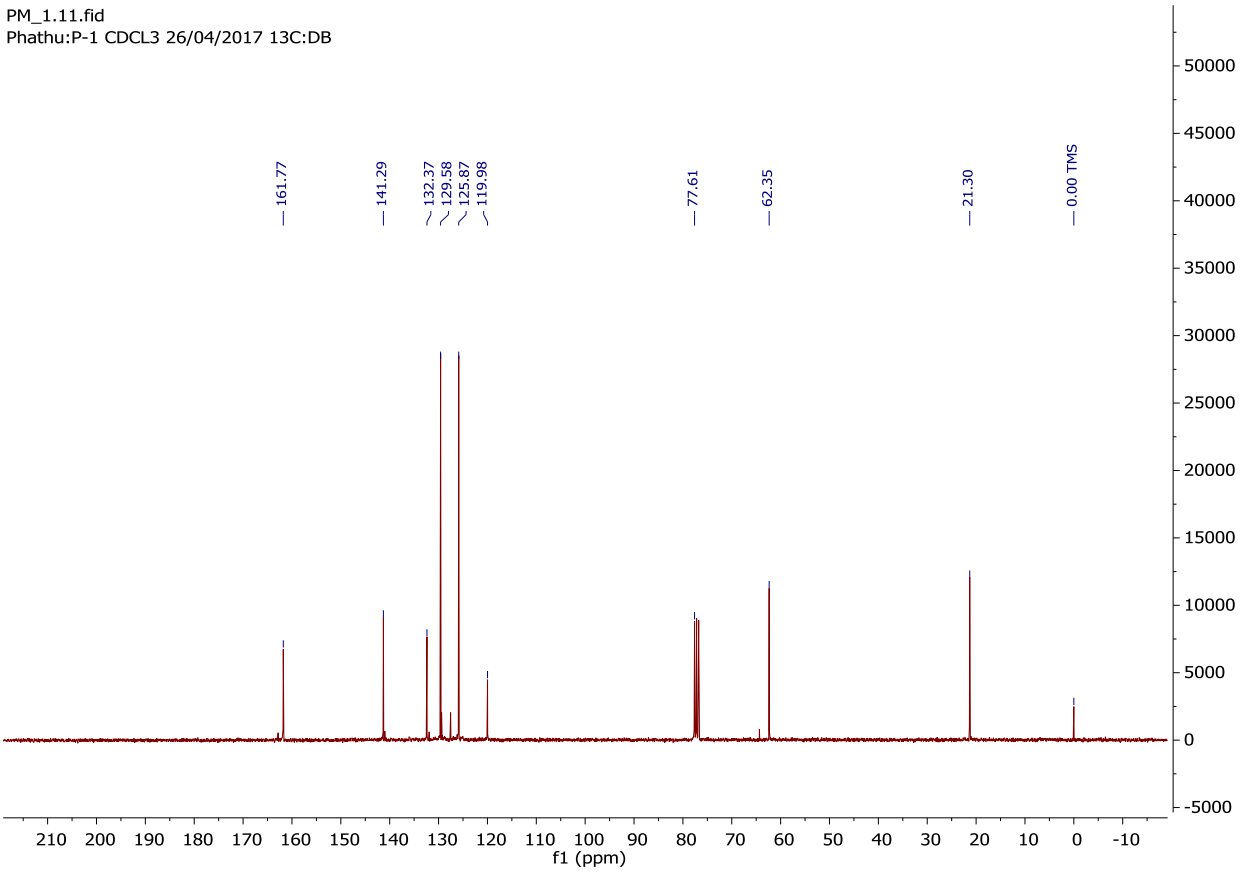


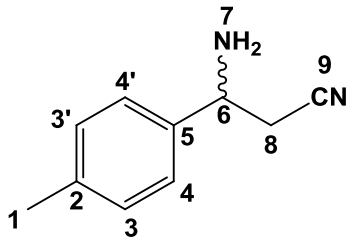
55

^{1}H NMR of 55


PM_1.10.fid
Phathu:P-1 CDCL3 26/04/2017 1H:DB
7.39
7.37
7.22
7.19
5.07
4.16
2.35
E (d)
7.20
D (d)
7.38
C (s)
5.07
B (s)
4.16
A (s)
2.35
1.81
1.91
1.77
0.85
3.00
f1 (ppm)

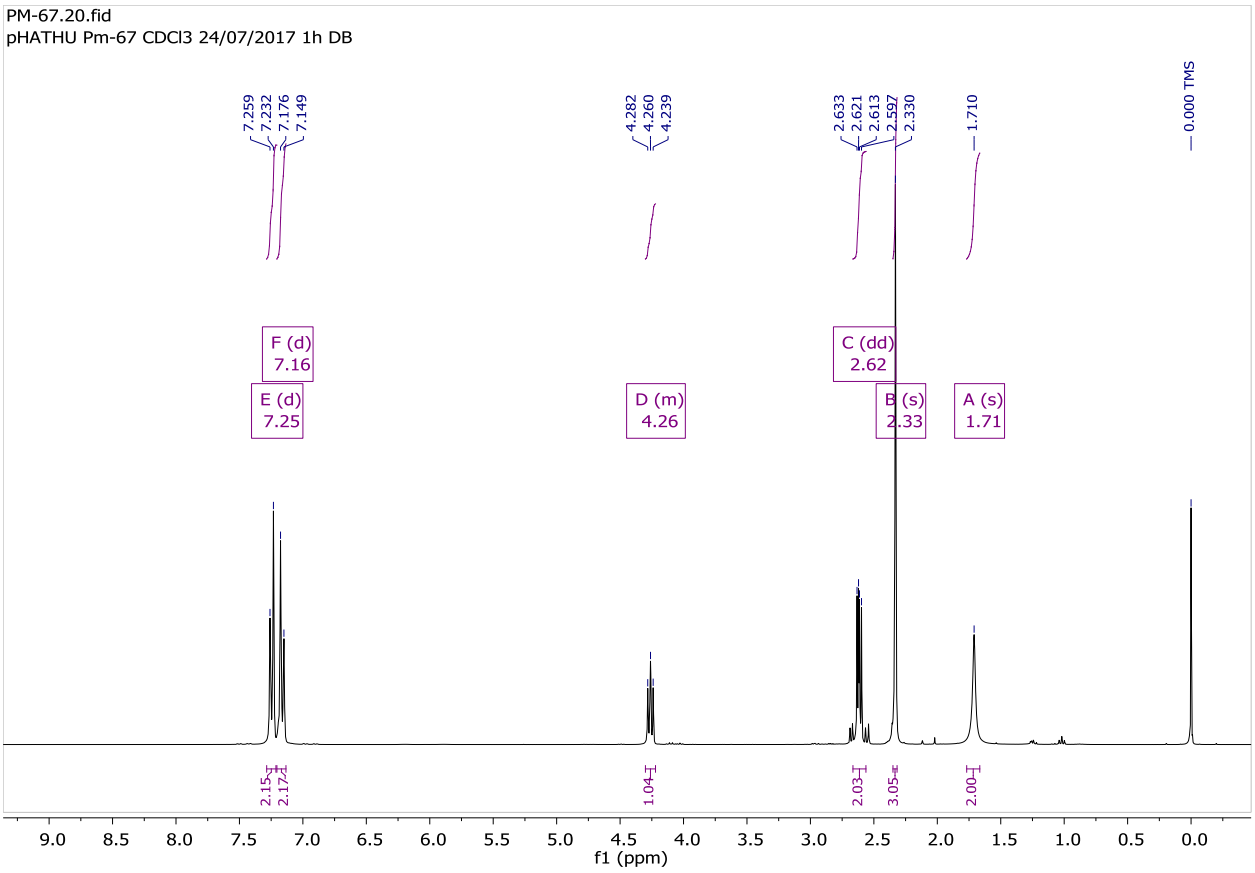
^{13}C NMR of 55



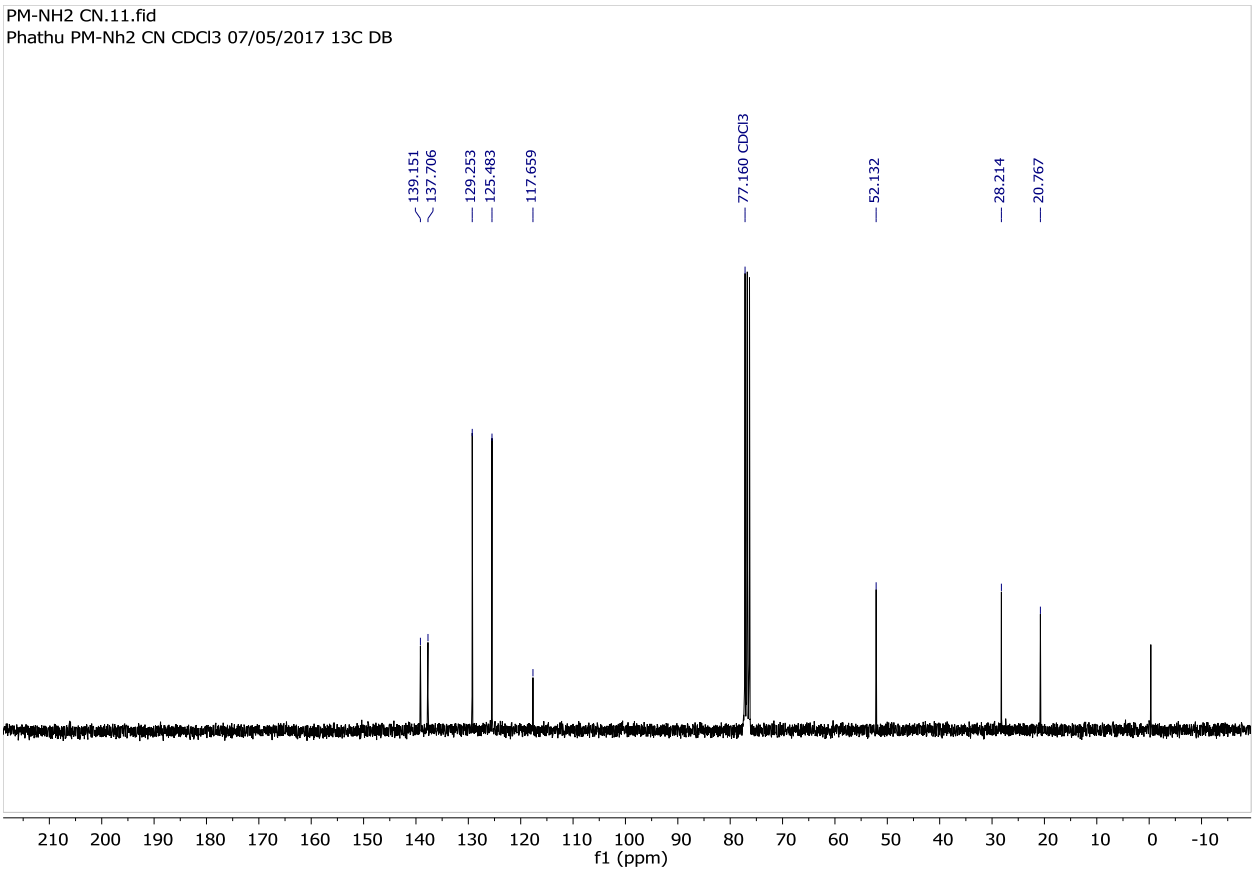


56

^{1}H NMR of 56c



^{13}C NMR of 56c



Analytical data for the compounds involved in the synthesis of 58

Display Report

Analysis Info

Analysis Name	I:\MY DOCUMENTS ONLY\LC-MS\phathu\06-06-17\PM-MBA 2uL_GE8_01_2272.d	Acquisition Date	07/Jul/2017 H20:34:52 PM
Method	Wits HPLC Std MS 50-1300 pos.m	Operator	Refilwe Moepya
Sample Name	PM-MBA 2uL	Instrument	compact 8255754.20116
Comment			

AcquisitionParameter

SourceType	ESI	IonPolarity	Positive	SetNebulizer	1.8 Bar
Focus	Not active	SetCapillary	4500 V	Set Dry Heater	220 °C
ScanBegin	50 m/z	Set End Plate Offset	-500 V	Set Dry Gas	9.0 l/min
ScanEnd	1300 m/z	SetChargingVoltage	2000 V	SetDivertValve	Waste
		SetCorona	0 nA	Set APCI Heater	0 °C

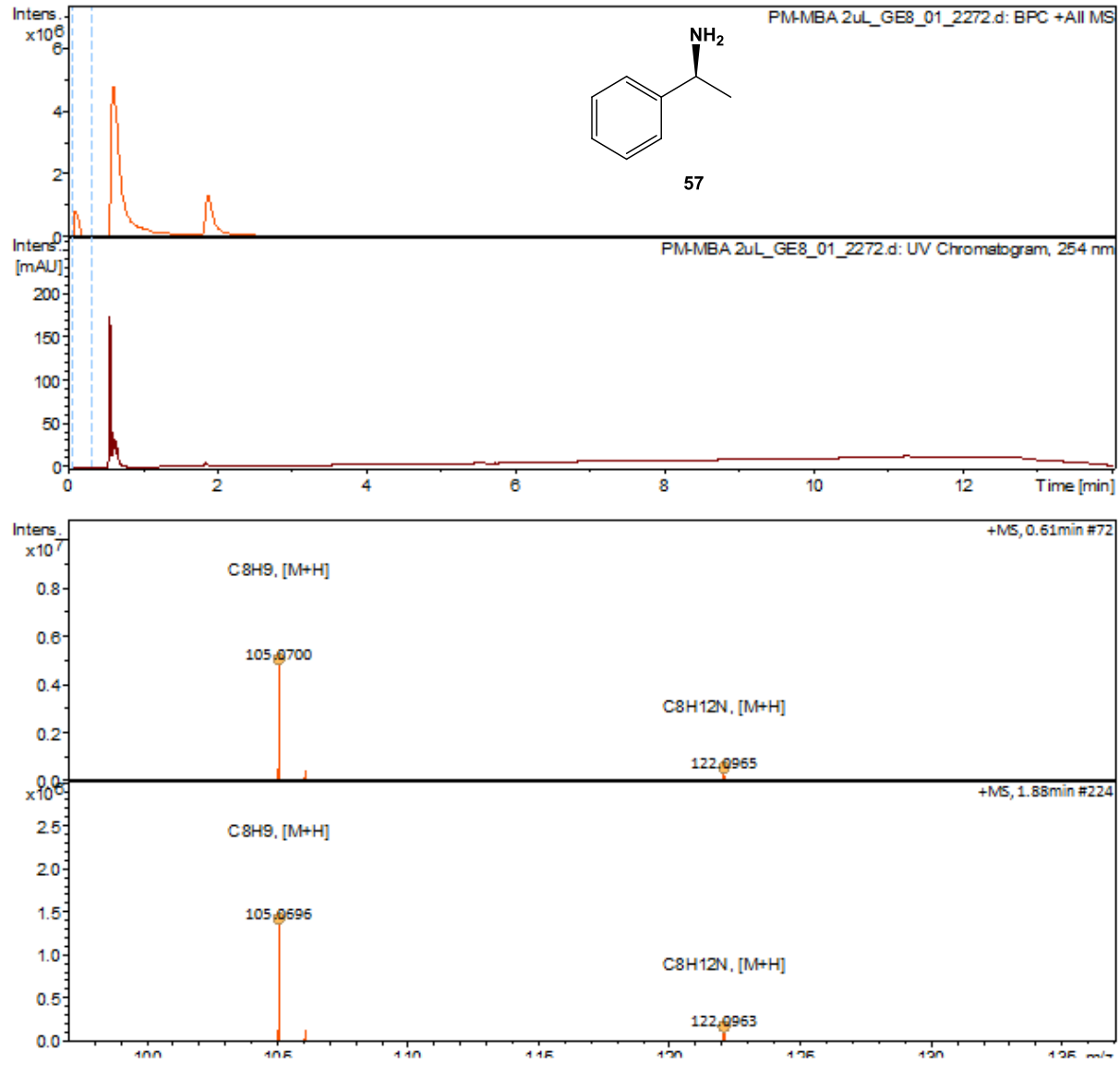


Figure A1. LC-MS data for the standard MBA **57**

Display Report

Analysis Info

Acquisition Date 07/Jul/2017 H21:04:25 PM

Analysis Name I:\MY DOCUMENTS ONLY\LC-MS\phathu\06-06-17\PM-Acetophenone 2uL_GE3_01_2274.d

Method Wits HPLC Std MS 50-1300 pos.m

Operator Refilwe Moepya

Sample Name PM-Acetophenone 2uL

Instrument compact 8255754.20116

Comment

AcquisitionParameter

SourceType	ESI	IonPolarity	Positive	SetNebulizer	1.8 Bar
Focus	Not active	SetCapillary	4500 V	Set Dry Heater	220 °C
ScanBegin	50 m/z	Set End Plate Offset	-500 V	Set Dry Gas	9.0l/min
ScanEnd	1300 m/z	SetChargingVoltage	2000 V	SetDivertValve	Waste
		SetCorona	0 nA	Set APCI Heater	0 °C

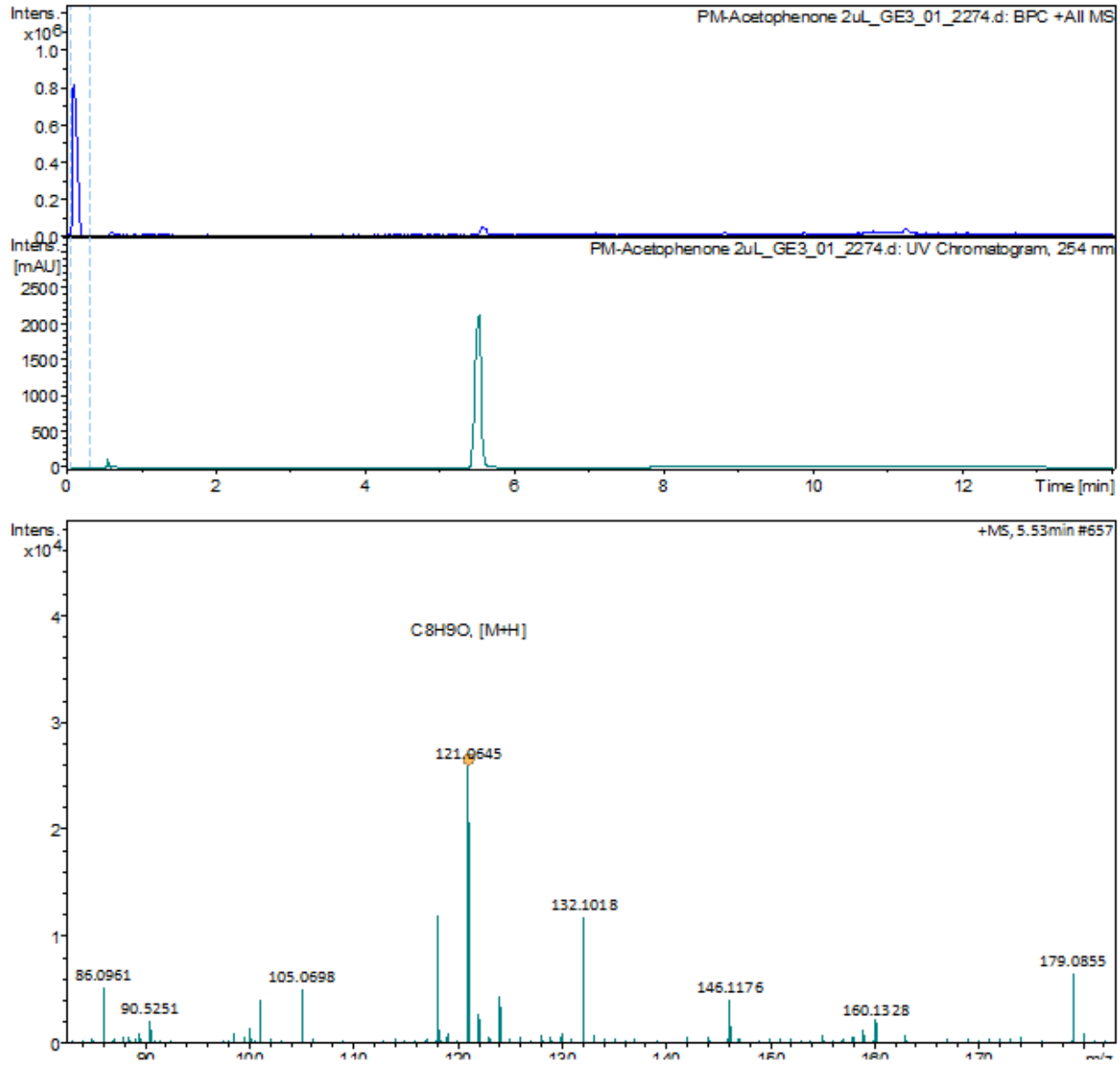


Figure A2. LC-MS data for the standard acetophenone **58**

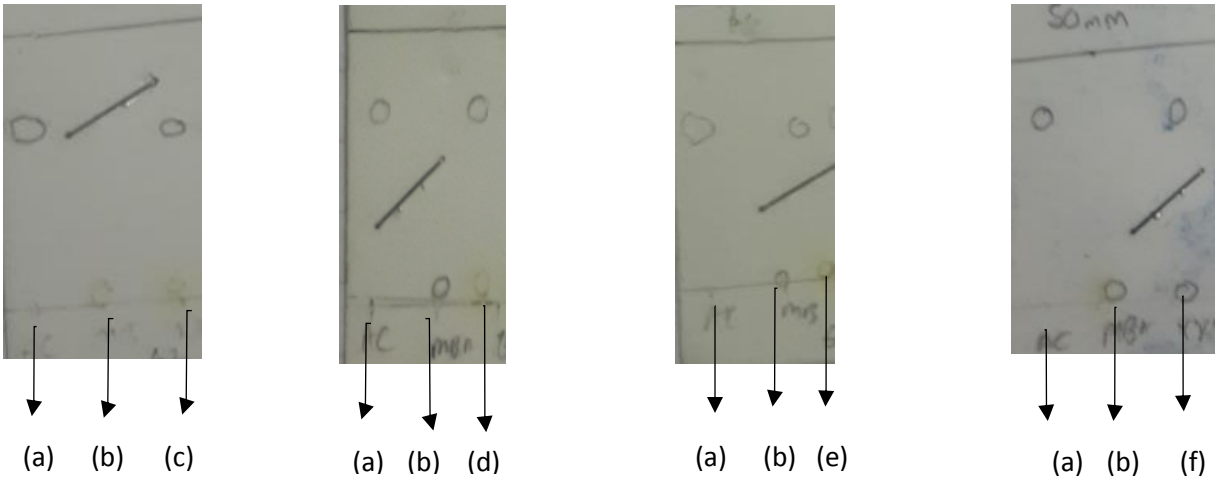


Figure A3. TLC for deamination of MBA (50 mM) (30 %EtOAc/Hexane); *(a) The acetophenone standard product. (b) The MBA standard starting material. (c) Reaction involving Prozomix-TA016, (d) Reaction involving Prozomix-TA030, (e) Reaction involving Prozomix-TA037, (f) Reaction involving Prozomix-TA045.*

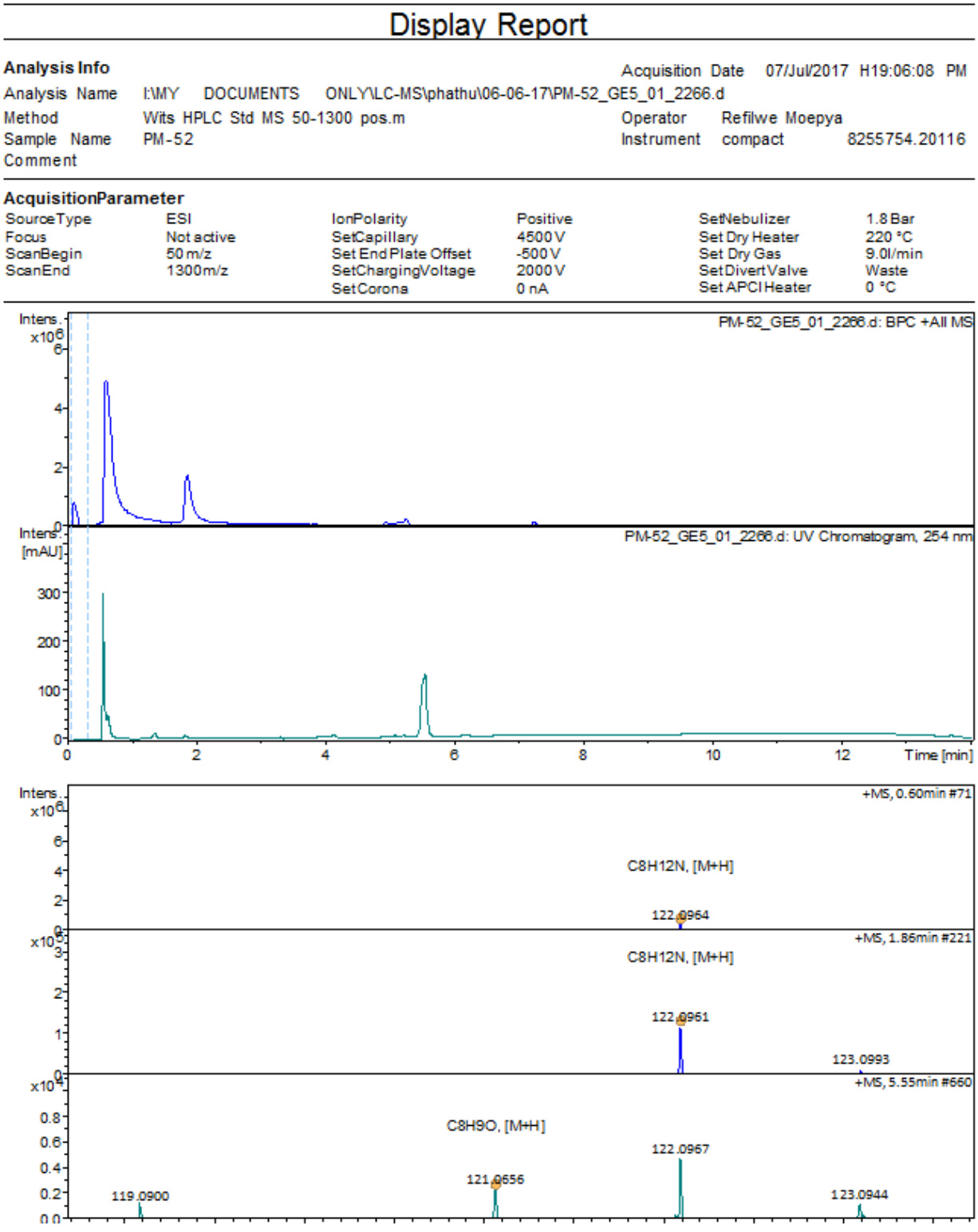


Figure A4. LC-MS analysis for deamination reaction of *S*-MBA involving Prozomix-TA045

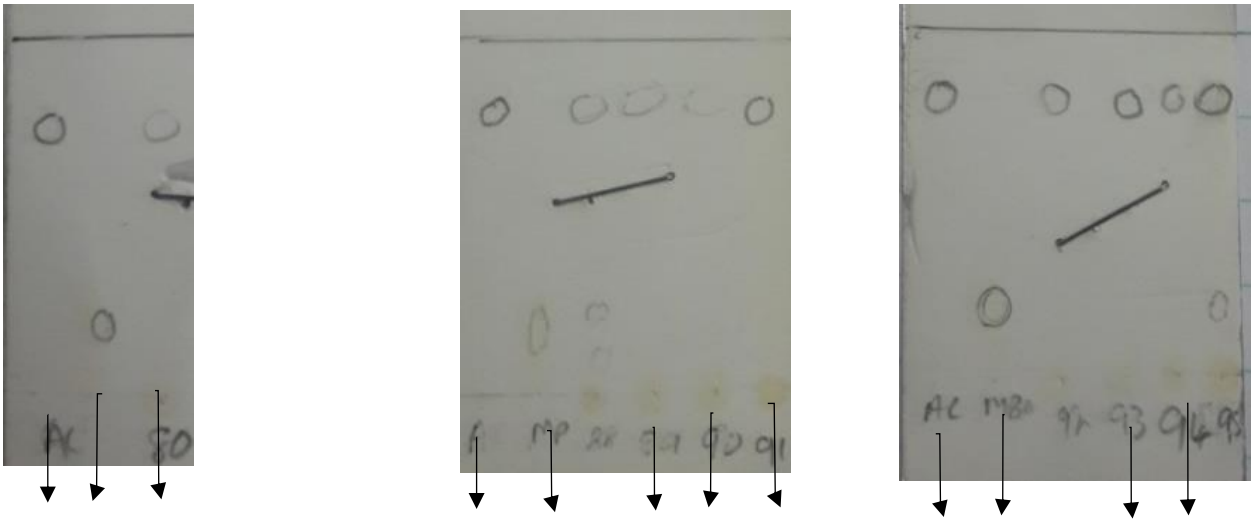


Figure A5. Reductive amination of **58** (50% EtOAc/Hexane); *(a) The acetophenone standard starting material **58.** (b) The MBA standard product **57**. (c) Reaction involved Prozomix-TA020, (d) Reaction involved Prozomix-TA023. (e) Reaction involved Prozomix-TA025. (f) Reaction involved Prozomix-TA027. (g) Reaction involved Prozomix-018. (h) reaction 94 involved Prozomix-TA050*

Display Report

Analysis Info

Acquisition Date 01/Aug/2017 H12:48:48 P M

Analysis Name I:\MY DOCUMENTS ONLY\LC-MS\phathu\01-08-17\PM-93 28,,July2017_RC2_01_3358.d

Method Wits HPLC Std MS 50-1300 pos.m

Operator Refilwe Moepya

Sample Name PM-93 28,,July2017

Instrument compact 8255754.20116

Comment

AcquisitionParameter

SourceType	ESI	IonPolarity	Positive	SetNebulizer	1.8 Bar
Focus	Not active	SetCapillary	4500 V	Set Dry Heater	220 °C
ScanBegin	50 m/z	Set End Plate Offset	-500 V	Set Dry Gas	9.0l/min
ScanEnd	1300 m/z	SetChargingVoltage	2000 V	Set Divert Valve	Waste
		SetCorona	0 nA	Set APCI Heater	0 °C

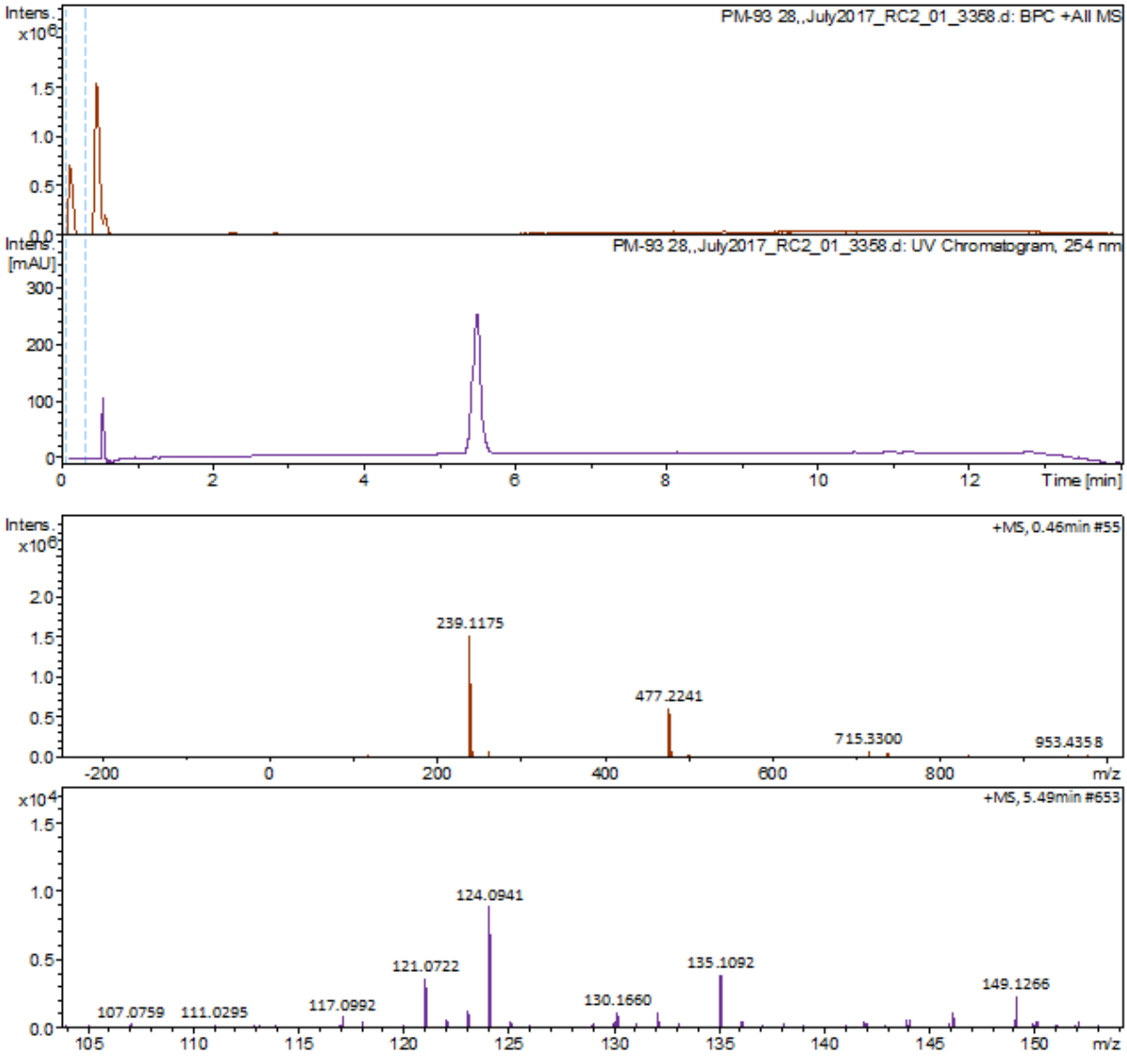


Figure A6. LC-MS analysis for Prozomix-TA018 reduction amination reaction of **58**

Display Report

Analysis Info

Acquisition Date 07/Jul/2017 H16:08:36 PM

Analysis Name I:\MY DOCUMENTS ONLY\LC-MS\phathu\06-06-17\PM-46_GE6_01_2254.d

Method Wits HPLC Std MS 50-1300 pos.m

Operator Refilwe Moepya

Sample Name PM-46

Instrument compact 8255754.20116

Comment

AcquisitionParameter

SourceType	ESI	IonPolarity	Positive	SetNebulizer	1.8 Bar
Focus	Not active	SetCapillary	4500 V	Set Dry Heater	220 °C
ScanBegin	50 m/z	Set End Plate Offset	-500 V	Set Dry Gas	9.0 l/min
ScanEnd	1300 m/z	SetChargingVoltage	2000 V	SetDivertValve	Waste
		SetCorona	0 nA	Set APCI Heater	0 °C

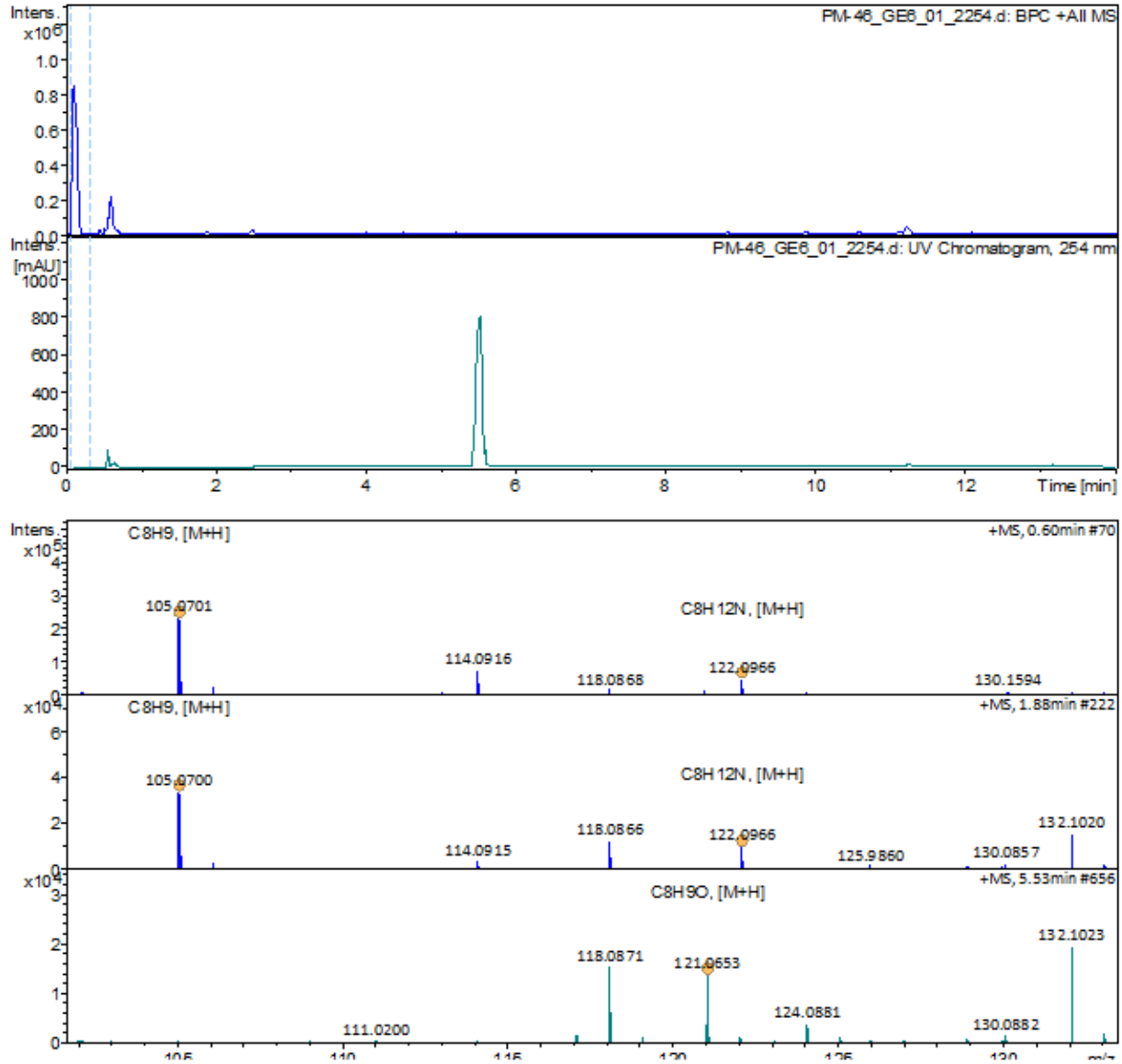


Figure A7. LC-MS analysis for reductive amination reaction involving ECS-TA02

Display Report

Analysis Info

Acquisition Date 07/Jul/2017 H16:52:54 PM

Analysis Name I:\MY DOCUMENTS ONLY\LC-MS\phathu\06-06-17\PM-48_GE7_01_2257.d

Method Wits HPLC Std MS 50-1300 pos.m

Operator Refilwe Moepya

Sample Name PM-48

Instrument compact 8255754.20116

Comment

AcquisitionParameter

SourceType	ESI	IonPolarity	Positive	SetNebulizer	1.8 Bar
Focus	Not active	SetCapillary	4500 V	Set Dry Heater	220 °C
ScanBegin	50 m/z	Set End Plate Offset	-500 V	Set Dry Gas	9.0l/min
ScanEnd	1300 m/z	SetChargingVoltage	2000 V	SetDivertValve	Waste
		SetCorona	0 nA	Set APCI Heater	0 °C

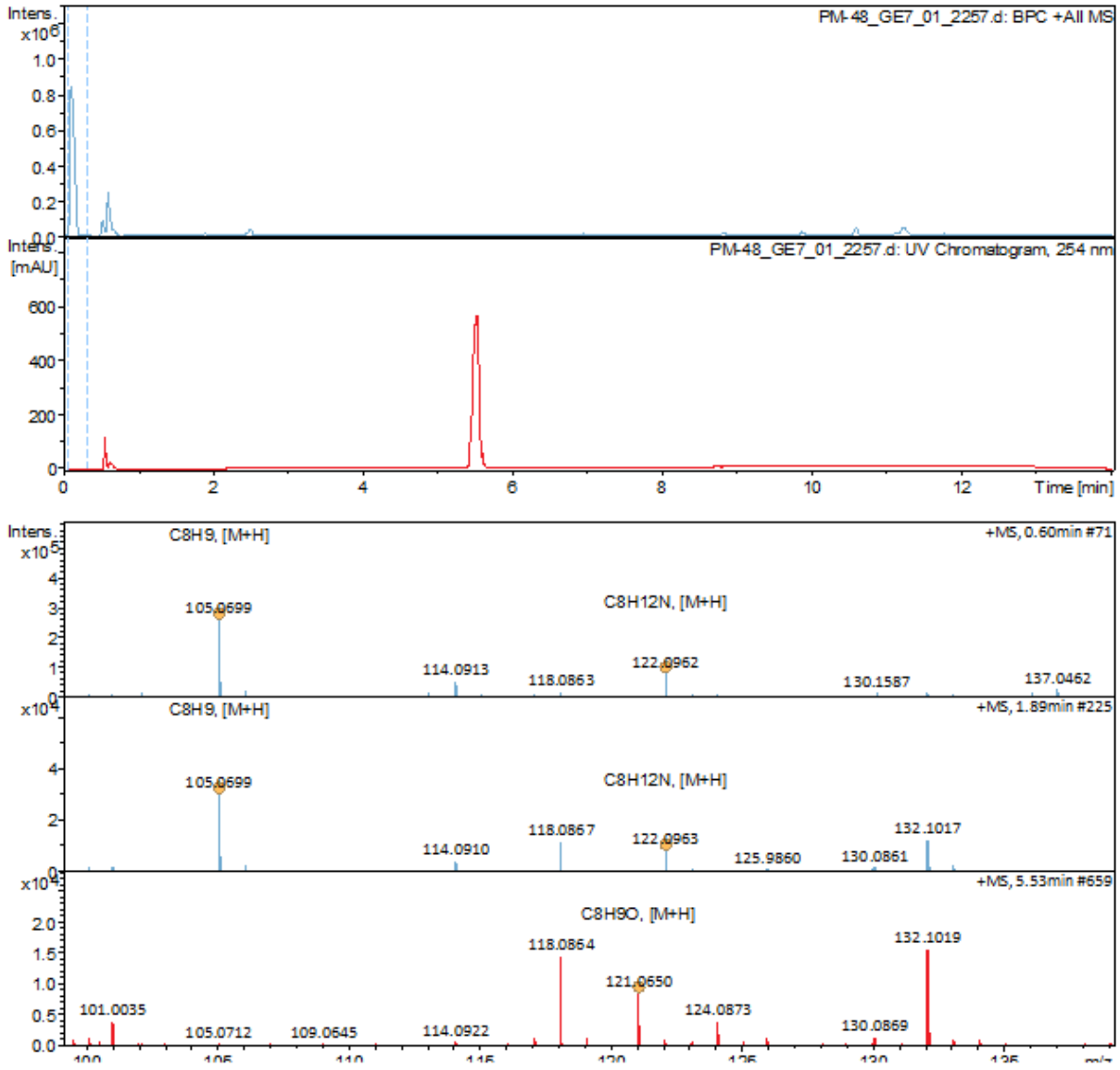


Figure A8. LC-MS analysis for reductive amination reaction involving Prozomix-TA024

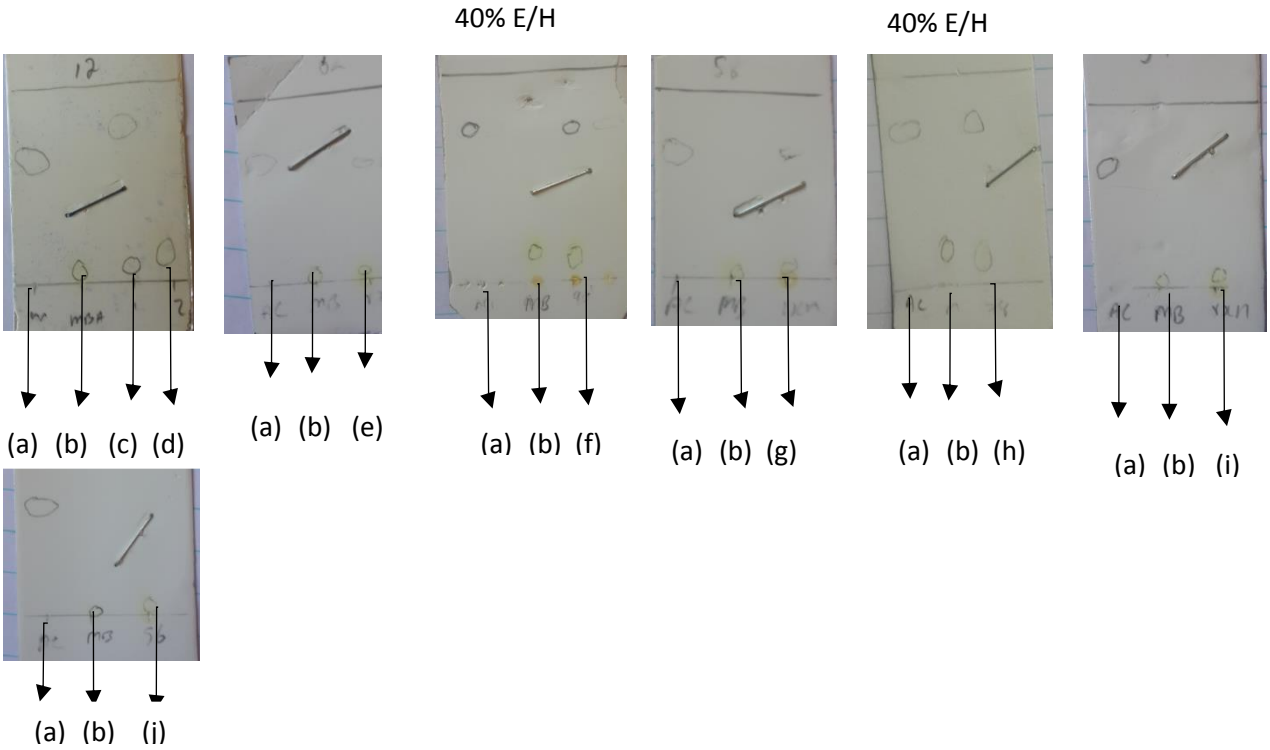


Figure A9. TLC for transaminase tested on different MBA concentrations (30% EtOAc/hexane); *(a) The acetophenone standard product. (b) The MBA standard starting material. (c) Reaction involved ECS-TA-03 with MBA (50 mM). (d) Reaction involved ECS-TA-03 with MBA (250 mM). (e) Involved Prozomix-TA016 with MBA (50 mM). (f) Involved Prozomix-TA002 with MBA (100 mM). (g) Involved Prozomix-TA045 with MBA (100 mM). (h) Involved Prozomix-TA041 with MBA (250 mM). (i) Involved Prozomix-TA045 with MBA (250 mM). (j) Involved Aspergillus fumigatus with MBA (250 mM).*

Display Report

Analysis Info

Acquisition Date 12/Jul/2017 H14:34:21 PM

Analysis Name I:\MY DOCUMENTS ONLY\LC-MS\phathu\06-06-17\PM-54_GA3_01_2419.d

Method Wits HPLC Std MS 50-1300 pos.m

Operator Refilwe Moepya

Sample Name PM-54

Instrument compact 8255754.20116

Comment

AcquisitionParameter

SourceType	ESI	IonPolarity	Positive	SetNebulizer	1.8 Bar
Focus	Not active	SetCapillary	4500 V	Set Dry Heater	220 °C
ScanBegin	50 m/z	Set End Plate Offset	-500 V	Set Dry Gas	9.0l/min
ScanEnd	1300 m/z	SetChargingVoltage	2000 V	SetDivertValve	Waste
		SetCorona	0 nA	Set APCI Heater	0 °C

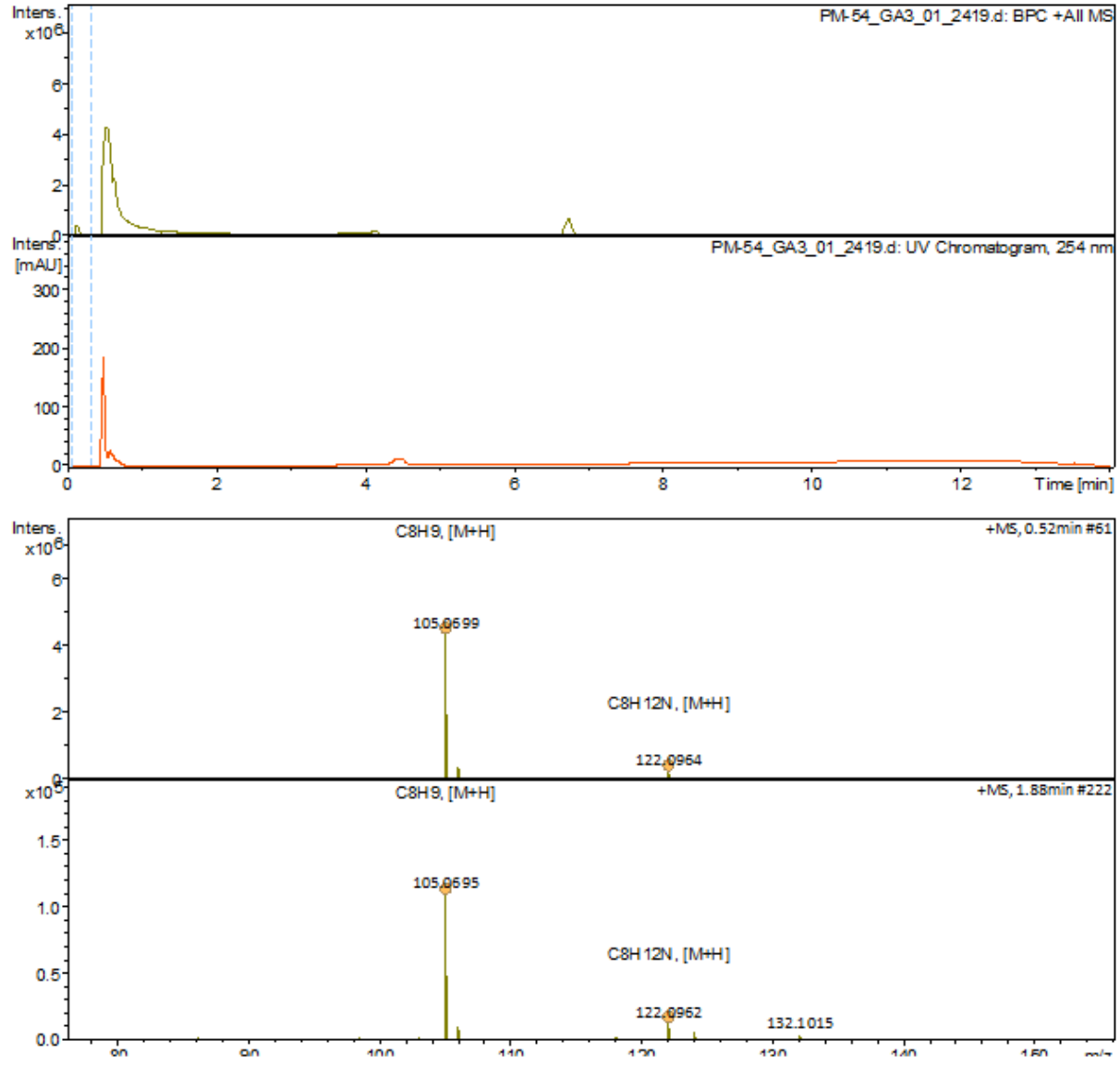


Figure A10. LC-MS analysis for deamination reaction involving Prozomix-TA045 at 250 mM

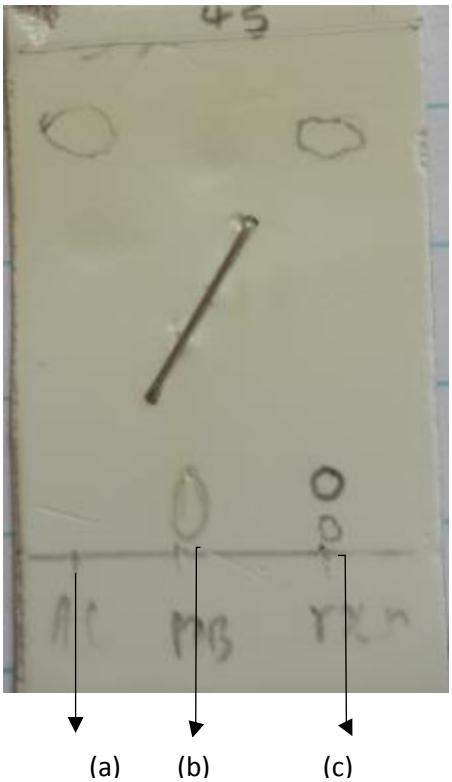


Figure A11. TLC analysis for reductive amination of **58** (30% EtOAc/hexane). *(a) The acetophenone standard starting material **58**. (b) The MBA standard product **57**. (c) Reaction involving Prozomix-TA022 at 25 mM of **58**.*

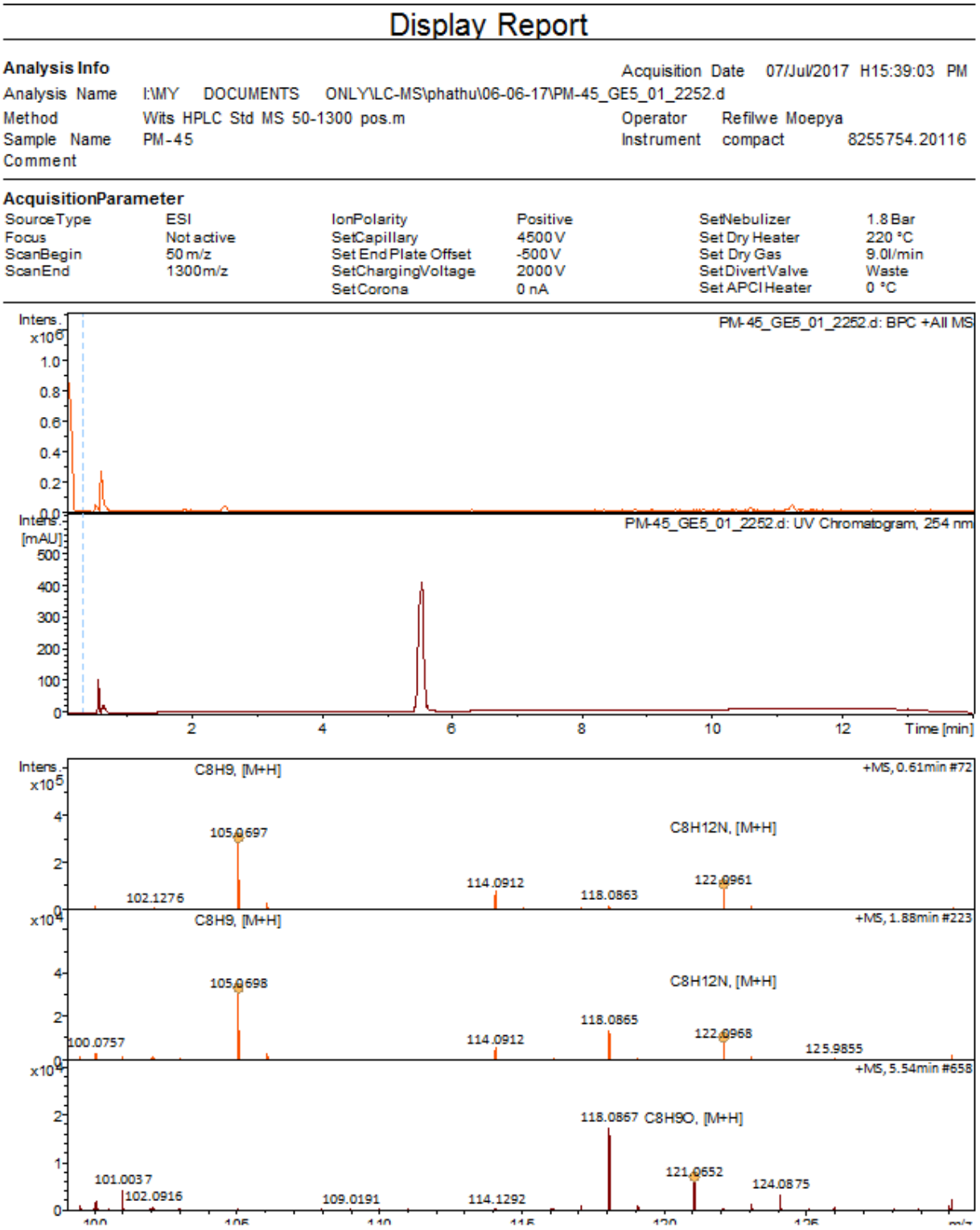


Figure A12. LC-MS analysis for reductive amination reaction involving Prozomix-TA022 at 25 mM of acetophenone

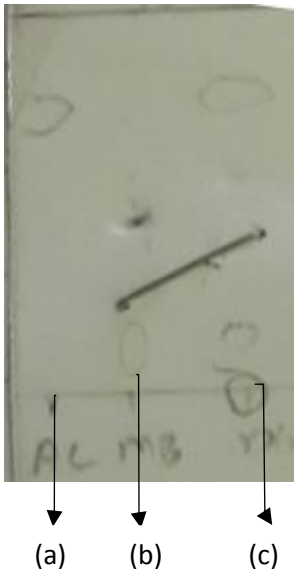


Figure A13. TLC analysis for reductive amination of **58**. *(a) Acetophenone standard starting material. (b) MBA standard product. (c) Reaction involving Prozomix-TA024 at 50 mM of acetophenone*

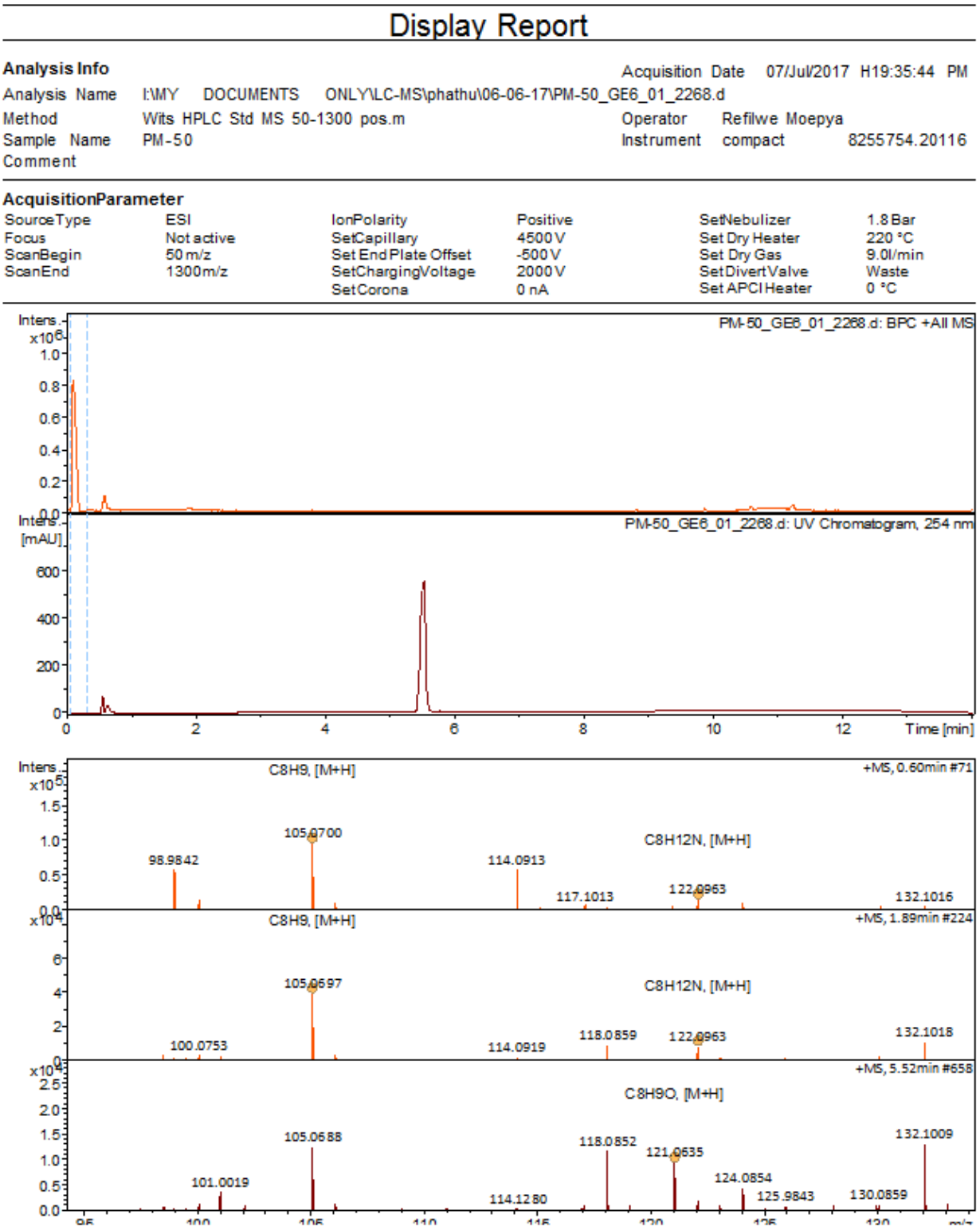


Figure A14. LC-MS analysis for reductive amination reaction involving Prozomix-TA024 at 50 mM of acetophenone



Figure A15. TLC analysis for reductive amination of **58** (30% EtOAc/hexane). *(a) Acetophenone standard starting material. (b) MBA standard product. (c) Reaction involving Prozomix-TA038 at 100 mM of acetophenone*

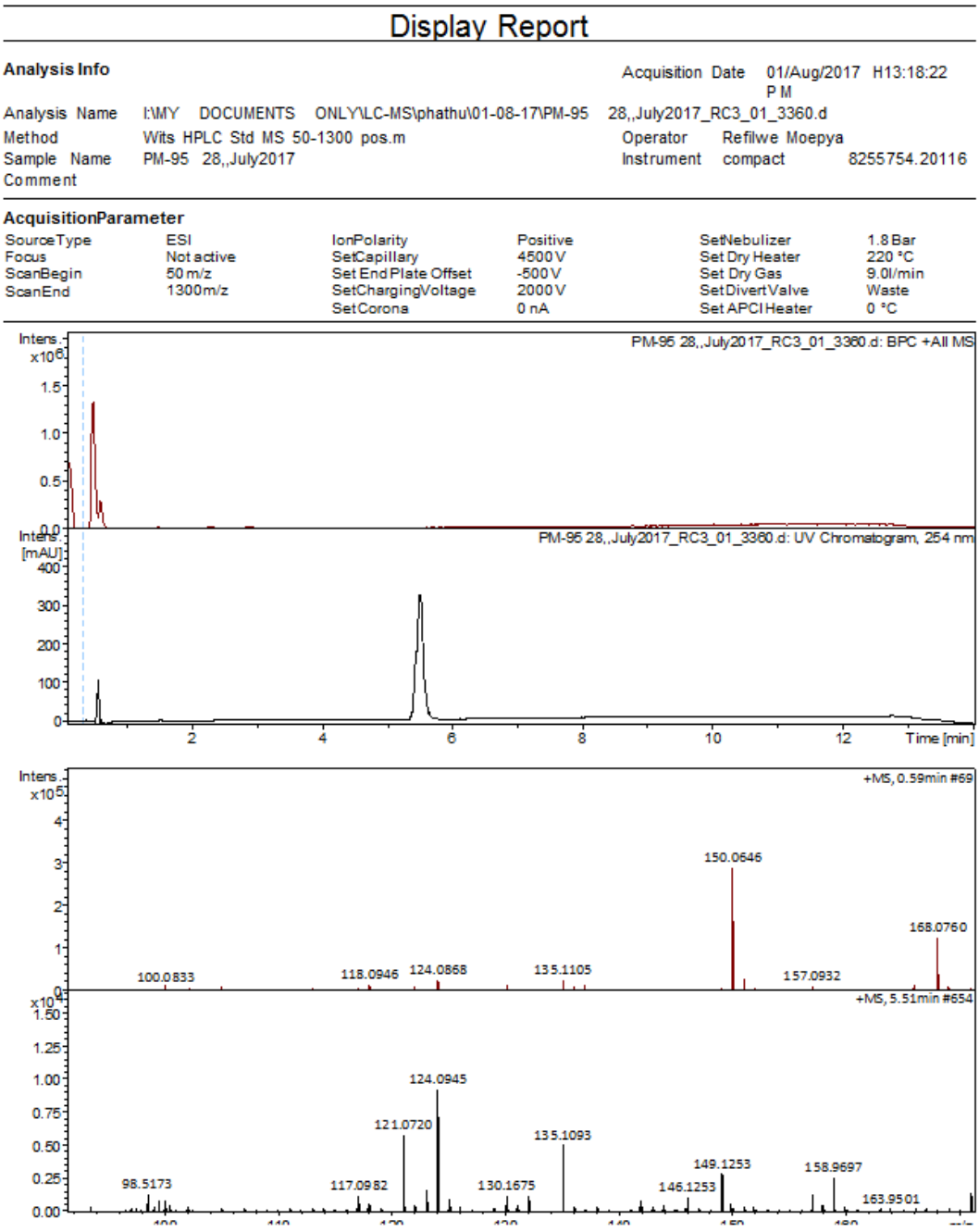


Figure A16. LC-MS analysis for reductive amination reaction involving Prozomix-TA038 at 100 mM of acetophenone

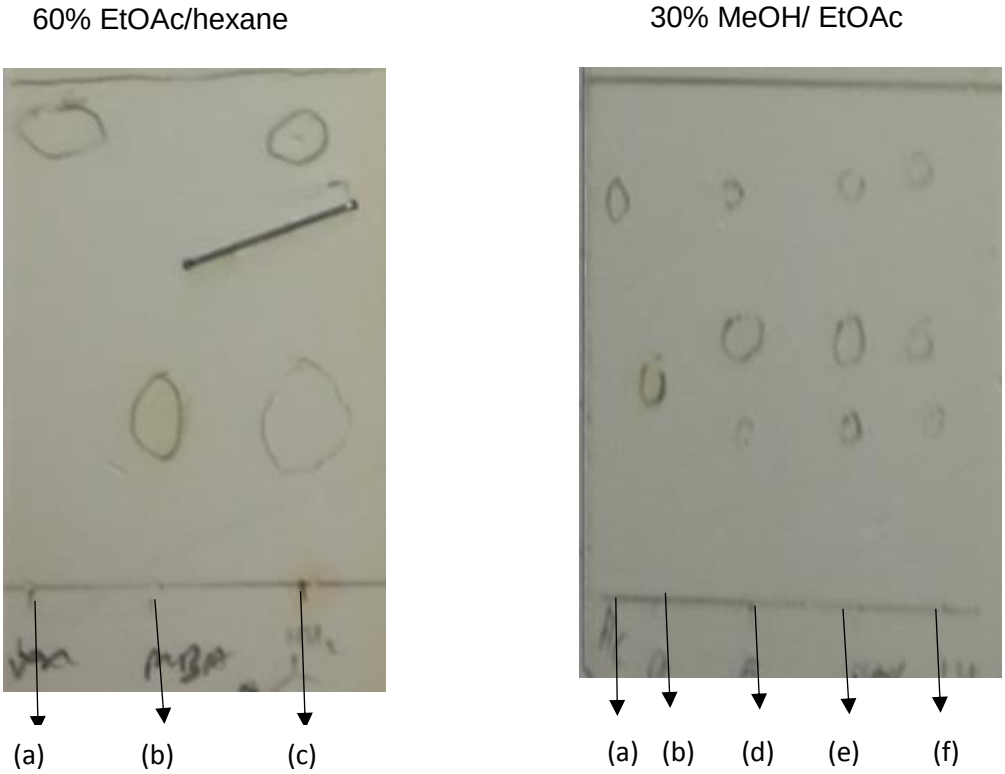


Figure A17. TLC for reductive amination of acetophenone using LDH mixture; *(a) Acetophenone standard starting material. (b) MBA standard product. (c) Reaction involving ECS-TA05 with Acetophenone (50 mM). (d) Reaction involved Prozomix-TA016 with Acetophenone (50 mM). (e) Reaction involved Prozomix-TA045 with Acetophenone (50 mM). (f) Reaction involved Aspergillus fumigatus with Acetophenone (50 mM).*

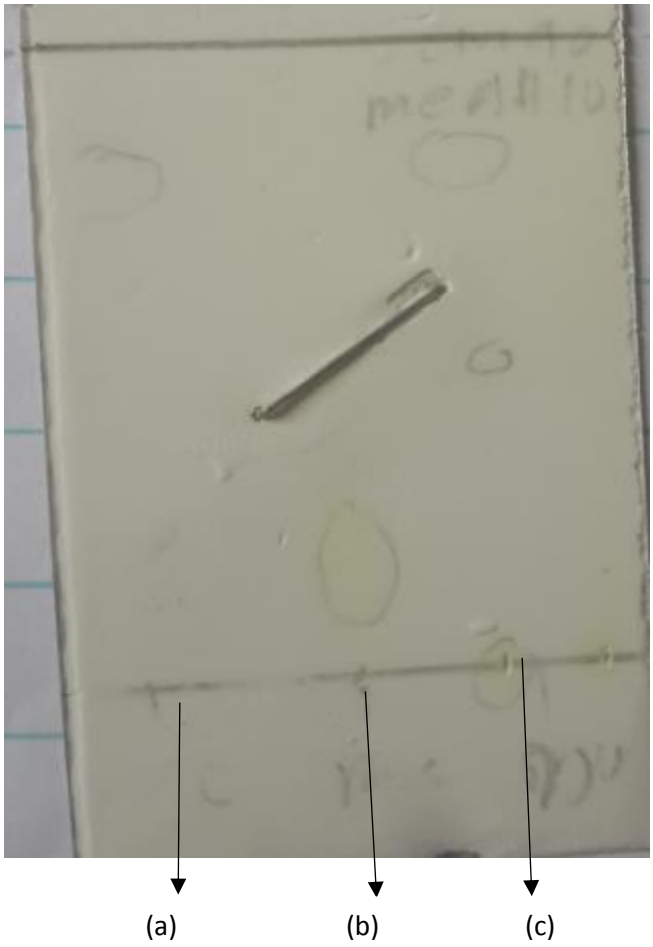


Figure A18. TLC analysis of reaction involving Prozomix-048 with **58** (10 mM) (c*)* (10% MeOH/EtOAc)*. (a) Acetophenone standard, (b) MBA standard*

Display Report

Analysis Info

Acquisition Date 20/Jul/2017 H12:04:54 PM

Analysis Name I:\MY DOCUMENTS ONLY\LC-MS\phathu\06-06-17\PM-70_RB3_01_2745.d

Method Wits HPLC Std MS 50-1300 pos.m

Operator Refilwe Moepya

Sample Name PM-70

Instrument compact 8255754.20116

Comment

AcquisitionParameter

SourceType	ESI	IonPolarity	Positive	SetNebulizer	1.8 Bar
Focus	Not active	SetCapillary	4500 V	Set Dry Heater	220 °C
ScanBegin	50 m/z	Set End Plate Offset	-500 V	Set Dry Gas	9.0 l/min
ScanEnd	1300 m/z	SetChargingVoltage	2000 V	Set Divert Valve	Waste
		SetCorona	0 nA	Set APCI Heater	0 °C

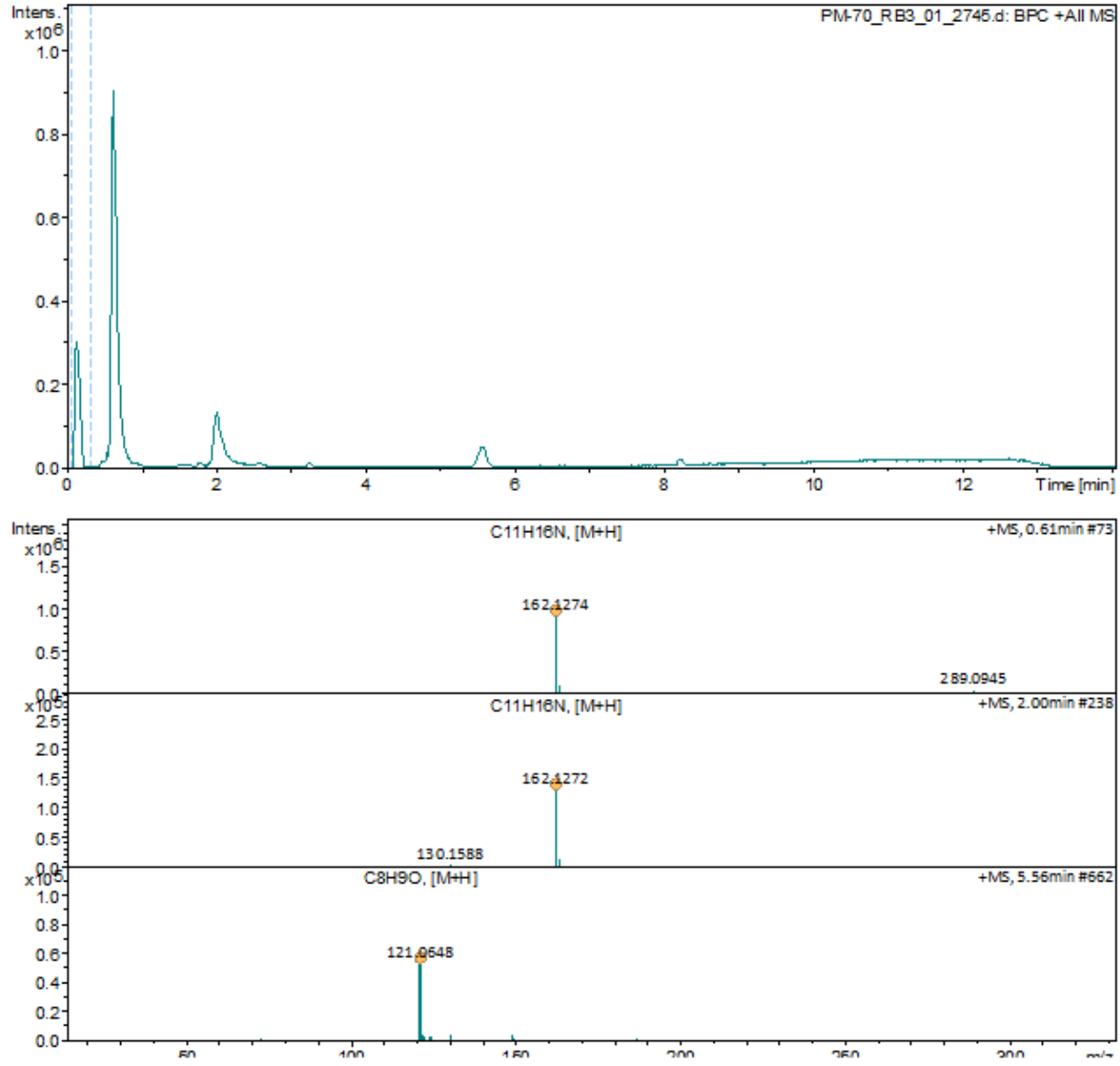


Figure A19. LC-MS analysis for reductive amination reaction involving Prozomix-TA048 with **58** (10 mM)

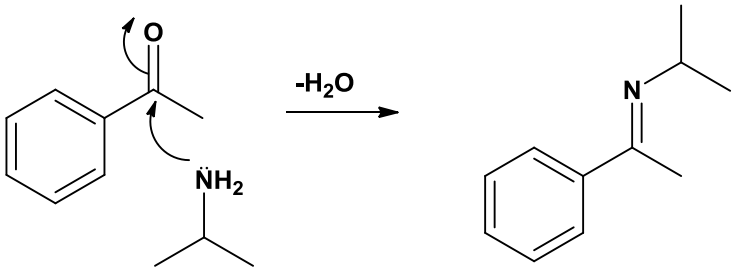


Figure A20. Mechanism for by-product formed by reaction between the isopropyl amine and acetophenone

Analytical data for the compounds involved in the synthesis of 57



Figure A21. Colour change for reductive amination of **58** using diamine donor and involving ECS-TA06

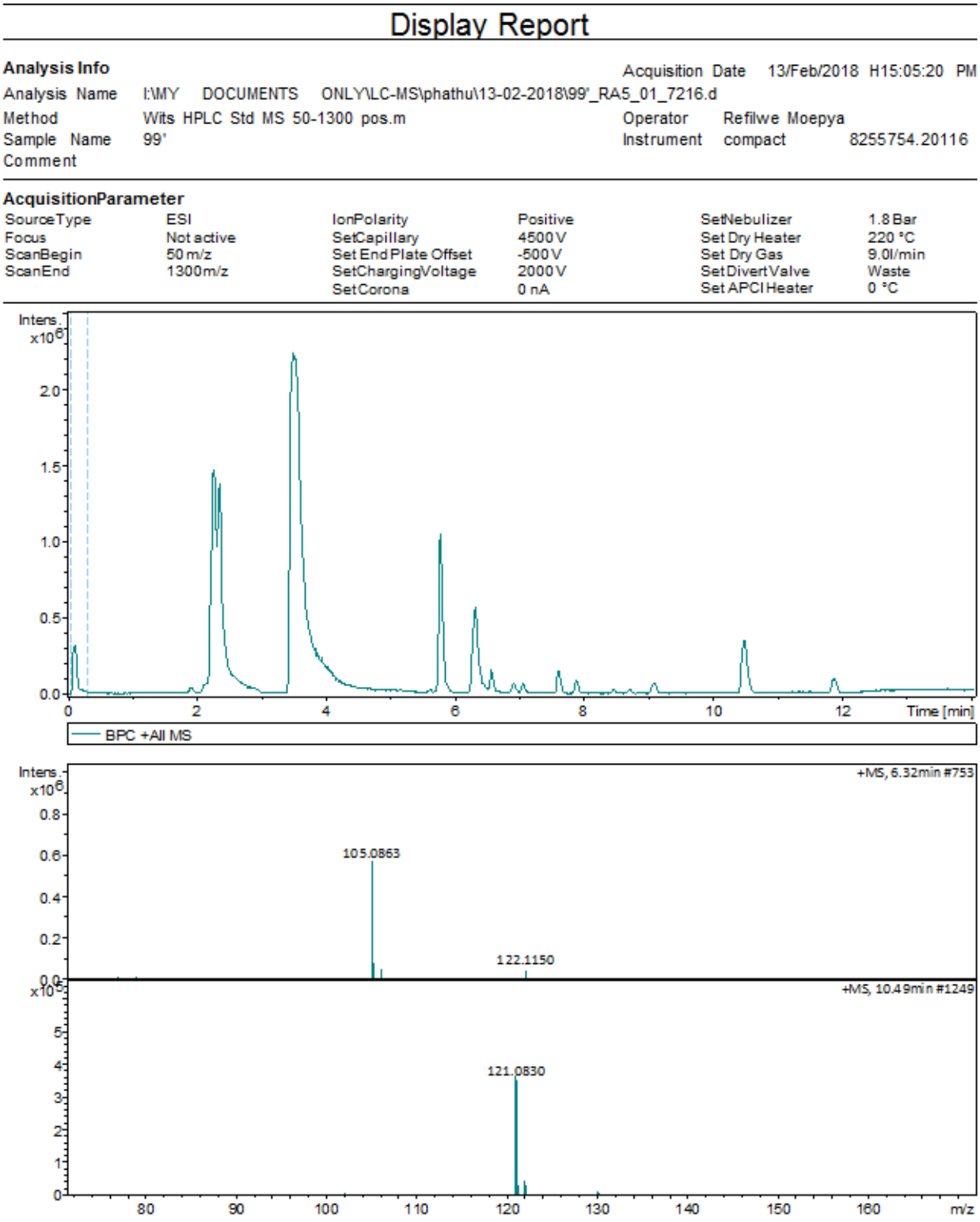


Figure A22. LC-MS analysis for reductive amination reaction involving ECS-TA06 at 10 mM of **58** using diamine donor

Analytical data for the compounds involved in the synthesis of 56c

Display Report

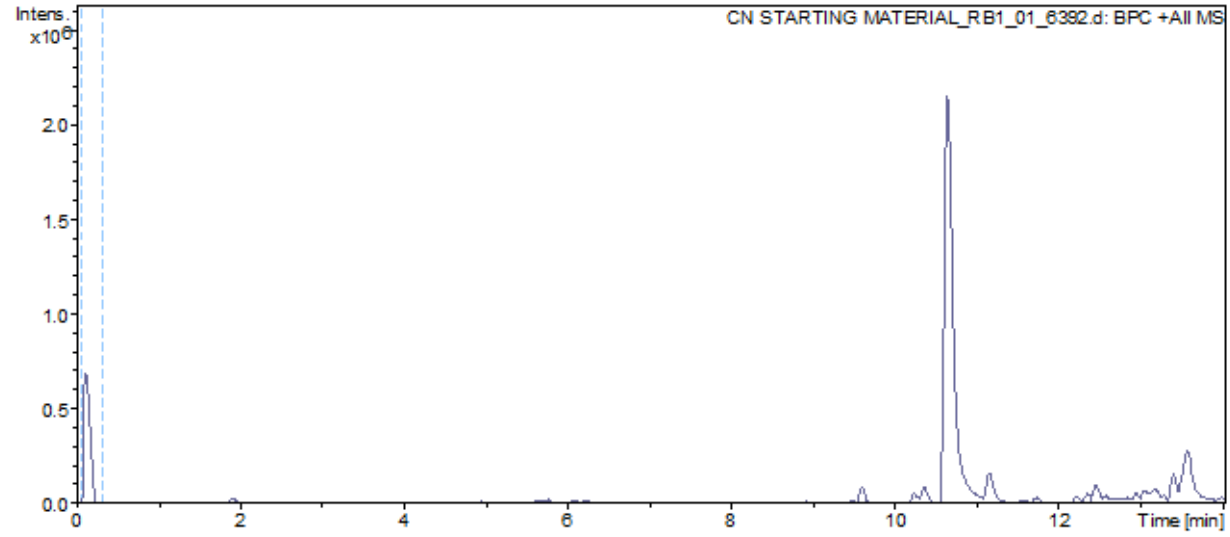
Analysis Info

Acquisition Date 15/Nov/2017 H01:48:42 AM

Analysis Name I:\MY DOCUMENTS ONLY\LC-MS\phathu\14-11-17 night\CN STARTING MATERIAL_RB1_01_6392.d
Method Wits HPLC Std MS 50-1300 pos.m
Operator Refilwe Moepya
Sample Name CN STARTING MATERIAL
Instrument compact 8255754.20116
Comment

AcquisitionParameter

SourceType	ESI	IonPolarity	Positive	SetNebulizer	1.8 Bar
Focus	Not active	SetCapillary	4500 V	Set Dry Heater	220 °C
ScanBegin	50 m/z	Set End Plate Offset	-500 V	Set Dry Gas	9.0 l/min
ScanEnd	1300 m/z	SetChargingVoltage	2000 V	SetDivertValve	Waste
		SetCorona	0 nA	Set APCI Heater	0 °C



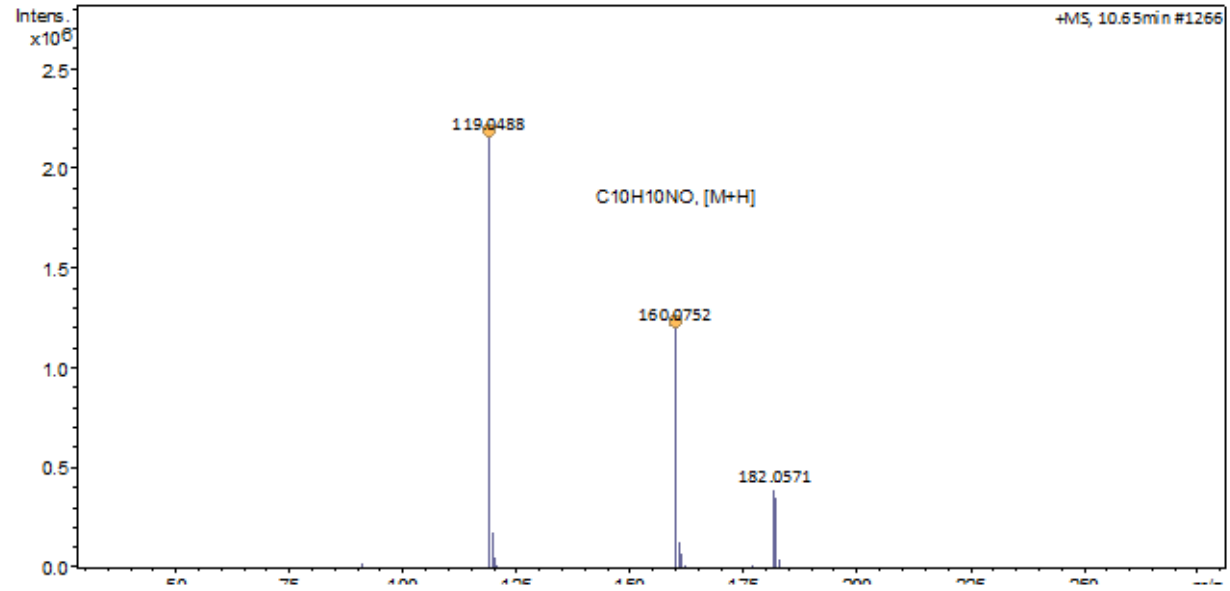


Figure A23. LC-MS analysis for standard **54c**

Display Report

Analysis Info

Acquisition Date 15/Nov/2017 H02:35:06 AM

Analysis Name I:\MY DOCUMENTS ONLY\LC-MS\phathu\14-11-17 night\NH2 PURE PRODUCT_RB2_01_6395.d

Method Wits HPLC Std MS 50-1300 pos.m

Operator Refilwe Moepya

Sample Name NH2 PURE PRODUCT

Instrument compact 8255754.20116

Comment

AcquisitionParameter

SourceType	ESI	IonPolarity	Positive	SetNebulizer	1.8 Bar
Focus	Not active	SetCapillary	4500 V	Set Dry Heater	220 °C
ScanBegin	50 m/z	Set End Plate Offset	-500 V	Set Dry Gas	9.0 l/min
ScanEnd	1300 m/z	SetChargingVoltage	2000 V	Set Divert Valve	Waste
		SetCorona	0 nA	Set APCI Heater	0 °C

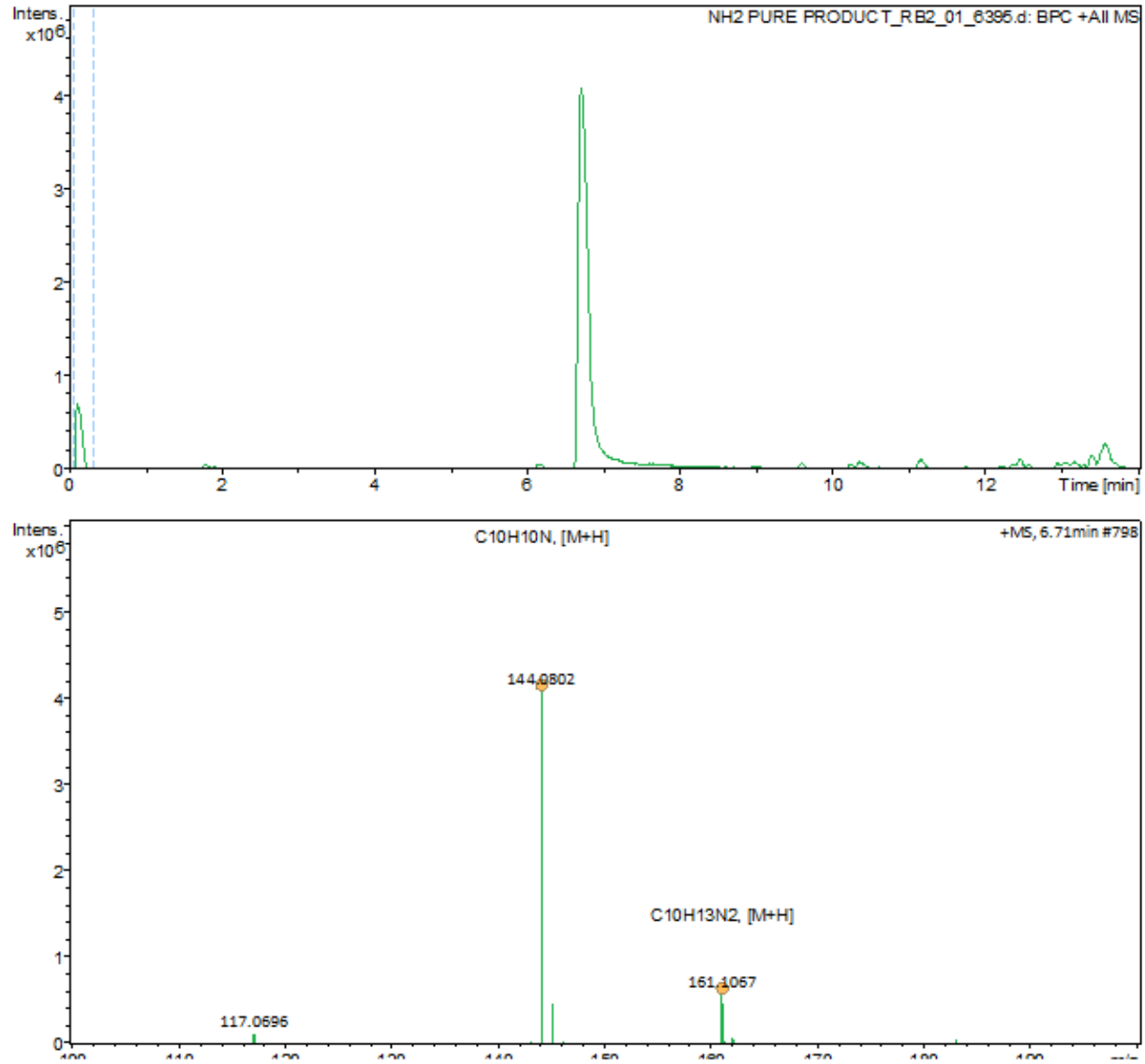


Figure A24. LC-MS analysis for standard **56c**

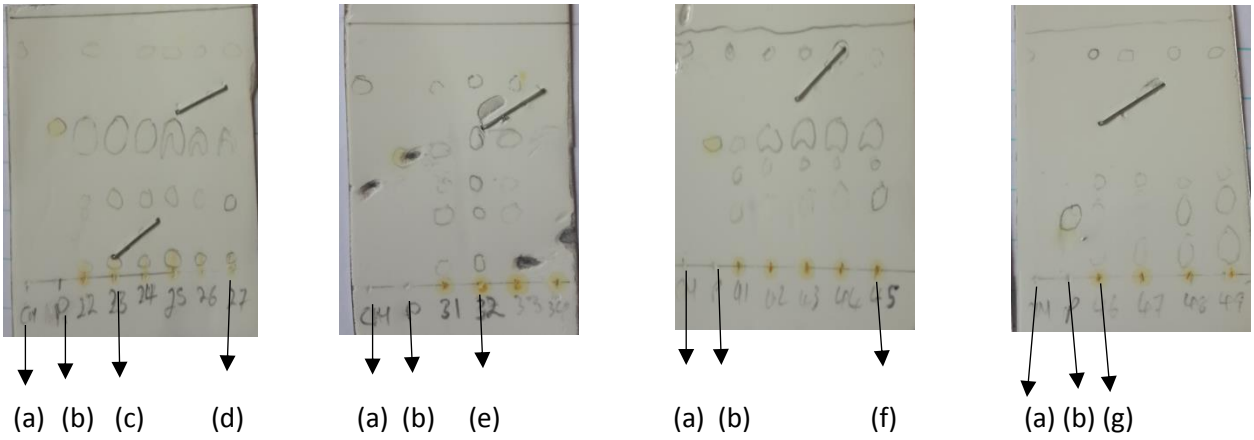


Figure A25. TLC for reductive amination of **54c** (10 mM) using diamine donor (10% MeOH/EtOAc); *(a) Standard substrate **54c**.(b) Standard amine product **56c**. (c) Reaction involved Prozomix-TA011. (d) Reaction involved prozomix-TA005. (e) Reaction involved Prozomix-TA010. (f) Reaction involved Prozomix-TA045. (g) Reaction 46 involved Prozomix-TA042 (40%. EtOAc/Hexane)*

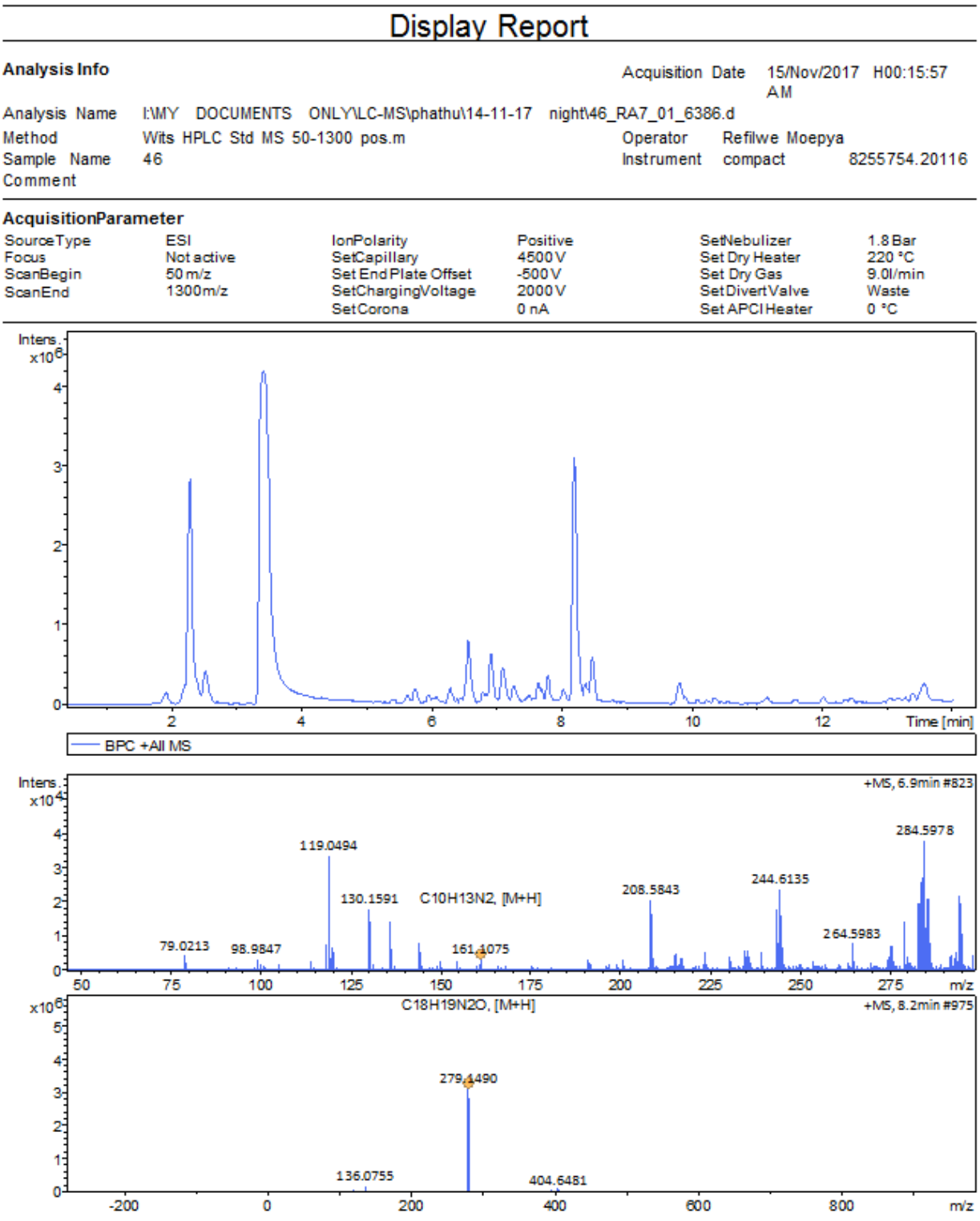


Figure A26. LC-MS analysis for reductive amination reaction involving Prozomix-TA042 at 10 mM of **54a** using diamine donor

Analytical data for the compounds involved in the synthesis of 56d

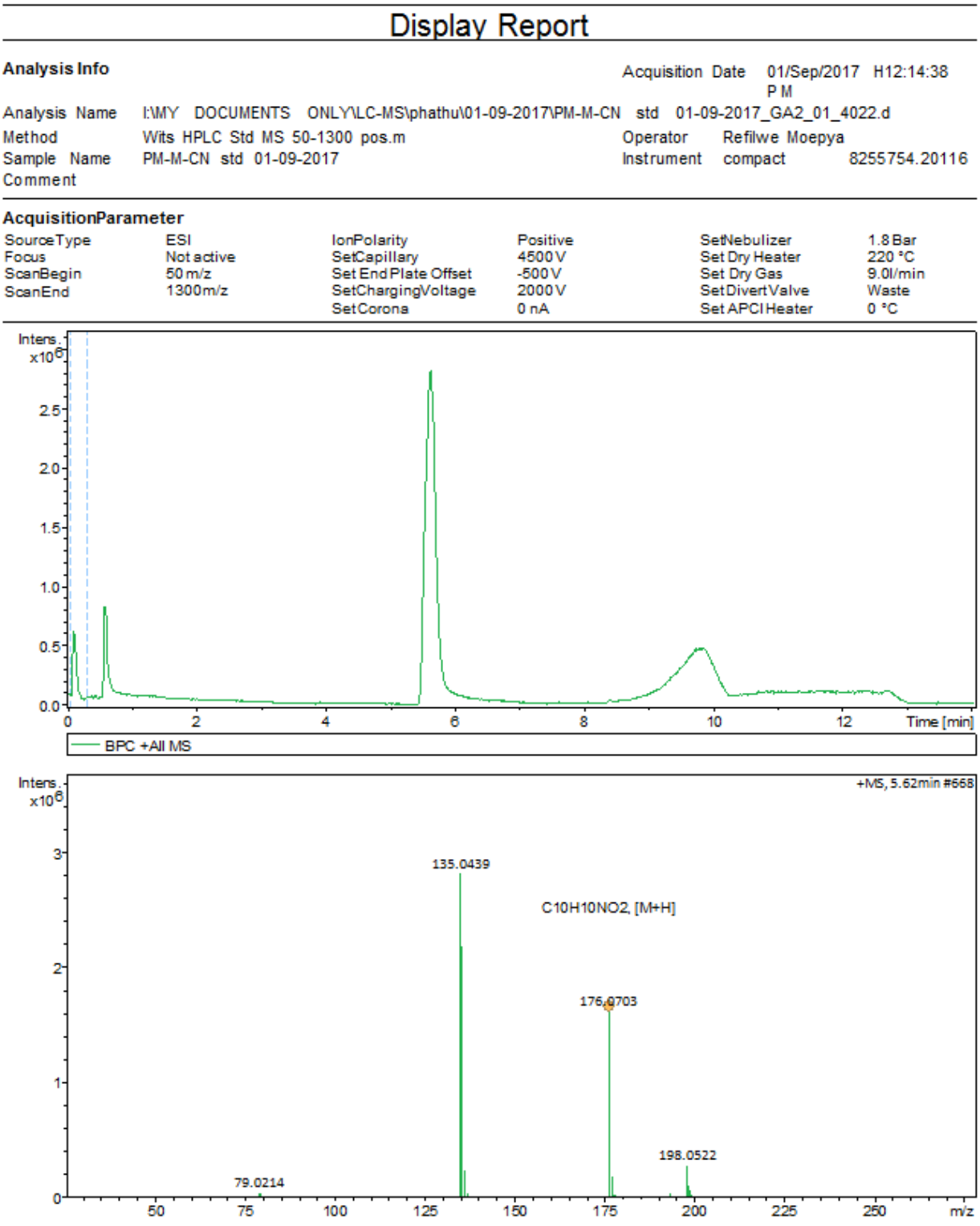


Figure A27. LC-MS analysis of standard **54b**

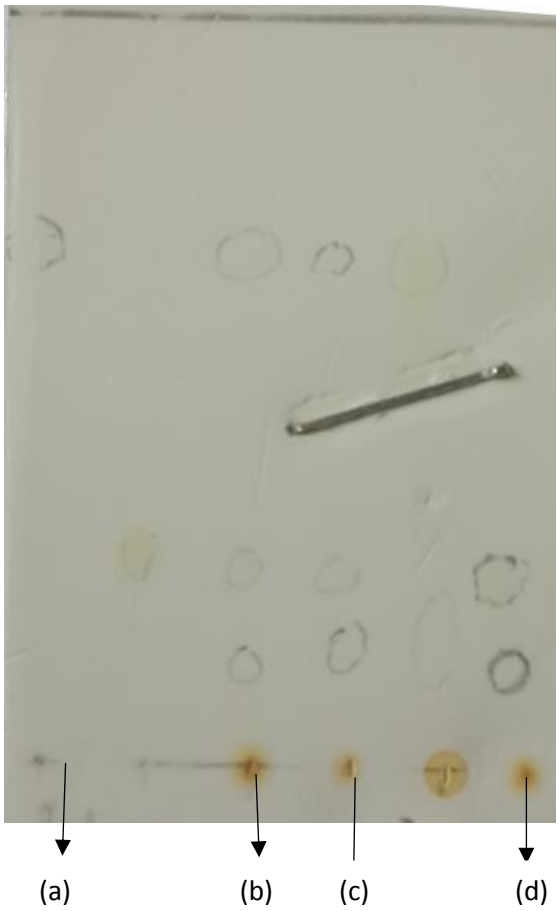


Figure A28. TLC for reductive amination of **54b** using diamine donor (40% EtOAc/Hexane). *(a) Standard starting material **54d**. (b Reaction involved Prozomix-TA046. (c) Reaction involving Aspergillus fumigatus. (d) Reaction involving prozomix-TA011.*

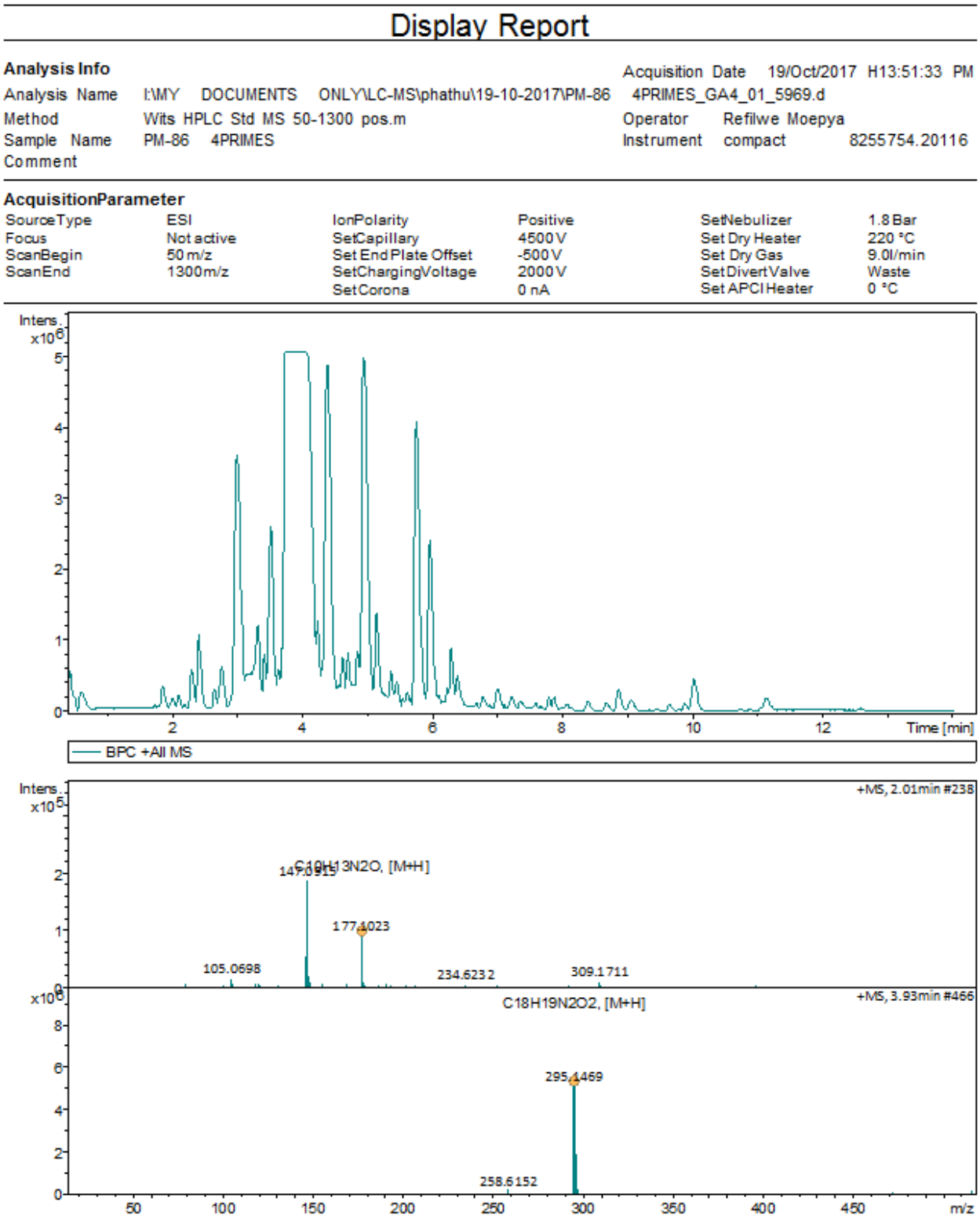


Figure A29. LC-MS analysis for reductive amination reaction involving Prozomix-TA011 at 10 mM of **54b** using diamine donor

Analytical data for the compounds involved in the synthesis of 65 and 66

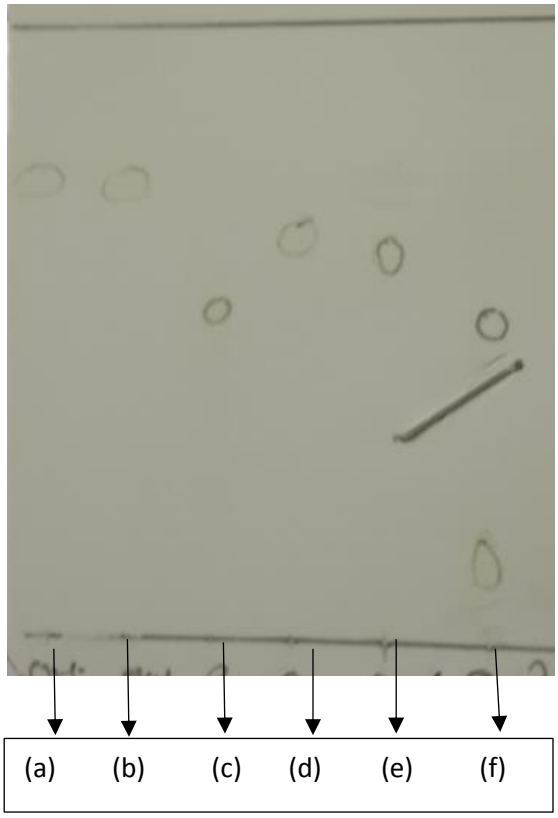


Figure A30. TLC analysis for hydrolysis of **56c** and **66** (40% EtOAc/Hexane); *(a) Standard starting material **54c**. (b) Standard starting material **54d**. (c) Standard starting material **56c**. (d) Reaction for hydrolysis of **54c**. (e) Reaction for hydrolysis of **54d**. (f) Reaction for hydrolysis of **56c**.*

Display Report

Analysis Info

Acquisition Date 09/Nov/2017 H20:26:17 P M

Analysis Name I:\MY DOCUMENTS ONLY\LC-MS\phathu\09-11-2017\PM-91(2)_GA2_01_6288.d
Method Wits HPLC Std MS 50-1300 pos.m
Operator Refilwe Moepya
Sample Name PM-91(2)
Instrument compact 8255754.20116
Comment

AcquisitionParameter

SourceType	ESI	IonPolarity	Positive	SetNebulizer	1.8 Bar
Focus	Not active	SetCapillary	4500 V	Set Dry Heater	220 °C
ScanBegin	50 m/z	Set End Plate Offset	-500 V	Set Dry Gas	9.0l/min
ScanEnd	1300 m/z	SetChargingVoltage	2000 V	Set Divert Valve	Waste
		SetCorona	0 nA	Set APCI Heater	0 °C

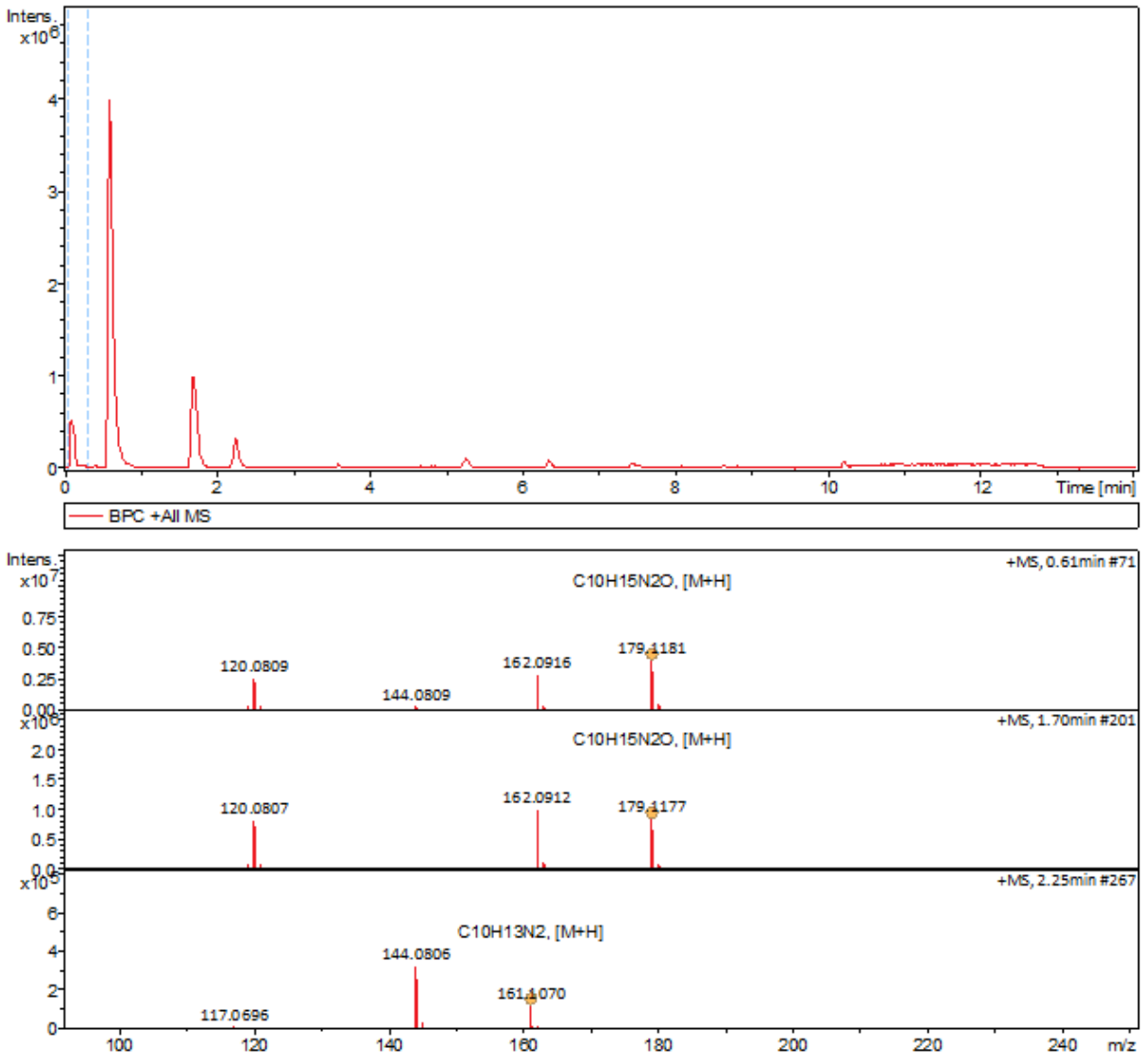


Figure A31. LC-MS analysis for hydrolysis of **56c**

Display Report

Analysis Info

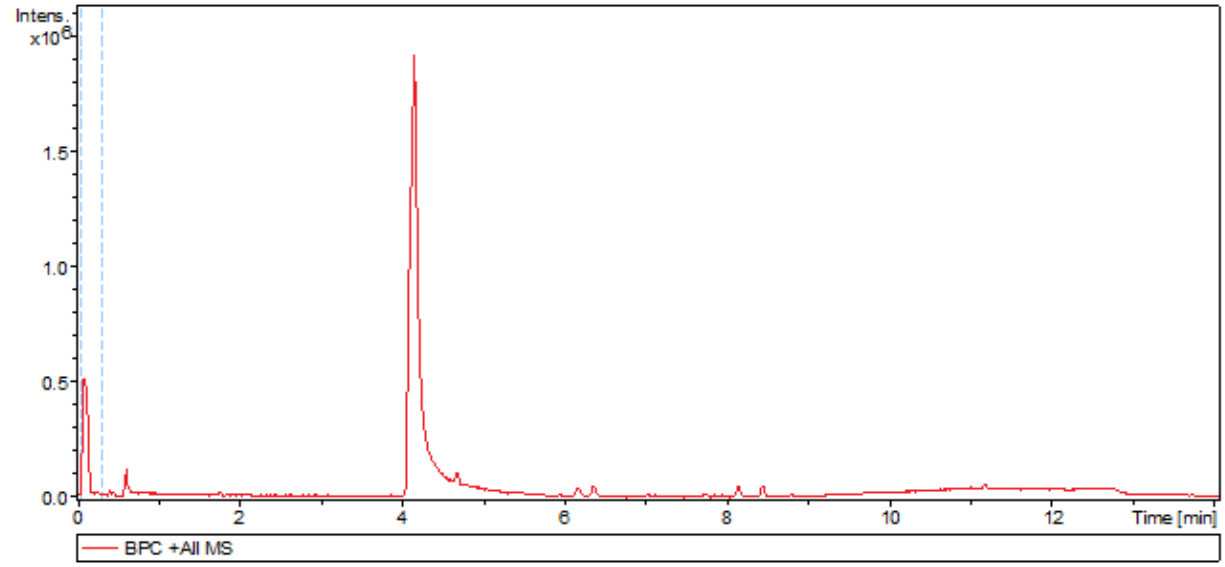
Acquisition Date 09/Nov/2017 H21:25:29 P M

Analysis Name I:\MY DOCUMENTS ONLY\LC-MS\phathu\09-11-2017\PM-91_GA4_01_6292.d
Method Wits HPLC Std MS 50-1300 pos.m
Sample Name PM-91
Comment

Operator Refilwe Moepya
Instrument compact 8255754.20116

AcquisitionParameter

SourceType	ESI	IonPolarity	Positive	SetNebulizer	1.8 Bar
Focus	Not active	SetCapillary	4500 V	Set Dry Heater	220 °C
ScanBegin	50 m/z	Set End Plate Offset	-500 V	Set Dry Gas	9.0 l/min
ScanEnd	1300 m/z	SetChargingVoltage	2000 V	Set Divert Valve	Waste
		SetCorona	0 nA	Set APCI Heater	0 °C



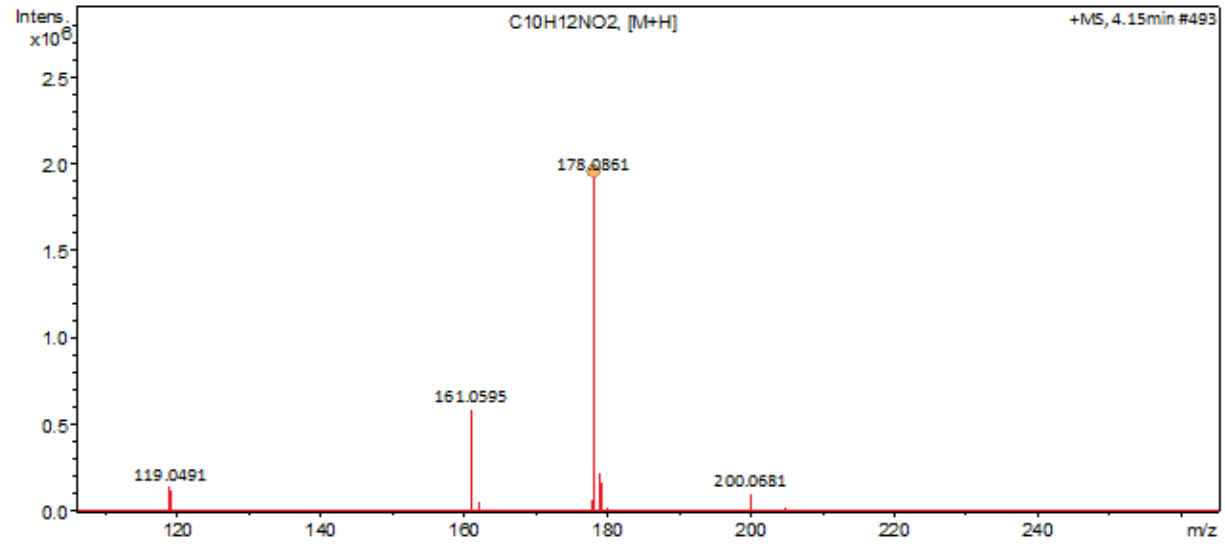


Figure A32. LC-MS analysis for hydrolysis of **54c**

Display Report

Analysis Info

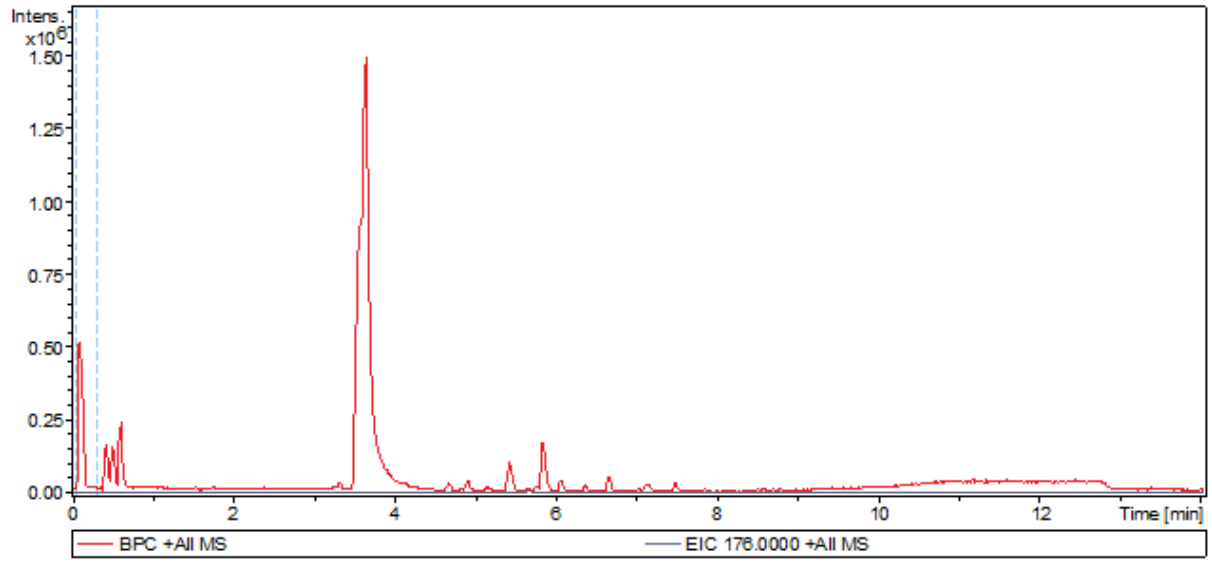
Acquisition Date 09/Nov/2017 H20:55:51 P M

Analysis Name I:\MY DOCUMENTS ONLY\LC-MS\phathu\09-11-2017\PM-91(1)_GA3_01_6290.d
Method Wits HPLC Std MS 50-1300 pos.m
Sample Name PM-91(1)
Comment

Operator Refilwe Moepya
Instrument compact 8255754.20116

AcquisitionParameter

SourceType	ESI	IonPolarity	Positive	SetNebulizer	1.8 Bar
Focus	Not active	SetCapillary	4500 V	Set Dry Heater	220 °C
ScanBegin	50 m/z	Set End Plate Offset	-500 V	Set Dry Gas	9.0l/min
ScanEnd	1300 m/z	SetChargingVoltage	2000 V	SetDivertValve	Waste
		SetCorona	0 nA	Set APCI Heater	0 °C



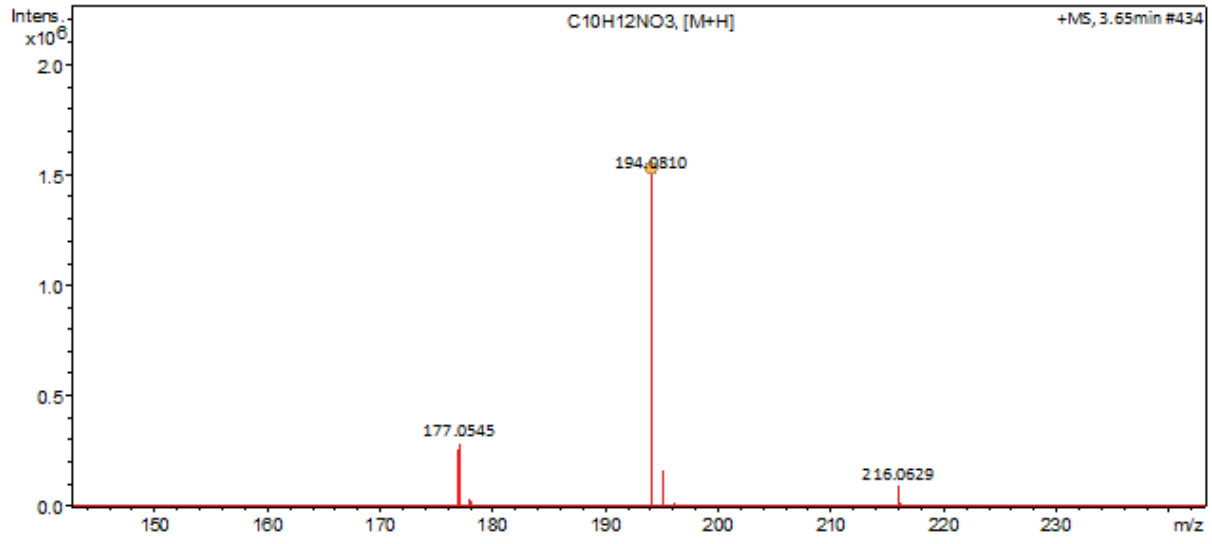


Figure A33. LC-MS of hydrolysis of **54d**

Analytical data for the compounds involved in the synthesis of α-peptide

Display Report

Analysis Info

Acquisition Date 12/Apr/2018 H05:03:31 AM

Analysis Name I:\MY DOCUMENTS ONLY\LC-MS\11-04-2018\G-F-O DILLUTED_GA7_01_9008.d

Method Wits HPLC Std MS 50-1300 pos.m

Operator Refilwe Moepya

Sample Name G-F-O DILLUTED

Instrument compact 8255754.20116

Comment

AcquisitionParameter

SourceType	ESI	IonPolarity	Positive	SetNebulizer	1.8 Bar
Focus	Not active	SetCapillary	4500 V	Set Dry Heater	220 °C
ScanBegin	50 m/z	Set End Plate Offset	-500 V	Set Dry Gas	9.0l/min
ScanEnd	1300 m/z	SetChargingVoltage	2000 V	Set Divert Valve	Waste
		SetCorona	0 nA	Set APCI Heater	0 °C

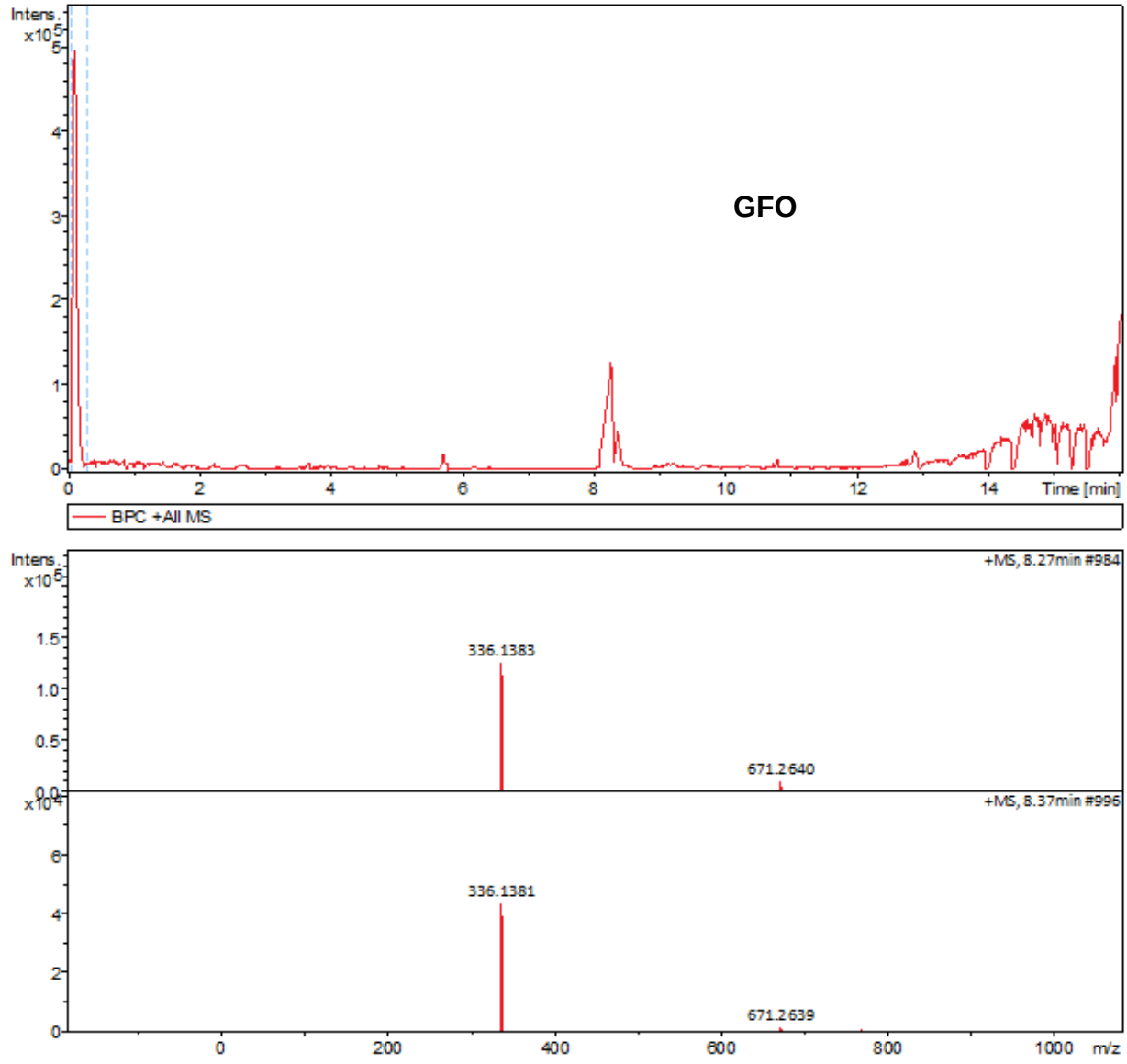


Figure A34. LC-MS analysis of GFO

Display Report

Analysis Info

Acquisition Date 12/Apr/2018 H06:13:16 AM

Analysis Name I:\MY DOCUMENTS ONLY\LC-MS\11-04-2018\G-F-O-G_GB2_01_9012.d

Method Wits HPLC Std MS 50-1300 pos.m

Operator Refilwe Moepya

Sample Name G-F-O-G

Instrument compact 8255754.20116

Comment

AcquisitionParameter

SourceType	ESI	IonPolarity	Positive	SetNebulizer	1.8 Bar
Focus	Not active	SetCapillary	4500 V	Set Dry Heater	220 °C
ScanBegin	50 m/z	Set End Plate Offset	-500 V	Set Dry Gas	9.0 l/min
ScanEnd	1300 m/z	SetChargingVoltage	2000 V	SetDivertValve	Waste
		SetCorona	0 nA	Set APCI Heater	0 °C

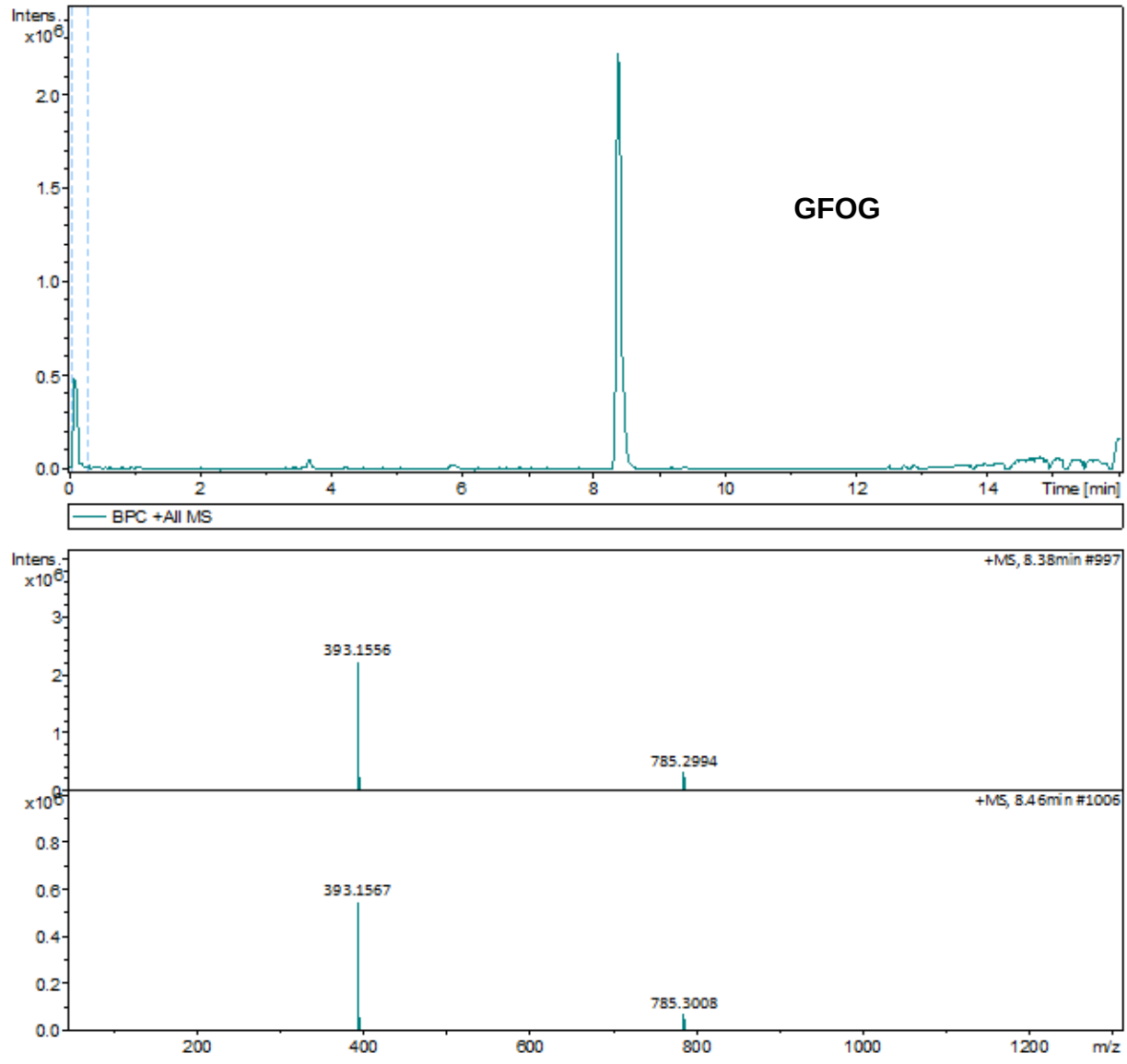


Figure A35. LC-MS analysis of GFOG

Display Report

Analysis Info

Analysis Name I:\MY DOCUMENTS ONLY\LC-MS\Peptides\G-F-O-G-R AD_RA7_01_8471.d
Method Wits HPLC Std MS 50-1300 pos.m
Sample Name G-F-O-G-R AD
Comment

Acquisition Date 13/Mar/2018 H13:49:15 PM
Operator Refilwe Moepya
Instrument compact 8255754.20116

AcquisitionParameter

SourceType	ESI	IonPolarity	Positive	SetNebulizer	1.8 Bar
Focus	Not active	SetCapillary	4500 V	Set Dry Heater	220 °C
ScanBegin	50 m/z	Set End Plate Offset	-500 V	Set Dry Gas	9.0 l/min
ScanEnd	1300 m/z	SetChargingVoltage	2000 V	Set Divert Valve	Waste
		SetCorona	0 nA	Set APCI Heater	0 °C

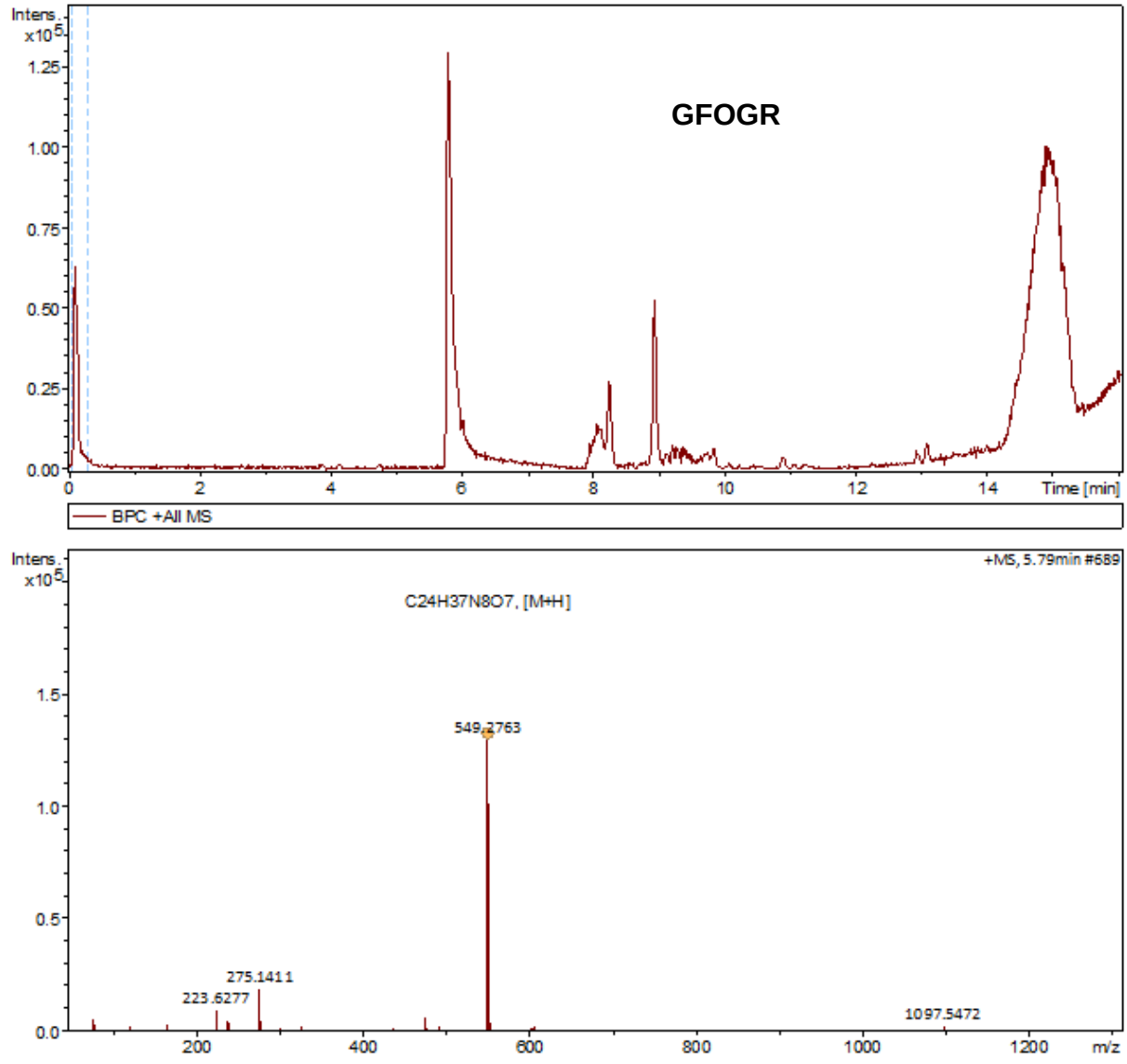


Figure A36. LC-MS analysis of GFOGR

Display Report

Analysis Info

Analysis Name	I:\MY DOCUMENTS ONLY\LC-MS\11-04-2018\G-F-O-G-R-G corr_GA3_01_8994.d	Acquisition Date	11/Apr/2018 H23:03:47 PM
Method	Wits HPLC Std MS 50-1300 pos.m	Operator	Refilwe Moepya
Sample Name	G-F-O-G-R-G corr	Instrument	compact 8255754.20116
Comment			

AcquisitionParameter

SourceType	ESI	IonPolarity	Positive	SetNebulizer	1.8 Bar
Focus	Not active	SetCapillary	4500 V	Set Dry Heater	220 °C
ScanBegin	50 m/z	Set End Plate Offset	-500 V	Set Dry Gas	9.0 l/min
ScanEnd	1300 m/z	SetChargingVoltage	2000 V	Set Divert Valve	Waste
		SetCorona	0 nA	Set APCI Heater	0 °C

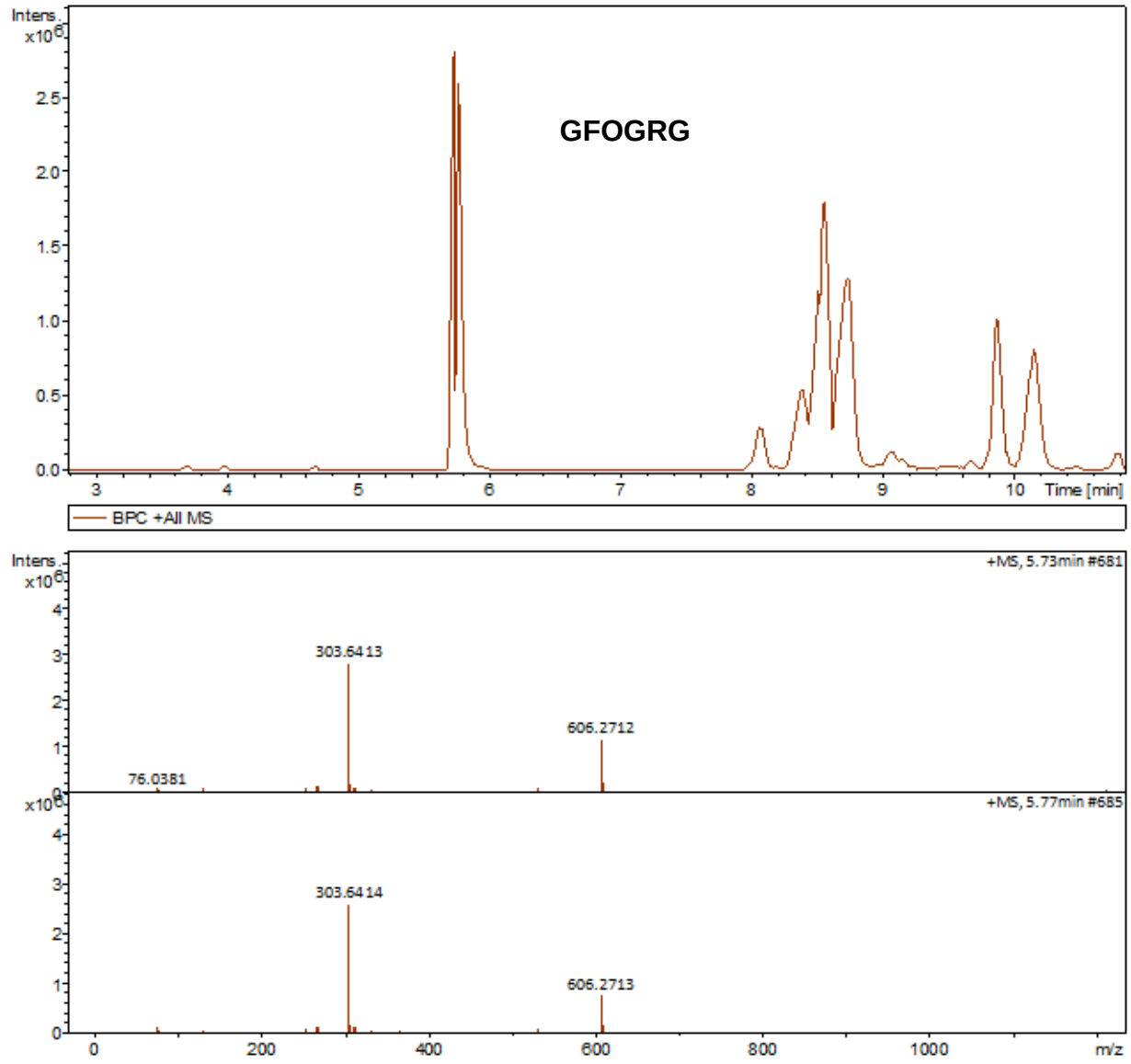


Figure A37. LC-MS analysis for GFOGRG

Display Report

Analysis Info

Acquisition Date 12/Apr/2018 H10:43:18 AM

Analysis Name I:\MY DOCUMENTS ONLY\LC-MS\11-04-2018\FULL PEP_GB5_01_9027.d

Method Wits HPLC Std MS 50-1300 pos.m

Operator Refilwe Moepya

Sample Name FULL PEP

Instrument compact 8255754.20116

Comment

AcquisitionParameter

SourceType	ESI	IonPolarity	Positive	SetNebulizer	1.8 Bar
Focus	Not active	SetCapillary	4500 V	Set Dry Heater	220 °C
ScanBegin	50 m/z	Set End Plate Offset	-500 V	Set Dry Gas	9.0 l/min
ScanEnd	1300 m/z	SetChargingVoltage	2000 V	Set Divert Valve	Waste
		SetCorona	0 nA	Set APCI Heater	0 °C

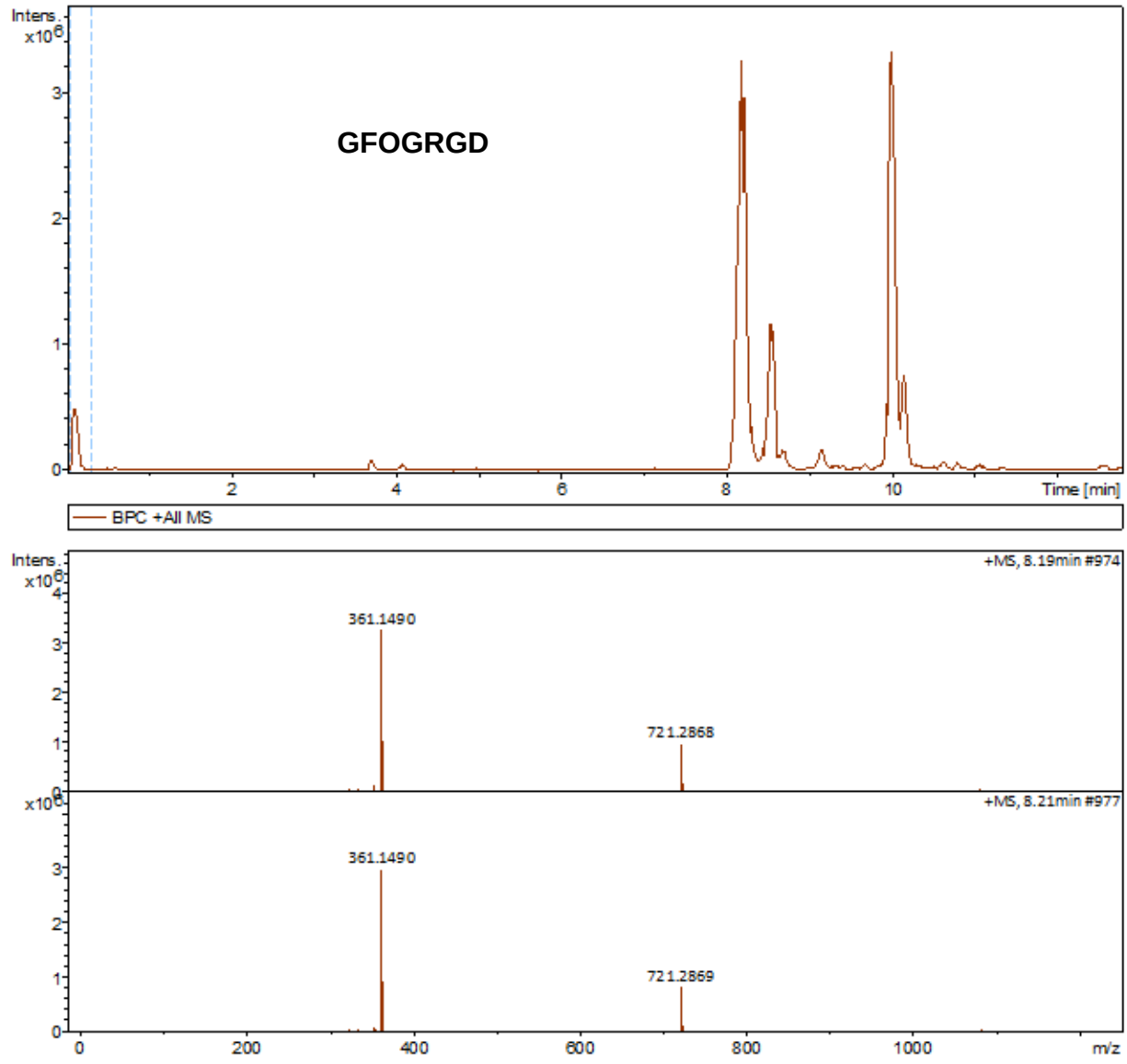


Figure A38. LC-MS analysis of GFOGRGD

Display Report

Analysis Info

Acquisition Date 11/Aug/2018 H22:14:12 P M

Analysis Name I:\MY DOCUMENTS ONLY\LC-MS\25-12-2018\R11 V14_GC2_01_12165.d

Method Wits HPLC Std MS 50-1300 pos.m

Operator Thapelo Mbhele

Sample Name R11 V14

Instrument compact 8255754.20116

Comment

AcquisitionParameter

SourceType	ESI	IonPolarity	Positive	SetNebulizer	1.8 Bar
Focus	Not active	SetCapillary	4500 V	Set Dry Heater	220 °C
ScanBegin	50 m/z	Set End Plate Offset	-500 V	Set Dry Gas	9.0 l/min
ScanEnd	1300 m/z	SetChargingVoltage	2000 V	SetDivertValve	Waste
		SetCorona	0 nA	Set APCI Heater	0 °C

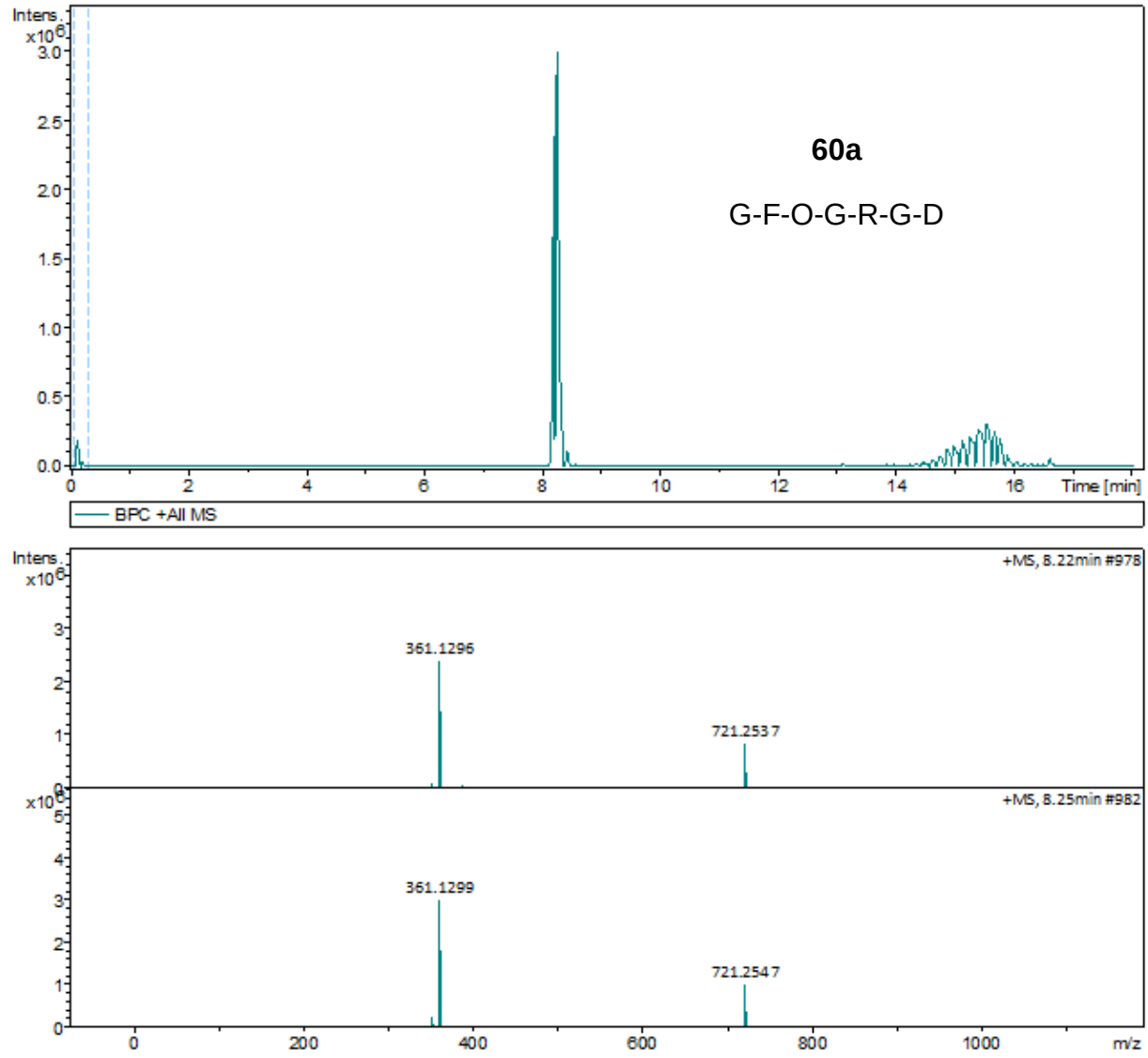


Figure A39. LC-MS analysis of **60a**

Display Report

Analysis Info

Acquisition Date 14/Jun/2018 H01:42:32 AM

Analysis Name I:\MY DOCUMENTS ONLY\LC-MS\11-02-2019\Direct runs 13-06-2018\NH2-PAL.d

Method DI Std MS 50-1300 pos.m

Operator Refilwe Moepya

Sample Name NH2-PAL

Instrument compact 8255754.20116

Comment

AcquisitionParameter

SourceType	ESI	IonPolarity	Positive	SetNebulizer	0.4 Bar
Focus	Not active	SetCapillary	4500 V	Set Dry Heater	180 °C
ScanBegin	50 m/z	Set End Plate Offset	-500 V	Set Dry Gas	4.0 l/min
ScanEnd	1300 m/z	SetChargingVoltage	2000 V	Set Divert Valve	Source
		SetCorona	0 nA	Set APCI Heater	0 °C

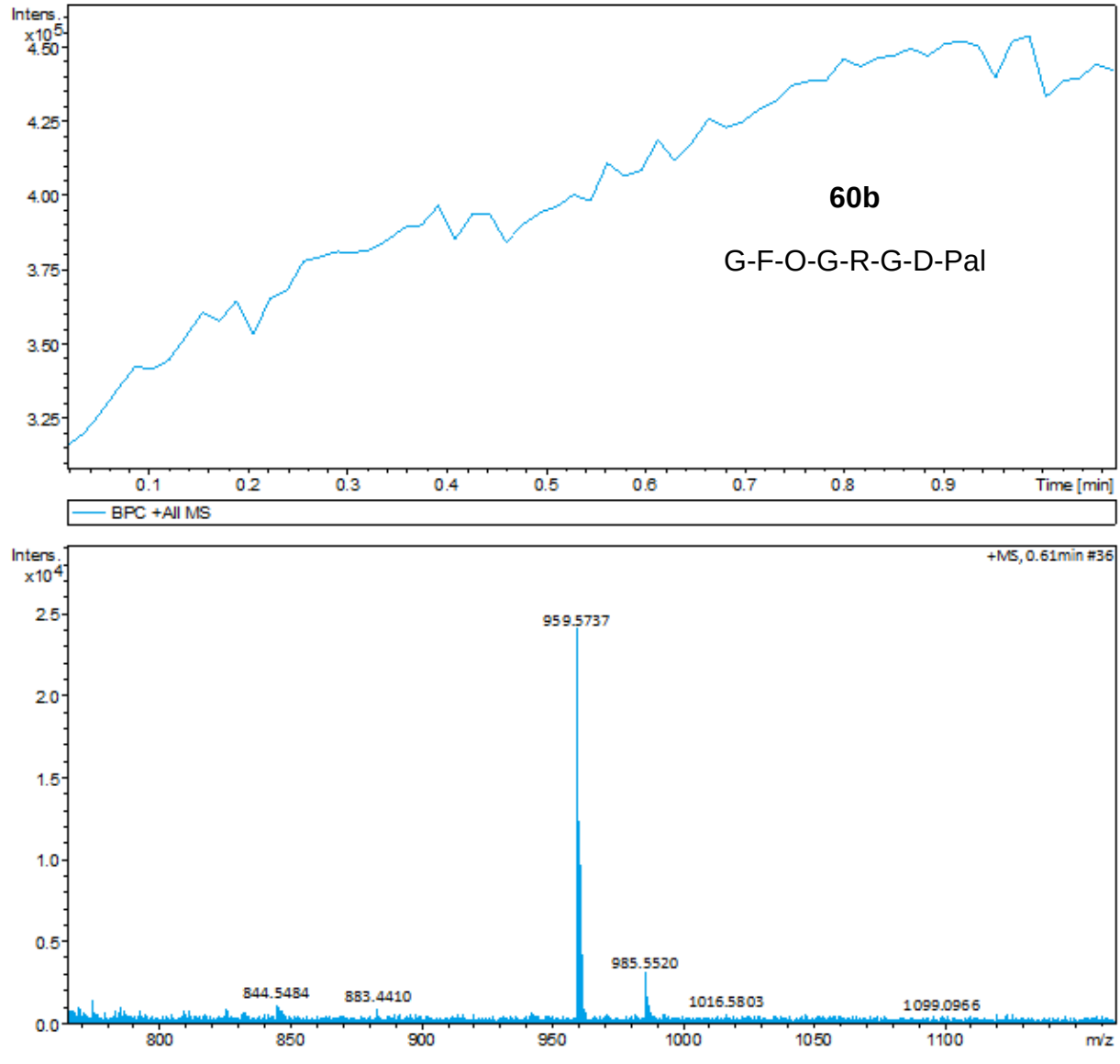


Figure A40. LC-MS analysis of GFOGRGD-Pal **60b**

Display Report

Analysis Info

Acquisition Date 23/Dec/2018 H20:39:26 P M

Analysis Name I:\MY DOCUMENTS ONLY\LC-MS\25-12-2018\Phathus\23-12-2018\ALPHA-ADA_RD8_01_18563.d

Method Wits HPLC high MS 100-3000 pos.m

Operator Thapelo Mbhele

Sample Name ALPHA-ADA

Instrument compact 8255754.20116

Comment

AcquisitionParameter

SourceType	ESI	IonPolarity	Positive	SetNebulizer	1.8 Bar
Focus	Not active	SetCapillary	4500 V	Set Dry Heater	220 °C
ScanBegin	100 m/z	Set End Plate Offset	-500 V	Set Dry Gas	9.0l/min
ScanEnd	3000 m/z	SetChargingVoltage	2000 V	Set Divert Valve	Waste
		SetCorona	0 nA	Set APCI Heater	0 °C

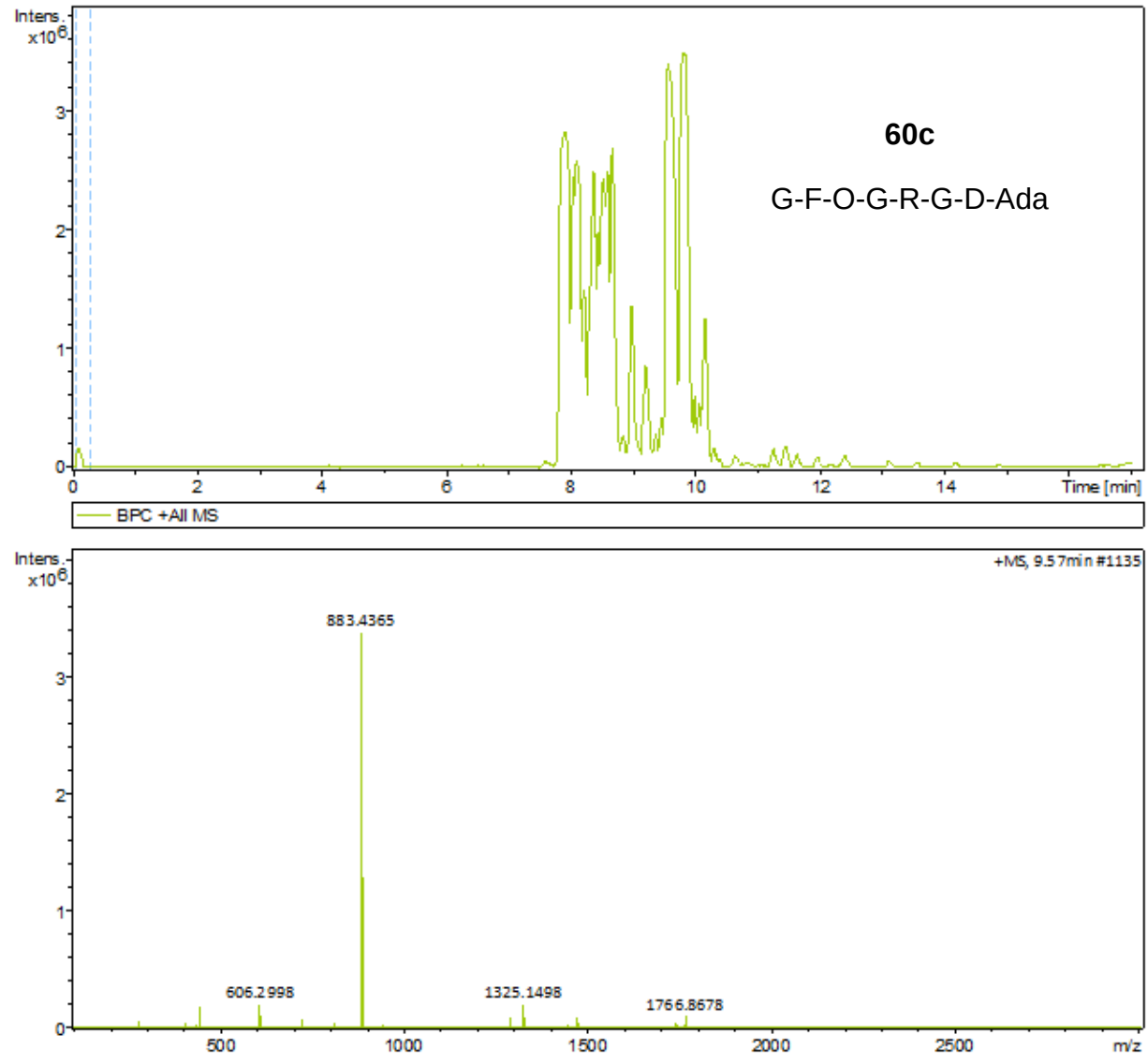


Figure A41. LC-MS analysis for GFOGRGD-Ada **60c**

Analytical data for the compounds involved in the synthesis of β-peptide

Display Report

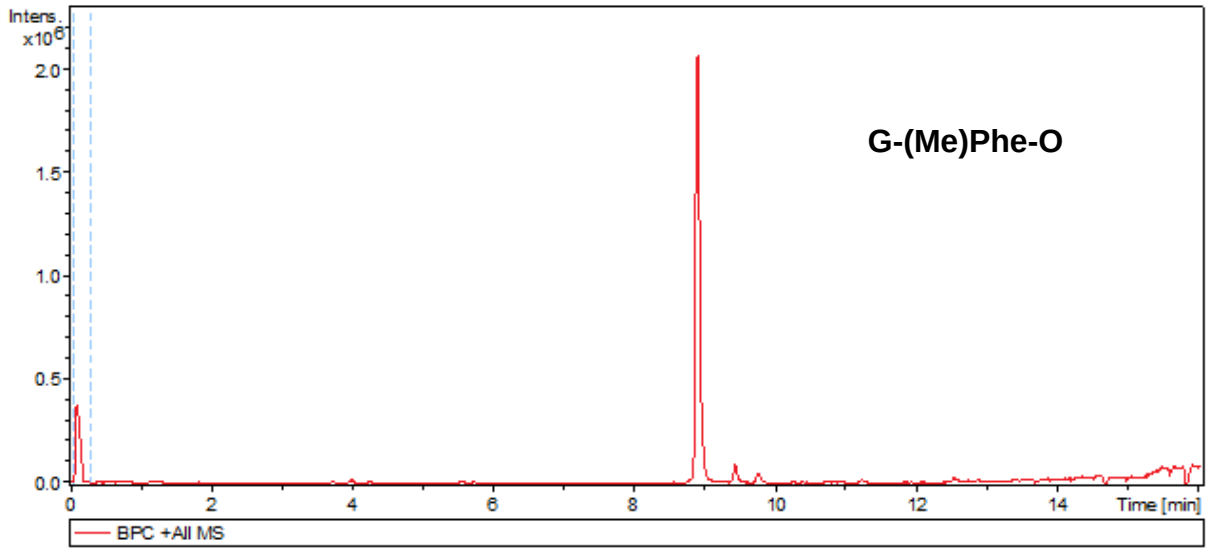
Analysis Info

Acquisition Date 30/May/2018 H15:23:26 P M

Analysis Name I:\MY DOCUMENTS ONLY\LC-MS\11-02-2019\30-05-2018\beta-CH3-O_RA4_01_9775.d
Method Wits HPLC Std MS 50-1300 pos.m
Operator Refilwe Moepya
Sample Name beta-CH3-O
Instrument compact 8255754.20116
Comment

AcquisitionParameter

SourceType	ESI	IonPolarity	Positive	SetNebulizer	1.8 Bar
Focus	Not active	SetCapillary	4500 V	Set Dry Heater	220 °C
ScanBegin	50 m/z	Set End Plate Offset	-500 V	Set Dry Gas	9.0 l/min
ScanEnd	1300 m/z	SetChargingVoltage	2000 V	Set Divert Valve	Waste
		SetCorona	0 nA	Set APCI Heater	0 °C



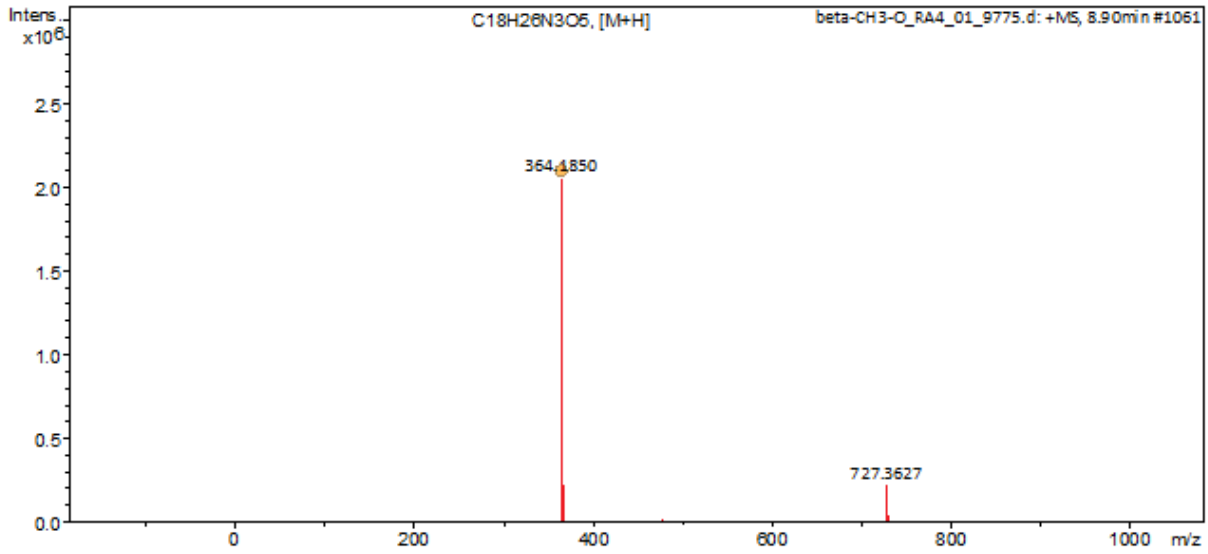


Figure A42. HMRS analysis for G-(Me)Phe-O

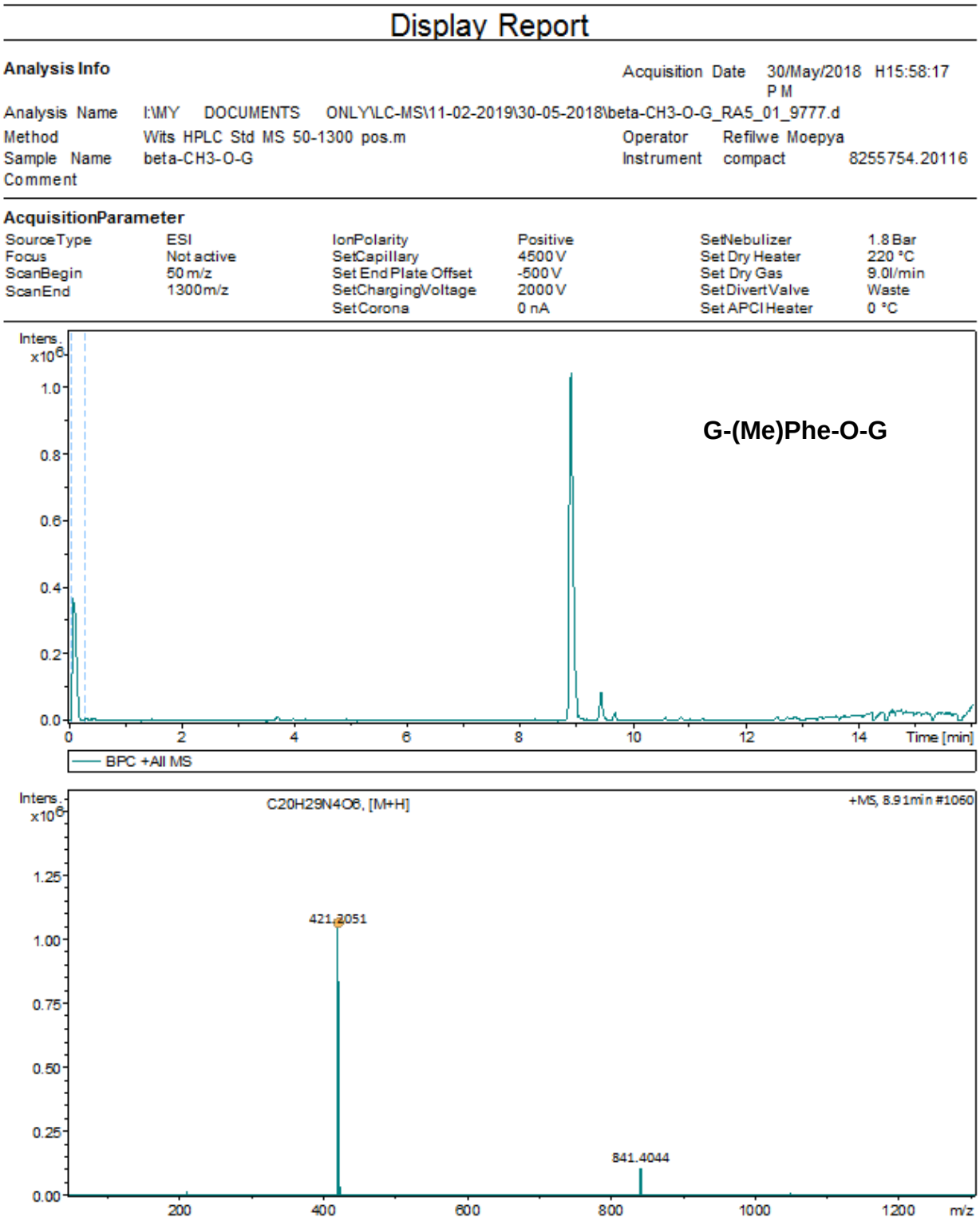


Figure A43. LC-MS analysis for G-(Me)Phe-O-G

Display Report

Analysis Info

Acquisition Date 30/May/2018 H20:37:24 P M

Analysis Name I:\MY DOCUMENTS ONLY\LC-MS\11-02-2019\30-05-2018\Beta-CH3---G-R_RB2_01_9793.d

Method Wits HPLC Std MS 50-1300 pos.m

Operator Refilwe Moepya

Sample Name Beta-CH3---G-R

Instrument compact 8255754.20116

Comment

AcquisitionParameter

SourceType	ESI	IonPolarity	Positive	SetNebulizer	1.8 Bar
Focus	Not active	SetCapillary	4500 V	Set Dry Heater	220 °C
ScanBegin	50 m/z	Set End Plate Offset	-500 V	Set Dry Gas	9.0 l/min
ScanEnd	1300 m/z	SetChargingVoltage	2000 V	Set Divert Valve	Waste
		SetCorona	0 nA	Set APCI Heater	0 °C

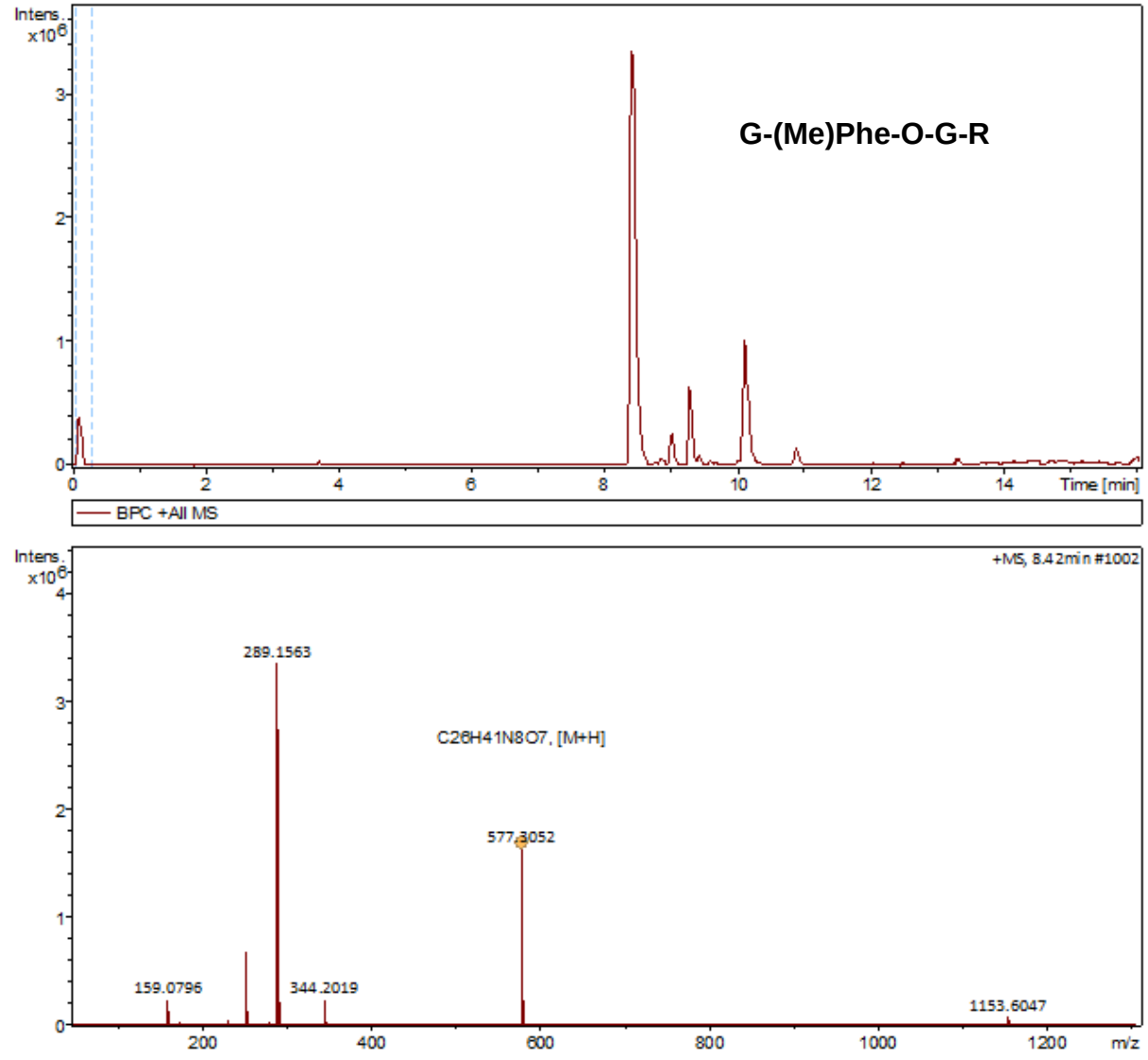


Figure A44. LC-MS analysis for G-(Me)Phe-O-G-R

Display Report

Analysis Info

Acquisition Date 30/May/2018 H21:12:20 P M

Analysis Name I:\MY DOCUMENTS ONLY\LC-MS\11-02-2019\30-05-2018\Beta-CH3---G-R-G_RB3_01_9795.d

Method Wits HPLC Std MS 50-1300 pos.m

Operator Refilwe Moepya

Sample Name Beta-CH3---G-R-G

Instrument compact 8255754.20116

Comment

AcquisitionParameter

SourceType	ESI	IonPolarity	Positive	SetNebulizer	1.8 Bar
Focus	Not active	SetCapillary	4500 V	Set Dry Heater	220 °C
ScanBegin	50 m/z	Set End Plate Offset	-500 V	Set Dry Gas	9.0 l/min
ScanEnd	1300 m/z	SetChargingVoltage	2000 V	Set Divert Valve	Waste
		SetCorona	0 nA	Set APCI Heater	0 °C

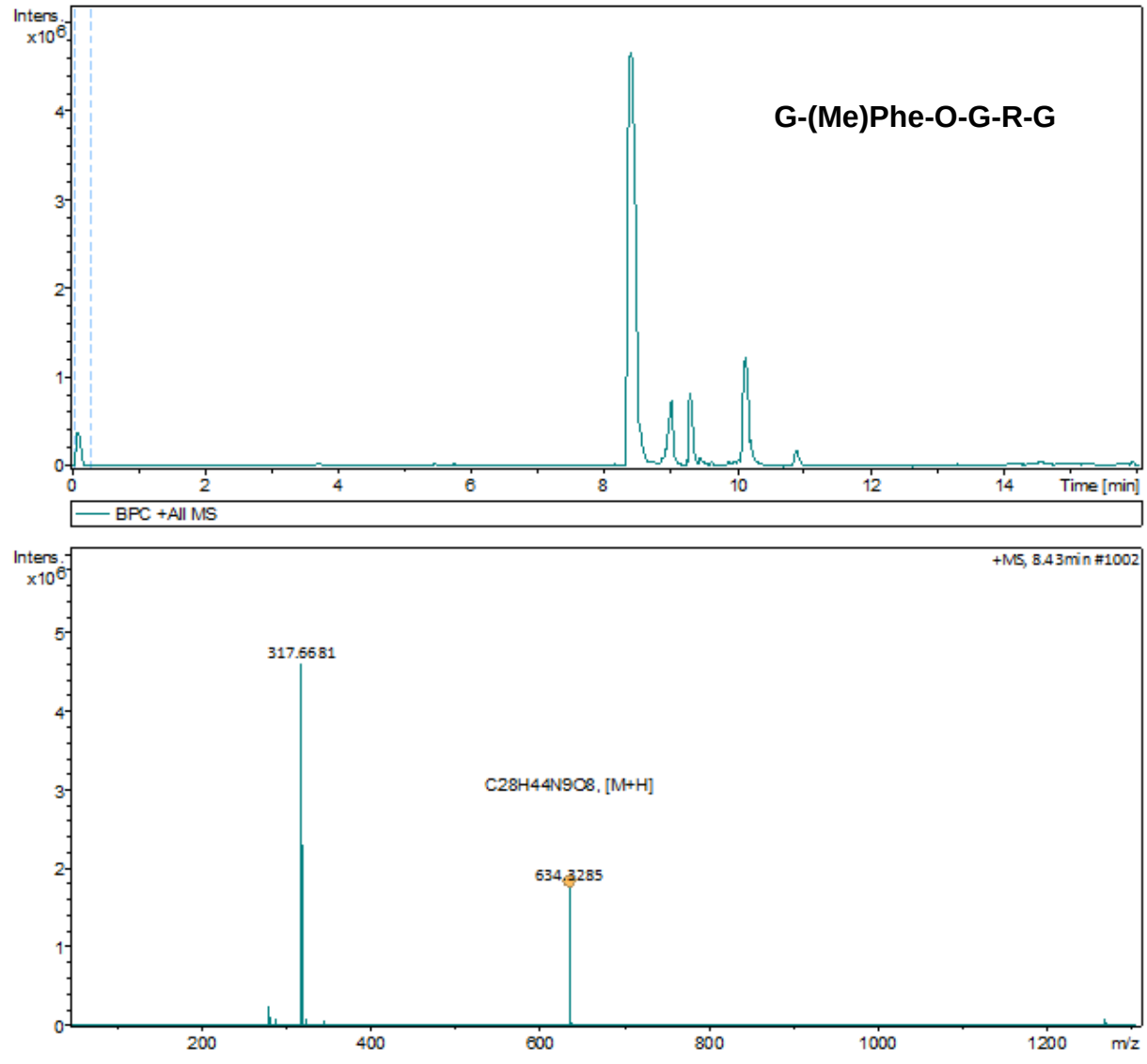


Figure A45. LC-MS analysis for G-(Me)Phe-O-G-R-G

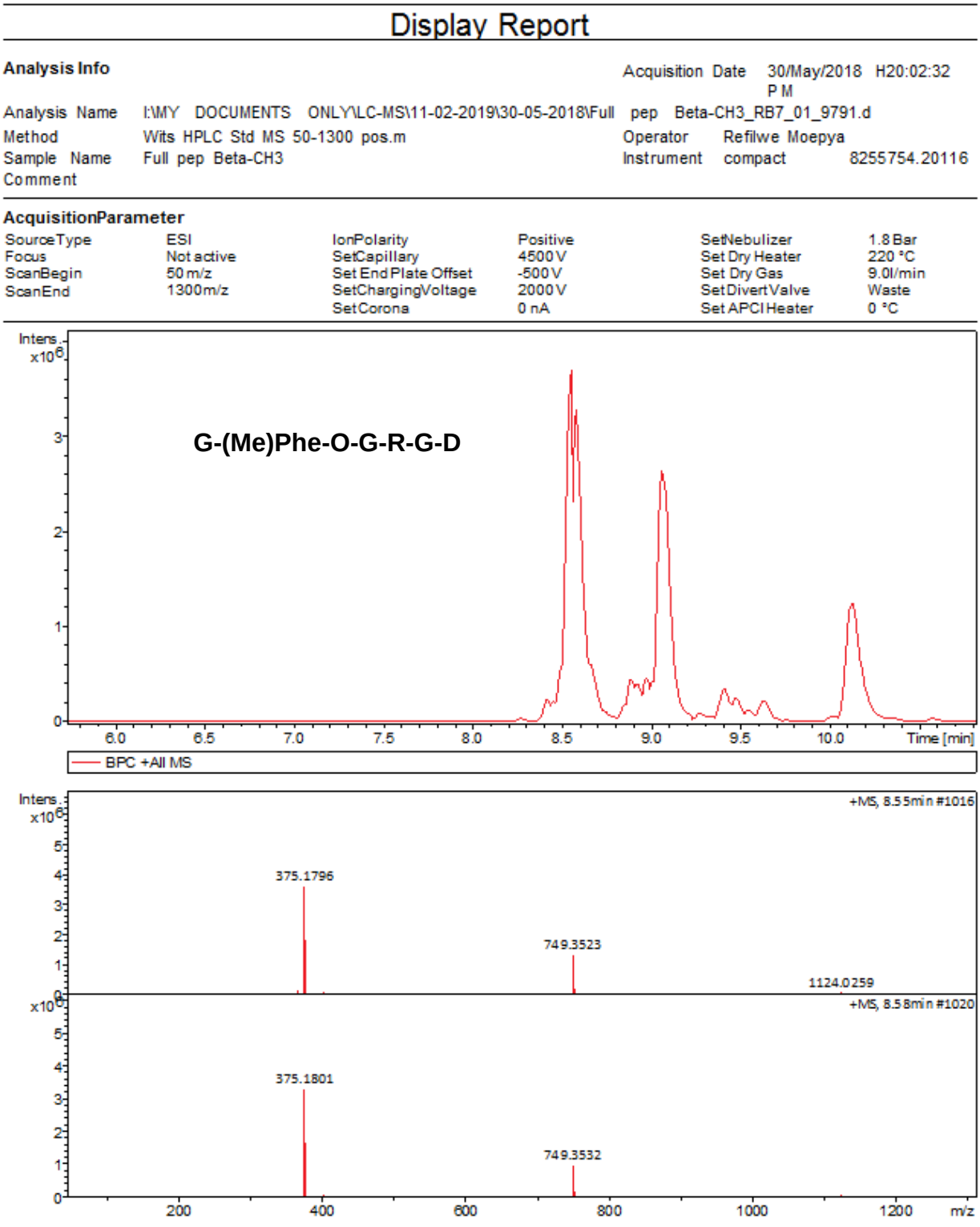


Figure A46. LC-MS analysis for G-(Me)Phe-O-G-R-G-D

Display Report

Analysis Info

Analysis Name	I:\MY DOCUMENTS ONLY\LC-MS\lc-ms 22-01-2019\V42 Phe-Nh2_RC2_01_19131.d	Acquisition Date	22/Jan/2019 H10:30:55 AM
Method	Wits HPLC high MS 100-3000 pos.m	Operator	Thapelo Mbhele
Sample Name	V42 Phe-Nh2	Instrument	compact 8255754.20116
Comment			

AcquisitionParameter

SourceType	ESI	IonPolarity	Positive	SetNebulizer	1.8 Bar
Focus	Not active	SetCapillary	4500 V	Set Dry Heater	220 °C
ScanBegin	100 m/z	Set End Plate Offset	-500 V	Set Dry Gas	9.0 l/min
ScanEnd	3000 m/z	SetChargingVoltage	2000 V	SetDivertValve	Waste
		SetCorona	0 nA	Set APCI Heater	0 °C

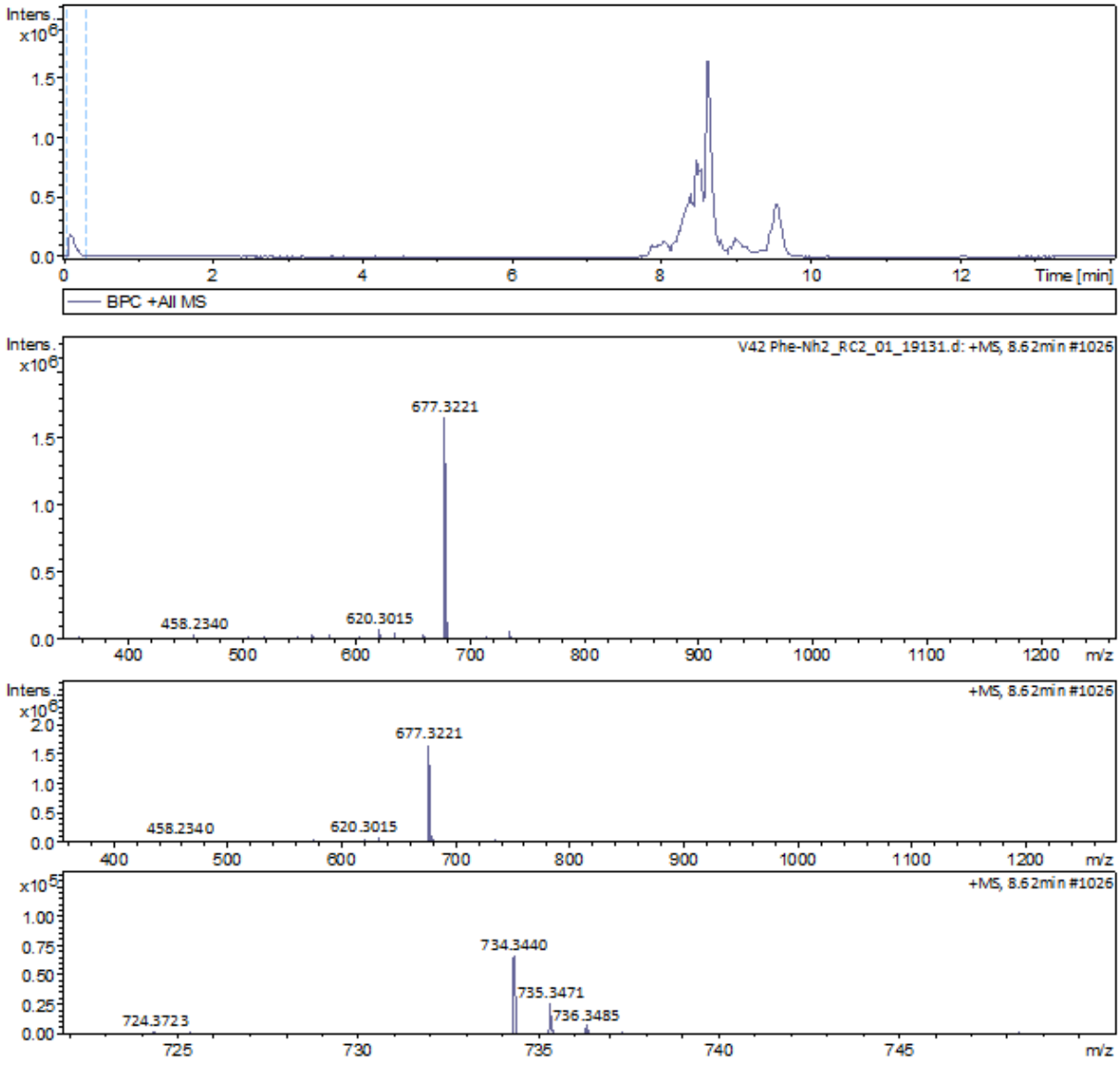


Figure A47. HRSM analysis for **61a**

Display Report

Analysis Info

Acquisition Date 23/Jan/2019 H18:15:05 PM

Analysis Name I:\MY DOCUMENTS ONLY\LC-MS\lc-ms 22-01-2019\V50 PHE-PAL_GD3_01_19227.d

Method Wits HPLC high MS 100-3000 pos.m

Operator Thapelo Mbhele

Sample Name V50 PHE-PAL

Instrument compact 8255754.20116

Comment

AcquisitionParameter

SourceType	ESI	IonPolarity	Positive	SetNebulizer	1.8 Bar
Focus	Not active	SetCapillary	4500 V	Set Dry Heater	220 °C
ScanBegin	100 m/z	Set End Plate Offset	-500 V	Set Dry Gas	9.0 l/min
ScanEnd	3000 m/z	SetChargingVoltage	2000 V	Set Divert Valve	Waste
		SetCorona	0 nA	Set APCI Heater	0 °C

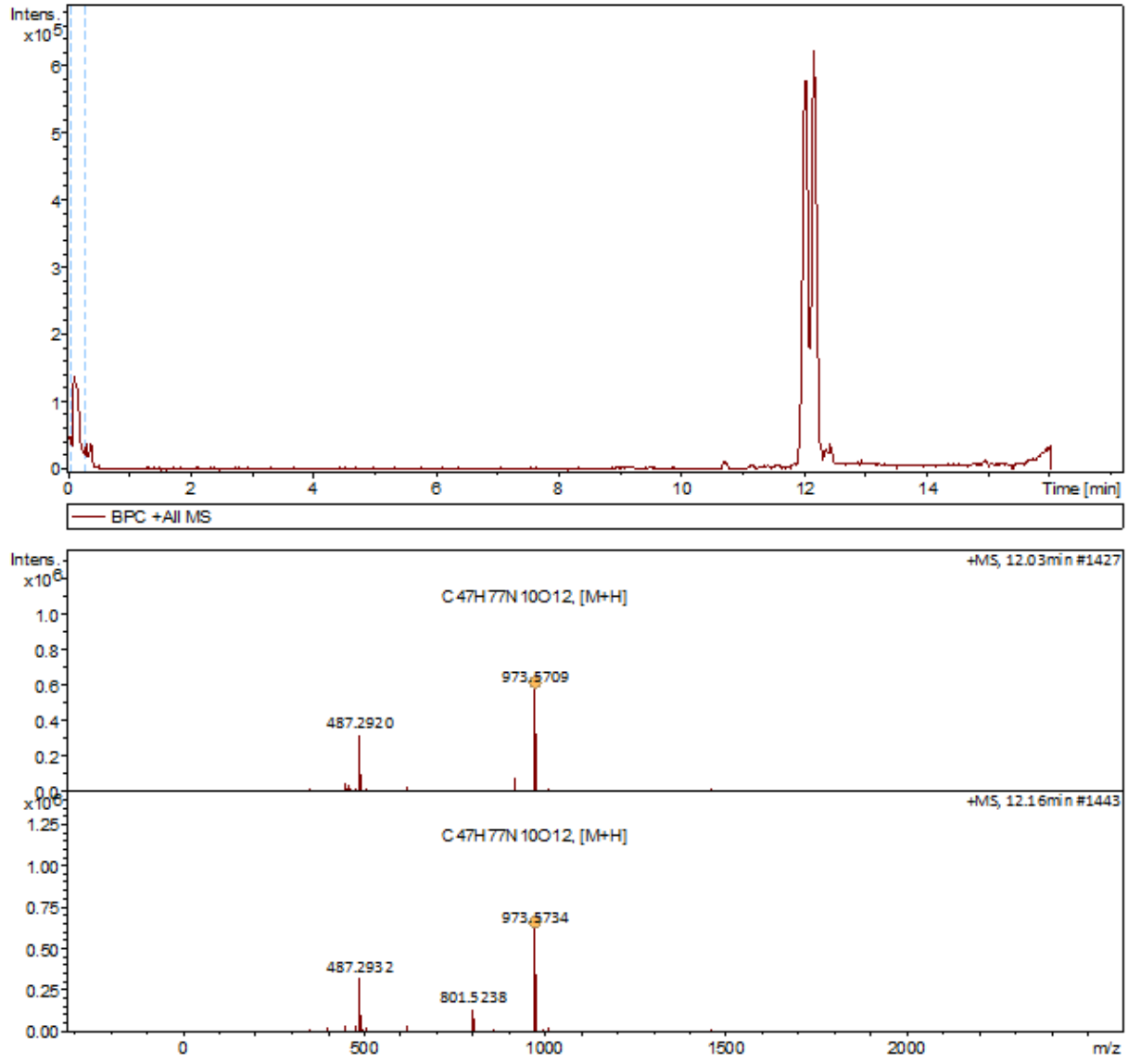


Figure A48. LC-MS analysis for **61b**

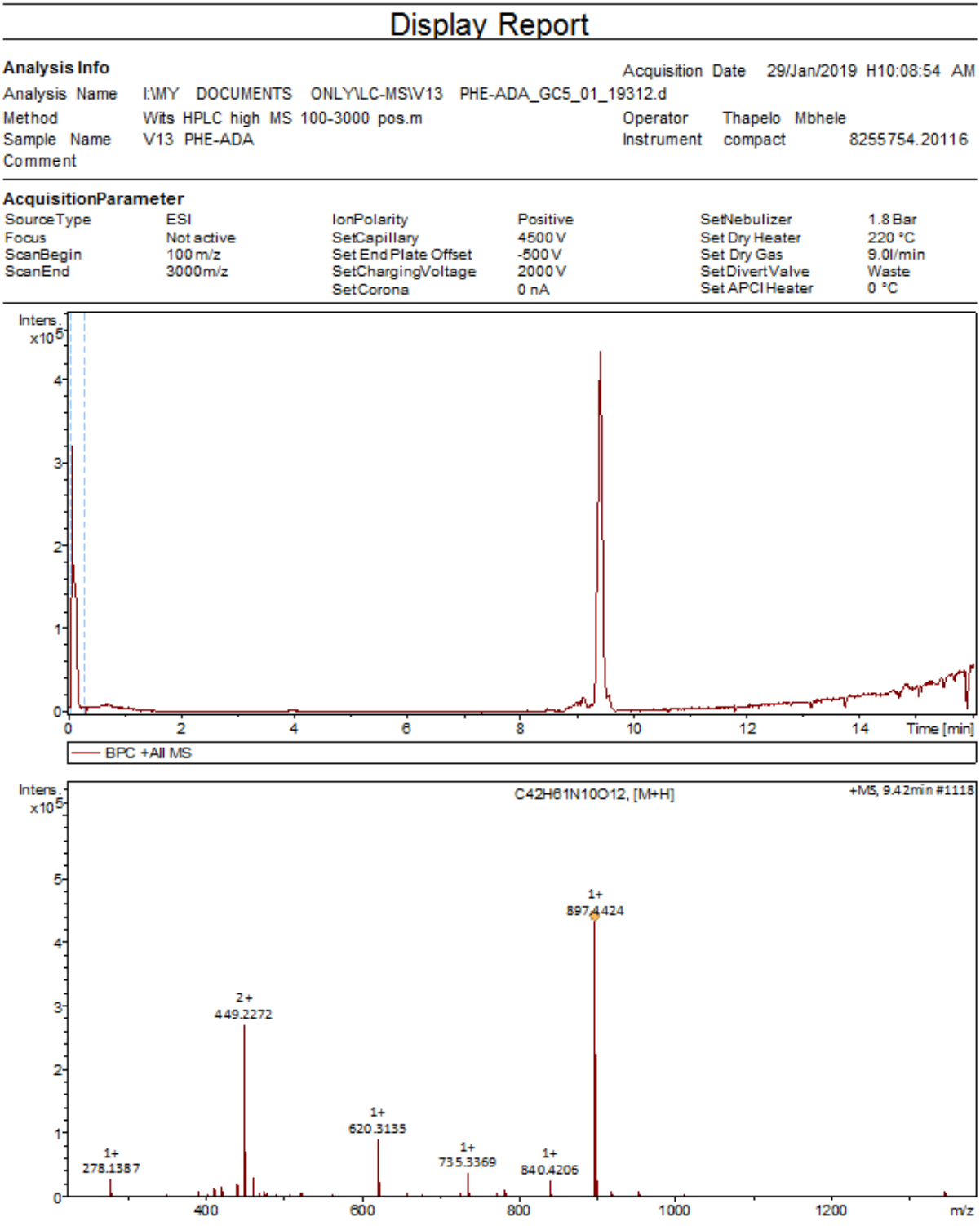


Figure A49. LC-MS analysis for **61c**

Display Report

Analysis Info

Acquisition Date 23/Jan/2019 H05:00:52 AM

Analysis Name I:\MY DOCUMENTS ONLY\LC-MS\lc-ms 22-01-2019\V93 CH3-NH2_RD6_01_19163.d

Method Wits HPLC high MS 100-3000 pos.m

Operator Thapelo Mbhele

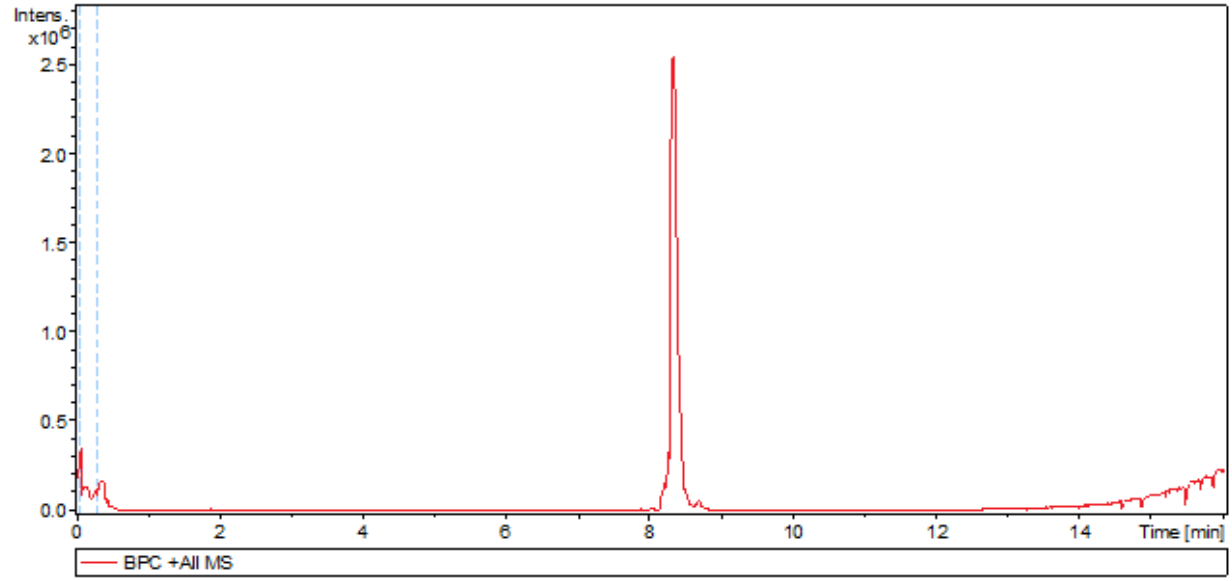
Sample Name V93 CH3-NH2

Instrument compact 8255754.20116

Comment

AcquisitionParameter

SourceType	ESI	IonPolarity	Positive	SetNebulizer	1.8 Bar
Focus	Not active	SetCapillary	4500 V	Set Dry Heater	220 °C
ScanBegin	100 m/z	Set End Plate Offset	-500 V	Set Dry Gas	9.0 l/min
ScanEnd	3000 m/z	SetChargingVoltage	2000 V	Set Divert Valve	Waste
		SetCorona	0 nA	Set APCI Heater	0 °C



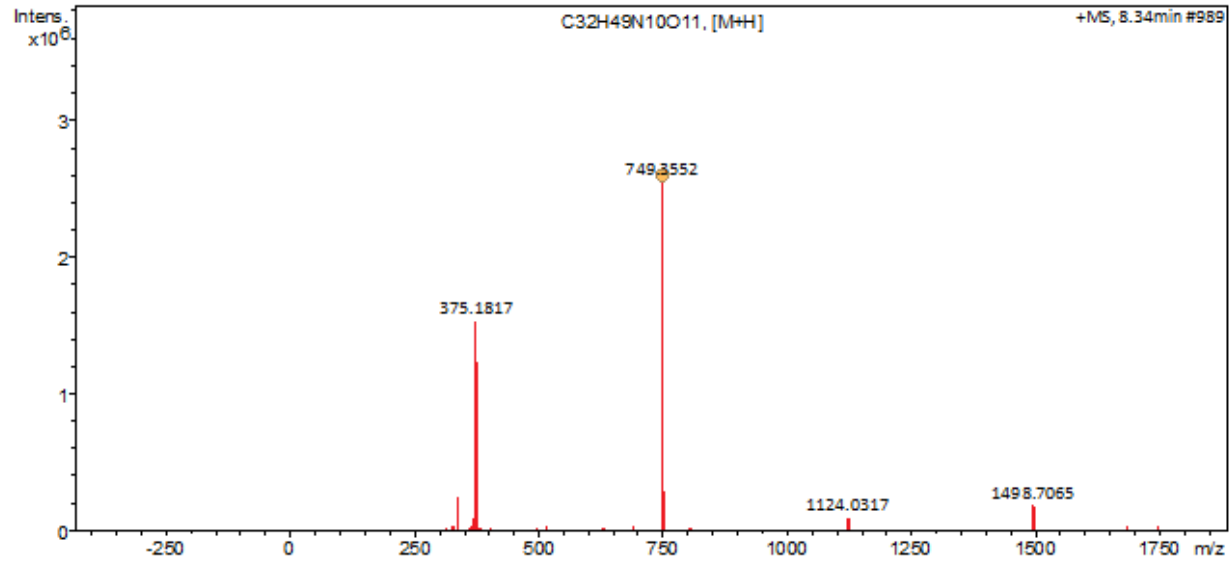


Figure A50. LC-MS analysis of **61d**

Display Report

Analysis Info

Acquisition Date 23/Dec/2018 H19:25:17 P M

Analysis Name I:\MY DOCUMENTS ONLY\LC-MS\25-12-2018\Phathus\23-12-2018\BETA-CH3-PAL_RD6_01_18559.d

Method Wits HPLC high MS 100-3000 pos.m

Operator Thapelo Mbhele

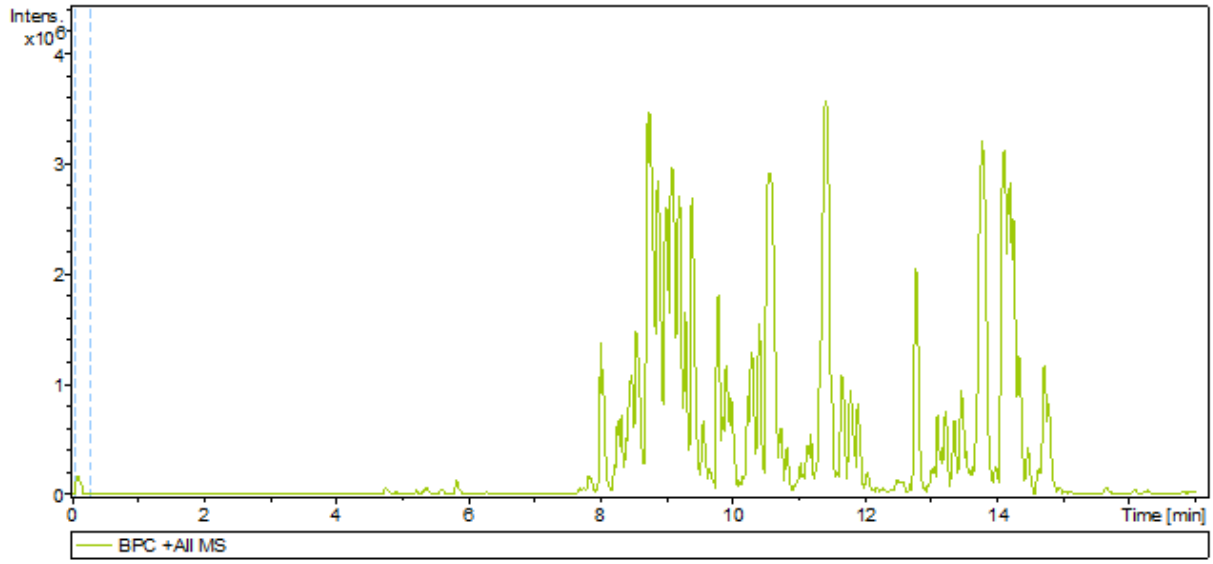
Sample Name BETA-CH3-PAL

Instrument compact 8255754.20116

Comment

AcquisitionParameter

SourceType	ESI	IonPolarity	Positive	SetNebulizer	1.8 Bar
Focus	Not active	SetCapillary	4500 V	Set Dry Heater	220 °C
ScanBegin	100 m/z	Set End Plate Offset	-500 V	Set Dry Gas	9.0 l/min
ScanEnd	3000 m/z	SetChargingVoltage	2000 V	SetDivertValve	Waste
		SetCorona	0 nA	Set APCI Heater	0 °C



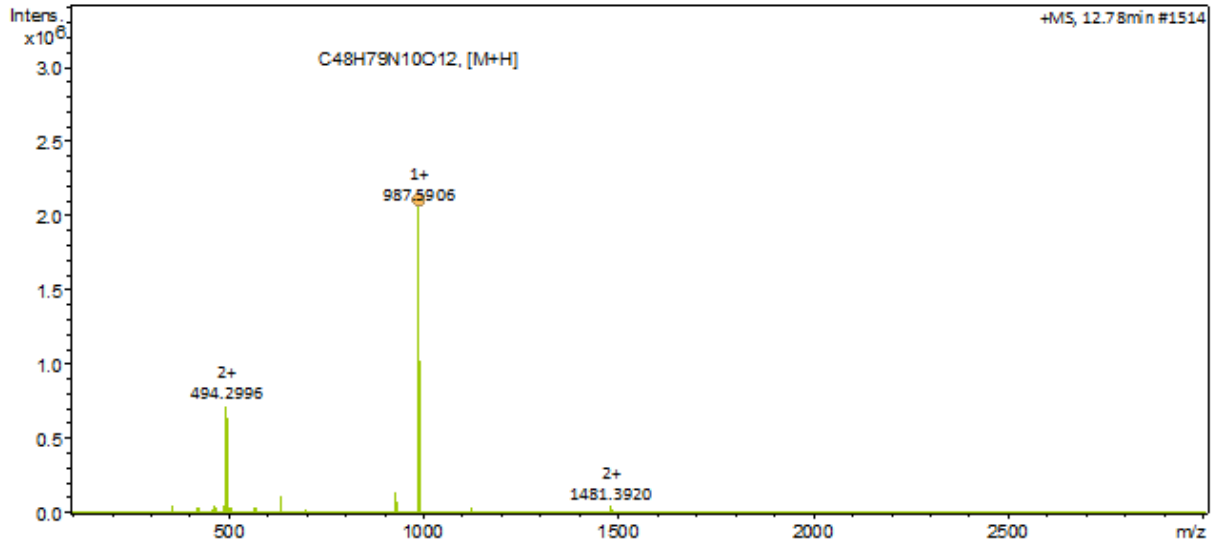


Figure A51. LC-MS analysis of **61e**

Display Report

Analysis Info

Analysis Name I:\MY DOCUMENTS ONLY\LC-MS\25-12-2018\9-10-2018 column\beta-CH3-ADA_GD7_01_15021.d
Method Wits HPLC high MS 100-3000 pos.m
Sample Name beta-CH3-ADA
Comment

Acquisition Date 10/Oct/2018 H07:23:13 AM
Operator Thapelo Mbhele
Instrument compact 8255754.20116

AcquisitionParameter

SourceType	ESI	IonPolarity	Positive	SetNebulizer	1.8 Bar
Focus	Not active	SetCapillary	4500 V	Set Dry Heater	220 °C
ScanBegin	100 m/z	Set End Plate Offset	-500 V	Set Dry Gas	9.0 l/min
ScanEnd	3000 m/z	SetChargingVoltage	2000 V	Set Divert Valve	Waste
		SetCorona	0 nA	Set APCI Heater	0 °C

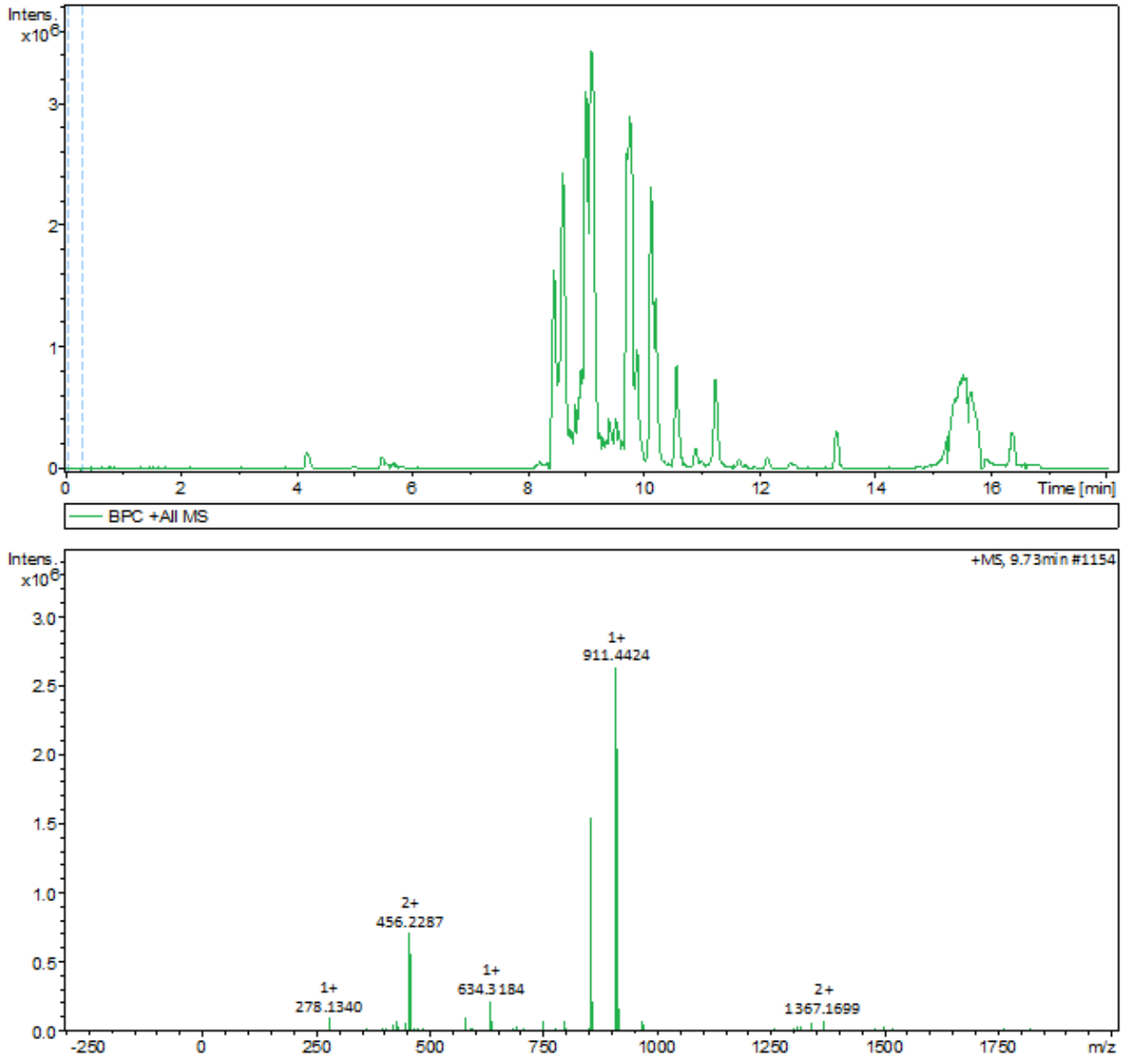


Figure A52. LC-MS analysis of **61f**

Display Report

Analysis Info

Acquisition Date 29/Jan/2019 H09:44:46 AM

Analysis Name I:\MY DOCUMENTS ONLY\LC-MS\V17 F-NH2_GC4_01_19310.d
Method Wits HPLC high MS 100-3000 pos.m
Operator Thapelo Mbhele
Sample Name V17 F-NH2
Instrument compact 8255754.20116
Comment

AcquisitionParameter

SourceType	ESI	IonPolarity	Positive	SetNebulizer	1.8 Bar
Focus	Not active	SetCapillary	4500 V	Set Dry Heater	220 °C
ScanBegin	100 m/z	Set End Plate Offset	-500 V	Set Dry Gas	9.0 l/min
ScanEnd	3000 m/z	SetChargingVoltage	2000 V	SetDivertValve	Waste
		SetCorona	0 nA	Set APCI Heater	0 °C

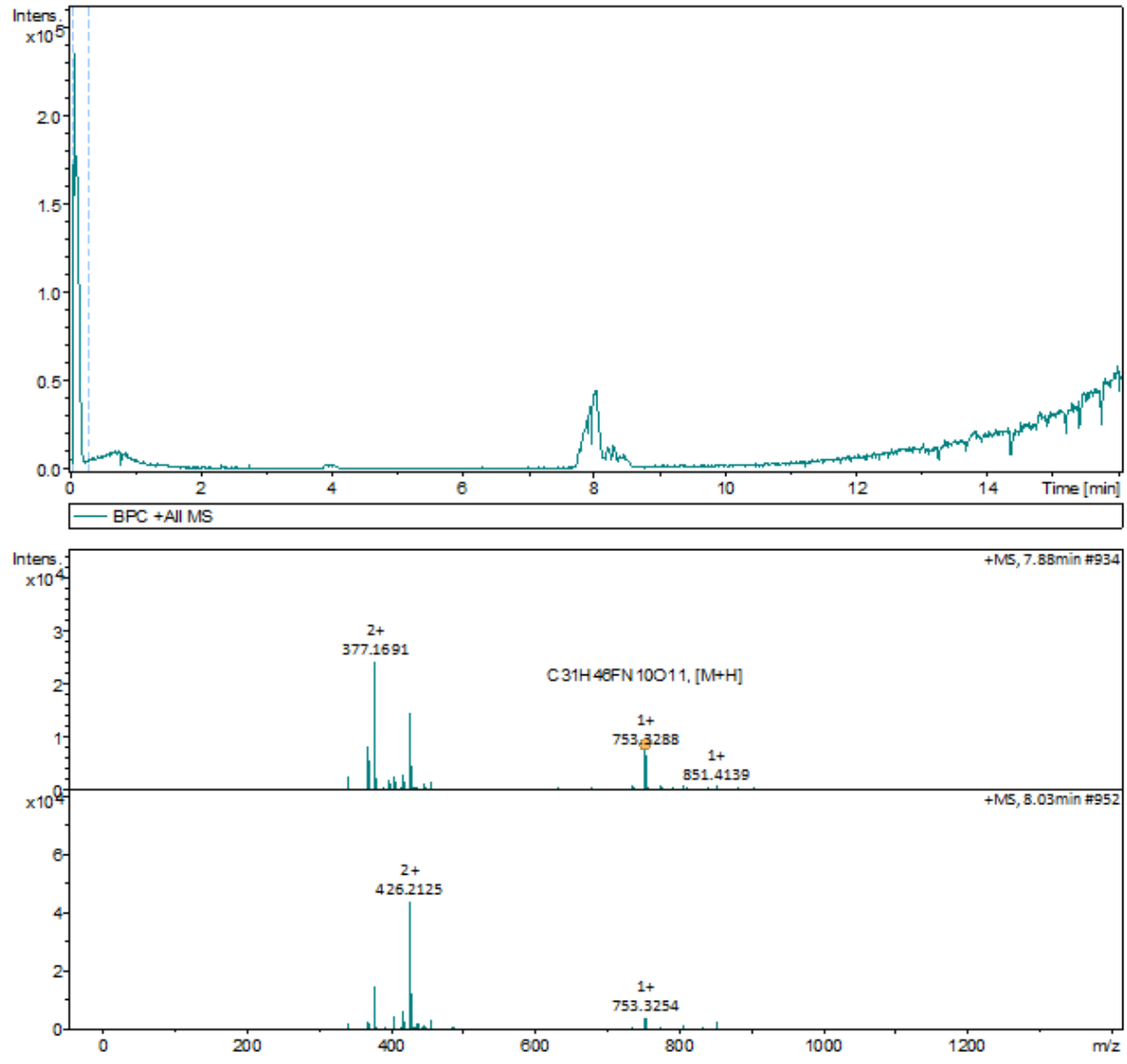


Figure A53. LC-MS analysis of **61g**

Display Report

Analysis Info

Acquisition Date 23/Dec/2018 H15:42:25 P M

Analysis Name I:\MY DOCUMENTS ONLY\LC-MS\25-12-2018\Phathus\23-12-2018\BETA-F-PAL IMPURE _RE5_01_18547.d

Method Wits HPLC high MS 100-3000 pos.m

Operator Thapelo Mbhele

Sample Name BETA-F-PAL IMPURE

Instrument compact 8255754.20116

Comment

AcquisitionParameter

SourceType	ESI	IonPolarity	Positive	SetNebulizer	1.8 Bar
Focus	Not active	SetCapillary	4500 V	Set Dry Heater	220 °C
ScanBegin	100 m/z	Set End Plate Offset	-500 V	Set Dry Gas	9.0 l/min
ScanEnd	3000 m/z	SetChargingVoltage	2000 V	Set Divert Valve	Waste
		SetCorona	0 nA	Set APCI Heater	0 °C

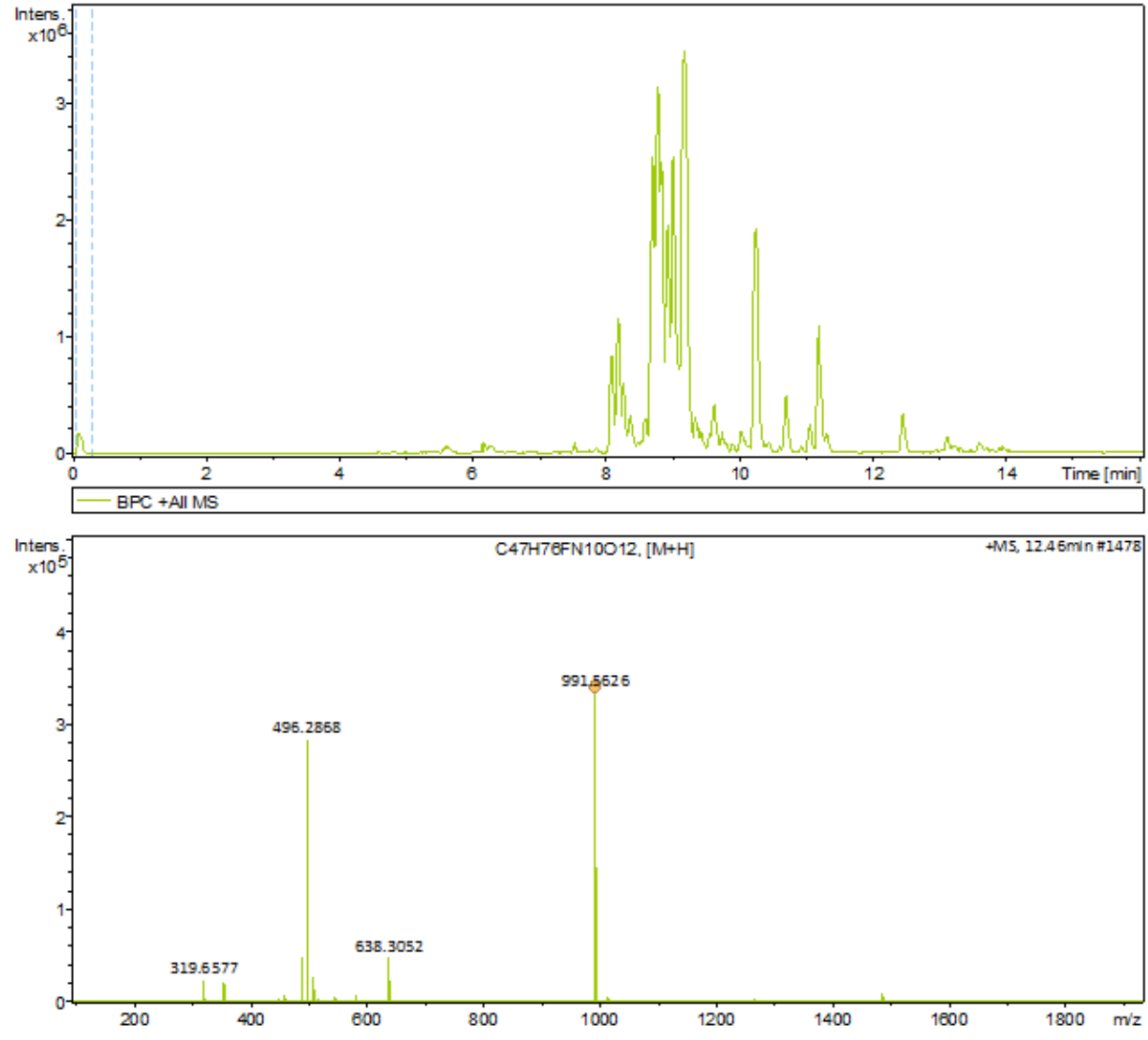


Figure A54. LC-MS analysis of **61h**

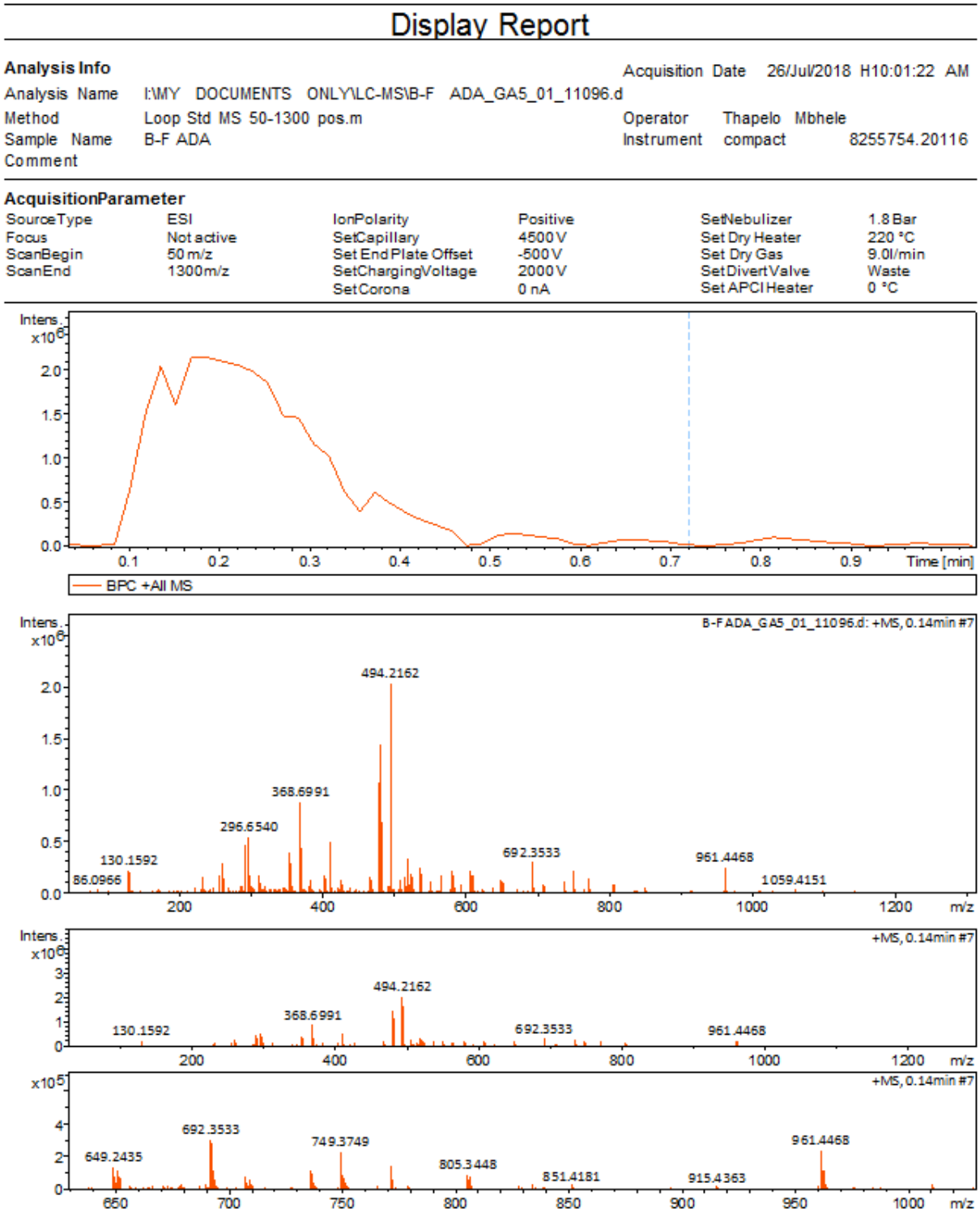


Figure A55. LC-MS analysis of **61i**